PACIFIC EARTHQUAKE ENGINEERING
RESEARCH CENTER

GEM-PEER Task 3 Project: Selection of a Global Set of Ground Motion Prediction Equations

Jonathan P. Stewart
University of California, Los Angeles

John Douglas
French Geological Survey

Mohammad B. Javanbarg
Carola Di Alessandro
Yousef Bozorgnia
Norman A. Abrahamson
Pacific Earthquake Engineering Research Center

David M. Boore
U.S. Geological Survey

Kenneth W. Campbell
EQECAT, Inc.

Elise Delavaud
ETH

Mustafa Erdik
Bogazici University

Peter J. Stafford
Imperial College

PEER 2013/22
DECEMBER 2013

Disclaimer

The opinions, findings, and conclusions or recommendations expressed in this publication are those of the author(s) and do not necessarily reflect the views of the study sponsor(s) or the Pacific Earthquake Engineering Research Center.

GEM-PEER Task 3 Project: Selection of a Global Set of Ground Motion Prediction Equations

Jonathan P. Stewart
University of California, Los Angeles

John Douglas
French Geological Survey

Mohammad B. Javanbarg
Carola Di Alessandro
Yousef Bozorgnia
Norman A. Abrahamson
Pacific Earthquake Engineering Research Center

David M. Boore
U.S. Geological Survey

Kenneth W. Campbell
EQECAT, Inc.

Elise Delavaud
ETH

Mustafa Erdik
Bogazici University

Peter J. Stafford
Imperial College

PEER Report 2013/22
Pacific Earthquake Engineering Research Center
Headquarters at the University of California, Berkeley

December 2013

ABSTRACT

Ground-motion prediction equations (GMPEs) relate a ground-motion parameter (e.g., peak ground acceleration, PGA) to a set of explanatory variables describing the earthquake source, wave propagation path and local site conditions. In the past five decades many hundreds of GMPEs for the prediction of PGA and linear elastic response spectral ordinates (e.g., pseudo-spectral acceleration, PSA) have been published. The Global Earthquake Model (GEM) Global GMPEs project, coordinated by the Pacific Earthquake Engineering Research Center (PEER), brought together ground-motion experts from various institutions around the world to develop recommendations on what GMPEs should be used by GEM when conducting global seismic hazard assessments. The GEM-PEER Project has seven tasks, as listed below:

Task 1a	Defining a Consistent Strategy for Modeling Ground Motions
Task 1b	Estimating Site Effects in Parametric Ground Motion Models
Task 2	Compile and Critically Review GMPEs
Task 3	Selection of a Global Set of GMPEs
Task 4	Include Near-Fault Effects
Task 5	Build an Inventory of Recorded Waveform Databases
Task 6	Design the Specifications to Compile a Global Database of Soil Classification

This report presents the methodology used in, and results of, Task 3, *Selection of a Global Set of GMPEs*. The reports of the other tasks of the GEM-PEER project are published by the GEM foundation and posted at: http://www.globalquakemodel.org.

For Task 3, a transparent and objective procedure was followed to reach the final recommendations. The procedure includes examination of the multi-dimensional (e.g., magnitude, distance and structural period) predicted ground-motion space, examination of functional forms, and evaluation of published quantitative tests of GMPE performance against observational data that was not used for their derivation.

The final selected GMPEs are a subset of the pre-selected models compiled during a previous task (Task 2) of this project. The recommendations for the prediction of PGA and PSA are:

- For stable continental regions: the models of Atkinson and Boore [2006], Pezeshk et al. [2011], Silva et al. [2002] (double corner with saturation) [but with its aleatory variability (standard deviation) model replaced by the variability model of EPRI [2006], and Toro et al. [1997] as modified by Toro [2002] to include finite-source geometric attenuation effects;
- For subduction zones: the models of Abrahamson et al. [2012, submitted], Atkinson and Boore [2003], and Zhao et al. [2006];

- For active shallow crustal regions: the models of Akkar and Bommer [2010], Chiou and Youngs [2008], and Zhao et al. [2006]; and
- For the three special regimes (volcanic zones, deep non-subduction Vrancea-type earthquakes and earthquakes with oceanic travel-paths), we recommend additional work be undertaken since the uncertainties in ground-motion prediction for these regimes is considerable.

Some of the recommended GMPEs have no site amplification term (i.e., three of the models for stable continental regions) or have linear site amplification terms. In either of those cases, we recommend application of the GMPEs for reference rock site conditions with modification by a nonlinear site term. The nonlinear site terms would ideally be region-specific, but in the absence of that information, we provide regime-specific recommendations. We consider the use of site amplification functions having nonlinearity to be important because linear models can significantly over-estimate ground motions for relatively large magnitude/close distance conditions, which often control the results of probabilistic seismic hazard analysis.

We emphasize that the goal of this project is to select a set of GMPEs for global hazard analysis; therefore, the number of selected GMPEs may be less than what might be used for site-specific analysis and/or development of national hazard maps. We also note that GMPE development is a continuously evolving research area, and new and/or updated GMPEs are published regularly as more empirical and simulated data become available and our knowledge of ground-motion hazard expands. Thus, the set of GMPEs recommended here should not be viewed as a long-term recommendation and should be re-evaluated on a regular basis.

ACKNOWLEDGMENTS

This study was funded by the GEM Foundation as part of the Pacific Earthquake Engineering Research Center's (PEER's) Global GMPEs project. Any opinions, findings, and conclusions or recommendations expressed in this material are those of the authors and do not necessarily reflect those of the sponsors.

CONTENTS

ABSTRACT iii

ACKNOWLEDGMENTS v

TABLE OF CONTENTS vii

LIST OF FIGURES ix

LIST OF TABLES xiii

1 INTRODUCTION 1
- 1.1 Project Motivation and Objectives 1
- 1.2 GEM Task 3 Project Requirements 2
- 1.3 Previous Related Work 3
- 1.4 GMPEs Pre-Selected in Task 2 5

2 PROCEDURE 9
- 2.1 International Panel of Experts 9
- 2.2 Selection Procedure and Factors Considered 9
  - 2.2.1 Synthesis of Functional Forms 12
  - 2.2.2 Comparative GMPE Scaling 12
  - 2.2.3 GMPE-Data Comparisons 12

3 TRELLIS PLOTS 15
- 3.1 Format of Plots 15
- 3.2 Model Evaluation from Trellis Plots including Epistemic Uncertainty 20
  - 3.2.1 Subduction Zones 20
  - 3.2.2 Stable Continental Regions 23
  - 3.2.3 Active Crustal Regions 29

4 GMPE DATA COMPARISONS 37
- 4.1 Requirements for Consideration of a Study 37
- 4.2 Application for GMPE Selection in this Study 38

5 RECOMMENDED GMPES 41

5.1 Subduction Zones 41

5.2 Stable Continental Regions 46

5.3 Active Crustal Regions 54

5.4 Three Special Regimes 58

5.4.1 Volcanic Zones 59

5.4.2 Vrancea-Type Earthquakes 59

5.4.3 Oceanic-Path Earthquakes 60

6 CONCLUSIONS 63

REFERENCES 65

APPENDIX A: PROJECT PLENARY MEETING, MAY 2012 69

LIST OF FIGURES

Figure 1.1 Number of published GMPEs per year (histogram) and cumulatively since 1964 (blue line). The red blocks indicate those models pre-selected in Task 2. 6

Figure 3.1 Trellis chart showing predicted PSAs for pre-selected SZ GMPEs for various interface earthquake scenarios for rock site conditions. Dashed lines indicated where the scenario falls outside the magnitude-distance range of validity of the model. 17

Figure 3.2 Trellis chart showing magnitude-scaling of predicted PSAs for pre-selected SZ GMPEs for various structural periods and source-to-site distances for rock site conditions. Dashed lines indicated where the scenario falls outside the magnitude-distance range of validity of the model. 18

Figure 3.3 Trellis chart showing distance decay of predicted PSAs for pre-selected SZ GMPEs for various structural periods and magnitudes for rock site conditions. Dashed lines indicated where the scenario falls outside the magnitude-distance range of validity of the model 19

Figure 3.4 Trellis chart showing inter- (between) and intra-(within) event and total natural log standard deviations of the pre-selected GMPEs for various interface SZ earthquake scenarios. 20

Figure 3.5 Trellis chart showing V_{s30}-scaling of the SZ GMPEs for a reference rock peak acceleration of $\text{PGA}_r = 0.1g$. Amplification has been computed relative to a consistent reference velocity of $V_{ref} = 1000$ m/sec, regardless of the reference condition used in the GMPE. Stepped relationships (e.g., AB03) describe site response relative to discrete categories whereas continuous relations use V_{s30} directly as the site parameter. The range shown for LL08 and YEA97 occurs because these relations do not have a formal site term but alternative GMPEs for rock and soil sites; the differences can be magnitude and distance dependent. 22

Figure 3.6 Trellis chart showing variation of site amplification with reference rock peak acceleration (for $V_{ref} = 1000$ m/sec) for various site classes and period. Representative velocities for each site class are based on category medians in the NGA-West2 database as described by Seyhan and Stewart [2012]. See Figure 3.5 caption for explanation of the ranges shown for LL08 and YEA97. 23

Figure 3.7 Trellis chart showing predicted PSAs for pre-selected SCR GMPEs for various earthquake scenarios for rock site conditions. Dashed lines indicated where the scenario falls outside the magnitude-distance range of validity of the model. 25

Figure 3.8 Trellis chart showing magnitude-scaling of predicted PSAs for pre-selected SCR GMPEs for various structural periods and source-to-site distances for rock site conditions. Dashed lines indicated where the scenario falls outside the magnitude-distance range of validity of the model..........26

Figure 3.9 Trellis chart showing distance decay of predicted PSAs for pre-selected SCR GMPEs for various structural periods and magnitudes for rock site conditions. Dashed lines indicated where the scenario falls outside the magnitude-distance range of validity of the model..........27

Figure 3.10 Period-dependent site terms in the SCR GMPEs for a reference rock peak acceleration of $\mathrm{PGA}_r = 0.1g$. Amplification has been computed relative to a consistent reference velocity of $V_{ref} = 1000$ m/sec..........28

Figure 3.11 Trellis chart showing inter- (between) and intra-(within) event and total natural log-standard deviations of the pre-selected SCR GMPEs. 29

Figure 3.12 Trellis chart showing predicted PSAs for pre-selected ACR GMPEs for various earthquake scenarios for rock site conditions. Dashed lines indicated where the scenario falls outside the magnitude-distance range of validity of the model. 31

Figure 3.13 Trellis chart showing magnitude-scaling of predicted PSAs for pre-selected ACR GMPEs for various structural periods and source-to-site distances for rock site conditions. Dashed lines indicated where the scenario falls outside the magnitude-distance range of validity of the model..........32

Figure 3.14 Trellis chart showing distance decay of predicted PSAs for pre-selected ACR GMPEs for various structural periods and magnitudes for rock site conditions. Dashed lines indicated where the scenario falls outside the magnitude-distance range of validity of the model..........33

Figure 3.15 Trellis chart showing V_{s30}-scaling of the ACR GMPEs for a reference rock peak acceleration of $\mathrm{PGA}_r = 0.1g$. Amplification has been computed relative to a consistent reference velocity of $V_{ref} = 1000$ m/sec, regardless of the reference condition used in the GMPE. Stepped relationships (e.g., AB10) describe site response relative to discrete categories whereas continuous relations use V_{s30} directly as the site parameter. 34

Figure 3.16 Trellis chart showing variation of site amplification with reference rock peak acceleration (for $V_{ref} = 1000$ m/sec) for various site classes and period. Representative velocities for each site class are based on category medians in the NGA-West2 database as described by Seyhan and Stewart [2012]. 35

Figure 3.17 Trellis chart showing variation of site amplification with period (for $V_{ref} = 1000$ m/sec and $\mathrm{PGA}_r = 0.1g$) for various site classes. 35

Figure 3.18 Trellis chart showing inter- (between) and intra-(within) event and total natural log standard deviations of the pre-selected ACR GMPEs. 36

Figure 5.1 PSAs trellis chart highlighting selected models (color) overlaid on non-selected models (grey). Conditions shown are for interface earthquake scenarios and rock site conditions....43

Figure 5.2 Magnitude scaling trellis chart highlighting selected models (color) overlaid on non-selected models (grey). Conditions shown are for interface earthquake scenarios and rock site conditions....44

Figure 5.3 Distance scaling trellis chart highlighting selected models (color) overlaid on non-selected models (grey). Conditions shown are for interface earthquake scenarios and rock site conditions....45

Figure 5.4 Standard deviation trellis chart highlighting selected models (color) overlaid on non-selected models (grey). Conditions shown are for interface earthquake scenarios and rock site conditions....46

Figure 5.5 Trellis plot for SCR GMPEs highlighting models of AB06′, PEA11, and SEA02....48

Figure 5.6 PSAs trellis chart highlighting selected models (color) overlaid on non-selected models (grey). Conditions shown are for SCR earthquake scenarios and rock site conditions....50

Figure 5.7 Magnitude scaling trellis chart highlighting selected models (color) overlaid on non-selected models (grey). Conditions shown are for SCR earthquake scenarios and rock site conditions....51

Figure 5.8 Distance scaling trellis chart highlighting selected models (color) overlaid on non-selected models (grey). Conditions shown are for SCR earthquake scenarios and rock site conditions....52

Figure 5.9 Standard deviation trellis chart highlighting selected models (color) overlaid on non-selected models (grey). Conditions shown are for SCR earthquake scenarios and rock site conditions. SEA02 model not highlighted in this plot since E06 standard deviation terms are used as a replacement....53

Figure 5.10 Frequency-dependent site amplification expressed as transfer functions (from AB06) and RRS (from seventh author). The RRS values can be used to correct PSA computed for very hard reference site conditions in SCRs ($V_s \geq 2.0$ km/sec , NEHRP site class A) to the BC boundary site condition ($V_{s30} = 760$ m/sec)....54

Figure 5.11 PSAs trellis chart highlighting selected models (color) overlaid on non-selected models (grey). Conditions shown are for ACR earthquake scenarios and rock site conditions....55

Figure 5.12 Magnitude scaling trellis chart highlighting selected models (color) overlaid on non-selected models (grey). Conditions shown are for ACR earthquake scenarios and rock site conditions....56

Figure 5.13 Distance scaling trellis chart highlighting selected models (color) overlaid on non-selected models (grey). Conditions shown are for ACR earthquake scenarios and rock site conditions....57

Figure 5.14 Standard deviation trellis chart highlighting selected models (color) overlaid on non-selected models (grey). Conditions shown are for ACR earthquake scenarios and rock site conditions. 58

LIST OF TABLES

Table 1.1 Summary of GMPEs selected in some GEM-related projects. 5
Table 1.2 List of pre-selected models in Task 2. 7

Table 2.1 The expert panel in alphabetical order. 11

Table 4.1 Summary of studies in literature with quantitative model-data comparisons for ACRs. Rows with light gray shading are for studies using an overall goodness-of-fit approach, rows with dark gray shading are for studies that test specific GMPE attributes through residuals analysis. 39
Table 4.2 Summary of studies in literature with quantitative model-data comparisons for SZs. Rows with light gray shading are for studies using an overall goodness-of-fit approach, rows with dark gray shading are for studies that test specific GMPE attributes through residuals analysis. 40
Table 4.3 Summary of studies in literature with model-data comparisons for SCRs. 40

1 Introduction

1.1 PROJECT MOTIVATION AND OBJECTIVES

Ground-motion prediction equations relate a ground-motion parameter [e.g., peak ground acceleration (PGA)] to a set of explanatory variables describing the earthquake source, wave propagation path, and local site conditions [e.g., Douglas [2003]). These independent variables invariably include magnitude, source-to-site distance, and local site conditions, and often style-of-faulting (mechanism). Some recent models also account for other factors affecting earthquake ground motions (e.g., hanging wall effects). In the past five decades many hundreds of GMPEs for the prediction of PGA and linear elastic response spectral ordinates have been published, which are summarized in a series of public reports by the second author of this report (Douglas [2011]). Therefore, the seismic hazard analyst is faced with the difficult task of deciding which GMPEs to use for a given project. This decision is a critical step in any hazard assessment because the resulting predicted spectra are strongly dependent on the GMPEs chosen.

This report discusses the selection of GMPEs undertaken within the framework of the Global Earthquake Model (GEM) Global GMPEs project, coordinated by the Pacific Earthquake Engineering Research Center (PEER). The overall GEM-PEER project is described by Di Alessandro et al. [2012]. The first step of the GMPE selection process was made by pre-selecting from all the available models the most robust GMPEs as candidates for final selection. As described by Douglas et al. [2011; 2012], this Task 2 of the GEM-PEER project led to the choice of roughly ten GMPEs for each of three major tectonic regimes [active crustal regions (ACRs); subduction zones (SZs); and stable continental regions (SCRs)]. For applications within GEM, the list of the pre-selected GMPEs in Task 2 is too long as the final selected GMPEs will be used by GEM for seismic hazard analysis of the entire world at quite a high resolution (thought to be a grid of 0.1 × 0.1°), i.e., tens of thousands of grid points. Therefore, for practical reasons (e.g., calculation times) the selected number of GMPEs for each tectonic environment should be in general less than that used for local and regional hazard analyses. However, it is important that epistemic uncertainty in ground motion prediction be accounted for in the Global GMPEs project by selecting a range of GMPEs that cover the center, body, and range of technically defensible interpretations [Bommer et al. 2005]. In that respect, our objective has similarities to other model-selection exercises used in the U.S. nuclear industry [U.S. NRC 2012].

It should also be noted that GMPE development is a continuously evolving research area, and new and/or updated GMPEs are published as more empirical and simulated data become available and our knowledge of ground-motion hazard expands. Thus, the set of GMPEs proposed within Task 3 should not be viewed as a long-term recommendation and should be re-evaluated on a regular basis.

This report describes the work undertaken in Task 3 of the GEM-PEER project to select a relatively small set of about three recommended GMPEs for each major tectonic regime. The rest of this introduction presents the project motivation and objectives, and GMPE selection in previous GEM-related projects, and the pre-selection step (Task 2) of this project is briefly summarized. Chapter 2 presents the procedure followed in Task 3, including the composition of the expert panel and the information considered during the selection process. Chapter 3 presents one of the main tools used in the selection process—namely trellis plots—which compare the ground-motion predictions from each of the GMPEs for various earthquake scenarios. The second principal tool used to guide the selection is presented in Chapter 4, where previously published studies quantitatively comparing predicted and observed response spectral accelerations in recent earthquakes. Chapter 5 provides our recommended GMPEs for GEM along with the rationale for their selection. We restrict our recommendations to the selection of GMPEs and not to what weights they should be assigned in a logic tree. The report ends with some brief conclusions (Chapter 6) and potential improvements for future studies. Not all of the material used by the experts to make the final selection is presented in Chapters 3 and 4 (only some representative figures are shown). Therefore, for completeness we provide updated versions of the Microsoft PowerPoint presentations shown at the project plenary meeting of May 2012 in Appendix A.

1.2 GEM TASK 3 PROJECT REQUIREMENTS

The GEM-PEER Global GMPEs project [Di Alessandro et al. 2012] seeks to provide to the GEM a set of ground-motion models with worldwide applicability that are based on a consensus view of dozens of international experts. These models should enable the prediction of peak ground acceleration (PGA) and linear elastic pseudo-absolute spectral acceleration (PSA) for 5% of critical damping for: (1) the structural period range of main engineering interest; (2) magnitudes from the lower limit generally considered in seismic hazard assessments (typical M 5) up to the largest earthquakes possible (roughly M 9.5 for subduction events); and (3) the source-to-site distances from the closest possible distance (i.e., 0 km, right next to the rupture) to the farthest distance considered important in hazard assessments (possibly 1000 km in stable continental regions).

The focus of this project is on the selection (and possible adjustment) of pre-existing already-parameterized GMPEs and not on the development of new models. For the prediction of strong-motion parameters (intensity measures) other than PGA and PSA, Douglas [2012] provides a summary table of GMPEs for peak ground velocity and displacement, Arias intensity, and significant duration published in the international literature. If spectral ordinates for damping levels other than 5% are required, we recommend use of the damping scaling factors developed by Rezaeian et al. [2012]. Our focus is on horizontal ground motions; none of the selected models allows the prediction of PGA and PSA for the vertical components. If GEM requires estimates of the vertical ground motions, we recommend use of the GMPEs for vertical-to-horizontal spectral ratios recently proposed by Gülerce and Abrahamson [2011], Bommer et al.

[2011], and Bozorgnia and Campbell [2004]. In addition, the on-going NGA-West 2 project is planning to publish GMPEs for vertical motions in 2013.

The GMPE selection process applied in this study assumes broad tectonic regionalization (listed below). We recognize the possibility for regional differences within tectonic classes, which we attempt to address in an admittedly approximate way through consideration of epistemic uncertainty in critical GMPE attributes (such as rate of distance decay). We principally considered the following broad tectonic regimes for GMPE selection:

- SCRs, which could possibly be divided further into shield and continental/foreland as was done by Delavaud et al. [2012]
- SZs, which includes intraslab and interface earthquakes (and potentially fore-arc and back-arc locations)
- ACRs having shallow crustal seismicity

As part of Task 3, we were asked to consider three other tectonic regimes of limited geographical extent that lack robust ground-motion models. The special regimes are:

- Volcanic zones
- Areas of deep focus non-subduction earthquakes, such as the Vrancea seismic zone (Romania)
- Areas where the travel paths are mainly through oceanic crust, such as earthquakes off coastal Portugal.

In Chapter 5 we make some limited recommendations concerning these special regimes.

1.3 PREVIOUS RELATED WORK

Similar GMPE selection tasks have been undertaken in other GEM-related projects: the GEM1 pilot project, Seismic Hazard Harmonization in Europe (SHARE) project and Earthquake Model of the Middle East Region (EMME) project. In this section, we provide brief summaries of these selections, including how they were made. It should be remembered that the selection undertaken here as part of Task 3 of the Global GMPEs project is not seeking to replace selections made in GEM regional programs, such as SHARE and EMME, but it is a first-order global recommendation that we expect would be applied principally in areas without regional programs.

GEM1 was a roughly one-year proof-of-concept implementation of GEM that sought not only to develop GEM's initial IT infrastructure and generate GEM's first products, but also to lay a foundation for further developments. It ran from January 2009 to March 2010. The aim was for an ‘80% solution’. As part of GEM1, a small subtask was initiated to propose a set of GMPEs for use in global hazard calculations within this project. The result of this subtask is the report by Douglas et al. [2009] and an associated standalone Matlab® program that allows the user to click on a global map and obtain the set of recommended GMPEs for that location. Table 1.1 lists the overall recommendations by Douglas et al. [2009], although these were slightly modified in areas for which local knowledge was available (e.g., French Antilles). Douglas et al. [2009]

generally recommended equal weights be applied to the GMPEs for each regime. This selection was based solely on expert judgment within a small task team and on previously published testing results.

Within the SHARE project, sponsored by the Seventh Framework Programme of the European Commission and the regional component of GEM for Europe, a task was dedicated to the development of a ground-motion logic tree for probabilistic seismic hazard assessment (PSHA) for Europe. The results of this task are summarized by Delavaud et al. [2012]. Table 1.1 presents the GMPE selection made by Delavaud et al. [2012]. These recommendations are associated with weights, but these weights are not reported here because they are not directly relevant, as we are not aiming to propose weights to GEM. The GMPE selection in SHARE was made based on a combination of expert judgment and quantitative comparisons between predicted and observed ground motions (two strong-motion databases were used: one containing only European data and the other containing records from large magnitude events worldwide).

The GEM regional component for the Middle East, the EMME project, has also constructed a GMPE logic tree [S. Akkar *written communication* 2012], whose models are listed in Table 1.1. The selection procedure followed in EMME was similar to that used in SHARE but it was solely based on quantitative comparisons between predicted and observed ground motions (a strong-motion database from the Middle East, principally Iranian and Turkish records, was used) rather than being a mixture of testing and expert judgment. In addition, the pre-selected GMPEs considered by EMME were slightly different from those that were the basis of SHARE (partly because EMME started slightly later than SHARE).

While the above-mentioned projects have focused on PGA and PSA, we note that the GMPE compilation of Douglas [2012] is a useful resource for GMPE selection involving other intensity measures, including peak ground velocity and displacement, Arias intensity, and significant duration.

Table 1.1 Summary of GMPEs selected in some GEM-related projects.

	GEM1	SHARE	EMME
ACR	Akkar and Bommer [2007] Boore and Atkinson [2008] Campbell and Bozorgnia [2008] Cauzzi and Faccioli [2008] Chiou and Youngs [2008]	Akkar and Bommer [2010] Cauzzi and Faccioli [2008] Chiou and Youngs [2008] Zhao et al. [2006]	Akkar and Bommer [2010] Akkar and Çağnan [2010] Chiou and Youngs [2008] Zhao et al. [2006]
SCR	Atkinson [2008] Atkinson and Boore [2006] Campbell [2003] Tavakoli and Pezeshk [2005] Toro et al. [1997]	Divided into shield and continental crust. For shield: Campbell [2003], Toro [2002] For continental crust: Campbell [2003], Toro [2002], Akkar and Bommer [2010], Cauzzi and Faccioli [2008], and Chiou and Youngs [2008]	N/A
SZ	Atkinson and Boore [2003] Kanno et al. [2006] Youngs et al. [1997]	Atkinson and Boore [2003] Lin and Lee [2008] Youngs et al. [1997] Zhao et al. [2006]	N/A

1.4 GMPES PRE-SELECTED IN TASK 2

As mentioned in Section 1.1, Task 3 of the GEM Global GMPEs project was preceded by Task 2, whose aim was to pre-select roughly ten GMPEs per region that would be the basis of discussions in Task 3. In this section, Task 2 is briefly summarized. For more information, the reader is referred to Douglas et al. [2012], to the Task 2 report [Douglas et al. 2011], and to the Tasks 1a, 1b, and 2 of the present report.

Since the publication of the first ground-motion model in the form of an equation with magnitude and source-to-site distance terms by Esteva and Rosenblueth [1964], the number of GMPEs has increased dramatically; over a dozen new studies are published every year (Figure 1.1). This high publication rate has been driven by: (1) increased recording (through lower-cost digital instruments and denser networks) and availability of strong-motion data [through online open-access databases, such as the Internet Site for European Strong-motion Data [Ambraseys et al. 2004], (2) more journals and conferences publishing engineering seismology research; and (3) large-scale initiatives, such as the Next Generation Attenuation (NGA) project [Power et al. 2008]. The latest compendium of published GMPEs by Douglas [2011] lists the characteristics of 289 empirical GMPEs for the prediction of PGA and 188 empirical models for the prediction of elastic response spectral ordinates. In addition, this report lists many dozens of simulation-based GMPEs.

This abundance of models, however, creates a difficulty. On one hand, it is feasible from a practical point of view to carefully consider only a small fraction (less than 10%) of available GMPEs in any project. On the other hand, predictions of the median ground motions from the available GMPEs show a large (and not noticeably narrowing) dispersion [Douglas 2010], which needs to be considered, since it demonstrates high epistemic uncertainty in ground-motion prediction. Consequently, a set of objective selection criteria need to be applied to the list of available models to pre-select GMPEs that are the most appropriate for the aims of a given project. While these selection criteria should involve careful review of the GMPE documentation, for ease of application, they should not require numerical evaluation or testing of models against local data, which is impractical for the vast majority of commercial projects. These selection criteria were discussed by the experts comprising the Task 2 working group and subsequently applied by the working group to the lists of models given in Douglas [2011]. The discussion process was conducted through a series of conference calls and email exchanges in order to obtain a consensus view, which also aimed to be objective so it could be supported by the wider community (within the GEM Global GMPEs project and beyond).

Because a GMPE excluded during this stage could not be subsequently re-instated, care was taken to avoid applying criteria that are too strict. About thirty GMPEs were finally pre-selected within Task 2 for closer inspection in Task 3 to obtain a final set of ground-motion models. This pre-selection was performed by applying the exclusion criteria of Cotton et al. [2006] to the complete list of published models in Douglas [2011]. The pre-selected models are listed in Table 1.2 along with their abbreviated titles, which are used subsequently.

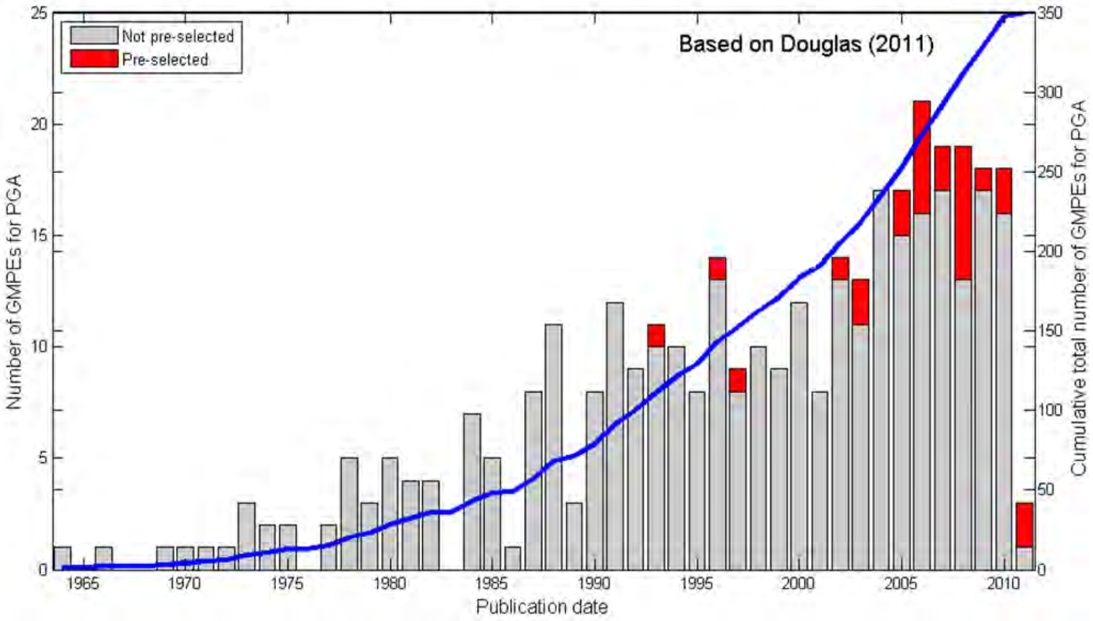

Figure 1.1 **Number of published GMPEs per year (histogram) and cumulatively since 1964 (blue line). The red blocks indicate those models pre-selected in Task 2.**

Table 1.2 List of pre-selected models in Task 2.

	Reference	Abbreviation
SCR	Atkinson [2008] as modified by Atkinson and Boore [2011]: Referenced empirical model for eastern North America	A08′
	Atkinson and Boore [2006] as modified by Atkinson and Boore [2011]: Extended stochastic model for eastern North America	AB06′
	Campbell [2003]: Hybrid empirical model for eastern North America	C03
	Douglas et al. [2006]: Hybrid empirical model for southern Norway	DEA06
	Frankel et al. [1996] as parameterized by EPRI [2004]: Stochastic model for eastern North America	FEA06
	Pezeshk et al. [2011]: Hybrid empirical model for eastern North America	PEA11
	Raghu Kanth and Iyengar [2006, 2007]: Peninsular India	RKI07
	Silva et al. [2002]: Stochastic model for eastern North America	SEA02
	Somerville et al. [2009]: Simulation-based model for Australia	SEA09
	Toro et al. [1997], originally published in EPRI [1993], modified by Toro [2002]: Stochastic model for eastern North America	TEA97′
SZ	Abrahamson et al. [2012]: Global	AEA12
	Arroyo et al. [2010]: Interface model for Mexico (complementary to Garcia et al. [2005]	AEA10
	Atkinson and Boore [2003]: Global	AB03
	Garcia et al. [2005]: Intraslab model for Mexico (complementary to Arroyo et al. [2010])	GEA05
	Kanno et al. [2006]: Japan	KEA06
	Lin and Lee [2008]: Taiwan	LL08
	McVerry et al. [2006]: New Zealand	MEA06
	Youngs et al. [1997]: Global	YEA97
	Zhao et al. [2006] with modifications by Zhao [2010]: Japan	ZEA06
ACR	Abrahamson and Silva [2008]: NGA model using worldwide data	AS08
	Akkar and Bommer [2010]: Model using Mediterranean and Middle Eastern data	AB10
	Boore and Atkinson [2008] as modified by Atkinson and Boore [2011]: NGA model using worldwide data	BA08′
	Campbell and Bozorgnia [2008] : NGA model using worldwide data	CB08
	Cauzzi and Faccioli [2008] as updated by Faccioli et al. [2010]: Model using worldwide data (mainly Japanese)	FEA10
	Chiou and Youngs [2008]: NGA model using worldwide data	CY08
	Kanno et al. [2006]: Model using mainly Japanese data	KEA06
	McVerry et al. [2006]: Model using mainly New Zealand data	MEA06
	Zhao et al. [2006]: Model using mainly Japanese data	ZEA06

2 Procedure

This chapter presents the overall procedure developed to select GMPEs for the three principal tectonic regimes (SZs, ACRs, and SCRs). Details of the two principal tools for making these selections are discussed in Chapter 3 (trellis plots) and Chapter 4 (GMPE-data comparisons).

2.1 INTERNATIONAL PANEL OF EXPERTS

Task 3 consisted of a core group of experts (the authors of this report) and a wider expert panel that comprised all members of the project (Table 2.1). The core group was responsible for preparing initial GMPE recommendations for the three regimes, which were then presented to the wider expert panel for discussion and potential revision.

2.2 SELECTION PROCEDURE AND FACTORS CONSIDERED

The GEM Task 3 core working group (the authors of this report) met by web conference on many occasions and in person before the project plenary meeting to discuss the selection of GMPEs for the three principal regimes. In addition, discussions continued by email within the working group and occasionally with GMPE developers for clarification of certain aspects of their models. The GMPEs were selected from the candidate list produced in Task 2 (see Section 1.4). We sought to select three GMPEs per regime to balance the desire for simplicity in the GEM hazard logic tree with a need to model epistemic uncertainty in ground-motion prediction; this is considerable for the many areas of the world with little or no strong-motion data. All members of the working group were present for at least one of the meetings, and all were included on the relevant correspondence including copies of slides, meeting minutes, and instructions for providing input to the working group chairs (the first two authors of this report).

In the first meeting, the working group decided on the criteria to be considered in the selection of GMPEs from the list provided in Table 1.2. There was agreement that relevant criteria for consideration in GMPE selection for SZ and ACR regimes include:

- Giving more emphasis to GMPEs derived from international than from local datasets. Exceptions can be made when a GMPE derived from a local dataset has been checked internationally and found to perform well.

- Giving more emphasis to GMPEs that have attributes of their functional form that we consider desirable, including saturation with magnitude, magnitude-dependent distance scaling and anelastic attenuation terms.
- If there are multiple GMPEs that are well constrained by data but exhibit different trends, it is desirable to capture those trends in the selected GMPEs to properly represent epistemic uncertainty.

For SCRs, where strong-motion data are scarce, these criteria were modified as follows:

- SCR GMPEs were derived principally from the results of numerical simulations. However, the manner in which the limited available data was used to constrain the input parameters for the simulations is critical. For example, the empirical calibration may influence stress drop parameters and site attenuation (kappa). We prefer GMPEs judged to be effective use the available data to constrain model parameters.
- Giving more weight to GMPEs that have attributes to their functional form that we consider desirable, including saturation with magnitude, magnitude-dependent distance scaling, and anelastic attenuation terms. Since data are very limited for SCRs, it is especially important that the selected models extrapolate in a reasonable manner beyond the data range.
- We seek GMPEs that meet the above criteria and which collectively: (i) represent diverse geographic regions and (ii) use alternate simulation methodologies. This is intended to capture epistemic uncertainty in the selected GMPEs.
- In the selection process, we decided not to down-weight GMPEs with difficult-to-implement parameters (e.g., basin depth terms or depth to top of rupture), because those issues can be overcome with appropriate parameter selection protocols (e.g., Kaklamanos et al. [2011]). We also decided not to down weight GMPEs that either lack site terms or whose modeling of site response is non-optimal (e.g., lack of nonlinearity), because GMPEs can be evaluated for a reference rock site condition in hazard analysis and site effects subsequently added in a hybrid process [Cramer 2003; Goulet and Stewart 2009].

To assist the working group members in making their selections according to the criteria above, two major compilations of information were prepared before the web conferences. First, so-called trellis plots were formulated that show spectral shapes for various magnitude and distance combinations, magnitude-scaling trends for different distance bins, distance-scaling trends for different magnitude bins, site-effect terms, hypocentral depth-scaling terms, and standard-deviation terms. Second, GMPE-data comparisons from the literature were compiled, emphasizing those studies that undertake formal analysis of residuals to provide insight into GMPE performance. These two compilations are described in more depth in subsequent sections.

Table 2.1 The expert panel in alphabetical order.

Name	Affiliation
Abrahamson, Norman	Pacific Gas and Electric Company, USA
Akkar, Sinan	Middle East Technical University, Turkey
Arefiev, Sergei†	Russian Academy of Sciences, Russia
Baker, Jack	Stanford University, USA
Boore, David	U.S. Geological Survey, USA
Boroschek, Ruben	University of Chile, Chile
Bozorgnia, Yousef	PEER, University of California, Berkeley, USA
Campbell, Kenneth	EQECAT Inc., USA
Cheng, Thomas	SinoTech, Taiwan
Chiou, Brian	California Department of Transportation, USA
Cotton, Fabrice	Université Joseph Fourier, France
Delavaud, Elise	ETH Zurich, Switzerland
Di Alessandro, Carola	PEER, University of California, Berkeley, USA
Douglas, John	BRGM (French Geological Survey), France
Erdik, Mustafa	Kandilli Observatory and Earthquake Research Institute (KOERI), Bogazici University, Turkey
Fajfar, Peter	University of Ljubljana, Slovenia
McVerry, Graeme	GNS Science, New Zealand
Midorikawa, Saburoh	Tokyo Institute of Technology, Japan
Midzi, Vunganai	Council for Geoscience, South Africa
Molas, Gilbert	Risk Management Solutions, USA
Saragoni, Rodolfo	University of Chile, Chile
Shoja-Taheri, Jafar	Ferdowsi University, Iran, and University of Nevada and USA
Silva, Walter	Pacific Engineering and Analysis, USA
Somerville, Paul	URS Corporation, USA, and Macquarie University, Australia
Stafford, Peter	Imperial College London, United Kingdom
Stewart, Jonathan	University of California, Los Angeles, USA

†Deceased 30 March 2012

Individual members of the working group provided their recommendations for GMPE selection either orally as part of an open discussion and/or in written correspondence to the group facilitators (C. Di Alessandro and M. B. Javanbarg]. The working group chairs reviewed the input received, including their own, and made recommendations that were put to the wider expert panel. These recommendations were presented at the project's plenary meeting in Istanbul in May 2012, and feedback from the meeting's attendees was received. The core group then adjusted the recommendations based on this feedback.

2.2.1 Synthesis of Functional Forms

It is sometimes difficult to compare how two or more GMPEs scale with magnitude, distance, and other independent parameters because of differences in the way functional forms are expressed. For example, in his compendium Douglas [2011] does not seek to unify the formulations of each model but simply repeats the equations using the same variable names. Therefore, since a principal aspect of the GMPE selection was how the models scale and extrapolate at the extremes of the magnitude-distance space, a unification of the functional forms was undertaken using consistent terminology and focusing only on the most important aspects of the models. These functional form summaries are given in the appendix for the three regimes. They highlight that some models assume simple scaling with magnitude (e.g., linear-dependency) and distance (e.g., $1/R$ decay), whereas others account for more complex effects (e.g., magnitude-saturation and magnitude-dependent distance scaling). The effect of these differences are more clearly seen when visually comparing how the predictions scale with magnitude and distance (and other independent parameters) within graphs.

2.2.2 Comparative GMPE Scaling

A more visual comparison of the scaling of the pre-selected GMPEs against independent parameters (e.g., magnitude and source-to-site distance) was prepared using sets of plots showing predicted PSA against different parameters. These are referred to as "trellis plots," and are discussed in more detail in Chapter 3. All of the generated plots are provided in the appendix for completeness.

2.2.3 GMPE-Data Comparisons

The original project plan called for a comparison of the pre-selected GMPEs to observed ground-motion data. To undertake this analysis, a standalone Matlab® program was written that undertook residual analysis (e.g., plotting of between- and within-event residuals against various independent parameters). It was planned to disseminate this code to members of the Task 3 expert panel to conduct quantitative analysis using their own sets of data. The advantage of this approach is that it would have led to a set of consistent residual analyses but keeping the ground-motion data with the owners, thereby avoiding data dissemination issues and problems with data formats. In addition, it would have required fewer resources than conducting all the data analysis within the Task 3 core.

Ultimately, this planned subtask was revised for a number of reasons. First, very few of the Task 3 experts expressed an interest in conducting such an analysis. Second, a literature survey of previously published quantitative GMPE-data comparisons highlighted a large number of previous analyses for ACRs and SZs; therefore, the requirement to undertake calculations within this project was not necessary for these regions. Such data analyses are lacking for SCRs, however. Although it would have been useful to conduct our own analyses for this tectonic regime, the limited number of records from earthquakes larger than **M**5 for SCRs makes such analyses of limited value. Chapter 4 describes the manner by which we considered GMPE-data comparisons within this project.

3 Trellis Plots

This chapter presents and interprets trellis plots, which comprise one of the two principal tools used to select GMPEs. We begin with an explanation of the format of these graphs and the criteria that were used to judge the behavior of the models that are displayed. The majority of the chapter presents key trellis plots for the three different regimes that were used to help guide the selection process.

3.1 FORMAT OF PLOTS

All of the GMPEs pre-selected in Task 2 were programmed within Matlab®. The predicted median ground motions and their aleatory variability from these implementations were checked against the original references and against the results from previous implementations in other programs (e.g., Kaklamanos et al. [2010]). As a standardized way of comparing the behavior of the GMPEs over the entire magnitude-distance (and other independent variables, e.g., site classification) range of interest, many trellis charts were drawn. With these charts we sought to display the multi-dimensional (magnitude, source-to-site distance, structural period etc.) predicted ground-motion space in various ways to understand the considered ground-motion models better. The aim was to help identify outliers with clearly nonphysical behavior but also to help guide the selection of models to capture epistemic uncertainty (e.g., the distance attenuation rate appears to be regionally dependent; therefore, it is important that this variation is captured). In this section, we present these plots for the example of interface SZ GMPEs in order to illustrate the plot formats. The interpretation of the findings from the plots is deferred to Section 3.2, which also presents plots for the other principal regimes (ACR and SCR).

The first type of these graphs (example in Figure 3.1 for SZs) show predicted response spectra (color-coded for each GMPE) where each graph within the trellis has an *x*-axis of period and a *y*-axis of PSA. The trellis has a super *x*- and *y*-axis of magnitude and distance, respectively, and each graph within the trellis has its own axes with a common scale. This type of chart enables examination of how the spectrum predicted by each GMPE compares to the others over the magnitude-distance range of interest, e.g., are there any models that are consistently high or low or any with a different spectral shape? Because of the requirements imposed by the planned application of the GMPEs within GEM at the physical extremes of magnitude and source-to-site distance, the GMPEs were evaluated from the smallest magnitude considered of importance within the seismotectonic regime of interest (often **M**5) to the largest magnitude that we felt to be possible in each of the different seismotectonic regimes and to the closest and farthest distance thought important on a global scale. Dotted lines are used for predictions for magnitudes and distances outside the limits of applicability stated by the GMPE developers or the range of data used for their derivation. However, since the goal of the GEM Global GMPEs project is to propose ground-motion models that work over all ranges of interest to GEM, the dotted lines were considered by the experts. The idea was to thoroughly examine the models even outside their ‘comfort zone’ [Bommer et al. 2010].

The second type of graph plotted within trellis charts (example in Figure 3.2 for SZs) are plots of predicted PSA against magnitude within a trellis chart with super *x*- and *y*-axes of period and source-to-site distance, respectively. This directly shows the magnitude scaling of ground motions. There are theoretical reasons why magnitude scaling is nonlinear (e.g., Fukushima [1996] and Douglas [2002]) and numerous observational studies have provided evidence for it. This effect is particularly important at large magnitudes (**M**>8) since otherwise ground motions can become unphysically large. The third set of trellis charts are similar to the previous type but show scaling with distance for different magnitudes and periods (Figure 3.3 for SZs). These plots show the decay rate for the various models, which can vary, for example, because of different anelastic attenuation representing variable crustal structures. Specifically for intraslab subduction earthquakes, the fourth type of chart shows the scaling with focal depth within a trellis chart having super axes of period and magnitude. Another set of trellis charts were produced that are similar to the first set (predicted median spectra) but showing the predicted between-event, within-event and total aleatory variabilities (standard deviations) as a function of magnitude, distance and period (Figure 3.4 for SZs). These are important since the modeling of the aleatory variability is a key component of a GMPE and PSHA. It was decided that we would prioritize the selection of complete ground-motion models (i.e., GMPEs for the median *and* the associated sigma model) rather than select separate models for the median and sigma.

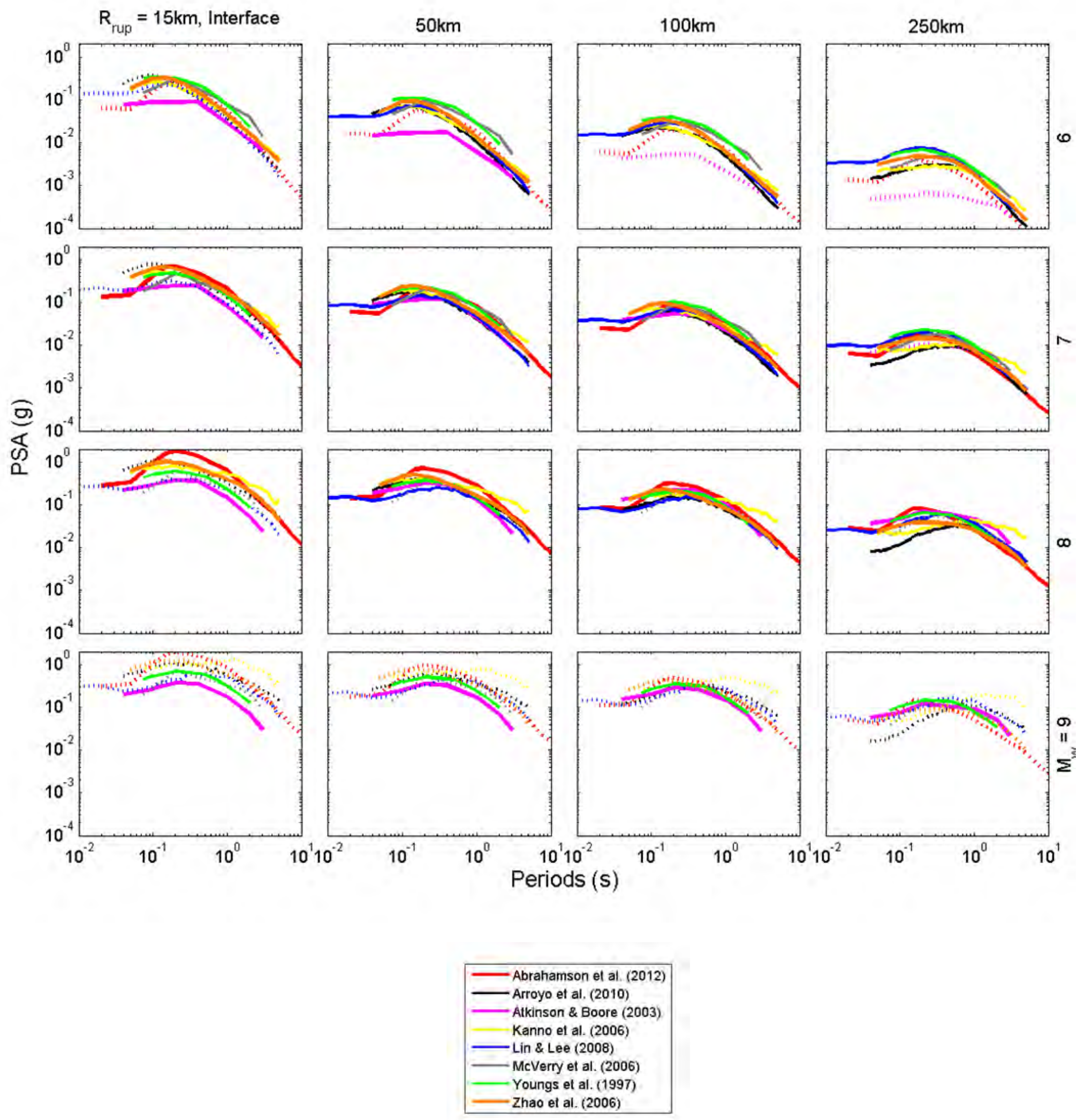

Figure 3.1 **Trellis chart showing predicted PSAs for pre-selected SZ GMPEs for various interface earthquake scenarios for rock site conditions. Dashed lines indicated where the scenario falls outside the magnitude-distance range of validity of the model.**

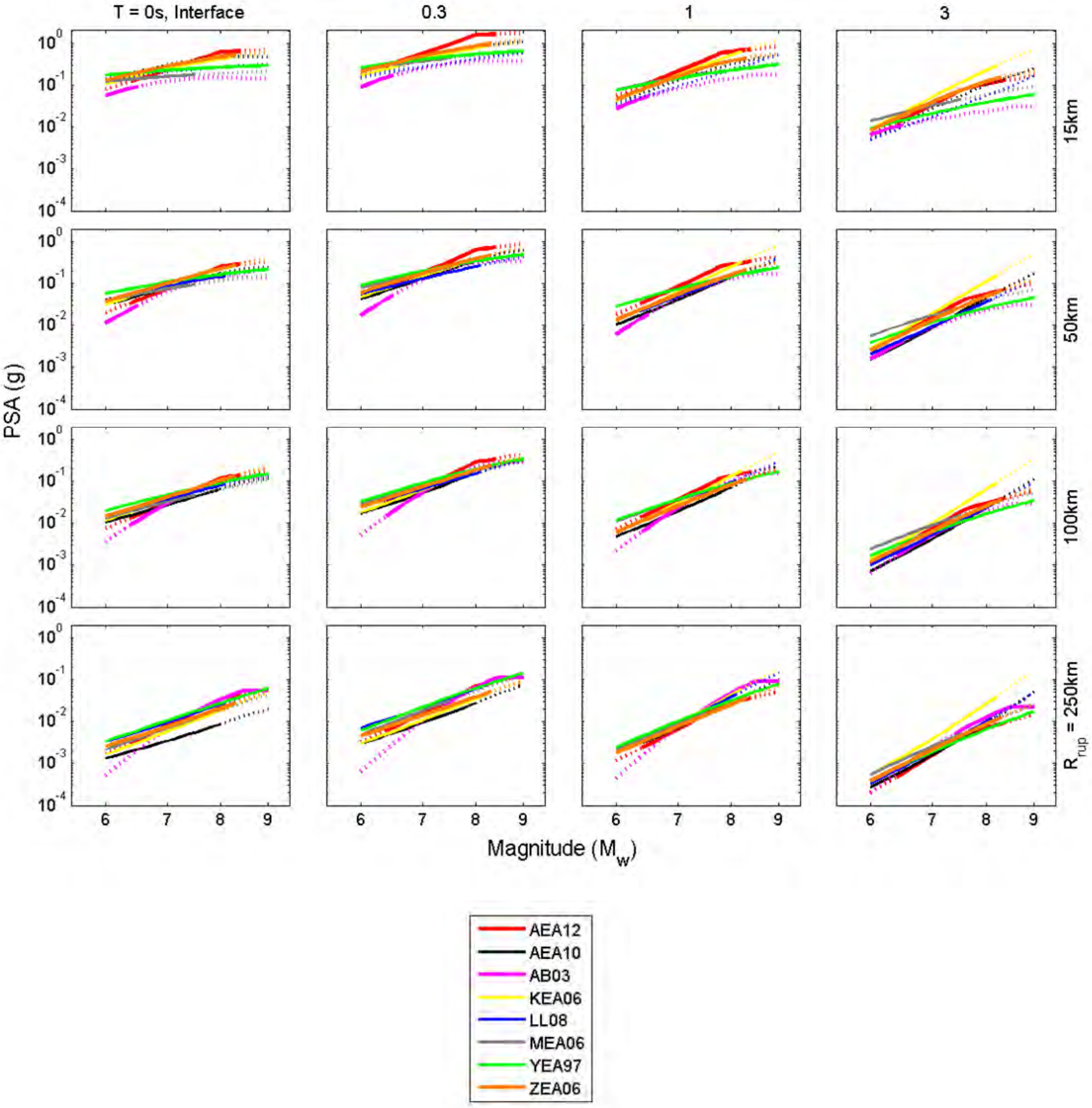

Figure 3.2 Trellis chart showing magnitude-scaling of predicted PSAs for pre-selected SZ GMPEs for various structural periods and source-to-site distances for rock site conditions. Dashed lines indicated where the scenario falls outside the magnitude-distance range of validity of the model.

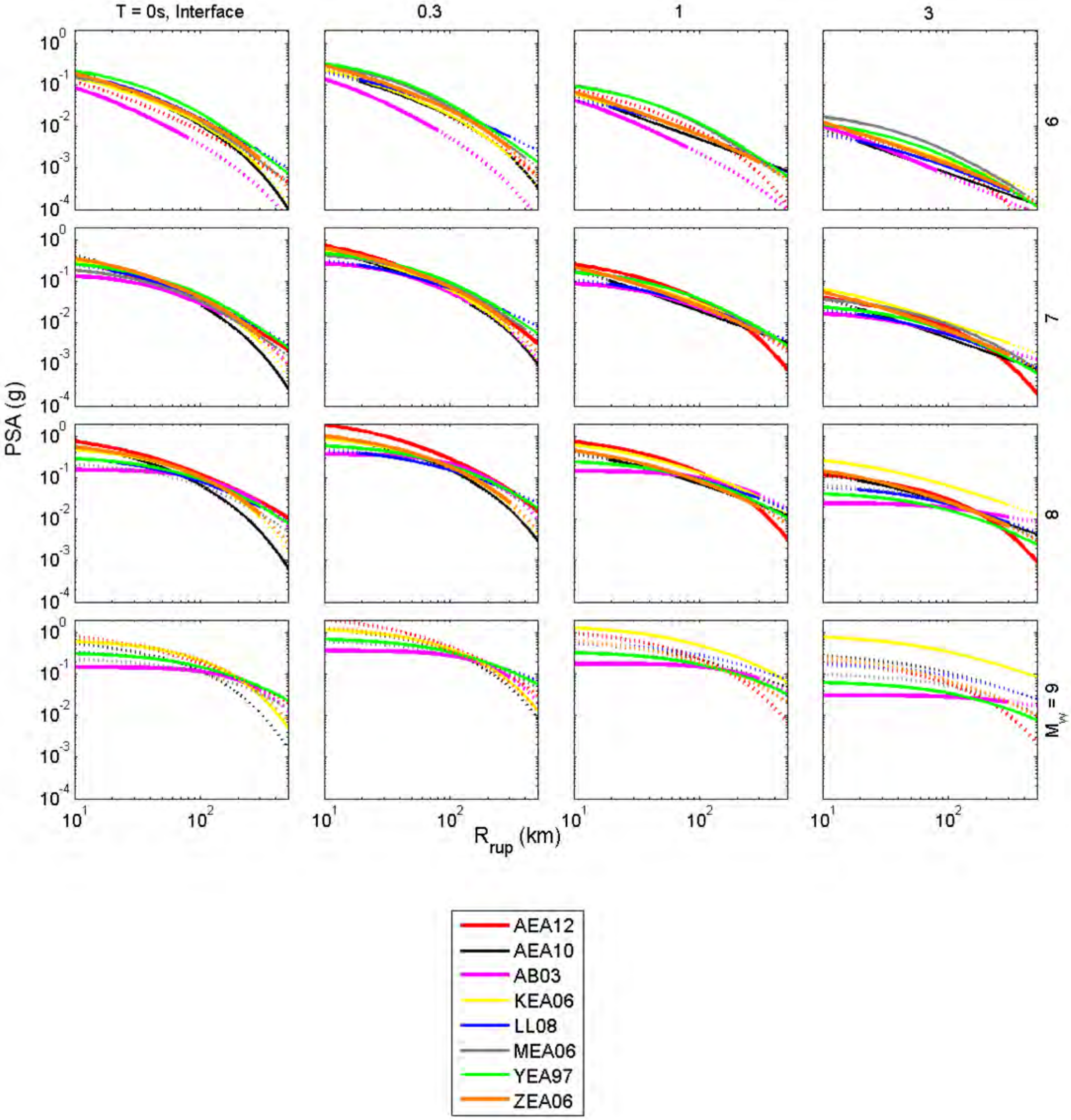

Figure 3.3 Trellis chart showing distance decay of predicted PSAs for pre-selected SZ GMPEs for various structural periods and magnitudes for rock site conditions. Dashed lines indicated where the scenario falls outside the magnitude-distance range of validity of the model.

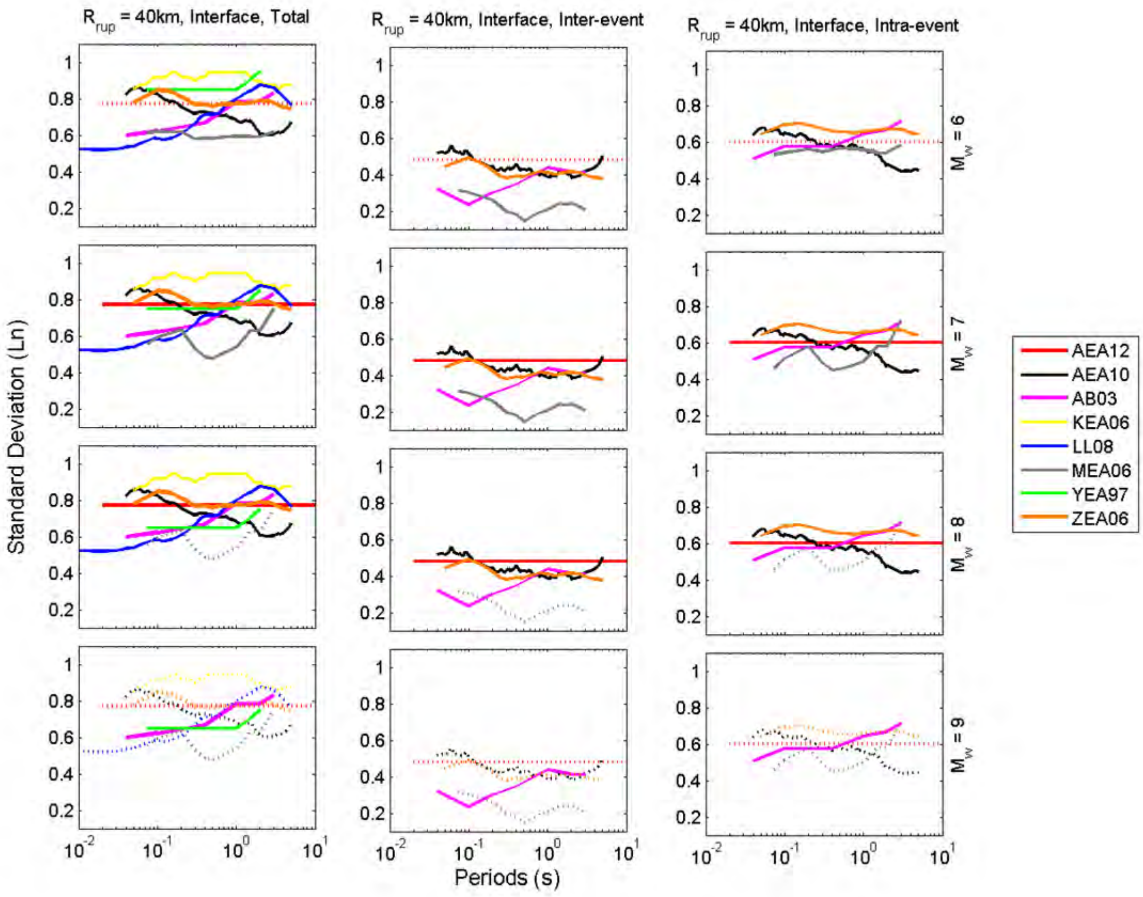

Figure 3.4 Trellis chart showing inter- (between) and intra-(within) event and total natural log standard deviations of the pre-selected GMPEs for various interface SZ earthquake scenarios.

Trellis charts were also produced to show the site amplifications predicted by the different models with respect to V_{s30} (i.e., time-averaged shear wave velocity in the upper 30 m of the site), spectral period and input ground motion amplitude on rock (important for models that account for soil nonlinearity).

3.2 MODEL EVALUATION FROM TRELLIS PLOTS INCLUDING EPISTEMIC UNCERTAINTY

This section presents the criteria used to evaluate the different GMPEs for each of the three main tectonic regimes are discussed. We do not discuss the GMPEs one-by-one but provide the overall philosophy that guided the selection process.

3.2.1 Subduction Zones

Trellis plots for SZs were presented in Section 3.1, with Figure 3.1 showing spectral shapes, Figure 3.2, showing magnitude-scaling, Figure 3.3 showing distance-scaling, and Figure 3.4 showing standard deviation terms. Examining the trellis charts for the SZ GMPEs shows that the

KEA06 model is an outlier, particularly at long periods, when evaluated for very large interface earthquakes (Figure 3.1) because linear magnitude-scaling is assumed (Figure 3.2).This suggests that this model is not a good candidate because this behavior may lead to erroneous hazard analyses for locations where very large events are possible. Linear magnitude scaling is also used by LL08, AEA10, and AB03, but these models also have a magnitude-dependent distance decay that effectively produces nonlinear magnitude-scaling, as shown in Figure 3.2.

As shown in Figure 3.3, distance attenuation rates are quite variable among the GMPEs, particularly at magnitudes of 8 and 9. At those large magnitudes, the AB03 model for interface events shows relatively flat attenuation rates, whereas AEA12, KEA06, and ZEA06 have relatively steep attenuation rates. These differences may reflect regional variations (i.e., genuine epistemic uncertainty) as the AB03 model is drawn heavily from Central and South American data; in contrast, AEA12, KEA06, and ZEA06 are based largely or entirely upon data from Japan. This issue is explored further in the model-data comparisons presented in Chapter.4. All of the considered models have magnitude-dependent distance attenuation rates.

Predictions from the AB03 model for interface events are typically a lower bound on estimates from the other considered GMPEs (Figure 3.1), except at long distances from very large earthquakes where the flat decay curve leads to high predicted PSAs (Figure 3.3). The models of AEA12 and ZEA06 often predict spectral ordinates at the upper end of the spread of the spectra. Predictions from the other GMPEs are more grouped, particularly within the rough center of the distribution of available data from SZs (Mw 6 to 7 and R from 50 to 150 km) (Figure 3.1).

Attributes of the site response functions of SZ GMPEs are shown in Figure 3.5 for V_{s30}-scaling and Figure 3.6 for nonlinearity. Note that the site response functions of the SZ GMPEs (Figure 3.5) predict similar dependency on V_{s30}, except that the KEA06 model is again an outlier, predicting higher amplification for low V_{s30} than the other GMPEs. Only three of the considered GMPEs account for nonlinear site response (AEA12, AB03 and MEA06), which leads to significant differences in predicted site amplification for large input motions (Figure 3.6). Since in GEM ground motions will need to be predicted on soil sites close to the largest subduction events, this consideration favors models that include a nonlinear site term.

The standard deviations associated with the KEA06 model are higher than other models (Figure 3.4) suggesting that the functional form is too simple to model the behavior of SZ ground motions. The MEA06 standard deviations tend to be on the low side relative to other models, which may be a peculiarity of the New Zealand motions from which it was derived. Standard deviation terms from the other models are generally relatively consistent. Five of the eight considered models (AEA12, AEA10/GEA05, AB03, MEA06, and ZEA06) split sigma into its two components (between- and within-event terms). Although standard PSHA computations of mean hazard do not require this separation, other applications require it including scenario-based risk assessments and PSHAs requiring confidence bounds. Hence, these models could be favored in that respect.

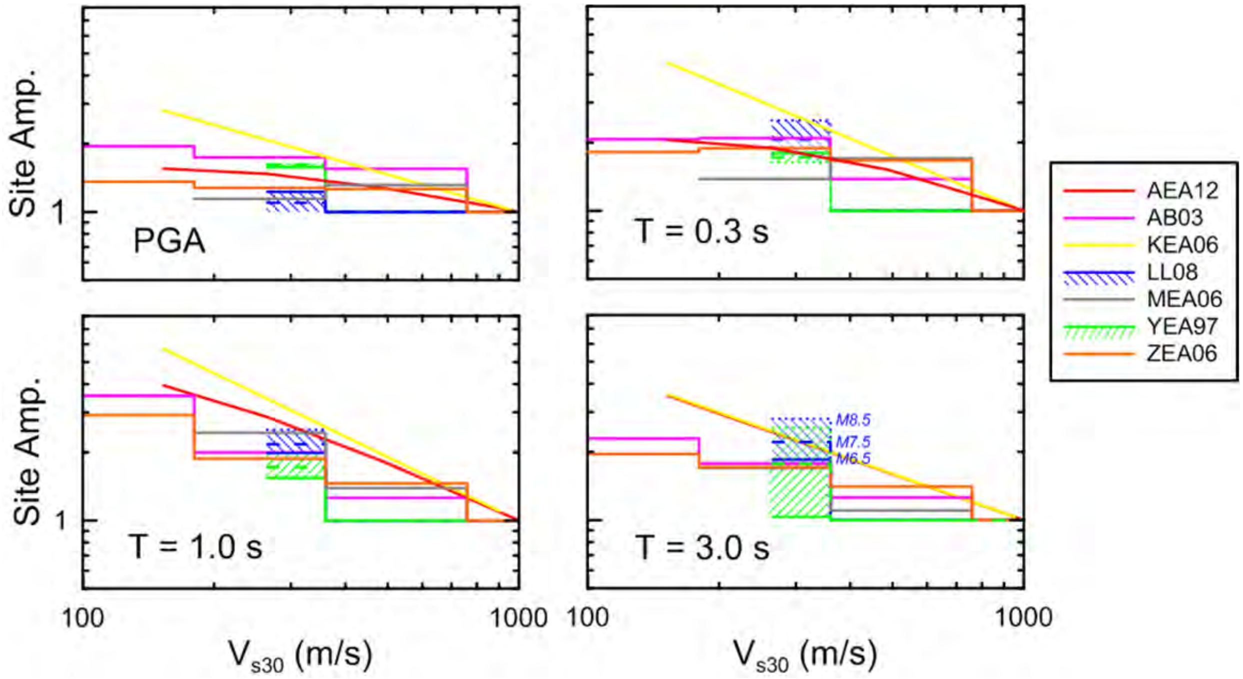

Figure 3.5 **Trellis chart showing V_{s30}-scaling of the SZ GMPEs for a reference rock peak acceleration of PGA$_r$ = 0.1*g*. Amplification has been computed relative to a consistent reference velocity of V_{ref} = 1000 m/sec, regardless of the reference condition used in the GMPE. Stepped relationships (e.g., AB03) describe site response relative to discrete categories whereas continuous relations use V_{s30} directly as the site parameter. The range shown for LL08 and YEA97 occurs because these relations do not have a formal site term but alternative GMPEs for rock and soil sites; the differences can be magnitude and distance dependent.**

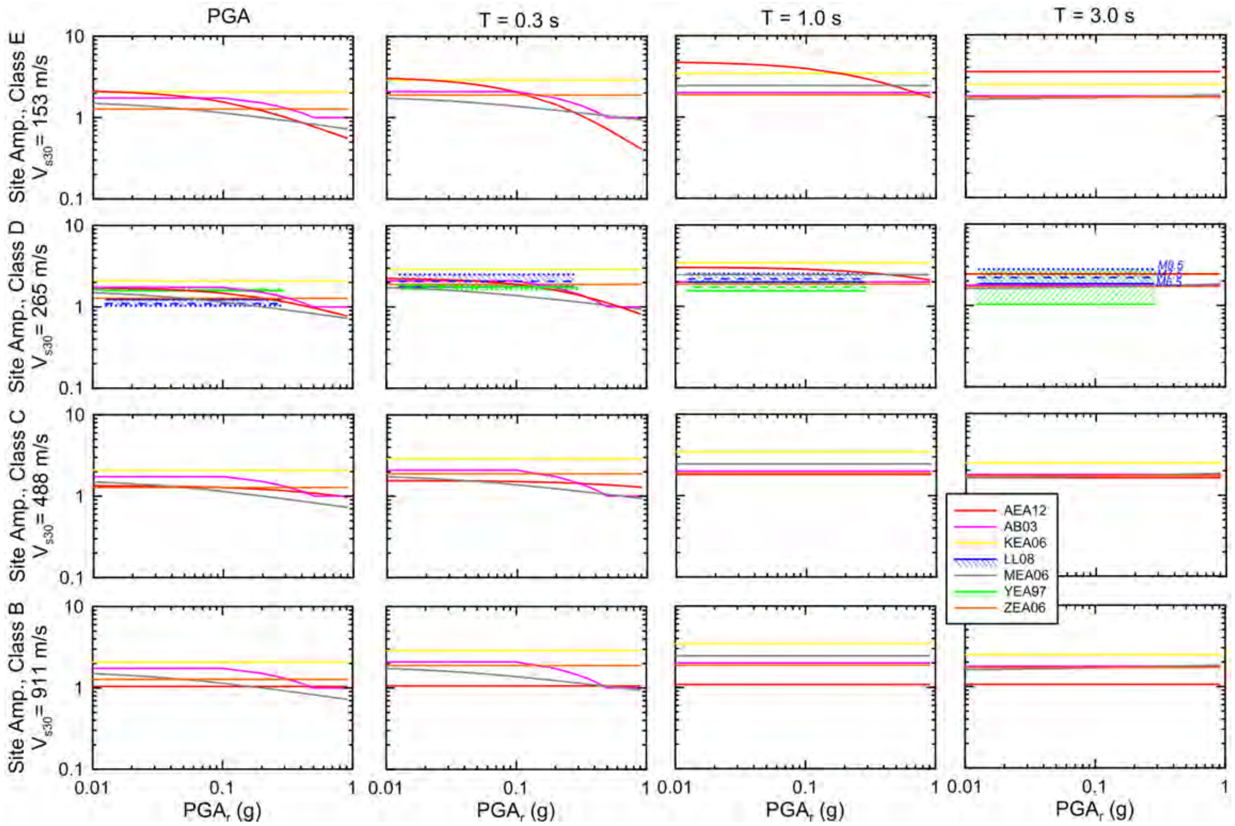

Figure 3.6 Trellis chart showing variation of site amplification with reference rock peak acceleration (for V_{ref} = 1000 m/sec) for various site classes and period. Representative velocities for each site class are based on category medians in the NGA-West2 database as described by Seyhan and Stewart [2012]. See Figure 3.5 caption for explanation of the ranges shown for LL08 and YEA97.

3.2.2 Stable Continental Regions

As will be discussed in the following chapter, published studies that compare the pre-selected GMPEs for SCRs to independent data are limited. Therefore, the trellis plots produced for SCR GMPEs were the major tool used to guide model selection.

By examining the predicted response spectra from the ten GMPEs (Figure 3.7) it can be seen that the variations among predictions is relatively large in comparison to other regimes (sometimes up to a factor of ten), particularly at higher magnitudes and closer distances. This is to be somewhat expected since there are practically no strong-motion records from earthquakes in SCRs for these magnitude-distance ranges and the manner by which the models are extrapolated will vary substantially between investigators. This comparison also shows that certain models predict greatly different PSAs than the majority of GMPEs at given distances and magnitudes. For example, DEA06 predicts much lower spectra at close distances, whereas the predicted spectra from SEA09 (Craton model) show a ‘bump’ at around 1 sec. Both of these features are the result of choices in modeling to capture local characteristics in the areas for which these GMPEs were derived. DEA06 assumed particularly deep focal depths when deriving their model (using Joyner-Boore distance as a predictor variable in the GMPEs) for southern

Norway, which leads to low near-source motions. SEA09 developed their model for the Yilgarn Craton in Western Australia, which has a specific combination of shallow earthquakes and a crustal structure that leads to large surface waves. The local peculiarities of these models mean that they may not be applicable for other SCRs that do not have these characteristics.

Figure 3.8 shows that the magnitude-scaling of the SCR GMPEs is quite variable with respect to magnitude saturation. Weak magnitude-saturation occurs in DEA06, FEA96, SEA09, and RKI07, which in some cases leads to the prediction of potentially unrealistically large PSAs from large earthquakes, particularly at long periods. Other models include stronger magnitude-saturation terms, which may be preferable for GEM application.

Figure 3.9 shows the predicted distance attenuation of the ten models, which again are quite variable. Developed for central and eastern North America, many of these models reflect a change towards flatter attenuation associated with Moho bounce effects between approximately 70 and 140 km (AB06, C03, FEA96, and PEA11). Other models for this same region (SEA02 and TEA97) do not model such effects. To account for epistemic uncertainty in the modeling of the effect of crustal structure and the requirement of global applicability of the selected GMPEs, it was thought desirable to select models that fall in both these categories. Another observation that can be made from Figure 3.9 is that for very large earthquakes, AB06 is often a lower bound on the predictions and SEA09 is generally the upper bound.

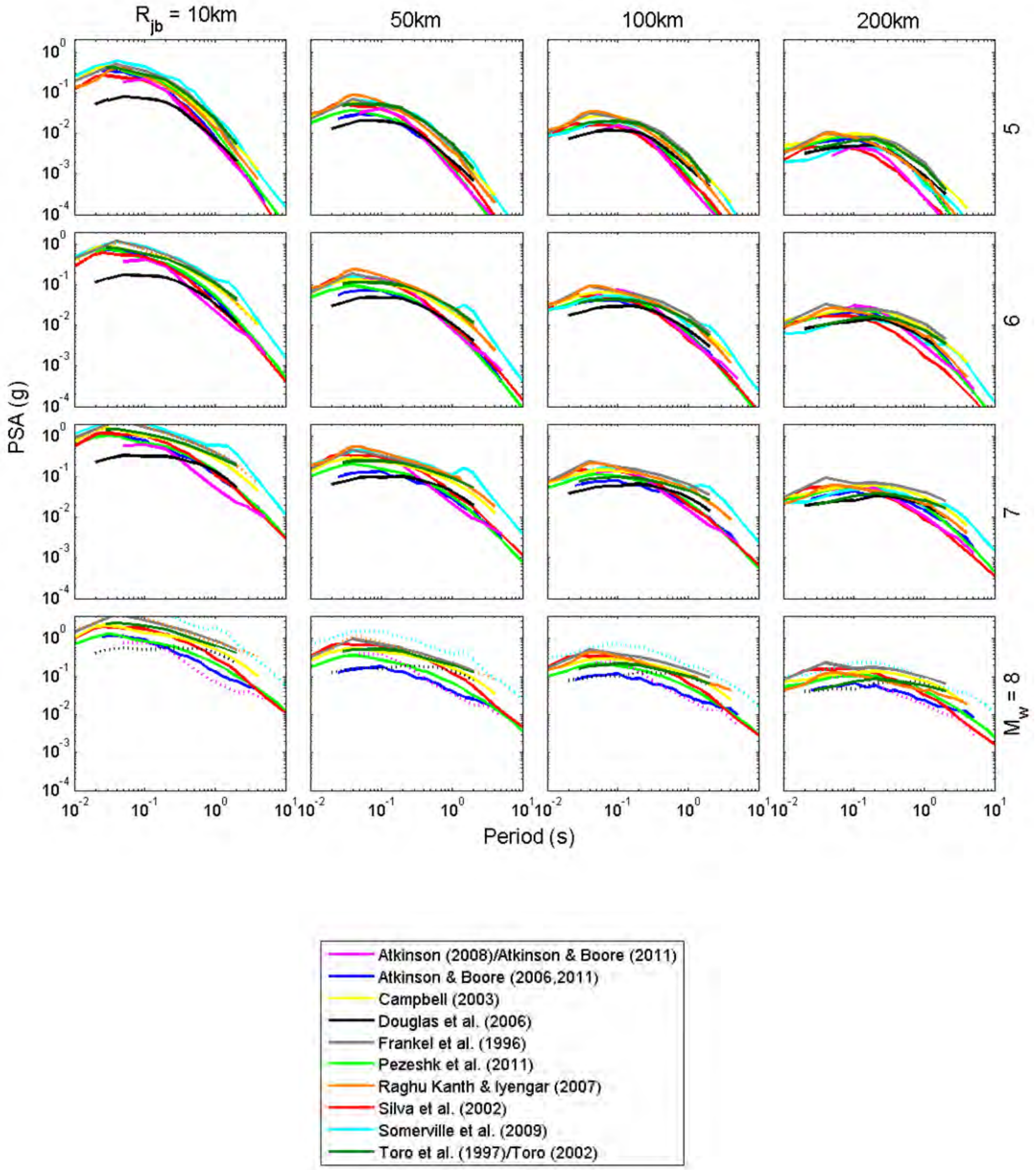

Figure 3.7 **Trellis chart showing predicted PSAs for pre-selected SCR GMPEs for various earthquake scenarios for rock site conditions. Dashed lines indicated where the scenario falls outside the magnitude-distance range of validity of the model.**

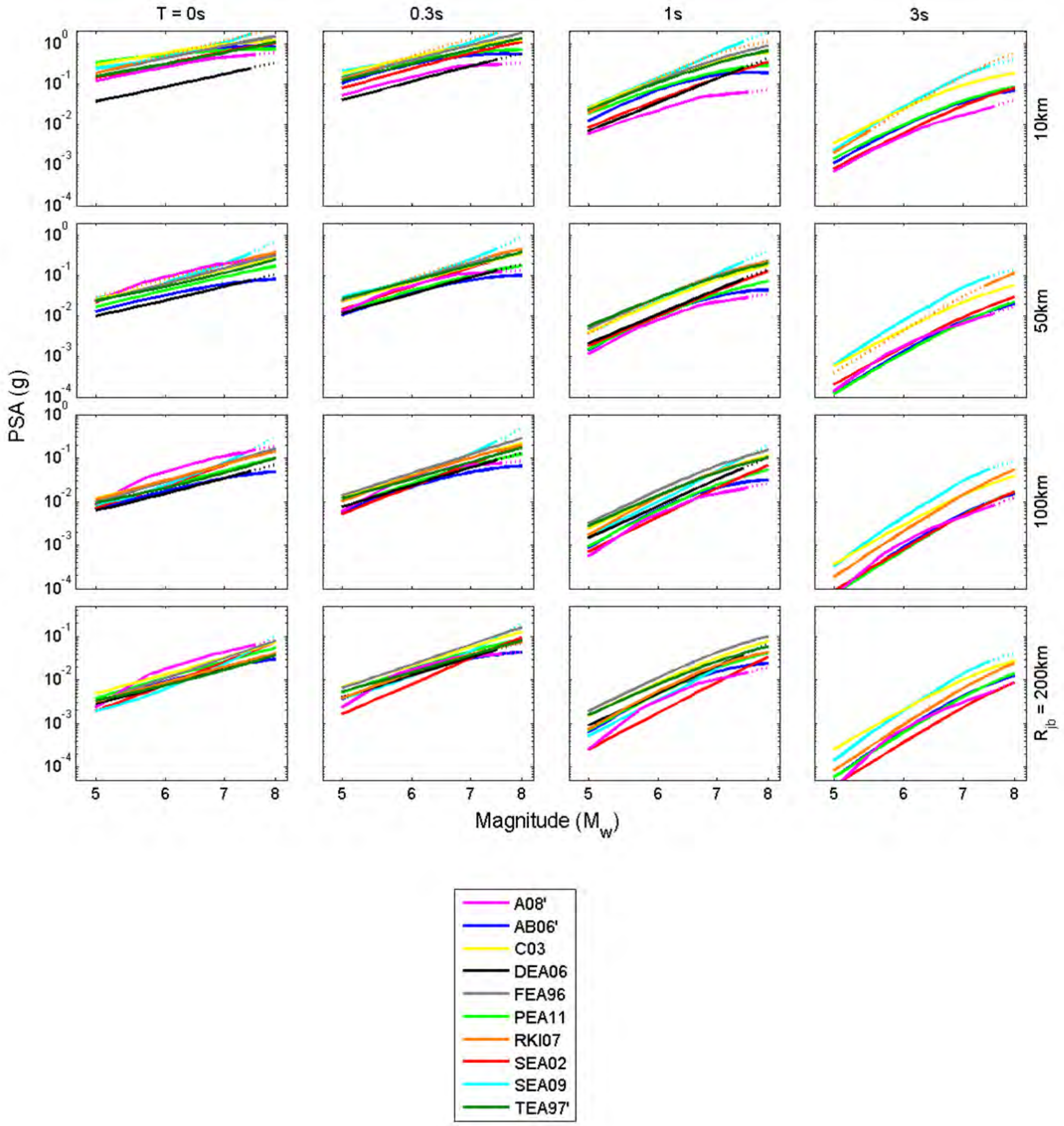

Figure 3.8 Trellis chart showing magnitude-scaling of predicted PSAs for pre-selected SCR GMPEs for various structural periods and source-to-site distances for rock site conditions. Dashed lines indicated where the scenario falls outside the magnitude-distance range of validity of the model.

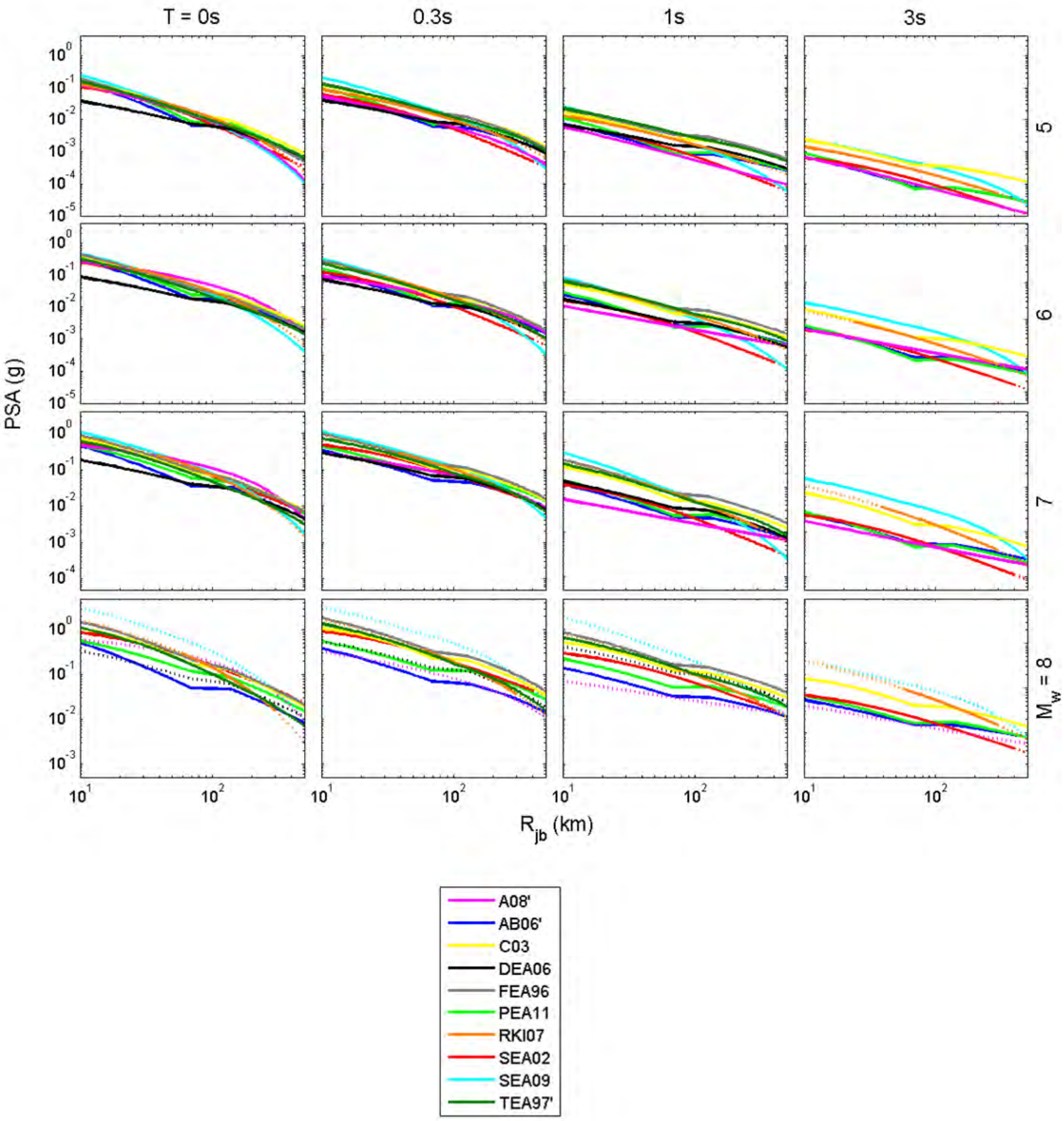

Figure 3.9 **Trellis chart showing distance decay of predicted PSAs for pre-selected SCR GMPEs for various structural periods and magnitudes for rock site conditions. Dashed lines indicated where the scenario falls outside the magnitude-distance range of validity of the model.**

Almost all of the SCR GMPEs do not include site terms allowing the ground motions on non-rock sites to be predicted. Only A08′, AB06, and RKI07 include such terms, which are shown for NEHRP classes B-E in Figure 3.10 for the conditions listed in the caption. In the case of A08′ and AB06 these were adopted from results for ACRs. In the case of RKI07, the predicted nonlinear effects are very strong, and the amplifications are not smooth but show large period-to-period variations. Most of the SCR GMPEs apply for hard rock site conditions with reference velocities much faster than those used as the reference in empirical site factors (e.g., 760 or around 1000 m/sec). Accordingly, before site factors of the type shown in Figure 3.10 can be applied for those models, an additional correction to adjust from hard rock to around 1000 m/sec must be made. This correction is generally not provided in the SCR GMPE documentation, nor is it well defined elsewhere in the literature. The aforementioned weaknesses with the SCR GMPE site terms are discussed further in Chapter 5 when making our final recommendations.

The standard deviation terms associated with the SCR GMPEs (Figure 3.11) show great model-to-model variability. These standard deviation models are generally a direct consequence of the simulation method used and the variability in the input parameters, rather than the result of statistical comparisons between data and prediction. The standard deviations associated with RKI07 are much lower than those from the other models because only the parametric component of the variability was included rather than also including the modeling component. This is an argument against its selection. The standard deviation models of DEA06, SEA02, and SEA09 show strong period dependencies, which is not observed in the standard deviations of SZ or ACR GMPEs; this behavior was again noted by the core group as an argument against selecting these models. Only three of the ten GMPEs separate standard deviations into between- and within-event components, which as discussed above could be valuable for some analyses. E06 [EPRI 2006] proposed generic standard deviation models for SCR GMPEs, which was considered by the core group of experts as a possible replacement for those standard deviations that were not thought to be physically realistic or are not spilt into the two components.

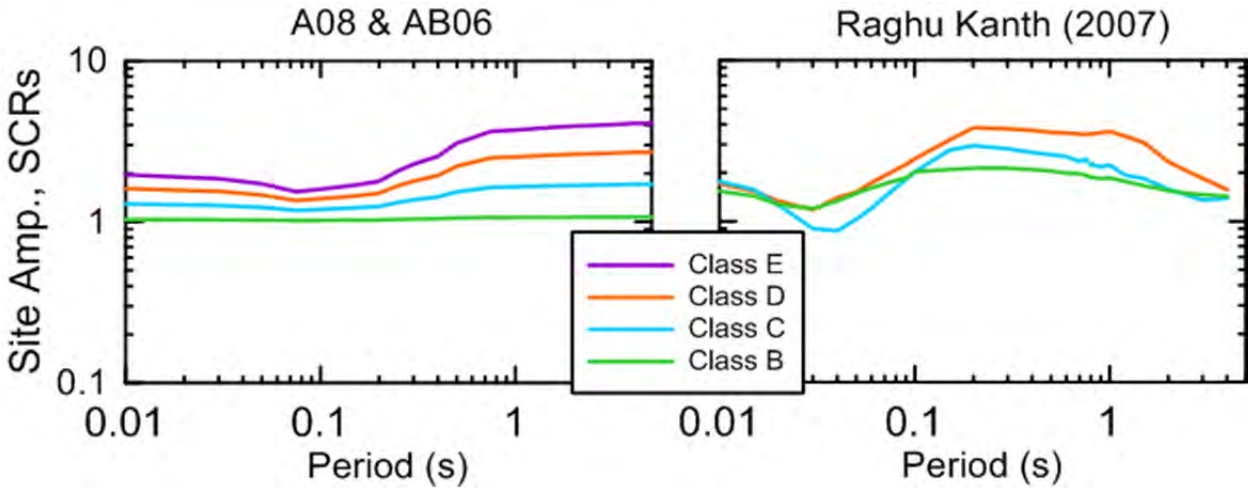

Figure 3.10 Period-dependent site terms in the SCR GMPEs for a reference rock peak acceleration of $PGA_r = 0.1g$. Amplification has been computed relative to a consistent reference velocity of $V_{ref} = 1000$ m/sec.

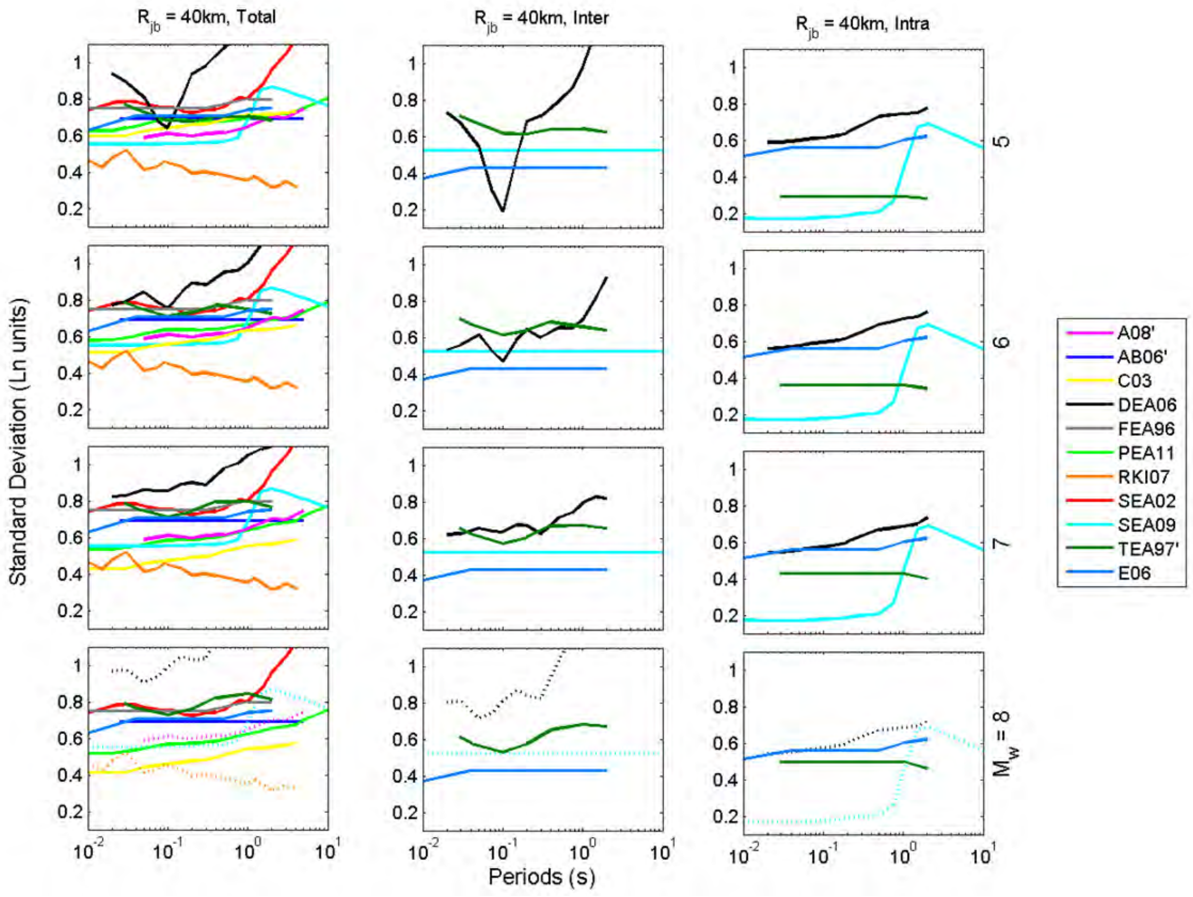

Figure 3.11 **Trellis chart showing inter- (between) and intra-(within) event and total natural log-standard deviations of the pre-selected SCR GMPEs.**

3.2.3 Active Crustal Regions

The predicted spectra of the nine ACR GMPEs show much less model-to-model variability than those from the other two tectonic regimes (Figure 3.12). The predicted spectra from MEA06 for **M**5 earthquakes are considerably higher than the others, perhaps because this magnitude is below the minimum considered magnitude. This characteristic makes this GMPE less appealing since possible over-prediction of ground motions from moderate earthquakes could have a large impact on hazard results for regions with relatively low rates of seismicity (but still qualifying as active), where such events are particularly important. Predictions from the FEA10 model often fall below the majority of models and display a different spectral shape (with two shallow peaks at longer source-to-site distances). This could be due to it being based on a limited number of records having rock-like V_{s30} values.

Figure 3.13 shows magnitude-scaling of the ACR GMPEs. The models of KEA06, MEA06, and FEA10 lack magnitude saturation, which argues against their selection since they can lead to the prediction of unphysically large or small ground motions at the edges of the magnitude-distance range of interest. Figure 3.14 shows the distance attenuation of the ACR GMPEs. All of the models have magnitude-dependent attenuation terms, but a point of differentiation is that some include anelastic attenuation that leads to steeper attenuation for distances beyond approximately 70–100 km (BA08, CY08, MEA06, and ZEA06) and some do not (AS08, AB10, CB08, FEA10, and KEA06).

The site response functions in the ACR GMPEs are shown in Figure 3.15 (V_{s30}-scaling), Figure 3.16 (soil nonlinearity), and Figure 3.17 (spectral amplification). Starting with $\mathrm{V_{s30}}$-scaling, three of the models (FEA10, KEA06, and ZEA06) are predominantly derived from Japanese data, yet have significantly different scaling at mid-to-short periods, with FEA10 and KEA06 being very strong relative to worldwide models and ZEA06 being somewhat weaker. Based on other on-going research in the NGA-West2 project, the ZEA06 trend is considered more representative for Japan. The V_{s30}-scaling from international models (e.g., AS08, BA08, CB08, and CY08) at short periods is stronger, indicating a potential regional dependency in site amplification, which should be considered in selecting GMPEs for ACRs. Turning next to nonlinearity (Figure 3.16), the models of AB10, FEA10, KEA06, MEA06, and ZEA06 are linear whereas the others are nonlinear at short periods. The lack of nonlinearity leads to significant overestimation of ground motions for strong levels of input motions for soil site conditions and mid-to-short-periods, which argues against the selection of these models. The spectral amplification plot (Figure 3.17) shows that the high amplifications predicted by some of the selected models for soft soil sites coupled with a lack of nonlinearity leads to very large differences (up to a factor of 10) in the predicted amplifications for high shaking levels–the large amplifications were not considered realistic.

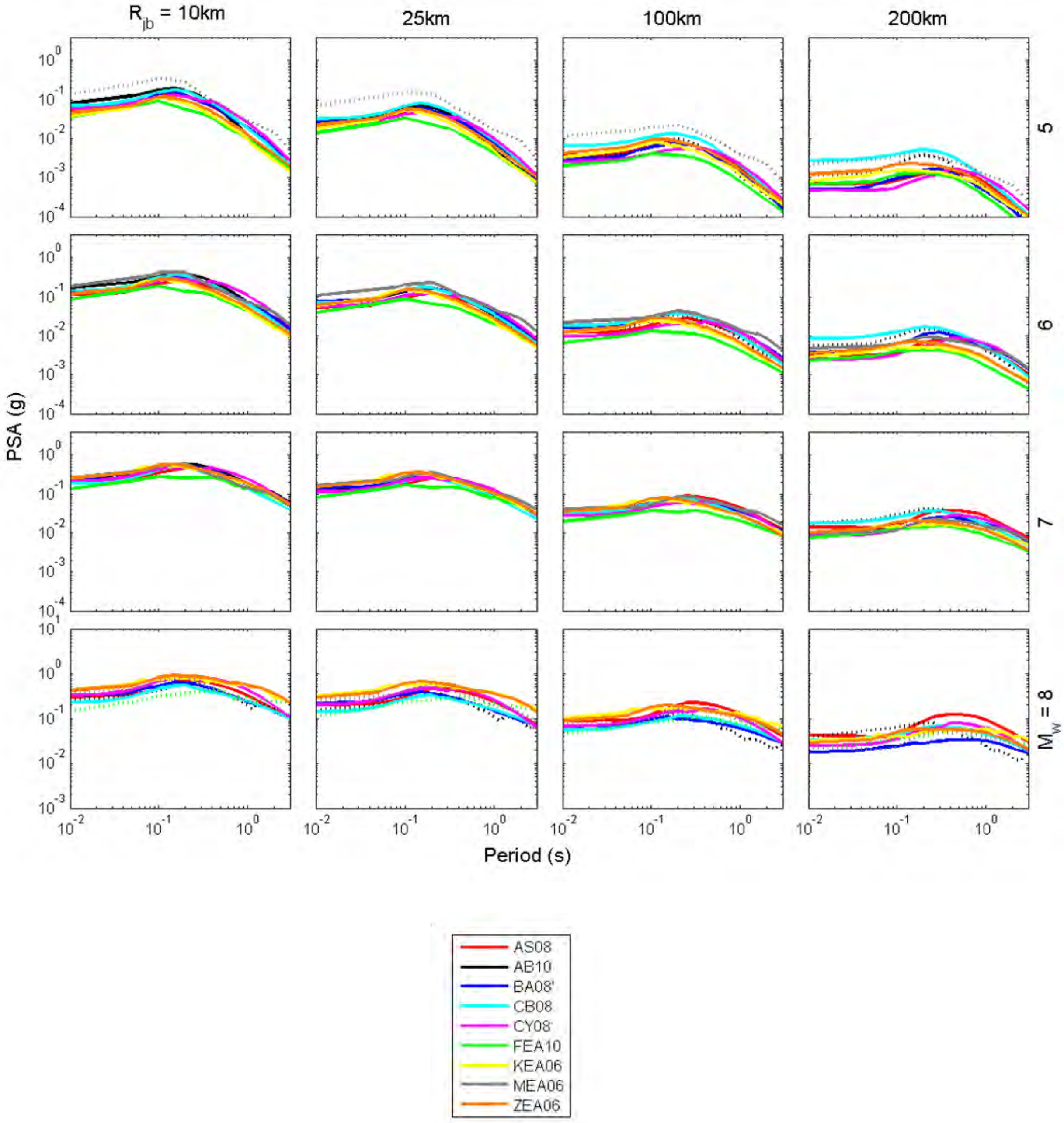

Figure 3.12 **Trellis chart showing predicted PSAs for pre-selected ACR GMPEs for various earthquake scenarios for rock site conditions. Dashed lines indicated where the scenario falls outside the magnitude-distance range of validity of the model.**

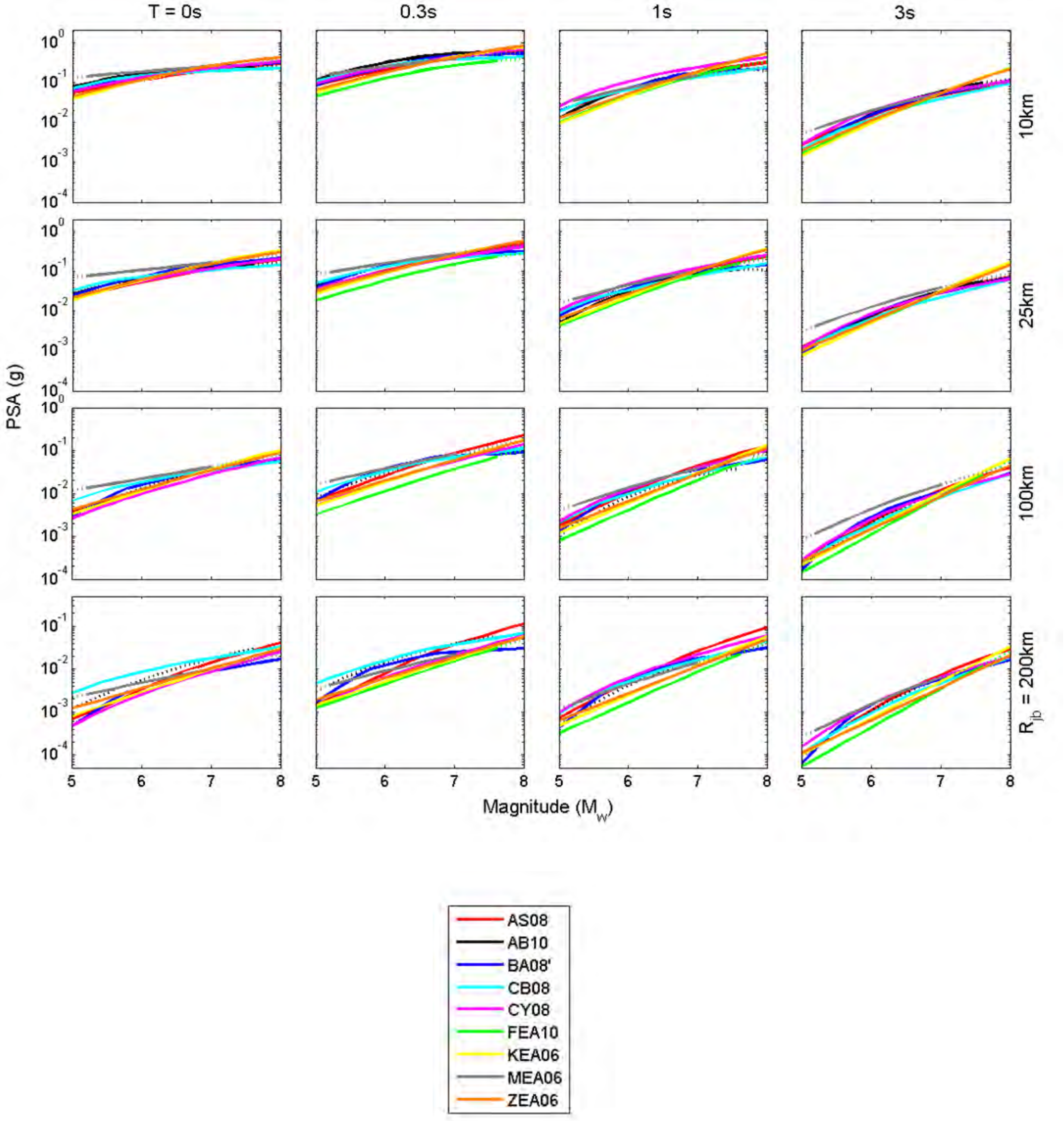

Figure 3.13 Trellis chart showing magnitude-scaling of predicted PSAs for pre-selected ACR GMPEs for various structural periods and source-to-site distances for rock site conditions. Dashed lines indicated where the scenario falls outside the magnitude-distance range of validity of the model.

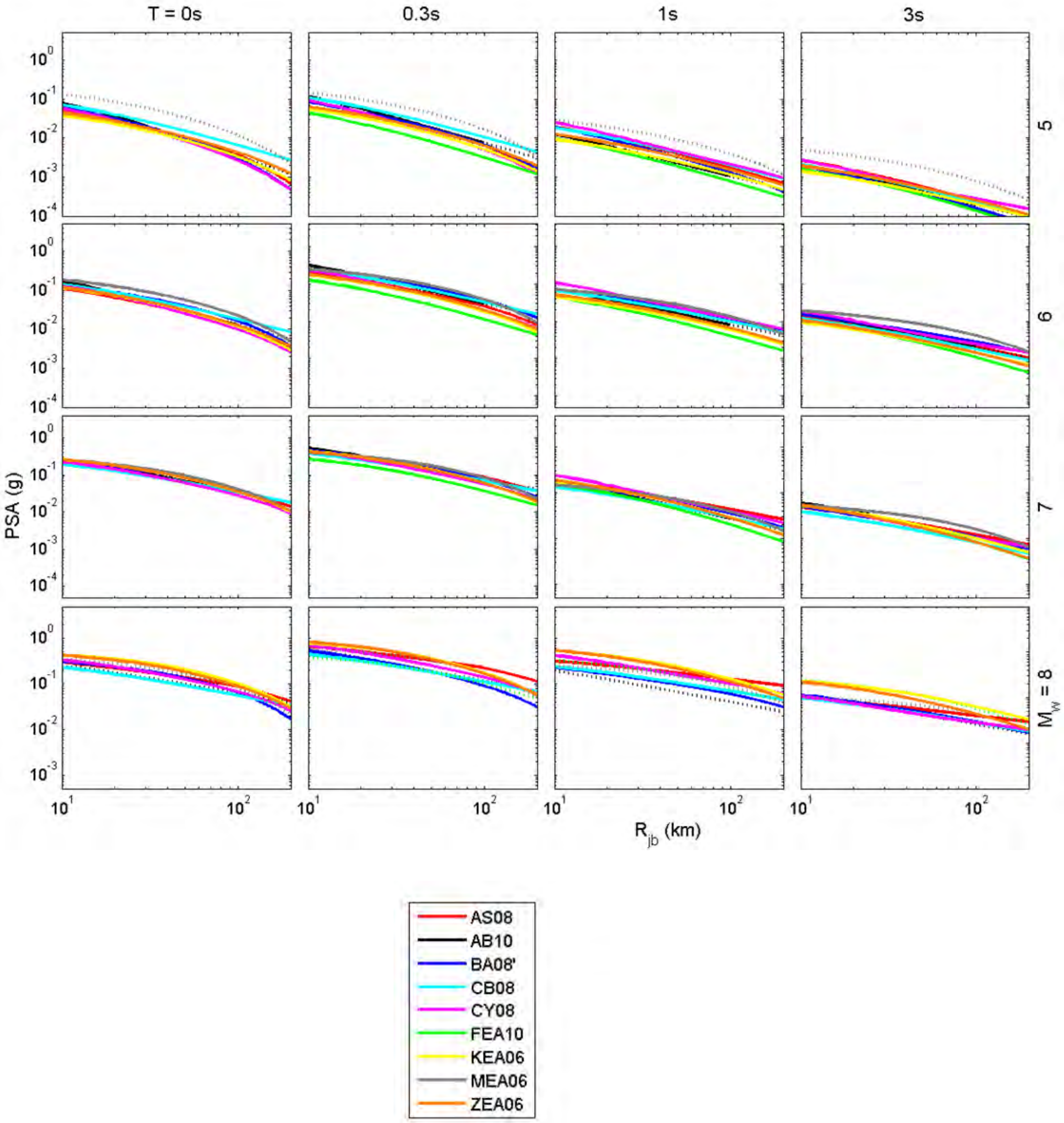

Figure 3.14 Trellis chart showing distance decay of predicted PSAs for pre-selected ACR GMPEs for various structural periods and magnitudes for rock site conditions. Dashed lines indicated where the scenario falls outside the magnitude-distance range of validity of the model.

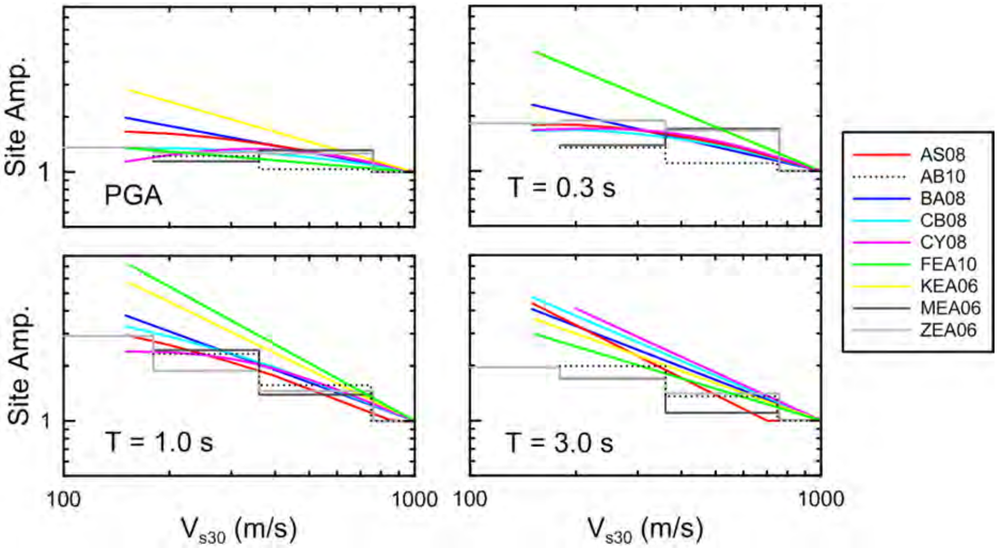

Figure 3.15 **Trellis chart showing V_{s30}-scaling of the ACR GMPEs for a reference rock peak acceleration of $PGA_r = 0.1g$. Amplification has been computed relative to a consistent reference velocity of V_{ref} = 1000 m/sec, regardless of the reference condition used in the GMPE. Stepped relationships (e.g., AB10) describe site response relative to discrete categories whereas continuous relations use V_{s30} directly as the site parameter.**

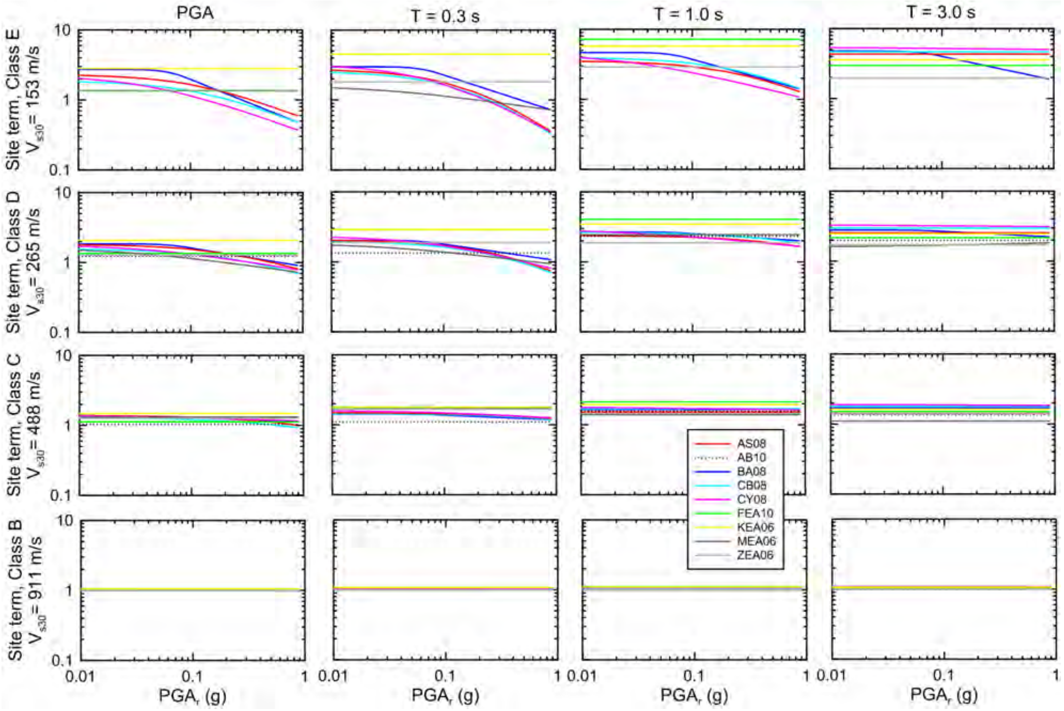

Figure 3.16 **Trellis chart showing variation of site amplification with reference rock peak acceleration (for V_{ref} = 1000 m/sec) for various site classes and period. Representative velocities for each site class are based on category medians in the NGA-West2 database as described by Seyhan and Stewart [2012].**

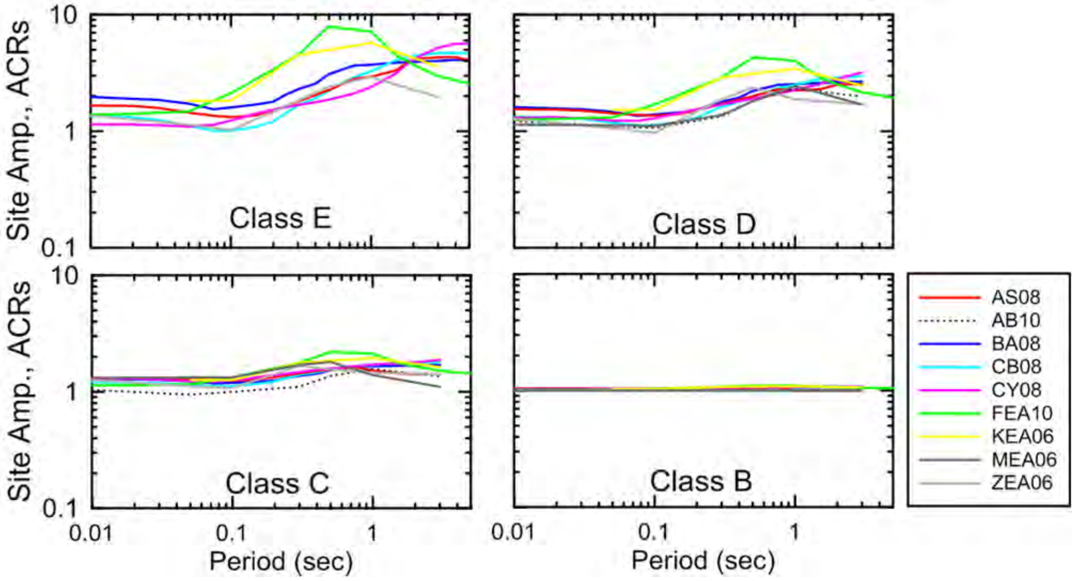

Figure 3.17 **Trellis chart showing variation of site amplification with period (for V_{ref} = 1000 m/sec and PGA$_r$ = 0.1g) for various site classes.**

Figure 3.16 shows trellis plots for aleatory variability (standard deviation terms). The results segregate into three sets of GMPEs: (1) KEA06 and FEA10 with relatively high total standard deviations (and no separation into between- and within-event components); (2) ZEA06 and AB10 with slightly lower standard deviations; and (3) the other five GMPEs with still lower standard deviations. Groups (2) and (3) provide estimates of the two components of standard deviation. Within the expert group, it was felt that the standard deviations presented by KEA06 and FEA10 were an indication of functional forms that are too simple. On the other hand, difference between the standard deviations of ZEA06 (principally Japanese data) and AB10 (European and Middle Eastern data) and the other (principally California and Taiwanese models) could be attributable to several possible sources including regional differences of within-event variability, the magnitude range of the data considered in model development, and the quality of metadata.

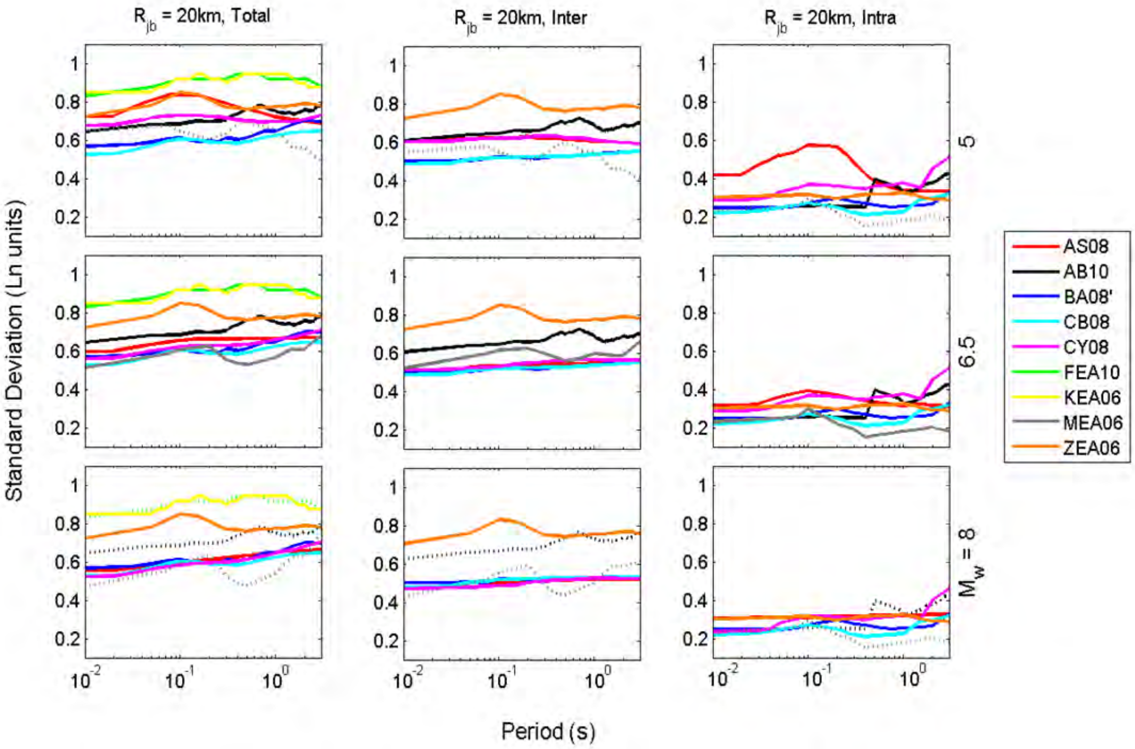

Figure 3.18 **Trellis chart showing inter- (between) and intra-(within) event and total natural log standard deviations of the pre-selected ACR GMPEs.**

4 GMPE Data Comparisons

This chapter discusses the other major tool used by the experts to select the GMPEs: quantitative comparisons between model predictions and observations.

4.1 REQUIREMENTS FOR CONSIDERATION OF A STUDY

Because the GMPEs for SZs and ACRs are invariably developed from the regression of strong-motion data, model-data comparisons are integral to the process by which they are prepared. Nonetheless, GMPE-data comparisons were considered a critical component of the selection process. GMPEs derived for SCRs are generally based on ground-motion simulations and, therefore, model-data comparisons are even more important for these equations. The value of these comparisons is often derived from the comparison dataset being beyond the parameter space considered for the original GMPE. For example, the data may be derived from a different region from that used in the original model development, which can be useful for studies of model applicability to the data region and regional variations of ground motions generally. Another significant example specific to SZs is the recent availability of datasets from large-magnitude earthquakes (Mw 8.8 Maule, Chile, and Mw 9.0 Tohoku, Japan) beyond the upper-bound magnitudes available during GMPE development.

Most GMPE-data comparisons in the literature consist of plots of ground-motion intensity measures versus distance along with GMPE median trend curves. Plots of this type have limited applicability for formal analysis of GMPE performance because it can be difficult to judge trends when the data span a very wide range on the *y*-axis and because event-specific bias (event terms) are seldom taken into account. Accordingly, we restricted our literature compilation for SZs and ACRs to studies that include a formal analysis of residuals into the GMPE-data comparisons. This still led to a considerable number of studies (8 for SZs and 13 for ACRs). For SCRs, however, restricting our compilation to only this type of analysis would lead to considering only one or two studies. Hence, it was decided for SCRs to also compile those studies only showing plots of predicted against observed ground motions. Even with this relaxation of the criterion, only a few studies were identified.

The three general methods of relatively rigorous model-data comparisons present in the collected literature are: (1) the maximum-likelihood approach of Scherbaum et al. [2004] and its extension to normalized within- and between-event residuals distributions by Stafford et al. [2008], which is intended to judge the overall fit of model to data; (2) the information theoretic approach of Scherbaum et al. [2009] for model-data comparisons, which also produces various overall goodness-of-fit metrics; and (3) analysis of within- and between-event residuals specifically targeted to investigations of GMPE scaling with respect to magnitude, distance, and site parameters (e.g., Scasserra et al. [2009]).

4.2 APPLICATION FOR GMPE SELECTION IN THIS STUDY

Tables 4.1 and 4.2 summarize the model-data comparisons considered in this study for ACRs and SZs, respectively. More information on each considered study and its individual findings are given in a consistent format within the Appendix A. The columns in Tables 4.1 and 4.2 indicate the GMPEs that were tested, whereas the rows correspond to the model-data comparison studies.

For ACRs, the most often tested models are the NGA models of AS08, BA08 (which is the single most-tested model), CB08, and CY08. Many of the studies seek to evaluate the applicability of the global NGA models to specific regions, including Europe, Japan, Iran, and New Zealand. The overall goodness-of-fit approaches find varying levels of fit for these and other models. Sometimes when poor fits are encountered, relatively local GMPEs that fit the data better are recommended by their developers, but which are likely to not extrapolate well to larger magnitude events. None of the NGA models or other pre-selected models stands out as clearly superior from these studies. Somewhat more useful are the second type of model-data comparisons in which specific GMPE attributes are tested. These studies find some instances of misfits in distance attenuation trends. In some cases when the data driving the misfit are from small magnitude events outside the range of applicability of the original models, a model by Chiou et al. [2010] performs well, although this was not a GEM pre-selected model from Task 2 because it only provides coefficients for a few structural periods.

For SZs, the most often tested models are AB03 and ZEA06, which reflect data globally and from Japan, respectively. The studies point rather clearly towards regional variations in subduction ground motions. Overall, goodness-of-fit approaches find Japan-based models such as ZEA06 performing better than other models for Japanese data. Those studies also find that the AB03 model performs relatively poorly against Japanese and Greek data (e.g., Beauval et al. [2011]; Delavaud et al. [2012]) and relatively well against central and south American data [Arango et al. 2012]. The AEA12 model, while tested relatively sparsely, has generally performed well in the tests. As with ACRs, somewhat more useful were the model-data comparisons in which specific GMPE attributes were tested. Applications of this approach to the Maule (Chile) and Tohoku (Japan) data [Boroschek et al. 2012; Stewart et al. 2012] identified different distance attenuation trends from these large events. In the case of the Maule earthquake, the relatively slow distance attenuation of the Atkinson and Boore [2003] model provided a good fit to the data; whereas the Tohoku data attenuated relatively fast with distance and was better matched by the model of Zhao et al. [2006].

Table 4.3 presents the model-data comparisons considered in this study for SCRs. Most of the studies show plots of recorded data against median fit lines, and between-event variability is not considered in the analysis or interpretation. Very few quantitative comparisons of the type undertaken for SZs and ACRs have been performed, and these have not provided conclusive results. We note that the AB06′ model has been the most well-tested model for SCRs.

Table 4.1 **Summary of studies in literature with quantitative model-data comparisons for ACRs. Rows with light gray shading are for studies using an overall goodness-of-fit approach, rows with dark gray shading are for studies that test specific GMPE attributes through residuals analysis.**

	AS 2008	AB 2010	BA 2008	CB 2008	FEA10	CY 2008	KEA 2006	MEA 2006	ZEA 2006
A (Euro-Med)		X	X						
B (Iran)			X	X		X			
C (Worldwide)	X	X	X	X	X (CF08)	X	X		X
D (CA)	X		X	X		X			
E (Japan)	X		X	X		X			
F (Portugal)		X	X			X			
G (Japan)	X	X	X		X (CF08)	X	X		X
H (Italy)	X	x (07)	X	X		X			
I (Greece)			X						
J (Iran)			X	X		X			
K (Japan)	X		X	X		X	X		
L (New Zealand)			X			X		X	X
M (CA)	X		X	X		X			

A = Stafford et al. [2008]; B = Ghasemi et al. [2008, 2009]; C = Delavaud et al. [2012]; D = Kaklamarios and Baise [2011]; E = Nishimura [2010]; F = Vilanova et al. [2012]; G = Beauval et al. [2012, in press]; H = Scasserra et al. [2009]; I = Margaris et al. [2010]; J = Shoja-Taheri et al. [2010]; K = Uchiyama and Midorikawa [2011]; L = Bradley [2012, in press]; M = Liao and Meneses [2012].

Table 4.2 Summary of studies in literature with quantitative model-data comparisons for SZs. Rows with light gray shading are for studies using an overall goodness-of-fit approach, rows with dark gray shading are for studies that test specific GMPE attributes through residuals analysis.

	AEA 2012	ARR2010	AB 2003	GAR 2005	KEA 2006	LL 2008	MEA 2006	YEA 1997	ZEA 2006
A (S. America)	X	X	X	X			X	X	X
B (L. Antilles)			X	X	X	X	X	X	X
C (India-Burma)			X						
D (Greece)			X		X	X	X	X	X
E (Worldwide)	X	X	X		X	X	X	X	X
F (New Zealand)			X				X		X
G (Chile)			X						X
H (Japan)			X						X

A = Arango et al. [2012]; B = Douglas and Mohais [2009]; C = Gupta [2010]; D = Delavaud et al. [2012]; E = Beauval et al. [2011]; F = Bradley [2010]; G = Boroschek et al. [2012]; H = Stewart et al. [2012, in press].

Table 4.3 Summary of studies in literature with model-data comparisons for SCRs.

	A 2008	AB 2006	C 2003	DEA 2006	FEA 1996	RKI 2007	SEA 2002	SEA 2009	PEA 2011	TEA 1997'
A (Global)		X	X							X
B (Portugal)	X	X	X							
C (Virginia)		X	X				X			X
D (Virginia)	X	X								
E (Thailand)										X

A = Allen and Wald [2009]; B = Vilanova et al. [2012]; C = Cramer et al. [2011]; D = Atkinson [2011]; E = Chintanapakdee et al. [2008].

5 Recommended GMPEs

The Task 3 core working group (the authors of this report) developed consensus (or near-consensus) selections based on the criteria and information presented previously for the three main tectonic regimes (shallow crustal seismicity in active regions, stable continental regions, and subduction zones). Our reasons for proposing each GMPE—and why others were not selected—were detailed in written documents and presentations, along with the material that led to our decisions. At the Global GMPEs plenary meeting in Istanbul, Turkey, on May 17 and 18, 2012, to which all experts of the project were invited, the arguments for each choice were carefully presented and the experts' feedback sought during the second day of the meeting, which focused on this key step of the project. As mentioned in Chapter 2, the wider Task 3 group consists of roughly 30 experts from dozens of countries with worldwide expertise in ground-motion modeling (Table 2.1). Based on the feedback from these experts, final sets of GMPEs for the different regimes were defined. This chapter presents our recommendations for GMPEs to be used by GEM for hazard calculations and is divided into four sections: the first three discuss our recommendations for the three principal tectonic regimes, and the last section discusses the three special regimes.

5.1 SUBDUCTION ZONES

We have selected the recent global model of AEA12 (Abrahamson et al. [2012]; also known as the 'BC Hydro' model), the global model of AB03 [Atkinson and Boore 2003] and the Japanese model of ZEA06 [Zhao et al. 2006]. These models were preferred based on the following criteria: (1) they have large datasets; (2) they have desirable attributes in terms of their magnitude and distance scaling functions; (3) they have been checked against data from well-recorded earthquakes (including the 2010 Maule, Chile, and 2011 Tohoku, Japan, event): and (4) they produce different distance attenuation trends that have been shown to match data trends from different global regions (thus bringing into the selection a degree of epistemic uncertainty).

There was some debate over inclusion of the AB03 model since the predicted decay rate from large (M_w>8) interface earthquakes is slow, meaning that the ground motions at great distances (>100 km) are not substantially reduced from those closer to the source. This behavior was considered physically unlikely by some members of the Task 3 expert panel, who therefore recommended that the model be rejected. Nevertheless, it was decided to retain this model since the slow decay rate has been observed in some earthquakes (e.g., Maule, Chile, Boroschek et al. [2012]), and because this model has been shown to work well in comparative studies for smaller magnitude events as well (see Section 4.2). Moreover, since variable distance attenuation rates were observed across global datasets for interface subduction zone earthquakes, and the AEA12 and ZEA06 models have relatively fast distance attenuation rates, use of the AB03 model was considered desirable to capture this important source of epistemic uncertainty. Nonetheless, we never reached a condition of full consensus on the selection of this particular model.

Figures 5.1–5.4 present re-plots of the trellis diagrams from Section 3.2.1 that highlight the selected models by greying out the predictions from the non-selected GMPEs. The figures present response spectra, magnitude scaling, distance scaling, and standard deviation terms for interface subduction events and rock site conditions. Additional similar plots for intraslab subduction events are presented in the Appendix. These plots show how the selected models reflect the range of behavior observed in the pre-selected GMPEs, especially with respect to variable rates of distance attenuation.

Each of the selected SZ models includes site terms, but we do not recommend application of the linear site terms of ZEA06. Instead, the ZEA06 model should be used for hard rock conditions (assumed V_{ref} = 1000 m/sec) and the nonlinear site amplification function from AEA12 applied to these hard-rock estimates. Since the assumed reference velocity is V_{ref} = 1000 m/sec for ZEA06 and the AEA12 site terms have period-dependent (and unspecified) values of V_{ref}, the appropriate site correction can be computed as follows from the AEA12 model (where f is the site function in natural log units):

- Compute site amplification using the appropriate V_{s30} for the site: $f_{site}\,(V_{s30}, PGA_r)$.
- Compute site amplification for V_{ref} = 1000 m/sec: f_{ref} (1000 m/sec, PGA_r).
- Calculate site amplification relative to V_{ref}: $f_{site}\,(V_{s30}, PGA_r)$- f_{ref} (1000 m/sec, PGA_r).

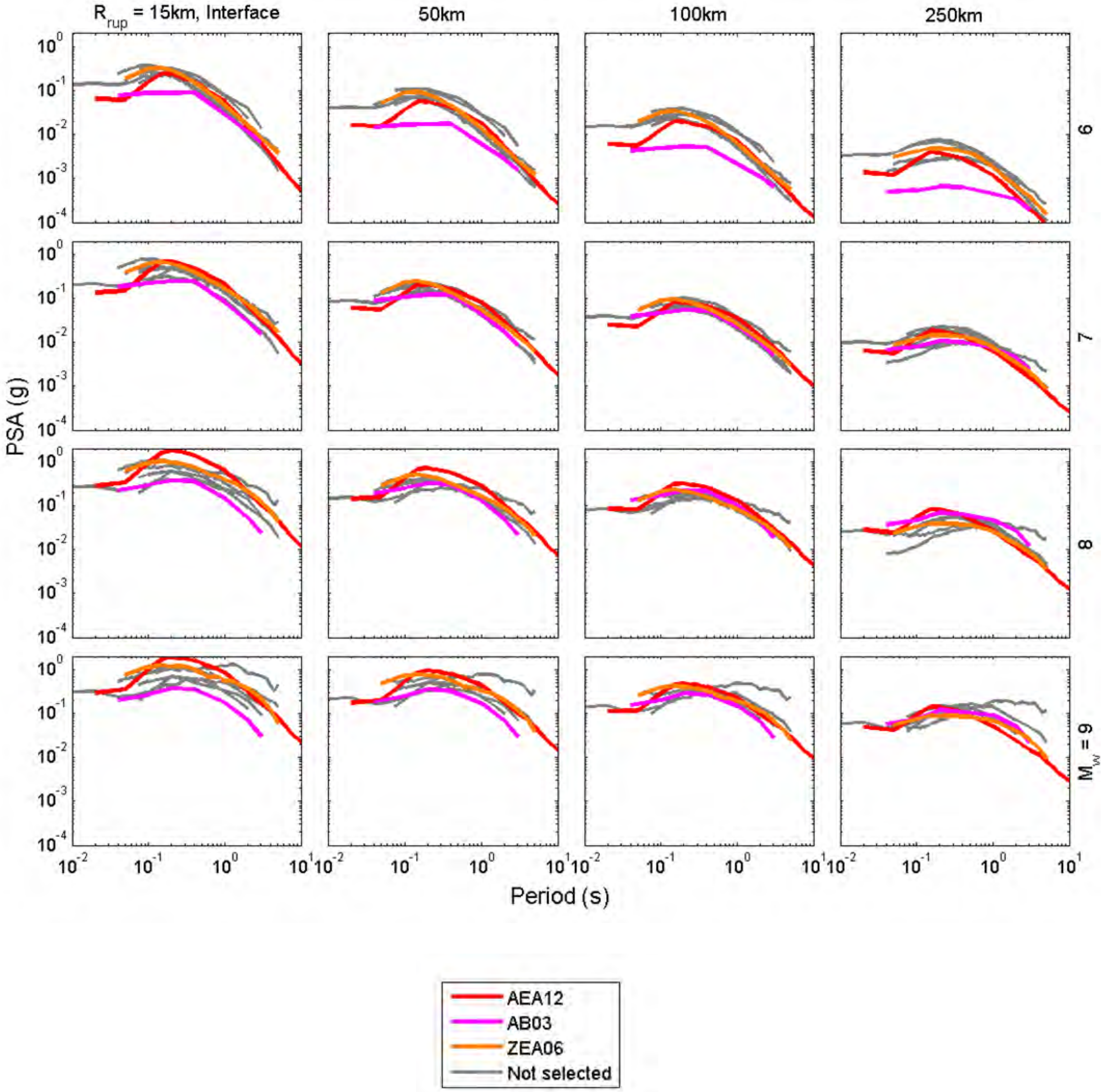

Figure 5.1 **PSAs trellis chart highlighting selected models (color) overlaid on non-selected models (grey). Conditions shown are for interface earthquake scenarios and rock site conditions.**

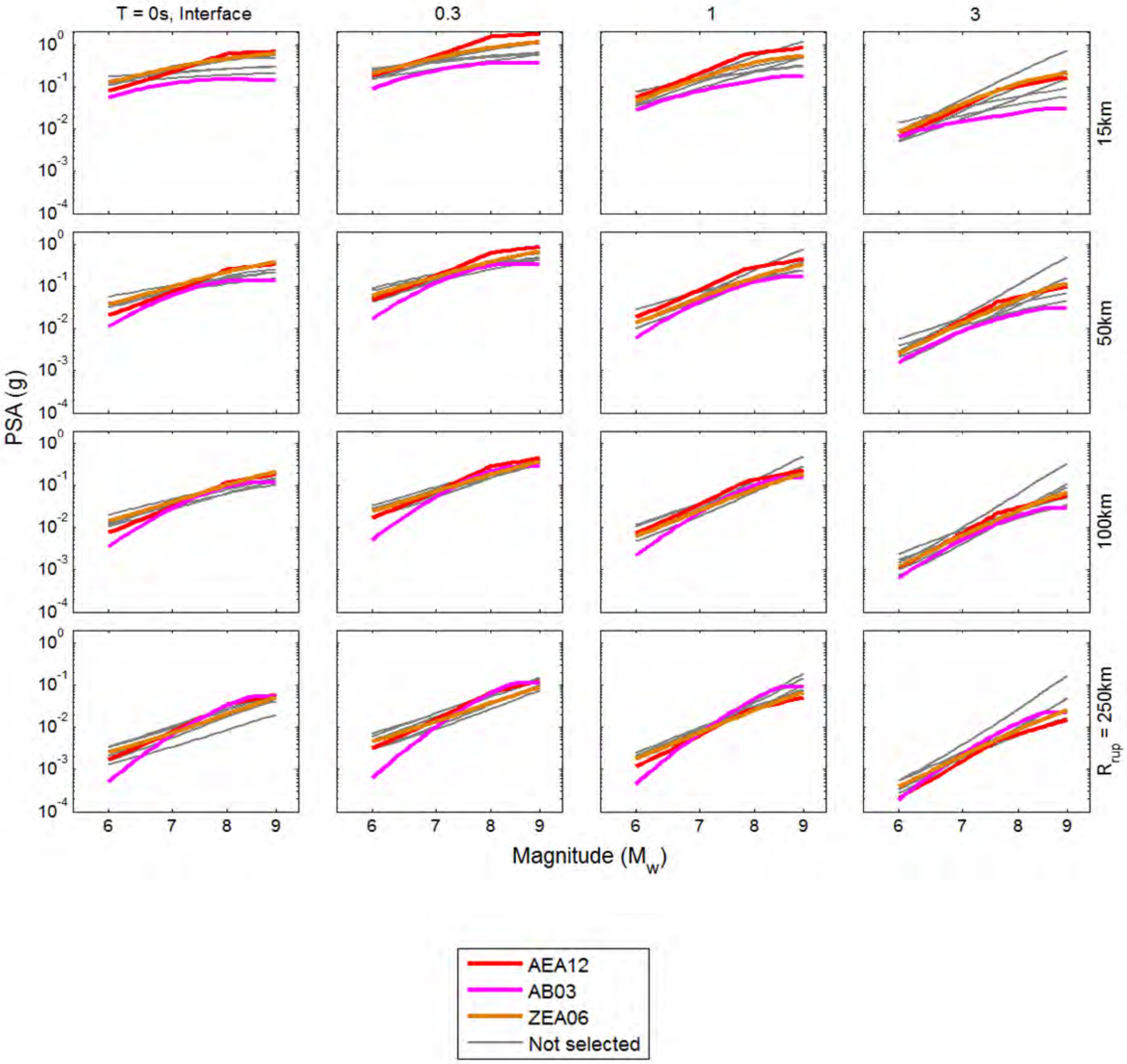

Figure 5.2 Magnitude scaling trellis chart highlighting selected models (color) overlaid on non-selected models (grey). Conditions shown are for interface earthquake scenarios and rock site conditions.

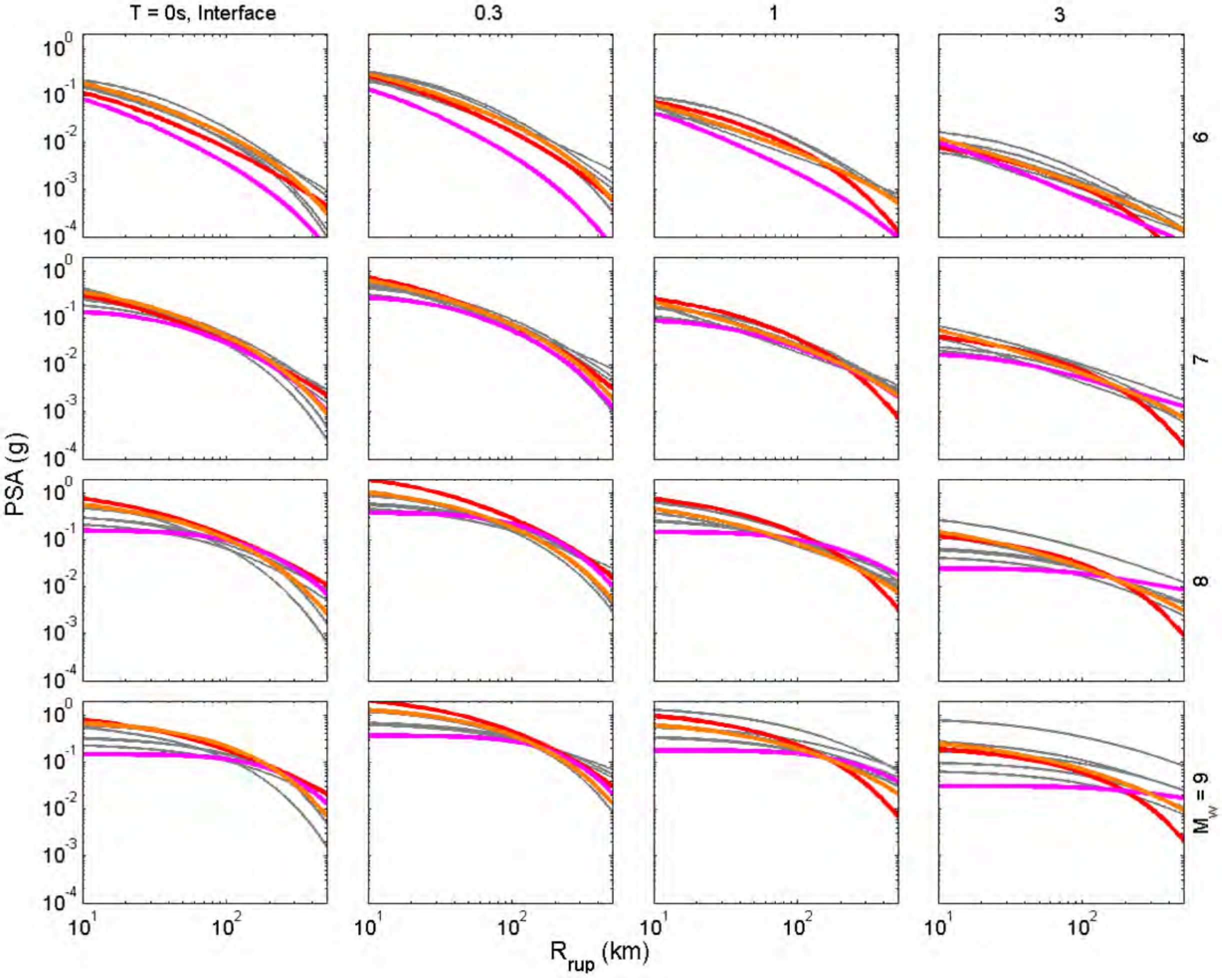

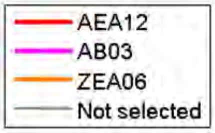

Figure 5.3 Distance scaling trellis chart highlighting selected models (color) overlaid on non-selected models (grey). Conditions shown are for interface earthquake scenarios and rock site conditions

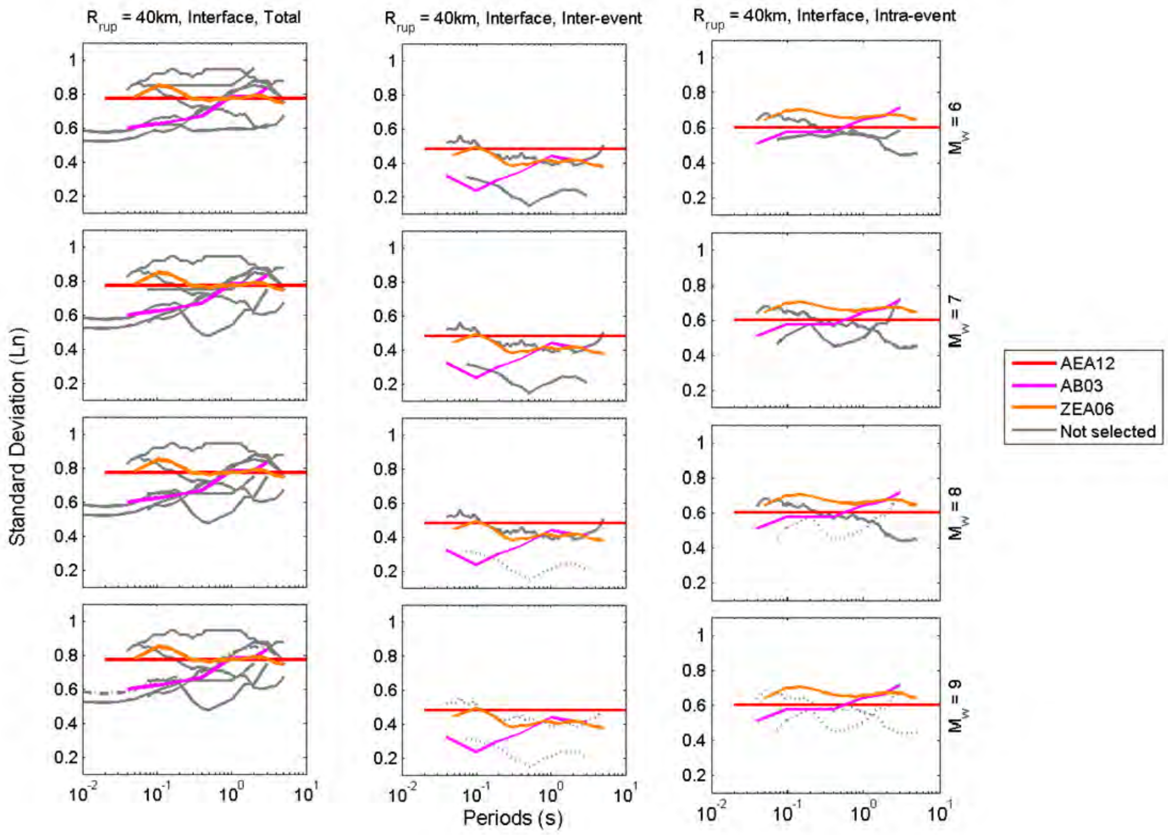

Figure 5.4 Standard deviation trellis chart highlighting selected models (color) overlaid on non-selected models (grey). Conditions shown are for interface earthquake scenarios and rock site conditions.

5.2 STABLE CONTINENTAL REGIONS

There was unanimous consensus on the selection of the PEA11 [Pezeshk et al. 2011] GMPE. Several lines of reasoning supported this selection: it is based on the hybrid empirical technique, which has desirable attributes and uses a recent and fairly complete dataset for eastern North America (ENA). Furthermore, it can be considered an update of C03 [Campbell 2012, submitted). AB06′ [Atkinson and Boore 2006; 2011] was also chosen. Arguments for this model, which is based on finite-source stochastic simulations, include the effective calibration of input parameters against available data, its broad usage in previous forms (including U.S. national hazard maps), an ability to apply the model for either very hard rock conditions or for V_{s30} = 760 m/sec conditions (thus avoiding the need for the correction factors mentioned in Section 3.2.2), and its position as the most prominent and well documented of the stochastic procedures. An argument against its selection is that elements of the model are similar to PEA11, so it can be argued that the use of PEA11 and AB06′ may artificially lower epistemic uncertainty. SEA02 [Silva et al. 2002], a double corner model with saturation, was the third model selected. The principal argument for this stochastic GMPE is its use of a point-source double corner model for the source spectrum, which has more realistic features than single corner models with respect to long period (> 1 sec) spectral ordinates. Single-corner models tend to over-predict observed long-period ground motions, whereas double-corner source spectra generally match these motions better, which could be important for applications involving high-rise and other long-period structures. As well as the arguments given in Section 3.2.2 based on the trellis plots for SCRs, we also note that the models of FEA96 and C03 have been superseded by AB06 and PEA11; hence, these newer models were preferred. In addition, predictions from DEA06 were felt to be too strongly based on a slightly arbitrary decision (because of a lack of observations) on what stress (drop) parameters to use within the stochastic simulations. A08′ was considered by the core to be a simple empirical adjustment from weak-motion data and to be lacking a strong physical background.

The three selected models of PEA11, AB06′, and SEA02 were all developed for application in the central and eastern U.S. To increase the geographical spread of the selected GMPEs, we considered including the model SEA09 [Somerville et al. 2009; Craton model) in lieu of the SEA02 model. The craton version of SEA09 applies to a SCR that is distinct geographically from ENA, which dominates many of the other pre-selected GMPEs. Moreover, this GMPE was developed using a different simulation procedure that is a hybrid of stochastic simulations at high frequencies and physics-based modeling at low frequencies. The diversity of the study region and simulation techniques were cited as advantages of this model. However, the weaknesses of this model were eventually considered to be too strong to select it. These weaknesses include: relatively poor documentation, some features of the model are specific to the study region and may not extrapolate well globally (e.g., properties of shallow earthquakes and large Moho bounce effect), the magnitude-scaling does not saturate but increases in slope with magnitude at short periods (see Figure 3.8), and the standard deviation term has an unrealistic step at around 1s (at the interface of the stochastic and physical models).

Figure 5.5 highlights predicted spectra from PEA11, AB06′, and SEA02 by greying out the predictions from the other GMPEs. These graphs show that the predictions from these three models are quite similar. We felt that this similarity in predictions does not accurately reflect the epistemic uncertainty in SCR GMPEs, which should be quite large given the lack of data. Therefore, we felt that some additional uncertainty should be introduced into the ground-motion logic tree for SCRs by adding another model. Various ways of generating this additional model were considered. This included the idea of scaling up or down one of the already selected GMPEs (the so-called backbone approach), but this was considered too arbitrary a method since it was difficult to decide on a scaling factor. In the end, it was decided to bring in a model that was not originally selected.

Therefore, following much discussion we decided to select the GMPE of TEA97′ [Toro et al. 1997; Toro 2002]. Although this model is also for ENA, its predictions are significantly different from those of the other three models. In addition, its modeling of epistemic uncertainty and aleatory variability is the most sophisticated of all stochastic models, and it has been used successfully in many previous projects. However, the data analyzed for this model are now more than 20 years old; it was originally published in 1993 as part of an EPRI report.

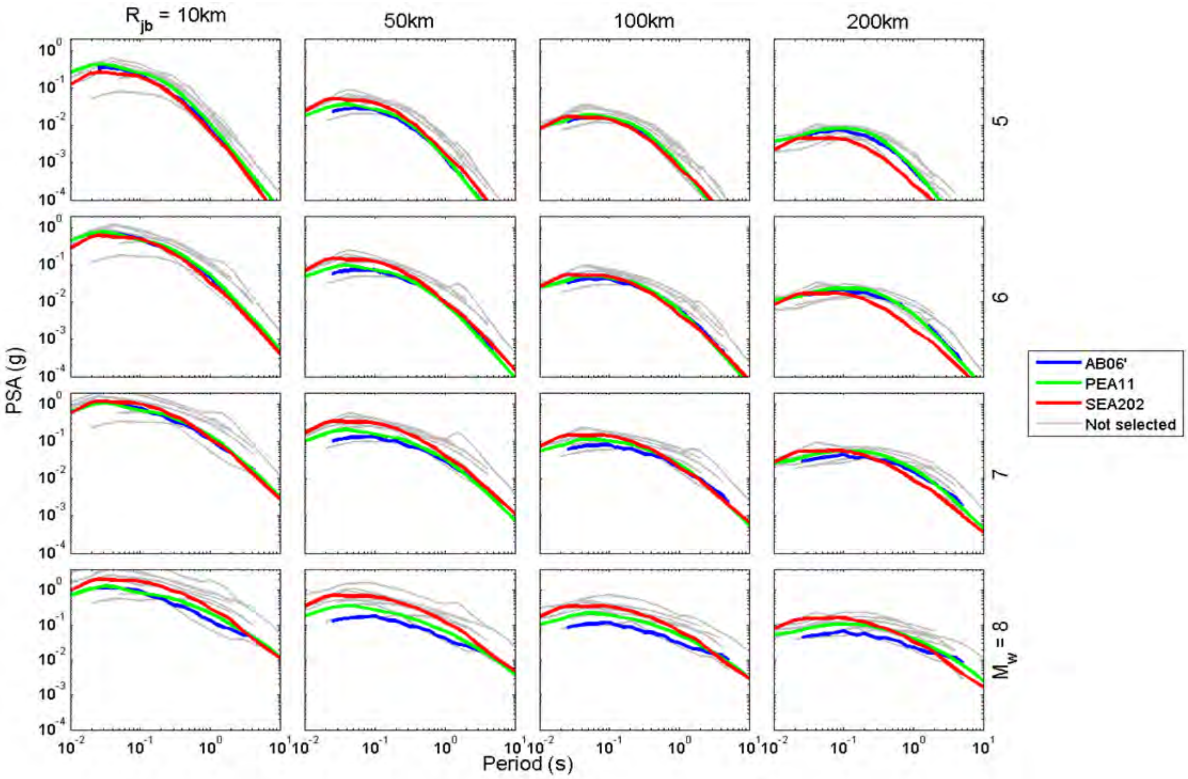

Figure 5.5 **Trellis plot for SCR GMPEs highlighting models of AB06′, PEA11, and SEA02.**

Figures 5.5–5.9 present re-plots of the trellis diagrams from Section 3.2.2 that highlight the four selected models by greying out the predictions from the non-selected GMPEs. The figures present response spectra, magnitude scaling, distance scaling, and standard deviation terms for rock site conditions. These plots show that the selected models approximately reflect the range of behavior observed in the pre-selected GMPEs.

Of the four selected models, only AB06′ includes recommendations for modeling site amplification. The AB06′ model can be applied for hard rock reference conditions ($V_s \geq 2.0$ km/sec; NEHRP Class A) or the NEHRP BC boundary (V_{s30} = 760 m/sec). When the BC model is used, a site amplification function can be applied, which was adopted from an empirical study of site amplification for active crustal regions [Choi and Stewart 2005]. For the other selected models (PEA11, SEA02, and TEA97′), we recommend the following procedure for incorporating site effects into ground motion prediction for SCRs:

1. Apply the selected models for their respective reference rock conditions (V_{ref} = 2.0 km/srv for PEA11; V_{ref} = 2.83 km/sec for SEA02 and TEA97′).
2. Adjust predicted spectra to the BC boundary (V_{s30} = 760 m/sec). Lacking more formal recommendations in the literature, we compile in Figure 5.10 transfer functions based on quarter-wavelength theory for crust-to-A (crustal velocities are approximately 3.7 km/sec) and crust-to-BC conditions from Tables 3 and 4 of AB06, respectively. We compute the ratio of these transfer functions, which represents the A-to-BC transfer function, although we recognize that this ratio

cannot be used directly as the desired correction factor both because varying kappa effects for A and BC sites are not reflected and because GMPEs predict response (not Fourier) spectra. Accordingly, we also show ratios of response spectra (RRS) derived by the seventh author (David M. Boore) in Figure 5.10. The ratios reflect the different V_s profiles for the two conditions, but also different levels of attenuation due to variable kappa effects. The ratios provided by Boore are more complex than illustrated in the figure because they have magnitude- and distance-dependence. The values shown in Figure 5.10 are reasonably stable averages over the parameter space typically of engineering interest for SCRs ($\mathbf{M} \geq 6$, $R_{jb} \approx$ 10–300 km). The results are relatively unstable (substantial epistemic uncertainty) for PGA; hence, they are not shown. The RRS values and transfer function ordinates match at low frequencies (<~ 1 Hz) but differ at higher frequencies. We recommend use of the RRS ordinates in Figure 5.10 for the A-to-BC correction for the indicated frequency range. More formal recommendations for this correction are in development as part of the NGA-East project.

3. Modify PSA from the reference V_{s30} = 760 m/sec to the site condition of interest using a suitable nonlinear amplification function for the target region. In the absence of appropriate region-specific site amplification functions, the site terms from NGA models can be applied. To apply the NGA site terms in a manner that ensures the reference velocity of 760 m/sec is maintained, the procedure given in Section 5.1 can be used (with substitution of 760 m/sec for the value of 1000 m/sec given in Section 5.1). Note that improved site amplification functions that reflect regional variations in geologic conditions are in development as part of the NGA-West2 project and should be used to replace the original NGA functions when available.

As mentioned in Section 3.3.2, there are problems with the standard deviation functions in some of the selected SCR GMPEs. We recommend application of the standard deviation terms from AB06′, PEA11, and TEA97′ in their as-published form (shown in Figure 5.9). We recommend that the standard deviations of EPRI [2006] be used in lieu of those from SEA02 because of the large increase in standard deviations for $T > 1$ sec for SEA02, which we consider unrealistic.

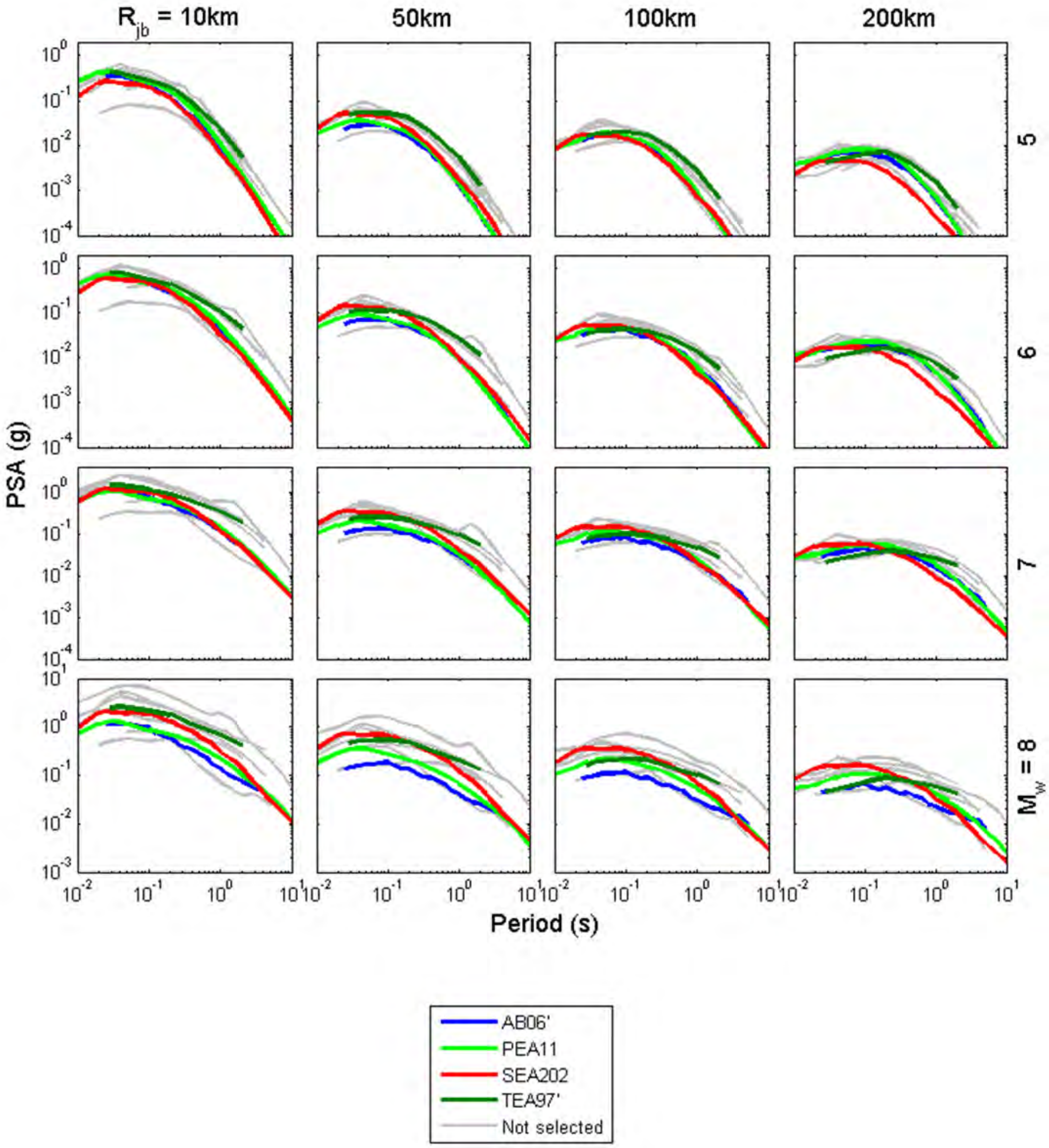

Figure 5.6 PSAs trellis chart highlighting selected models (color) overlaid on non-selected models (grey). Conditions shown are for SCR earthquake scenarios and rock site conditions.

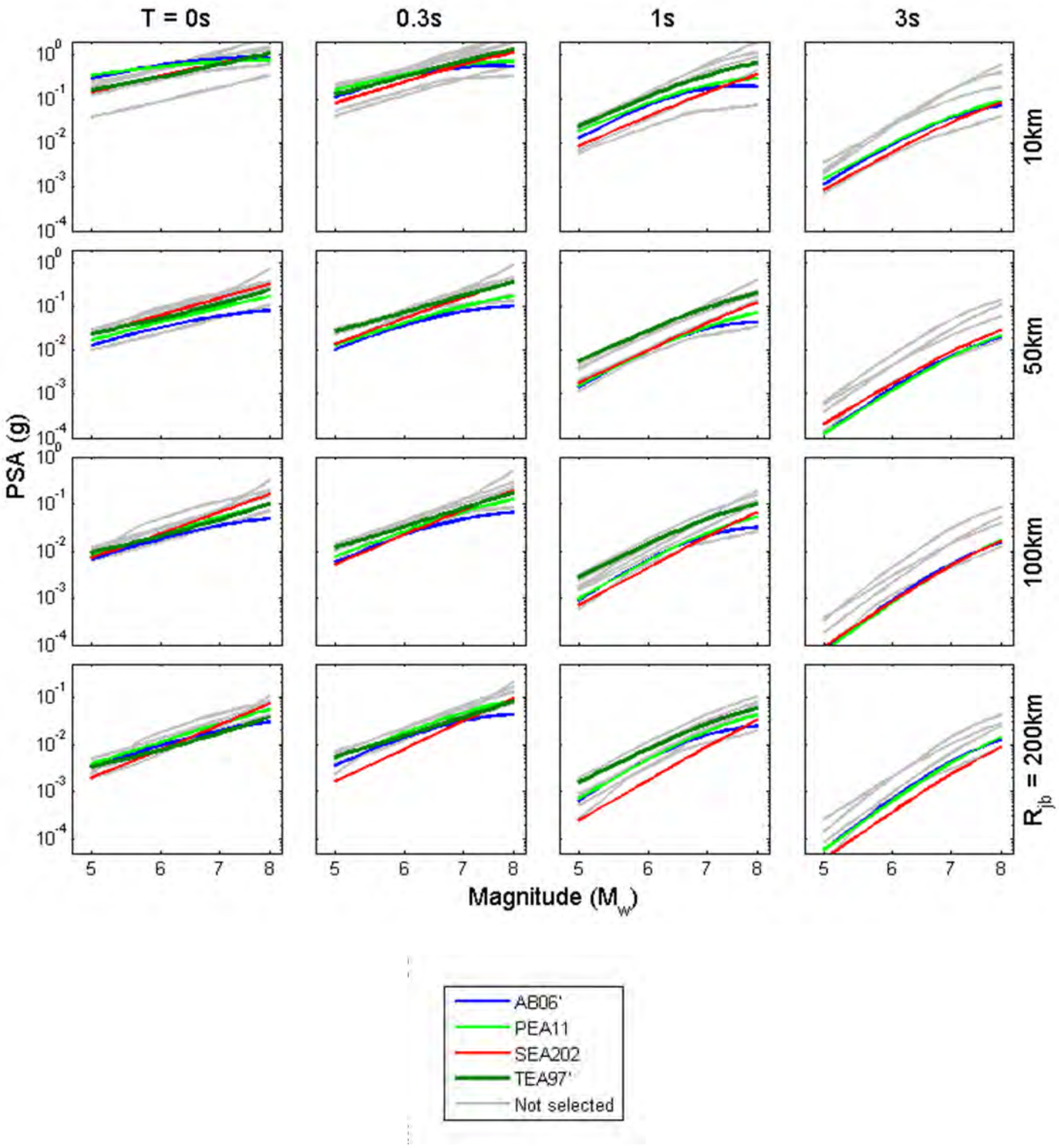

Figure 5.7 Magnitude scaling trellis chart highlighting selected models (color) overlaid on non-selected models (grey). Conditions shown are for SCR earthquake scenarios and rock site conditions.

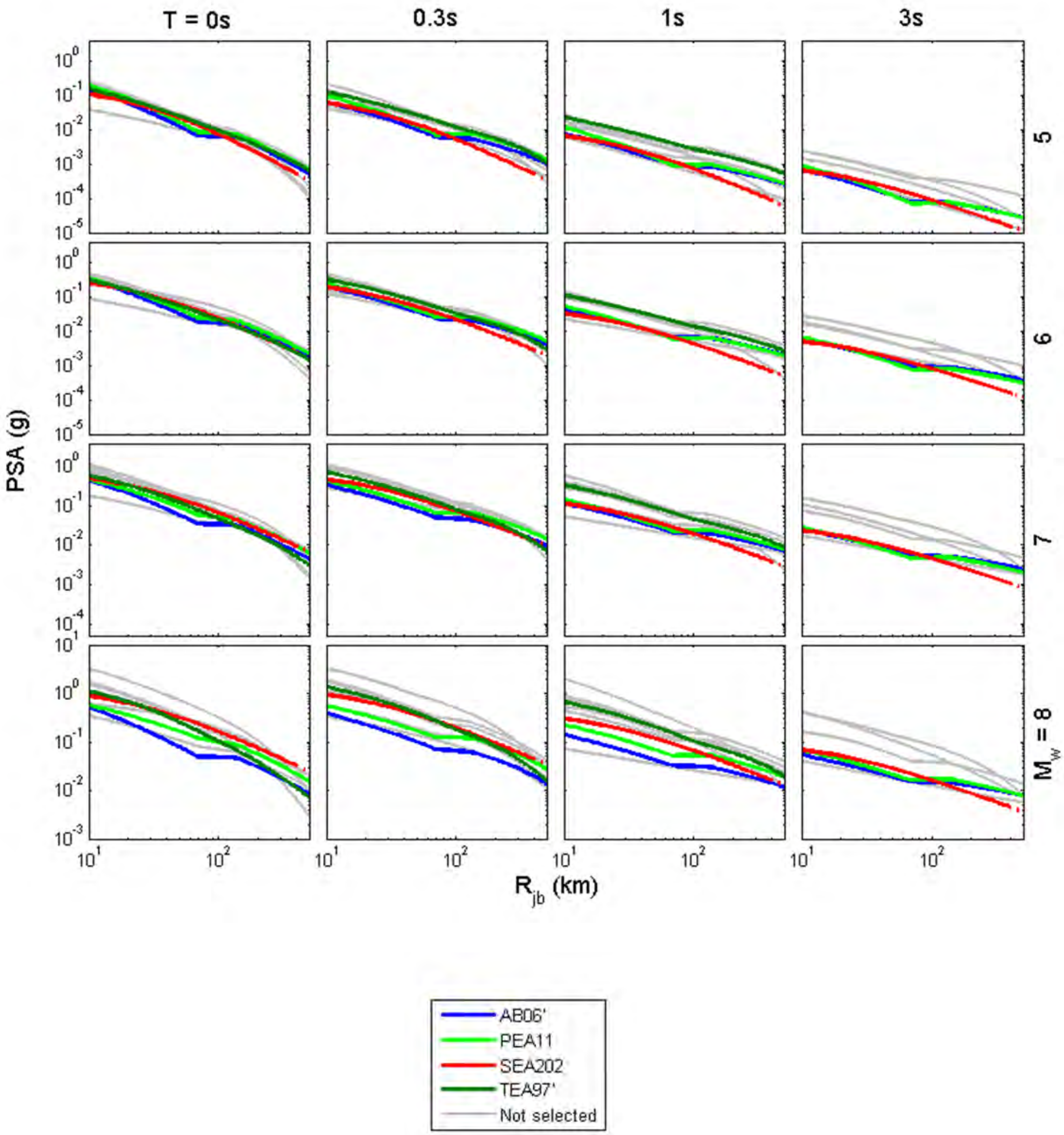

Figure 5.8 Distance scaling trellis chart highlighting selected models (color) overlaid on non-selected models (grey). Conditions shown are for SCR earthquake scenarios and rock site conditions.

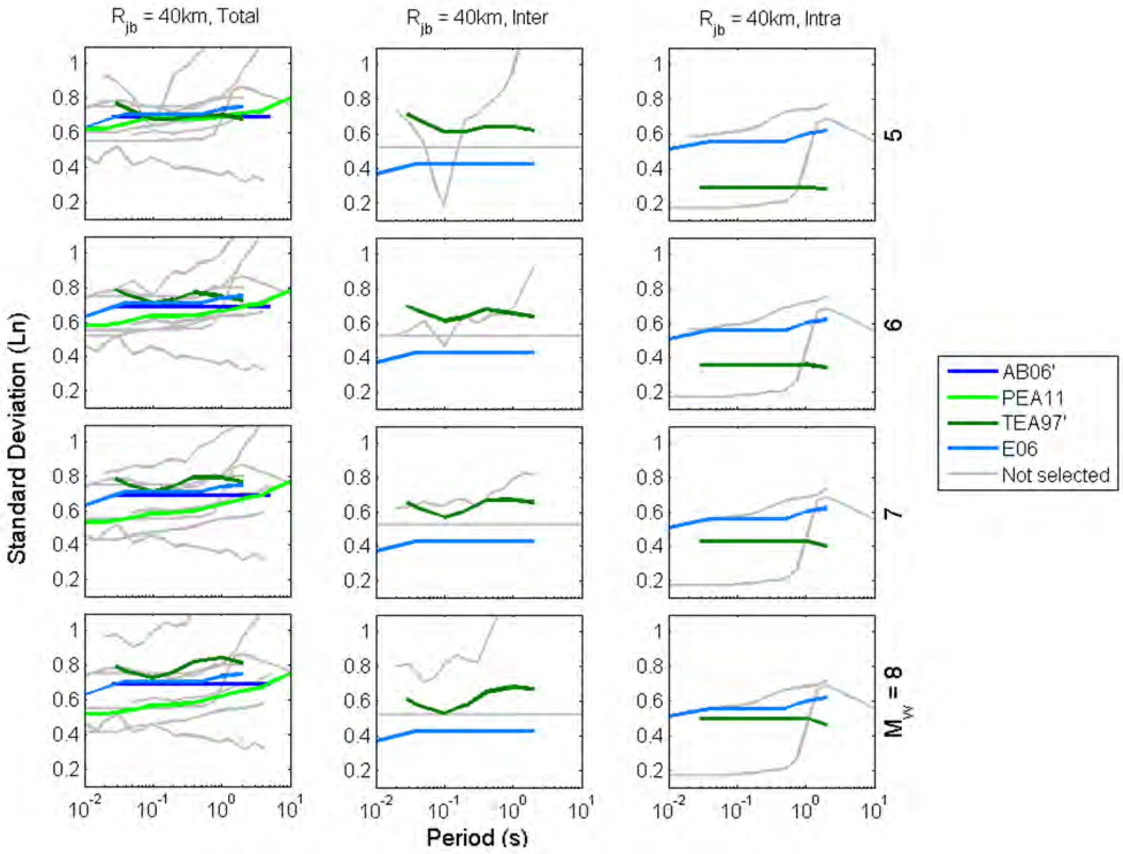

Figure 5.9 Standard deviation trellis chart highlighting selected models (color) overlaid on non-selected models (grey). Conditions shown are for SCR earthquake scenarios and rock site conditions. SEA02 model not highlighted in this plot since E06 standard deviation terms are used as a replacement.

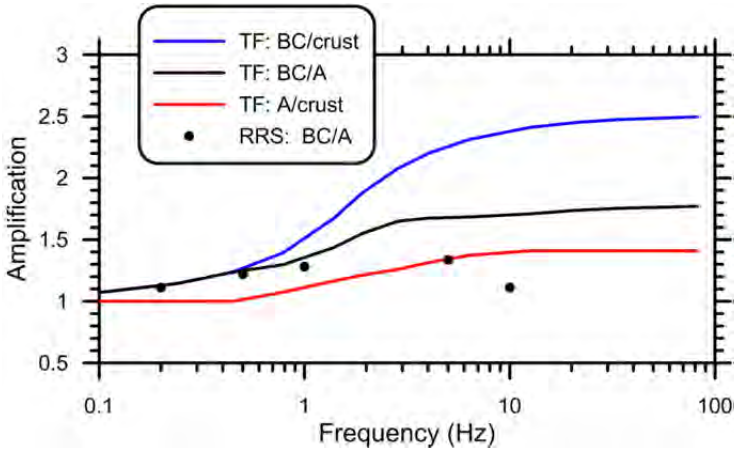

Figure 5.10 **Frequency-dependent site amplification expressed as transfer functions (from AB06) and RRS (from seventh author). The RRS values can be used to correct PSA computed for very hard reference site conditions in SCRs ($V_s \geq 2.0$ km/sec , NEHRP site class A) to the BC boundary site condition (V_{s30} = 760 m/sec).**

5.3 ACTIVE CRUSTAL REGIONS

The following three models were selected for ACRs: AB10 [Akkar and Bommer 2010], CY08 [Chiou and Youngs 2008], and ZEA06 [Zhao et al. 2006]. These models provide a good geographical spread (one for Europe and the Middle East, one global, and one predominantly for Japan). Their scaling shows desirable features, such as magnitude and distance saturation and anelastic attenuation terms, which means that they can be applied across the magnitude-distance range of interest to GEM. CY08 was preferred over the other pre-selected NGA models because (1) its magnitude-scaling for small and moderate events was considered to be more appropriate than the other NGA models; and (2) it has an anelastic attenuation term that has produced relatively favorable model-data comparisons in past studies. The BA08 model was seriously considered for selection as an alternate or supplement to CY08 as it also has generally compared well to international data and has many of the desirable functional form attributes of CY08 (but with simpler equations). It was not selected because we did not want to have four ACR models.

Figures 5.11–5.14 present re-plots of the trellis diagrams from Section 3.2.3 that highlight the selected models by greying out the predictions from the non-selected GMPEs. The figures present response spectra, magnitude scaling, distance scaling, and standard deviation terms for ACR events and rock site conditions.

Each of the selected ACR models includes site terms, but we do not recommend application of the linear site terms of AB10 or ZEA06. The ZEA06 and AB10 models should be used for hard rock and rock conditions, respectively (assumed V_{ref} =1000 m/sec). The nonlinear site amplification function from CY08 can be applied to correct the ground motions for the V_{s30} of the site. The CY08 amplification function was developed relative to a reference condition of 1130 m/sec, which is sufficiently close to 1000 m/sec that the model can be directly applied (additional corrections of the type discussed in Section 5.1 are not required).

There was some discussion within the core group about whether epistemic uncertainty in ground motions in ACRs is being sufficiently captured by these three models since for some magnitudes and distances the three sets of results are quite similar (e.g., Figure 5.11). After some deliberation, we decided to not select a fourth GMPE or to scale up or down one of the selected models. However, we note that the within-event standard deviation terms of the selected models (Figure 5.14) have significant differences, reflecting epistemic uncertainty.

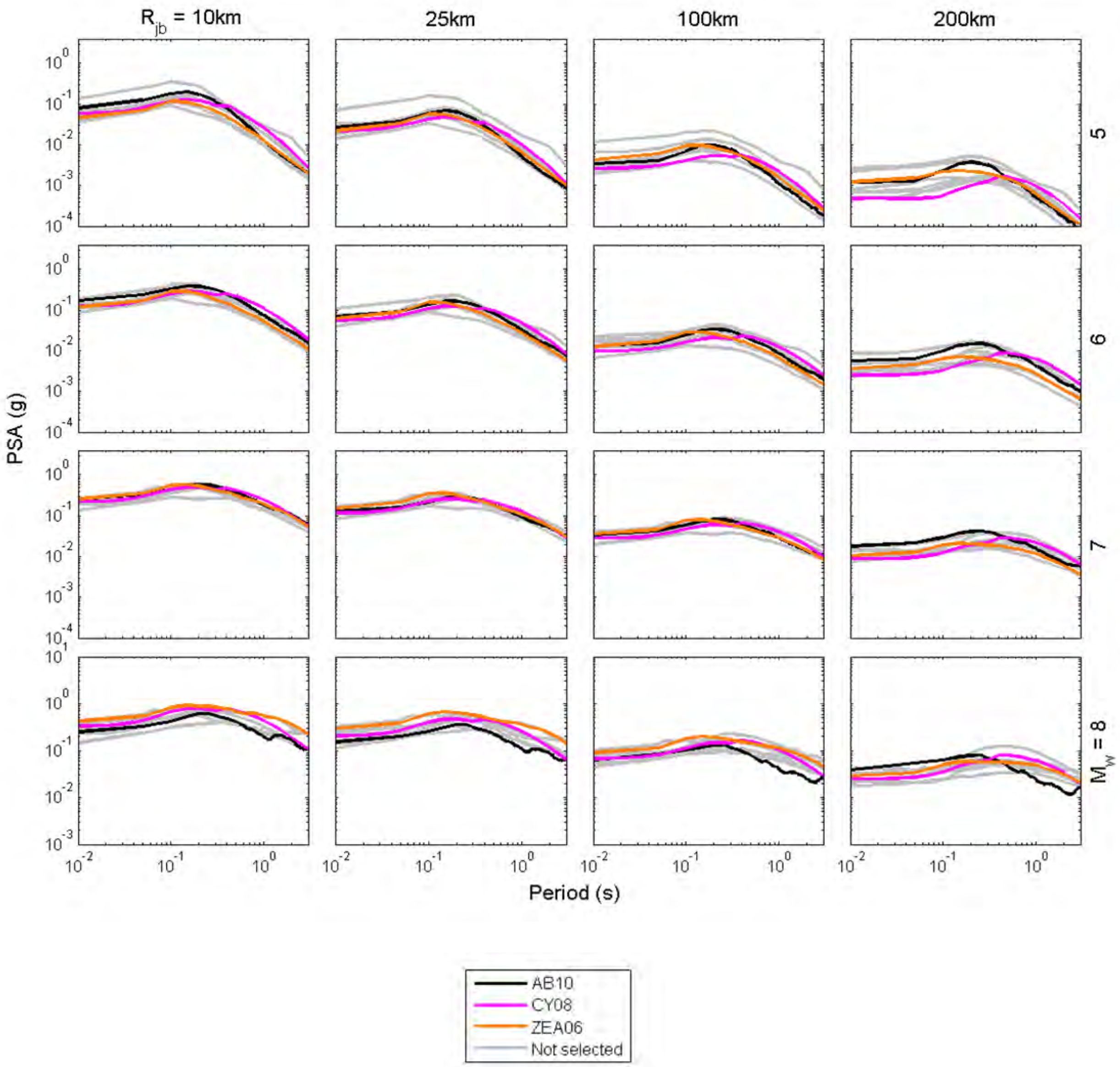

Figure 5.11 PSAs trellis chart highlighting selected models (color) overlaid on non-selected models (grey). Conditions shown are for ACR earthquake scenarios and rock site conditions.

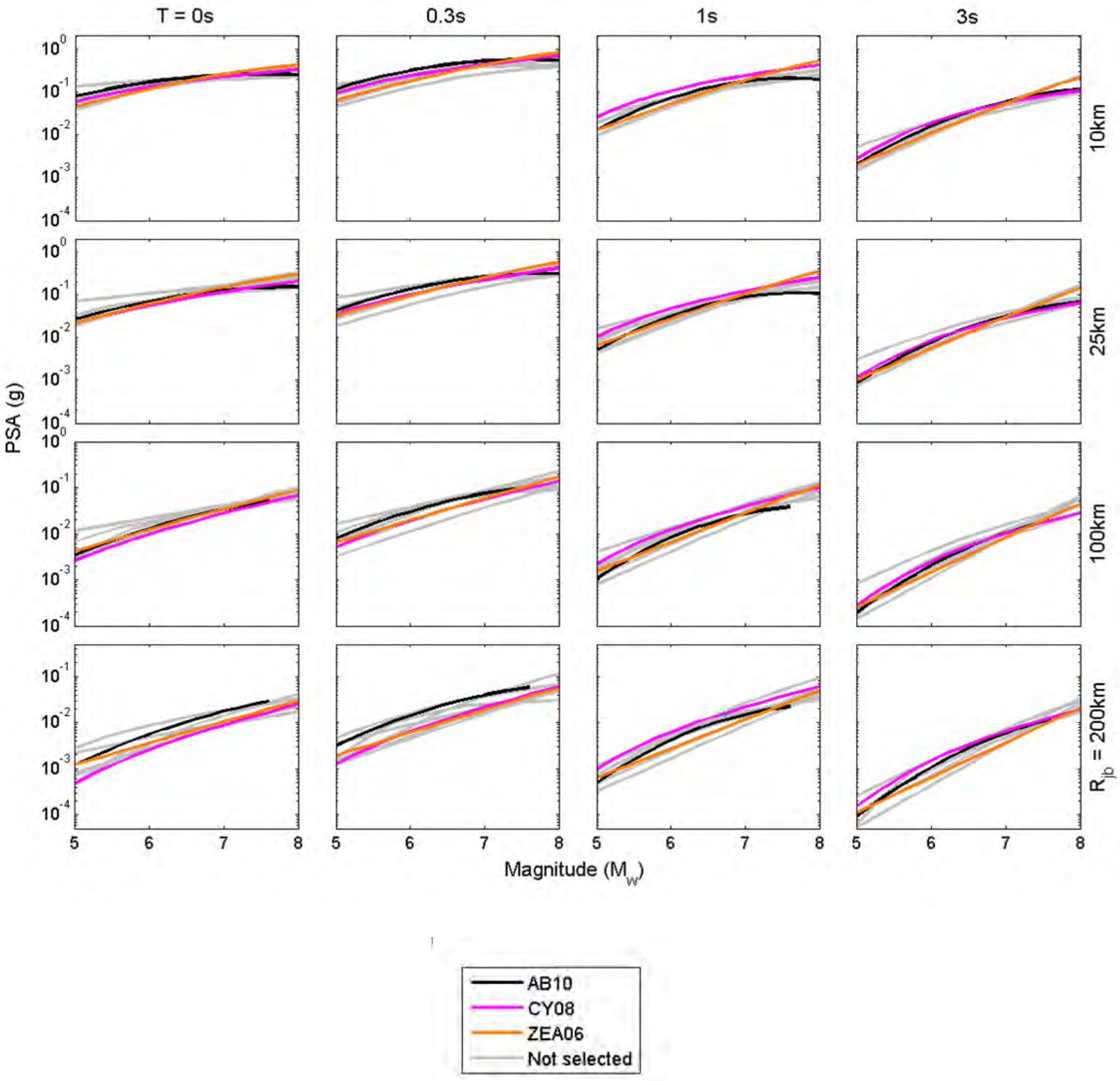

Figure 5.12 Magnitude scaling trellis chart highlighting selected models (color) overlaid on non-selected models (grey). Conditions shown are for ACR earthquake scenarios and rock site conditions.

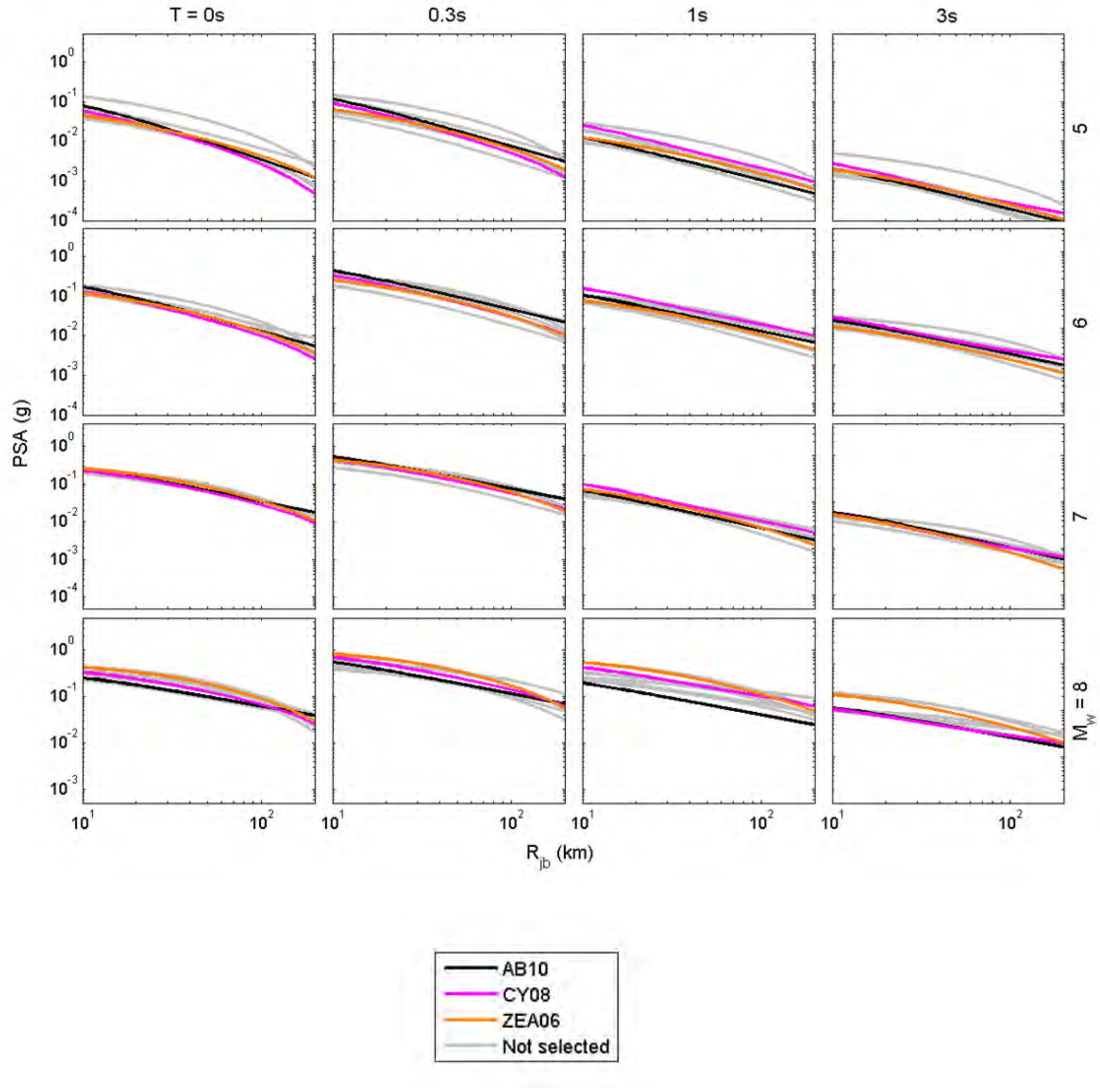

Figure 5.13 Distance scaling trellis chart highlighting selected models (color) overlaid on non-selected models (grey). Conditions shown are for ACR earthquake scenarios and rock site conditions.

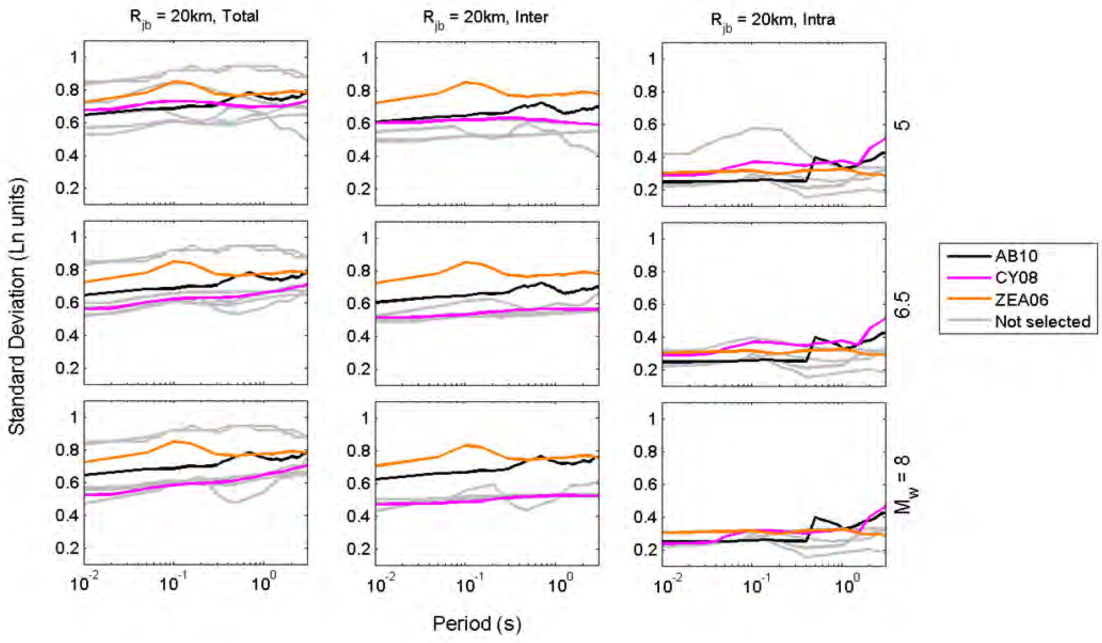

Figure 5.14 Standard deviation trellis chart highlighting selected models (color) overlaid on non-selected models (grey). Conditions shown are for ACR earthquake scenarios and rock site conditions.

5.4 THREE SPECIAL REGIMES

As noted above, there exist at least three tectonic regimes with characteristics that may lead to significantly different ground motions for the same-sized earthquake at a similar distance than GMPEs derived for SCRs, SZs, or ACRs. These three regimes are: volcanic zones (e.g., close to Mount Etna in Sicily, parts of New Zealand, and parts of Iceland); areas of deep focus non-subduction earthquakes, such as the Vrancea Seismic Zone (Romania); and areas where the travel paths are mainly through oceanic crust, such as offshore coastal Portugal and off the coast of northern California. Volcanic zones in this case cover both small shallow events related to volcanic activity (e.g., Mount Etna) and also the possible additional travel-path attenuation that comes from seismic waves passing through active volcanic regions (e.g., Taupo volcanic zone, TVZ, in New Zealand). These three special regimes were not the focus of the GEM Global GMPEs project and, therefore, we do not make any recommendations here concerning GMPEs to be used in such zones. We do, however, propose some analysis that could be performed to help inform recommendations. These analyses generally are variants of the referenced-empirical technique proposed by Atkinson [2008] and applied by her to derive GMPEs for eastern North America.

5.4.1 Volcanic Zones

Previous studies by Graeme McVerry and others (e.g., McVerry et al. [2006]; Zhao [2010]) concerning the modification to ground motions coming from additional attenuation due to volcanic travel-paths could be adapted to derive adjustment factors for this situation. The general procedure that could be followed is the following.

1. Collect observed PSAs obtained from strong-motion data recorded in areas potentially affected by volcanic travel-paths. Two obvious examples are the TVZ and data from earthquakes occurring in the South Iceland Seismic Zone but recorded outside this area (e.g., in Reykjavik). For each record, the distance travelled through the volcanic zone needs to be estimated.
2. For all three GMPEs recommended for ACRs (the most appropriate tectonic regime), compute the within-event residuals for all PSAs and plot against distance through the volcanic zone.
3. Fit regression lines through the within-event residuals for all periods and all three GMPEs and check if the coefficients are statistically significant. It is expected that the slope should be negative (meaning that the seismic waves are attenuated faster when they pass through the volcanic zone) and significant for short structural periods (longer periods should be less affected by low Q values).
4. For those GMPEs and periods for which statistically significant best-fit lines are obtained this additional term can be added to these GMPEs when used in seismic hazard assessments for sites affected by volcanic paths.

One complication of this approach is that PSHA taking account of additional attenuation along travel paths passing through a volcanic zone would be challenging since it is thought not to be included in any PSHA code. Graeme McVerry [*personal communication* 2011] has stated that when conducting PSHA for the New Zealand national hazard map they made a simplification and assumed that the distance through the volcanic zone equals the source-to-site distance for sites within this zone. This is because the additional attenuation coming from the volcanic zone dominates when near this zone.

5.4.2 Vrancea-Type Earthquakes

Deep (>70 km) non-subduction earthquakes occur in at least three areas (sometimes known as nests): Vrancea (Romania), which contributes to high seismic risk in Bucharest, Bucaramanga (Colombia), and the Hindu Kush (Afghanistan). GMPEs have only been published for Vrancea [Douglas 2011]. Sokolov et al. [2008] presented the most recent and well-documented model for this region, which was considered by SHARE. We reached the same conclusion as the participants of SHARE, namely that this model is too complex and Vrancea-specific for regional/global PSHA application because of its azimuthal dependency, for example. In addition, only selecting a single model for this type of region would not account for the large epistemic uncertainty present in the prediction of ground motions from Vrancea-type earthquakes. Therefore, we propose, as did the experts of SHARE, that the recommended intra-slab GMPEs for SZs be used for this type of source. It is also recommended that some data analysis be performed to justify and possibly adjust these GMPEs to make them more applicable for this type of earthquake. The proposed analysis is the following:

1. Collect observed PSAs obtained from strong-motion data recorded from deep-focus non-subduction earthquakes. It is thought that only for Vrancea are there enough strong-motion data from moderate and large magnitude events with good quality metadata.
2. Compute the between- and within-event residuals for these data with respect to the three GMPEs for SZs evaluated for intraslab events.
3. Plot the between-event residuals with respect to magnitude and depth and examine possible trends for all structural periods. If significant trends are observed, then regression lines could be fit to these residuals derive an adjustment of the original GMPEs for application in these special areas.
4. Similarly, plot the within-event residuals with respect to source-to-site distance and fit regression curves if significant trends are observed. These best-fit functions could be included as extra terms to the GMPEs when applying them in these special areas.

5.4.3 Oceanic-Path Earthquakes

Earthquakes occuring within oceanic crust and consequently whose travel paths to onshore stations are predominantly through oceanic crust (e.g., offshore Portugal) are thought to generate significantly different ground motions than earthquakes occurring in continental crust. For this reason there have been some attempts to derive GMPEs specifically for this situation (e.g., Carvalho [2008]). None of these models, however, have been published in an international peer-reviewed journal; therefore, they were not considered here. Based on analysis presented by Vilanova et al. [2012] we suggest that our recommended models for SCRs be used for this type of situation, although for the SHARE project Delavaud et al. [2012] suggest that ACR GMPEs be applied for these regions. Nevertheless, it would be beneficial for this situation to undertake some data analysis to justify this recommendation and to possibly improve it. The analysis proposed is the following.

1. Collect observed PSAs obtained from strong-motion data recorded from earthquakes occuring in oceanic crust. It is thought that data is available from both Portugal and earthquakes occuring in the Gorda plate region off northern California.
2. Compute the between- and within-event residuals for these data with respect to the GMPEs for ACRs, SCRs and SZs (intraslab but evaluated for shallower focal depths than is usual). It is not yet clear which tectonic regime’s GMPEs would be most appropriate for this situation and hence it would be useful to check data against all models.
3. Plot the between-event residuals with respect to magnitude and depth and examine possible trends for all structural periods.
4. Identify the three or four GMPEs whose residuals present the weakest trends and recommend those for use in hazard assessments for this type of situation.

If the between- and within-event residuals from the best-fitting GMPEs present significant trends, then fit regression curves with respect to magnitude and source-to-site distance and add these as additional terms to the recommended GMPEs.

6 Conclusions

This report presents and applies a methodology for selection of ground-motion models for the GEM-PEER Global GMPEs Project. This procedure aims to be transparent, objective, and repeatable in future projects (e.g., for possible updates of the GEM hazard assessments). The procedure consists of expert review of several information sources, including (1) trellis plots showing the scaling of candidate GMPEs against period, magnitude, distance, and site condition, along with within- and between-event standard deviation terms; (2) functional forms of candidate GMPEs; and (3) review of quantitative model-data comparison studies in the literature.

Based on expert review of the aforementioned information sources summarized in Chapters 3 and 4, a set of GMPEs for each of the tectonic regimes was proposed as described in Chapter 5. These consisted of three GMPEs for subduction zones, three GMPEs for active crustal regimes, and four GMPEs for stable continental regions. For the majority of these GMPEs, their associated standard deviation models and site terms were selected as well. The only exception for the standard deviation component of the models was for stable continental regions where a standard deviation model by EPRI [2006] was preferred over that derived by Silva et al. [2002]. In the case of site amplification models, we do not recommend the linear site amplification functions used in several of the selected GMPEs. In those cases, we recommend application of the GMPEs for reference rock site conditions, and we provide relatively specific recommendations on how nonlinear site corrections can be applied to those prediction. These recommendations are provided in Sections 5.1–5.3.

We are pleased to recommend several follow-up studies that would be useful if a GMPE selection exercise of this type is undertaken in the future. These include:

1. More systematic model-data comparisons for regions worldwide. This is especially important for SCRs.
2. Consistent implementation of the models in an open-source code such as OpenSHA (http://www.opensha.org/) so that they can readily be applied by a wide variety of users.
3. The data analysis work described in Section 5.4 for the three special regimes.
4. GMPE selection for other intensity measures that may be useful to GEM (e.g., PGV, significant duration or other duration measures, Arias intensity, and cumulative absolute velocity).
5. Assigning weights to the selected GMPEs.

6. Development of a more quantitative approach to add extra epistemic uncertainty for regions where we suspect that the true uncertainty is being under represented (e.g., ACRs and SCRs).
7. As noted in the introduction, GMPE development is a continuously evolving research area, and new and/or updated GMPEs are published as more empirical and simulated data become available and our knowledge of ground-motion hazard expands. Thus, the set of GMPEs proposed within this project should not be viewed as a long-term recommendation but be reevaluated on a regular basis.

REFERENCES

Abrahamson N.A., Gregor N., Addo K. (2012). BCHydro ground motion prediction equations for subduction earthquakes, *Earthquake Spectra*, submitted.

Akkar S., Bommer J.J. (2007). Prediction of elastic displacement response spectra in Europe and the Middle East, *Earthq. Eng. Struct. Dyn.*, 36(10): 1275–1301.

Akkar S., Bommer J J. (2010). Empirical equations for the prediction of PGA, PGV and spectral accelerations in Europe, the Mediterranean region and the Middle East, *Seismol. Res. Lett.*, 81(2): 195–206.

Akkar S., Çağnan Z. (2010). A local ground-motion predictive model for Turkey and its comparison with other regional and global ground-motion models, *Bull. Seismol. Soc. Am.*, 100(6): 2978–2995.

Ambraseys N.N., Smit P., Douglas J., Margaris B., Sigbjörnsson R., Ólafsson S., Suhadolc P., Costa G. (2004). Internet site for European strong-motion data, *Bollettino di Geofisica Teorica ed Applicata*, 45(3): 113–129.

Arango M.C., Strasser F.O., Bommer J.J., Cepeda J.M., Boroschek R., Hernandez D.A., Tavera H. (2012). An evaluation of the applicability of current ground-motion models to the South and Central American subduction zones, *Bull. Seismol. Soc. Am.*, 102(1): 143–168, doi: I: 10.1785/0120110078.

Arroyo D., García D., Ordaz M., Mora M.A., Singh S.K. (2010). Strong ground-motion relations for Mexican interplate earthquakes, *J. Seismology*, 14(4): 769–785.

Atkinson G.M. (2008). Ground-motion prediction equations for eastern North America from a referenced empirical approach: Implications for epistemic uncertainty, *Bull. Seismol. Soc. Am.*, 98(3): 1304–1318, doi: 10.1785/0120070199.

Atkinson G.M., Boore D.M. (2003). Empirical ground-motion relations for subduction zone earthquakes and their application to Cascadia and other regions, *Bull. Seismol. Soc. Am.*, 93(4): 1703–1729.

Atkinson G.M., Boore D.M. (2006). Earthquake ground-motion prediction equations for eastern North America, *Bull. Seismol. Soc. Am.*, 96(6): 2181–2205, doi: 10.1785/0120050245.

Atkinson G.M., Boore D.M. (2011). Modifications to existing ground-motion prediction equations in light of new data, *Bull. Seismol. Soc. Am.*, 101(3) 1121–1135, doi: 10.1785/0120100270.

Bommer J.J., Akkar S., Kale, Ö (2011). A model for vertical-to-horizontal response spectral ratios for Europe and the Middle East, *Bull. Seismol. Soc. Am.*, 101: 1783–1806, doi: 10.1785/0120100285.

Bommer J.J., Douglas J., Scherbaum F., Cotton F., Bungum H., Fäh D. (2010). On the selection of ground-motion prediction equations for seismic hazard analysis, *Seismol. Res. Lett*, 81(5): 783–793.

Bommer J.J., Scherbaum F., Bungum H., Cotton F., Sabetta F., Abrahamson N.A. (2005). On the use of logic trees for ground motion prediction equations in seismic hazard assessment, *Bull. Seismol. Soc. Am.*, 95(2): 377–389.

Boore D.M., Atkinson G.M. (2008). Ground-motion prediction equations for the average horizontal component of PGA, PGV, and 5%-damped PSA at spectral periods between 0.01s and 10.0 s, *Earthq. Spectra*, 24(1): 99–138.

Boroschek R., Contreras V., Kwak D.Y., Stewart J.P. (2012). Strong ground motion attributes of the 2010 M_w 8.8 Maule Chile earthquake, *Earthq. Spectra*, 28(S1): S19–38.

Bozorgnia Y., Campbell K.W. (2004). The vertical-to-horizontal response spectral ratio and tentative procedures for developing simplified V/H and vertical design spectra, *J. Earth1. Eng.*, 8(2): 175–207.

Campbell K.W. (2003). Prediction of strong ground motion using the hybrid empirical method and its use in the development of ground motion (attenuation) relations in eastern North America, *Bull. Seismol. Soc. Am.*, 93: 1012–1033.

Campbell K.W. (2012). A comparison of ground motion prediction equations developed for eastern North America using the hybrid empirical method, *Bulletin of the Seismological Society of Am.*, submitted.

Campbell K.W., Bozorgnia, Y. (2008). NGA ground motion model for the geometric mean horizontal component of PGA, PGV, PGD and 5% damped linear elastic response spectra for periods ranging from 0.01 to 10 s, *Earthq. Spectra*, 24(1): 139–171, doi:10.1193/1.2857546.

Carvalho A. (2008). *Modelação estocástica da acção sísmica em Portugal continental*, Ph.D. thesis, Instituto Superior Técnico, Universidade Técnica de Lisboa, Portugal, in Portuguese.

Cauzzi C., Faccioli E. (2008). Broadband (0.05 to 20 s) prediction of displacement response spectra based on worldwide digital records, *J. Seismology*, 12(4): 453–475, doi: 10.1007/s10950-008-9098-y.

Chiou B.S.-J., Youngs R.R. (2008). An NGA model for the average horizontal component of peak ground motion and response spectra, *Earthq. Spectra*, 24(1), 173–215, doi: 10.1193/1.2894832.

Choi Y., Stewart J.P. (2005). Nonlinear site amplification as function of 30 m shear wave velocity, *Earthq. Spectra*, 21(1): 1–30.

Cotton F., Scherbaum F., Bommer J.J., Bungum H. (2006). Criteria for selecting and adjusting ground-motion models for specific target regions: Application to central Europe and rock sites, *J. Seismology*, 10(2): 137–156, doi: 10.1007/s10950-005-9006-7.

Cramer C.H. (2003). Site specific seismic hazard analysis that is completely probabilistic, *Bull. Seismol. Soc. Am.*, 93: 1841–1846.

Delavaud E., Cotton F., Akkar S., Scherbaum F., Danciu L., Beauval C., Drouet S., Douglas J., Basili R., Sandikkaya M.A., Segou M., Faccioli E., Theodoulidis N. (2012). Toward a ground-motion logic tree for probabilistic seismic hazard assessment in Europe, *J. Seismology*, 16(3): 451–473, doi: 10.1007/s10950-012-9281-z.

Di Alessandro C., Bozorgnia Y., Abrahamson N.A., Akkar S., Erdik, M. (2012).GEM–PEER Global Ground Motion Prediction Equations Project: An Overview, *Proceedings, 15th World Conference on Earthquake Engineering*, Lisbon, Portugal.

Douglas J. (2002). Note on scaling of peak ground acceleration and peak ground velocity with magnitude, *Geophys. J. Inter.*, 148(2): 336–339.

Douglas J. (2003).Earthquake ground motion estimation using strong-motion records: A review of equations for the estimation of peak ground acceleration and response spectral ordinates, *Earth-Science Reviews*, 61(1–2): 43–104.

Douglas J. (2010). Consistency of ground-motion predictions from the past four decades, *Bull. Earthq. Eng.*, 8(6): 1515–1526. DOI 10.1007/s10518-010-9195-5.

Douglas J. (2011). Ground motion prediction equations 1964-2010, *PEER Report No. 2011/102*, Pacific Earthquake Engineering Research Center, University of California, Berkeley, CA.

Douglas J. (2012). Consistency of ground-motion predictions from the past four decades: Peak ground velocity and displacement, Arias intensity and relative significant duration, *Bull. Earthq. Eng.*, in press. DOI 10.1007/s10518-012-9359-6.

Douglas J., Bungum H., Scherbaum F. (2006). Ground-motion prediction equations for southern Spain and southern Norway obtained using the composite model perspective, *J. Earthq. Eng.*, 10(1): 33–72.

Douglas J., Faccioli E., Cotton F., Cauzzi C. (2009). Selection of ground-motion prediction equations for GEM1, *GEM Technical Report*, GEM Foundation, Pavia, Italy.

Douglas J., Cotton F., Abrahamson N.A., Akkar S., Boore D.M., Di Alessandro C. (2011). Pre-selection of ground-motion prediction equations (Task 2), PEER GEM–Global GMPEs Task 2 WG, URL www.nexus.globalquakemodel.org/gem-gmpes/posts/.

Douglas J., Cotton F., Di Alessandro C., Boore D.M., Abrahamson N.A., Akkar S. (2012). Compilation and critical review of GMPEs for the GEM-PEER global GMPEs project, *Proceedings, 15th World Conference on Earthquake Engineering*, Lisbon, Portugal.

Electric Power Research Institute (1993). Guidelines for determining design basis ground motions, Electric Power Research Institute, Vol. 1–5, *EPRI TR-102293*, Palo Alto, CA.

Electric Power Research Institute (2004). CEUS ground motion project final report, *Technical Report 1009684*. EPRI, Palo Alto, CA, Dominion Energy, Glen Allen, VA, Entergy Nuclear, Jackson, MS, and Exelon Generation Company, Kennett Square, PA.

Electric Power Research Institute (2006). Program on Technology Innovation: Truncation of the lognormal distribution and value of the standard deviation for ground motion models in the central and eastern United States, *Technical Report 1014381*, EPRI, Palo Alto, CA and U.S. Department of Energy, Germantown, MD.

Esteva L., Rosenblueth E. (1964). Espectros de temblores a distancias moderadas y grandes, *Boletin Sociedad Mexicana de Ingenieria Sesmica*, 2: 1–18, in Spanish.

Frankel A., Mueller C., Barnhard T., Perkins D., Leyendecker E.V., Dickman N., Hanson S., Hopper M. (1996). National Seismic-Hazard Maps: Documentation June 1996, U.S. Geological Survey, *USGS Open-File Report 96-532*. Menlo Park, CA.

Fukushima Y. (1996). Scaling relations for strong ground motion prediction models with M^2 terms, *Bull. Seismol. Soc. Am.*, 86(2): 329–336.

Garcia D., Singh S.K., Herraiz M., Ordaz M., Pacheco J.F. (2005). Inslab earthquakes of central Mexico: Peak ground-motion parameters and response spectra, *Bull. Seismol. Soc. Am.*, 95(6): 2272–2282, doi: 10.1785/0120050072.

Goulet C.A., Stewart J.P. (2009). Pitfalls of deterministic application of nonlinear site factors in probabilistic assessment of ground motions, *Earth. Spectra*, 25(3): 541–555.

Gülerce Z., Abrahamson N.A. (2011). Site-specific design spectra for vertical ground motion, *Earthq. Spectra*, 27(4): 1023–1047.

Kanno T., Narita A., Morikawa N., Fujiwara H., Fukushima Y. (2006). A new attenuation relation for strong ground motion in Japan based on recorded data, *Bull. Seismol. Soc. Am.*, 96(3): 879–897, doi: 10.1785/0120050138.

Kaklamanos J., Baise L.G., Boore D.M. (2011). Estimating unknown input parameters when implementing the NGA ground-motion prediction equations in engineering practice, *Earthq. Spectra*, 27: 1219–1235.

Kaklamanos J., Boore D.M., Thompson E.M., Campbell K.W. (2010). Implementation of the Next Generation Attenuation (NGA) ground-motion prediction equations in Fortran and R, *U.S. Geological Survey Open-File Report 2010-1296*, 43 pgs.

Lin P.-S., Lee C.-T. (2008). Ground-motion attenuation relationships for subduction-zone earthquakes in northeastern Taiwan, *Bull. Seismol. Soc. Am.*, 98(1): 220–240, doi:10.1785/0120060002.

McVerry G.H., Zhao J.X., Abrahamson N.A., Somerville P.G. (2006). New Zealand acceleration response spectrum attenuation relations for crustal and subduction zone earthquakes, *Bull. NZ Soc. Earthq. Eng.*, 39(4) 1–58.

Pezeshk S., Zandieh A., Tavakoli B. (2011). Hybrid empirical ground-motion prediction equations for eastern North America using NGA models and updated seismological parameters, *Bull. Seismol. Soc. Am.*, 101(4): 1859–1870, doi: 10.1785/0120100144.

Power M., Chiou B.S.-J., Abrahamson N.A., Bozorgnia Y., Shantz T., Roblee, C. (2008). An overview of the NGA project, *Earthq. Spectra*, 24(1): 3–21, doi: 10.1193/1.2894833.

Raghu Kanth, S.T.G., Iyengar R.N. (2006). Seismic hazard estimation for Mumbai city, *Current Science*, 91(11): 1486–1494.

Raghu Kanth S.T.G., Iyengar R.N. (2007). Estimation of seismic spectral acceleration in peninsular India, *J. Earth System Sci.*, 116(3): 199–214.

Rezaeian S., Bozorgnia Y., Idriss I.M., Campbell K.W., Abrahamson N.A., Silva W.J. (2012). Spectral damping scaling factors for shallow crustal earthquakes in active tectonic regions, *PEER Report 2012/01*, Pacific Earthquake Engineering Research Center, University of California, Berkeley. CA.

Scasserra G., Stewart J.P., Bazzurro P., Lanzo G., Mollaioli F. (2009). A comparison of NGA ground-motion prediction equations to Italian data, *Bull. Seismol. Soc. Am.*, 99(5) 2961–2978.

Scherbaum F., Cotton F., Smit, P. (2004). On the use of response spectral reference data for the selection and ranking of ground motion models for seismic hazard analysis in regions of moderate seismicity: The case of rock motion, *Bull. Seismol. Soc. Am.*, 94(6): 2164–2185.

Silva W.J., Gregor N., Darragh R. (2002). Development of regional hard rock attenuation relations for central and eastern North America, Technical Report, Pacific Engineering and Analysis, El Cerrito, CA.

Sokolov V., Bonjer K.-P., Wenzel F., Grecu B., Radulian M. (2008). Ground-motion prediction equations for the intermediate depth Vrancea (Romania) earthquakes, *Bull. Earthq. Eng.*, 6: 367–388.

Somerville P., Graves R.W., Collins N., Song S.G., Ni S., Cummins P. (2009). Source and ground motion models of Australian earthquakes, *Proceedings, 2009 Annual Conference of the Australian Earthquake Engineering Society*, Newcastle, Australia.

Stafford P.J., Strasser F.O., Bommer J.J. (2008). An evaluation of the applicability of the NGA models to ground motion prediction in the Euro-Mediterranean region, *Bull. Earthq. Eng.*, 6: 149–177.

Stewart J.P., Midorikawa S., Graves R.W., Khodaverdi K., Kishida T., Miura H., Bozorgnia Y., Campbell K.W. (2012). Implications of Mw 9.0 Tohoku-oki Japan earthquake for ground motion scaling with source, path, and site parameters, *Earthq. Spectra*, submitted.

Tavakoli B., Pezeshk S. (2005). Empirical-stochastic ground-motion prediction for eastern North America, *Bull. Seismol. Soc. Am.*, 95(6): 2283–2296.

Toro G.R. (2002). Modification of the Toro et al. (1997) attenuation equations for large magnitudes and short distances, Technical Report, Risk Engineering.

Toro G.R., Abrahamson N.A., Schneider J.F. (1997). Model of strong ground motions from earthquake in central and eastern North America: Best estimates and uncertainties, *Seismol. Res. Lett.*, 68(1): 41–57.

U.S. NRC (2012). Practical implementation guidelines for SSHAC Level 3 and 4 hazard studies, U.S. Nuclear Regulatory Commission, *Report NUREG-2117*, Washington, D.C.

Vilanova S.P., Fonseca J.F.B.D., Oliveira C.S. (2012). Ground-motion models for seismic hazard assessment in western Iberia: Constraints from instrumental data and intensity observations, *Bull. Seismol. Soc. Am.*, (1):169–184, doi: 10.1785/0120110097.

Youngs R.R., Chiou B.S.-J. Silva W.J., Humphrey J.R. (1997). Strong ground motion attenuation relationships for subduction zone earthquakes, *Seismol. Res. Lett.*, 68(1): 58–73.

Zhao J.X. (2010). Geometric spreading functions and modeling of volcanic zones for strong-motion attenuation models derived from records in Japan, *Bull. Seismol. Soc. Am.*, 100(2): 712–732, doi: 10.1785/0120090070.

Zhao J.X., Zhang J., Asano A., Ohno Y., Oouchi T., Takahashi T., Ogawa H., Irikura K., Thio H.K., Somerville P.G., Fukushima Y., Fukushima Y. (2006). Attenuation relations of strong ground motion in Japan using site classification based on predominant period, *Bull. Seismol. Soc. Am.*, 96(3): 898–913, doi: 10.1785/0120050122.

Appendix A: Project Plenary Meeting, May 2012

For completeness, this appendix presents the Microsoft Powerpoint slides that were shown to the expert panel during the project plenary meeting on May 17–18, 2012. Some slides have been slightly updated because of minor errors. These presentations contain many additional trellis plots and summarize all identified studies that compare the pre-selected GMPEs and observation ground motions and that comply with the study-selection criteria discussed in Section 4.1

Introduction to Task 3 “Select a Global Set of GMPEs” and Protocol for selection of GMPEs

John Douglas & Jonathan P. Stewart (co-chairs)

C. di Alessandro, D. M. Boore, Y. Bozorgnia
N. A. Abrahamson, E. Delavaud, P. J. Stafford, K. W. Campbell, M. Erdik & Mohammad B. Javanbarg

PEER

GEM
GLOBAL EARTHQUAKE MODEL

Objective

- To select, from the pre-selected GMPEs (Task 2), models for these regimes:
  - Stable continental regions (SCRs), which can possibly be divided further into shield and continental/foreland;
  - Subduction zones, which includes intraslab and interface earthquakes (and potentially fore-arc and back-arc locations);
  - Active regions with shallow crustal seismicity (ACRs);
  - Volcanic zones;
  - Areas of deep focus non-subduction earthquakes, such as Vrancea (Romania);
  - Areas where the travel paths are mainly through oceanic crust, such as coastal Portugal.
- No testing against observations undertaken due to time/data constraints
- Special consideration for final three regimes for which very few models exist
- Finally selected models should enable:
  - prediction of **PGA** and linear elastic (pseudo-)spectral acceleration (**PSA**) for 5% damping

  for:

  - **T** of main engineering interest (0 to roughly 4s);
  - **M** from roughly M_w 5 to the largest earthquakes (e.g. M_w~9.5 for subduction events);
  - **R** from ~0km to farthest distance of importance (e.g. ~1 000km in SCRs).

GMPEs for SCRs

1. **Atkinson [2008] as modified by Atkinson & Boore [2011]:**
   Referenced empirical model for eastern North America
2. **Atkinson & Boore [2006] as modified by Atkinson & Boore [2011]:**
   Extended stochastic model for eastern North America
3. **Campbell [2003]:**
   Hybrid model for eastern North America
4. **Douglas *et al*. [2006]:**
   Hybrid model for southern Norway
5. **Frankel *et al*. [1996] as parameterized by EPRI [2004]:**
   Stochastic model for eastern North America
6. **Raghu Kanth & Iyengar [2006, 2007]:**
   Stochastic model for peninsular India
7. **Silva *et al*. [2002]:**
   Stochastic model for eastern North America
8. **Somerville *et al*. [2009]:**
   Simulation-based models for Australia
9. **Pezeshk *et al*. [2011]:**
   Hybrid model for eastern North America
10. **Toro *et al*. [1997] modified by Toro [2002]:**
   Stochastic model for eastern North America

+ various variants to account for epistemic uncertainty

GMPEs for subduction

1. **BC Hydro [2011]:**
   Worldwide
2. **Arroyo *et al*. [2010]:**
   Interface model for Mexico (complementary to Garcia *et al*. [2005])
3. **Atkinson & Boore [2003]:**
   Worldwide
4. **Garcia *et al*. [2005]:**
   Intraslab model for Mexico (complementary to Arroyo *et al*. [2010])
5. **Kanno *et al*. [2006]:**
   Japan
6. **Lin & Lee [2008]:**
   Taiwan
7. **McVerry *et al*. [2006]:**
   New Zealand
8. **Youngs *et al*. [1997]:**
   Worldwide
9. **Zhao *et al*. [2006]:**
   Japan

GMPEs for ACRs

1. **Abrahamson & Silva [2008]:**
   NGA model using worldwide data
2. **Akkar & Bommer [2010]:**
   Model using Mediterranean and Middle Eastern data
3. **Boore & Atkinson [2008] as modified by Atkinson & Boore [2011]:**
   NGA model using worldwide data
4. **Campbell & Bozorgnia [2008]:**
   NGA model using worldwide data
5. **Cauzzi & Faccioli [2008]: updated by Faccioli *et al*. [2010]:**
   Model using worldwide data (mainly Japanese)
6. **Chiou & Youngs [2008]:**
   NGA model using worldwide data
7. **Kanno *et al*. [2006]:**
   Model using mainly Japanese data
8. **McVerry *et al*. [2006]:**
   Model using mainly New Zealand data
9. **Zhao *et al*. [2006]:**
   Model using mainly Japanese data

Aim

- GEM plans to conduct PSHA for the entire globe
- These calculations are time- and resource- hungry
- Need to keep the GMPE logic-trees as simple as possible (but no simpler)
- Reduce the:
  - 10+ models for SCRs;
  - 9 for subduction zones; and
  - 9 for ACRs

  to roughly 3 per regime
- Select GMPEs that cover the center, body and range of opinion
- Propose some workarounds for the special regimes
- Aim is not to replace regional logic-trees (e.g. SHARE and EMME)
- No logic-tree weights proposed
- New and/or updated GMPEs constantly being developed
- GMPEs proposed here are not a very long-term recommendation
- Within the core Task 3 group consensus reached
- Today we present this consensus for your comments and suggestions

Procedure

- Background information prepared (principally C. Di Alessandro, under direction of chairs)
  - Papers/reports collected, posted to pass-word protected website.
  - GMPEs coded in Matlab
  - Occasional contact with GMPE developers for necessary clarifications
  - Range of applicability selected by region
  - Trellis plots prepared (spectra, M-scaling, R-scaling, site-scaling, sigma)
  - GMPE – data comparisons summarized
- Materials distributed to Task 3 working group (WG)

Procedure

- Initial WG meeting to review materials, provide recommendations for needed revisions.
- Revised materials distributed with instructions for submitting selections.
- Second WG meeting. Discussion related to GMPE selection. Discussion of input received.
- All members of the WG were present for at least one of the meetings
- Consensus decision written by co-chairs and distributed to WG for comment.

Attributes considered in selection process

- Are the GMPEs local or global?
  - Suggest more weight to international.
  - Exception: local relations checked against earthquakes outside the study region.
  - N/A for SCRs
- Desirable attributes of the functional form. Examples:
  - Saturation with magnitude
  - Magnitude-dependent distance scaling; distance saturation effect; anelastic term (long distance).
- Epistemic uncertainty considerations:
  - When we have multiple GMPEs that are well constrained by data but exhibit different trends, we sought to capture those trends in the selected GMPEs

Attributes considered in selection process

- For SCRs:

– Derived from simulations.

– Hence, consideration given to the manner by which available data used to constrain input parameters

Attributes **not** considered

- Lack of site terms or undesirable form of site term (e.g., linear)
  - Hazard can be run for reference site & site term added
  - We have not provided site term recommendations
- Utilization in GMPE of parameters that are difficult to estimate
  - Examples: basin depth, depth to top of rupture,
  - Can be overcome with appropriate parameter selection protocols (e.g., Kaklamanos et al., 2011)

Information Compiled

- Trellis plots
- GMPE summary tables (functional forms, etc.)
- GMPE – data comparisons

Trellis Plots

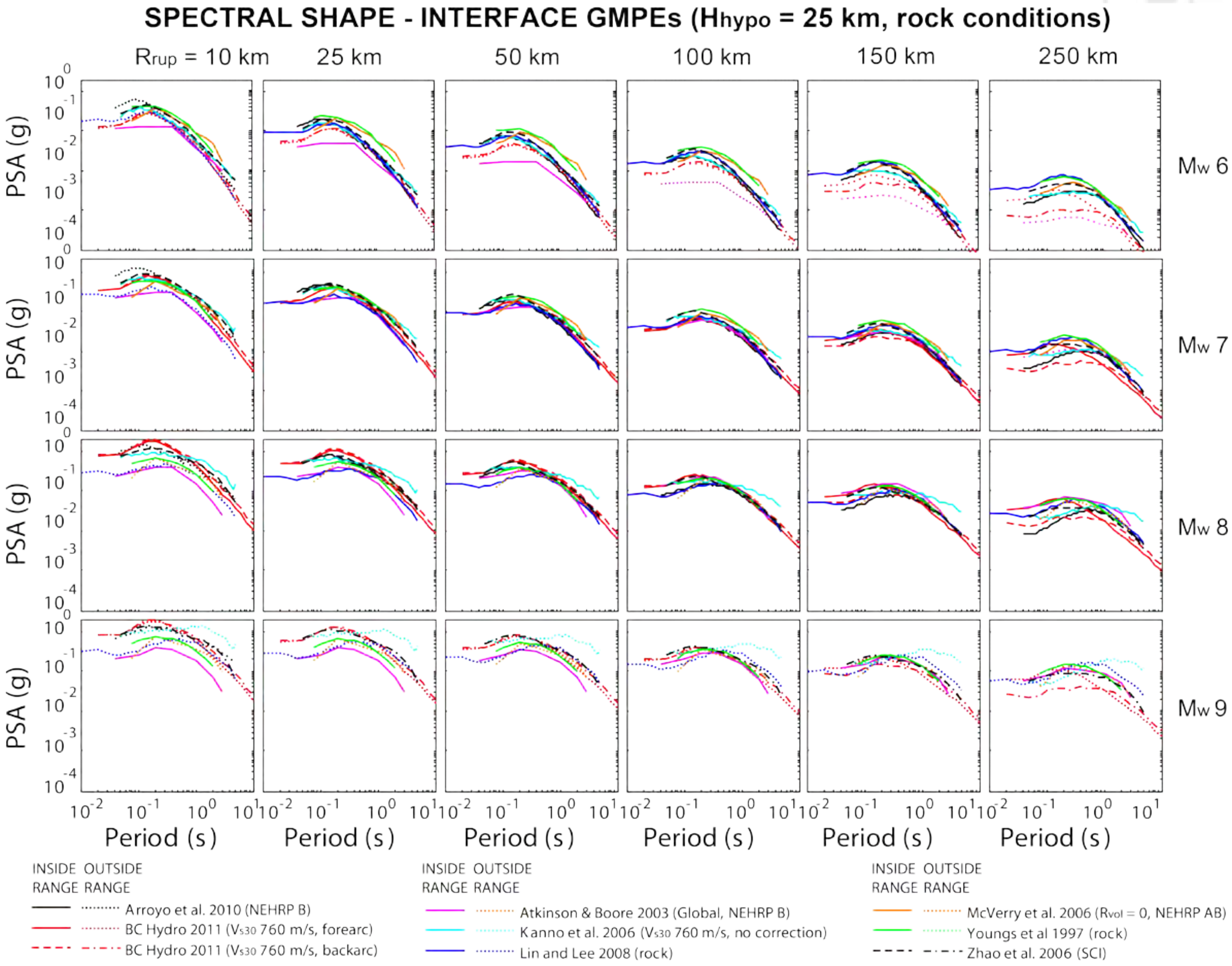

SPECTRAL SHAPE - INTERFACE GMPEs (H_{hypo} = 25 km, rock conditions)

Summary Tables

MODEL	RECORDS (H)	EVENTS	Mw	DIST. (km)	H (km)	SITEs
BC Hydro (2011)	Interface 1378 Intraslab 3946	Interface 46 Intraslab 76	Interface 6.5 - 8.4 Intraslab 5 - 7.9	Interface 5 - 551 Intraslab 34 – 991	Interface < 30 Intraslab > 30	Continuous (Vs30)
Arroyo et al (2010)	Interface 418	Interface 40	Interface 5.0 - 8.0	Interface 20 - 400	Interface 10 – 29	3 (NZ classes)
Atkinson & Boore (2003)	Interface 349 Intraslab + crustal 761	Interface 49 Intraslab + crustal 30	Interface 5.5 - 8.3 Intraslab 5 - 7.9	Interface 5 – 420 Intraslab 34 – 575 (r300)	Interface < 50 Intraslab 50 – 100	4 (Vs30; NEHRP B to E)
Garcia et al. (2005)	Intraslab 267	Intraslab 16	Intraslab 5.2 - 7.4	Intraslab 40 – 400	Intraslab 35 - 138 (m75)	N/A (Sites NEHRP B)
Kanno et al. (2006)	Interf. + cr. 3769 Intraslab 8150	Interf. + cr. 83 Intraslab 111	Interf.+ cr. 5.2 - 8.2 Intraslab 5.5 – 8	Interface 1 - 400 Intraslab 30 – 500	Shallow < 30 Deep 30 - 180	Cont. (Vs30)
Lin & Lee (2008)	Interface 873 Intraslab 3950	Interface 17 Intraslab 37	Interface 5.3 - 8.1 Intraslab 4.1 – 6.7	Interface 20 - 40 Intraslab 40 - 600	Interface 4 - 30 Intraslab 43 - 161	2 (Vs30; NEHRP B,C or D,E)
McVerry et al. (2006)	535 Subduct. + crustal	Interface 6 Intraslab 19	5.08 – 7.09	6 - 400	Interf. 15 – 24 Intrasl. 26 - 50 50 - 149	3 (NZ classes)
Youngs et al. (1997)	Interface 181 Intraslab 53	Interface 57 Intraslab 26	Interface 5 - 8.2 Intraslab 5 - 7.8	Interface 8.5 - 551 Intraslab 45 – 774	10 – 229 (not distinguished)	2 (Rock/Soil)
Zhao et al. (2006)	Interface 1508 Intraslab 1725 Crustal 1285	289 (not distinguished)	5.0 - 8.3 (not distinguished)	0 - 300 (not distinguished)	Interf. 10 - 50 Intraslab 15–162 (c125)	5 (HR + 4 Jap. Rail. Ass., Tg)

Summary Tables

MODEL	MAGNITUDE TERM(s)	NOTES	Mw RANGE
BC Hydro (2011)	$f_{Mag}(M) = \begin{cases} \theta_4 * (M - (C_1 + \Delta C_1)) + \theta_{13} * (10 - M)^2 & for \quad M \le C_1 + \Delta C \\ \theta_5 * (M - (C_1 + \Delta C_1)) + \theta_{13} * (10 - M)^2 & for \quad M > C_1 + \Delta C \end{cases}$ $(\theta_2 + \theta_{14} * F_{event} + \theta_3 * (M - 7.8)) * \ln(R + C_4 * \exp[(M-6) * \theta_9])\cdot$	Break in magnitude scaling atc1 = 7.8, +- period dependent variation (deltaC1) refined after Maule and Tohoku events	Interface 6.5 - 8.4
Arroyo et al (2010)	$\alpha_2(T)\ M_w \quad ; \quad r_0^2 = 1.4447 \times 10^{-5} e^{2.3026 M_w}$	Allows for oversaturation	Interface 5.0 - 8.0
Atkinson & Boore (2003)	$fn(\mathbf{M}) = c_1 + c_2\ \mathbf{M}$ $\Delta = 0.00724 \times 10^{0.507\mathbf{M}}$ $g = 10^{(1.2 - 0.18\mathbf{M})}$	use M=8.5 for interface events of M>8.5 The interface events show a much more pronounced magnitude dependence to the attenuation. Amplitudes at large Mw controlled by Cascadia events which differ by more than a factor of 2 from those in Japan for the same conditions.	Interface 5.5 - 8.3
Kanno et al. (2006)	$a_1 M_w \quad ; \quad - \log(X + d_1 \cdot 10^{e_1 M_w})$	Mainly controlled by crustal events at short distances for shallow model	Interf.+ cr. 5.2 - 8.2
Lin & Lee (2008)	$C_2 M_i + C_3 \ln(R_{ij} + \alpha_1 e^{\alpha_2 M_i})$		Interface 5.3 - 8.1
McVerry et al. (2006)	$C_{11}(T) + \underline{C_{12}^{*}(T)}\,(M-6) + C_{13Y}(T)(10-M)^3$ $+C_{17}(T)\ln(r + C_{18Y}\exp(C_{19Y}\,M))$ where $\underline{C_{12}^{*}(T)} = C_{12Y} + (C_{17Y}(T) - C_{17}(T))\,C_{19Y}$		5.08 – 7.09

GMPE-Data Comparisons

- We neglect (generally) studies emphasizing IM vs R and GMPE median
- We seek a meaningful analysis of residuals.

Two approaches generally taken:

- Overall goodness-of-fit (Scherbaum et al, 2004; Stafford et al., 2008)
- Residuals vs. predictive parameters: M, R, etc. (Scasserra et al. 2009)

GMPE-Data Comparisons

Overall goodness-of-fit approach

- Select data within range of model
- Calculate residuals

Data

$$Z_{T,ij} = \frac{\ln\left(IM_{obs,ij}\right) - \ln\left(IM_{\mathrm{mod},ij}\right)}{\sigma_T}$$

GMPE

- Plot histogram of $Z_{t,ij}$
- Compare to standard normal variate

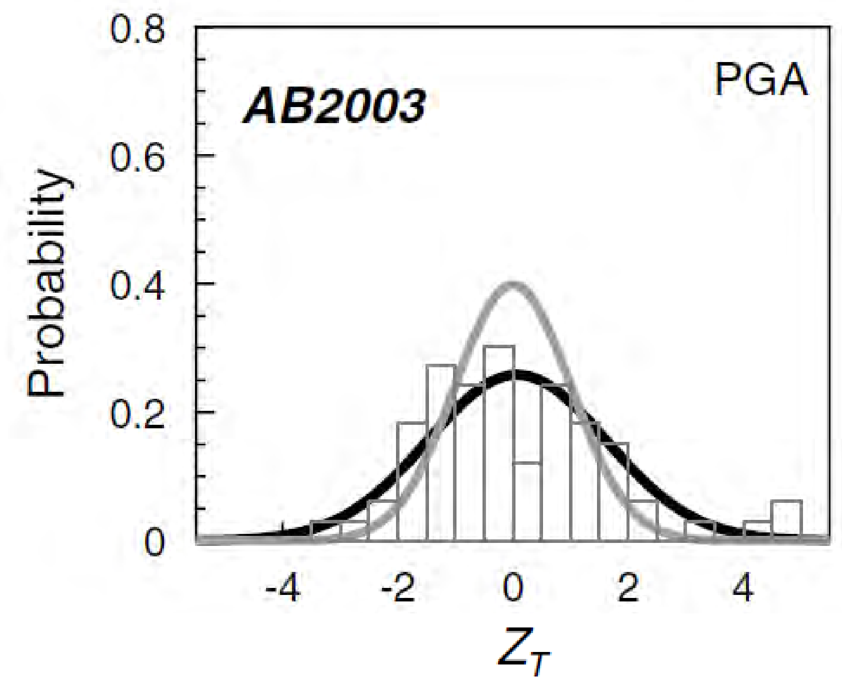

Scherbaum et al. (2004);
Stafford et al. (2008)

GMPE-Data Comparisons

Overall goodness-of-fit approach

- Select data within range of model
- Calculate residuals

Data

$$Z_{T,ij} = \frac{\ln\left(IM_{obs,ij}\right) - \ln\left(IM_{\mathrm{mod},ij}\right)}{\sigma_T}$$

GMPE

- Plot histogram of $Z_{t,ij}$
- Compare to standard normal variate

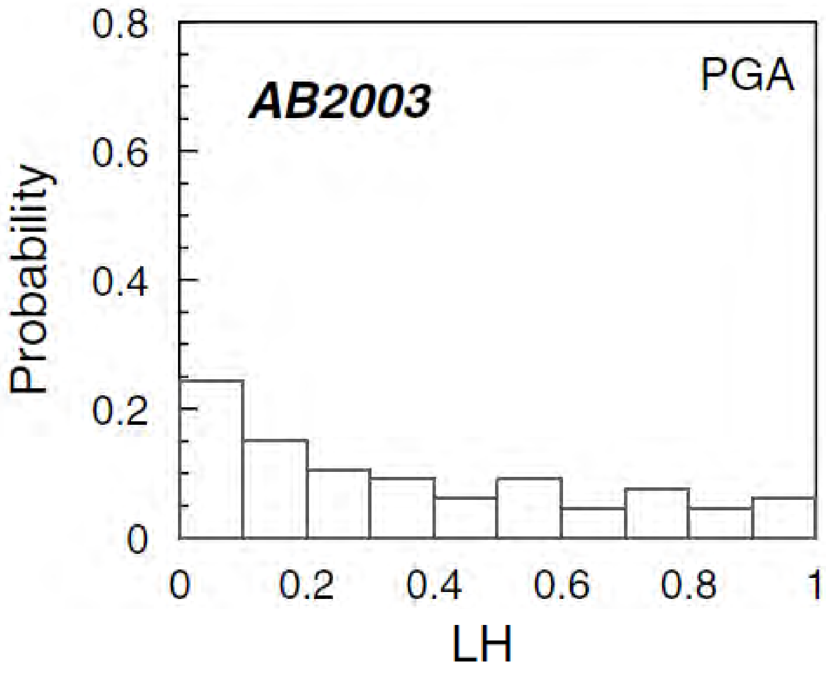

Scherbaum et al. (2004);
Stafford et al. (2008)

GMPE-Data Comparisons

Overall goodness-of-fit approach

- Select data within range of model
- Calculate residuals

Data

$$Z_{T,ij} = \frac{\ln\left(IM_{obs,ij}\right) - \ln\left(IM_{\mathrm{mod},ij}\right)}{\sigma_T}$$

GMPE

- Plot histogram of $Z_{t,ij}$
- Compare to standard normal variate

Grade	Med LH	$Z_{T,med}$, μ_Z	σ_Z
A	> 0.4	<0.25	<1.125
B	> 0.3	<0.5	<1.25
C	> 0.2	<0.75	<1.5
D			

Scherbaum et al. (2004);
Stafford et al. (2008)

GMPE-Data Comparisons

Overall goodness-of-fit approach

- Can obscure misfits

Zero mean
Small std. dev.

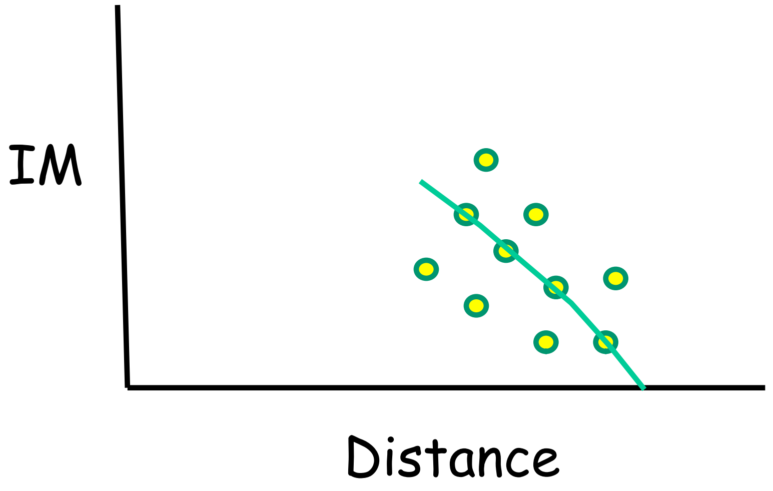

Zero mean
Larger std. dev.

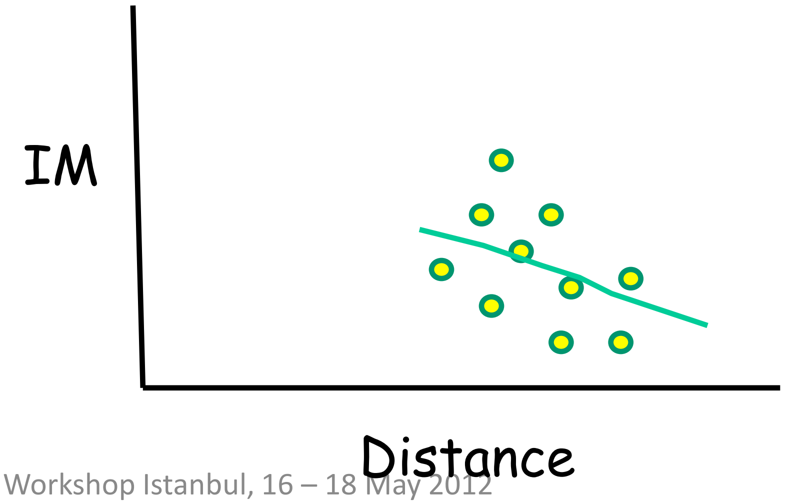

GMPE-Data Comparisons

Overall goodness-of-fit approach

- LLH Interpretation
- KL divergence between models *g* and *f*

$$D(f,g) = E_f[\log_2(f)] - E_f[\log_2(g)],$$

  - *f* = nature (observed).
    Unknown but drops out in model comparisons
  - *g* = conditional PDF from GMPE
    (given M, R, etc at stations)
  - Second term approximated as: $\mathrm{LLH}(g,\mathbf{x}) := -\frac{1}{N}\sum_{i=1}^{N}\log_2(g(x_i)),$
- LLH: measure of the distance between model and the data-generating distribution

Scherbaum et al., 2009; Delavaud et al. 2012

GMPE-Data Comparisons

Overall goodness-of-fit approach

- LLH Interpretation

Model 0: *f*

Models i; Variations of mean and standard deviation relative to 0

Increasing LLH indicates worsening fit

Procedure for assigning wts

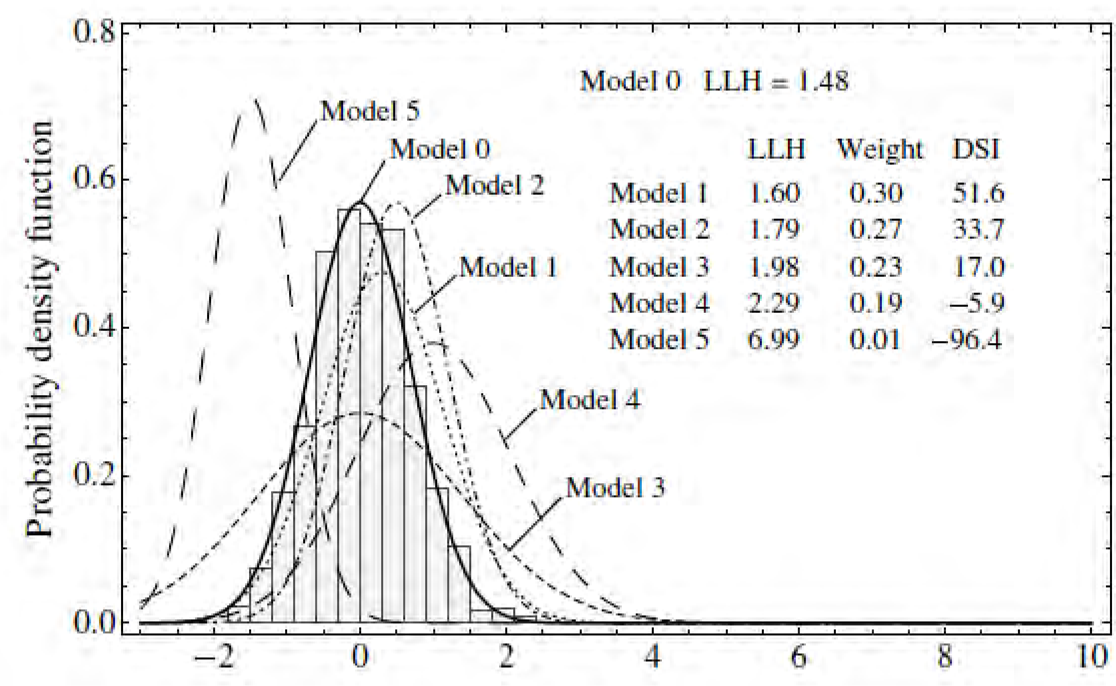

	LLH	Weight	DSI
Model 1	1.60	0.30	51.6
Model 2	1.79	0.27	33.7
Model 3	1.98	0.23	17.0
Model 4	2.29	0.19	−5.9
Model 5	6.99	0.01	−96.4

Scherbaum et al., 2009; Delavaud et al. 2012

GMPE-Data Comparisons

Residual trends approach

- Select data within range of model
- Calculate residuals $R_{i,j} = \ln\left(IM_{i,j}\right)_{data} - \ln\left(IM_{i,j}\right)_{gmpe,\mu}$
- Random effect analysis: Separate event term (η_i) from within-event residual ($\varepsilon_{i,j}$)

$$R_{i,j} = c + \eta_i + \varepsilon_{i,j}$$

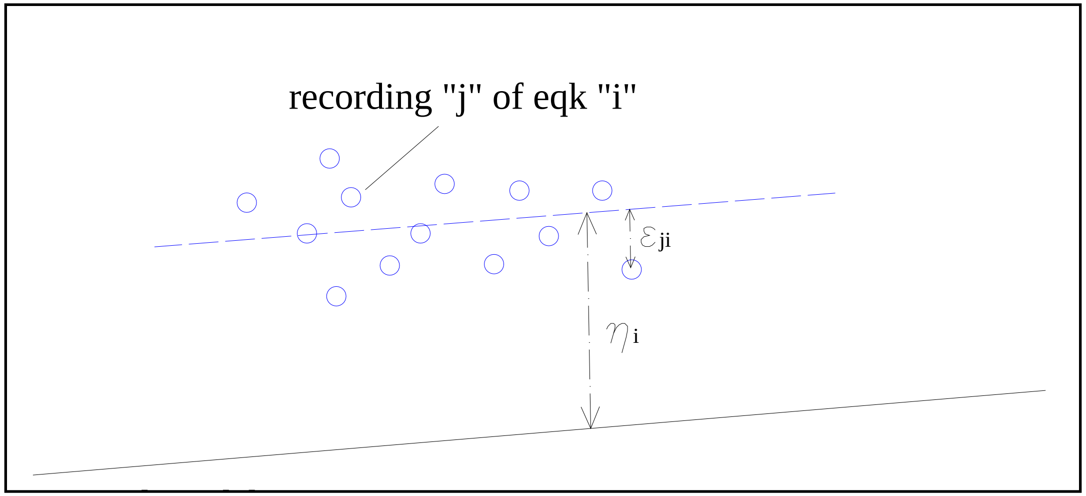

Scasserra et al. (2009)

GMPE-Data Comparisons

Residual trends approach

- Select data within range of model
- Calculate residuals
- Random effect analysis: Separate event term (η_i) from within-event residual ($\varepsilon_{i,j}$)
- Evaluate M-dependence from η_i
- Evaluate R-dependence from $\varepsilon_{i,j}$

Scasserra et al. (2009)

GMPE-Data Comparisons

Residual trends approach

- Check of distance scaling (Chilean example)

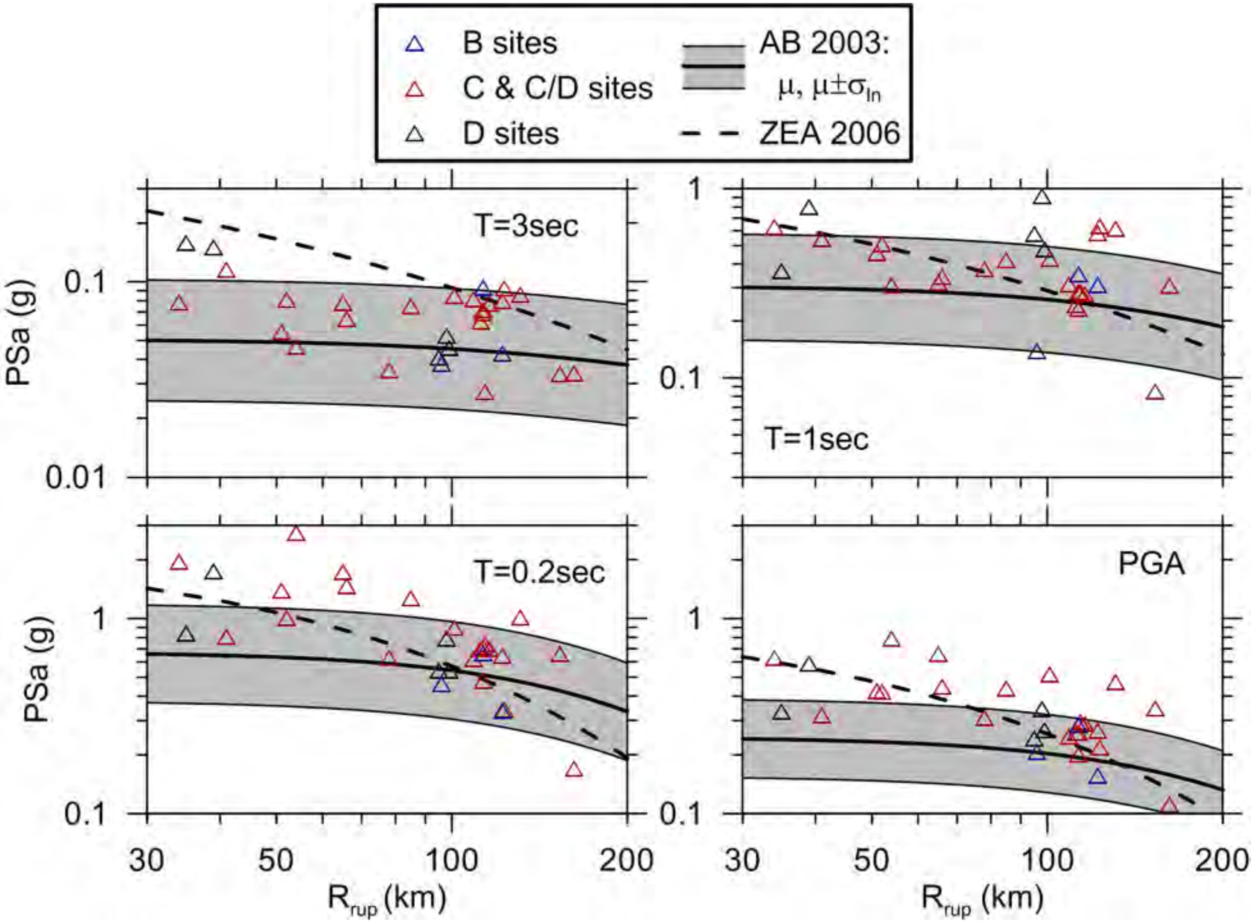

Boroschek et al. (2012)

GMPE-Data Comparisons

Residual trends approach

- Check of distance scaling (Chilean example)

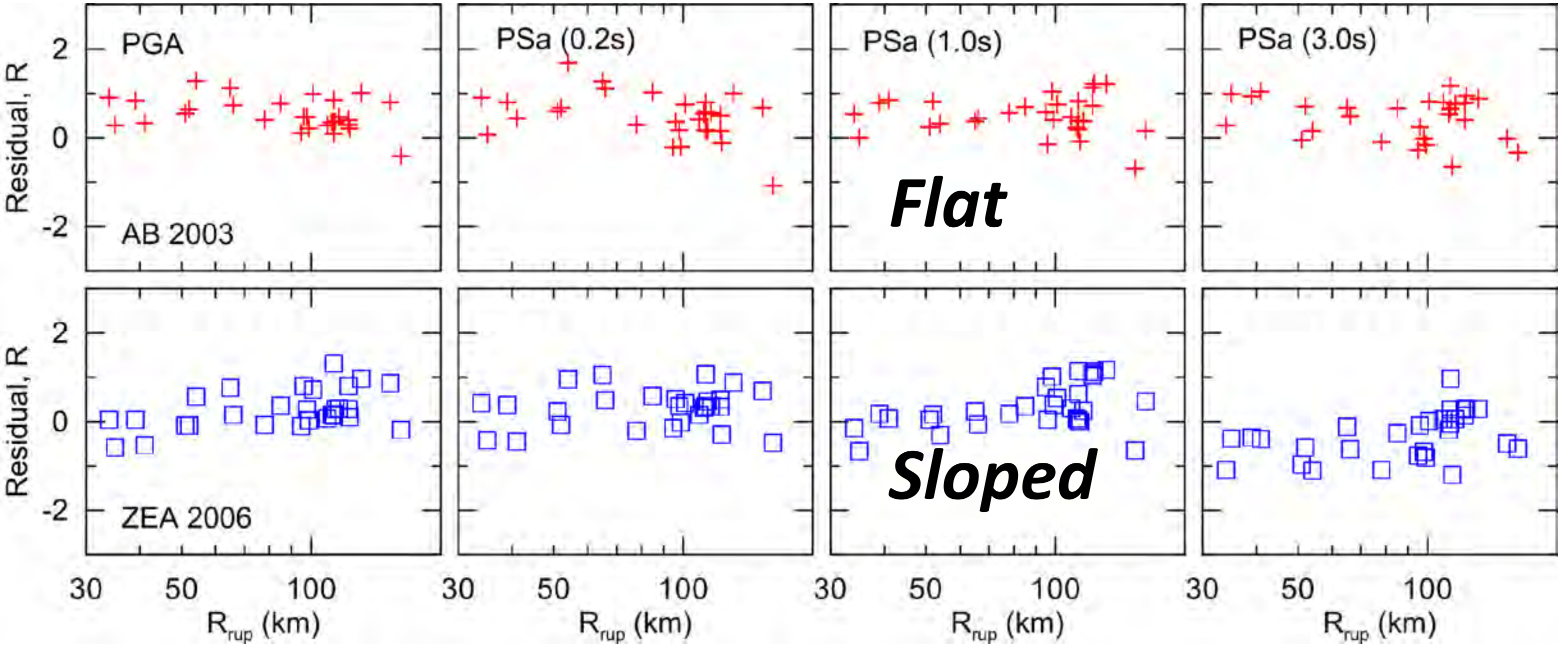

Flat

Sloped

Boroschek et al. (2012)

GMPE-Data Comparisons

Residual trends approach

- Check of distance scaling (Chilean example)
- Check of magnitude scaling (Italian example)

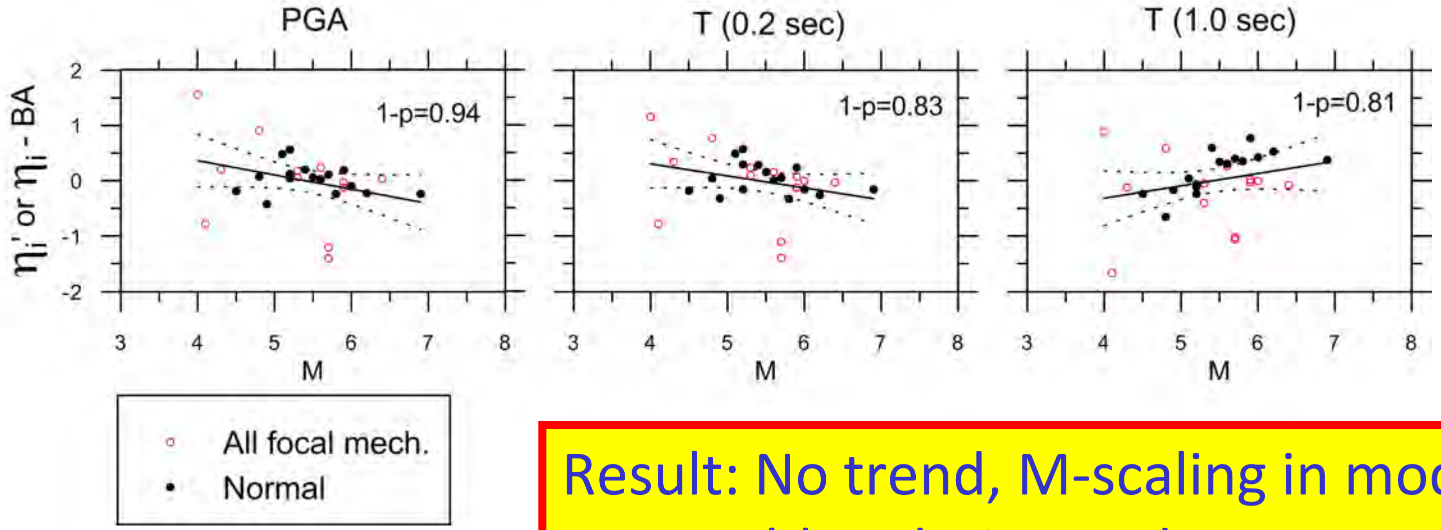

Result: No trend, M-scaling in model acceptable relative to data set.

Scasserra et al. (2009)

GMPE-Data Comparisons

Residual trends approach

- Check of standard deviation terms (Italian example)

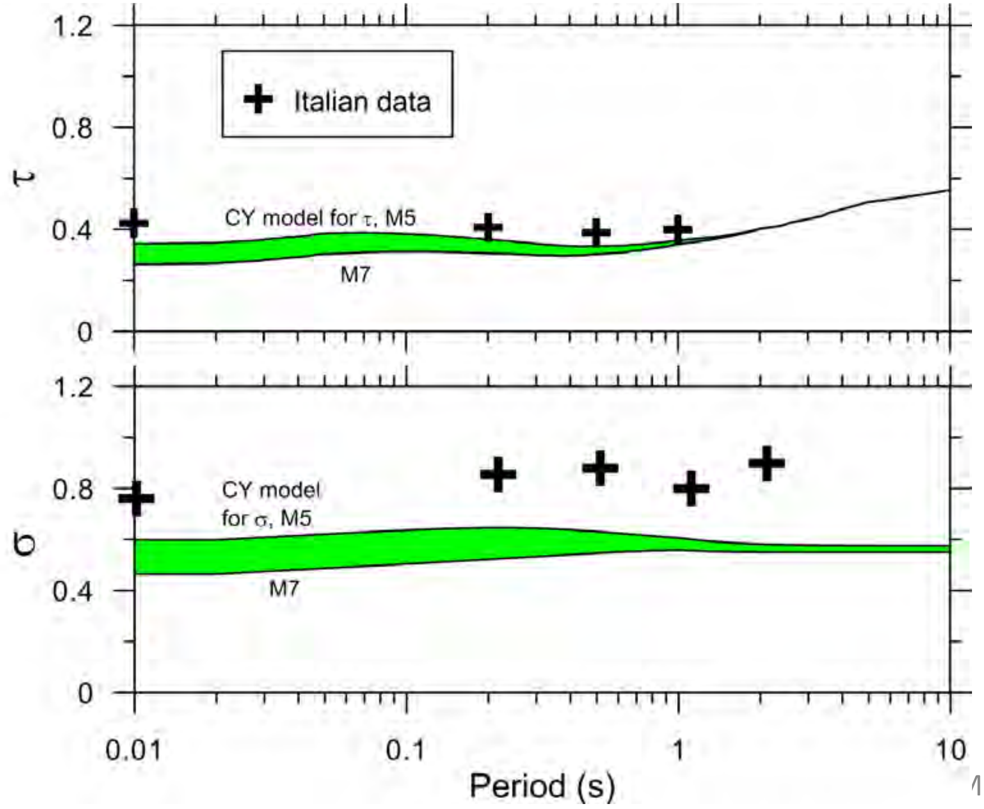

Scasserra et al. (2009)

GMPE Selection

- Each WG member considers available data (trellis plots, tables, GMPE-data comparisons)
- No formal point system. Relative weight given to each information source variable.
- All have opportunity to present their opinion in conference calls or emails
- Selections submitted either via confidential email or openly expressed in call.

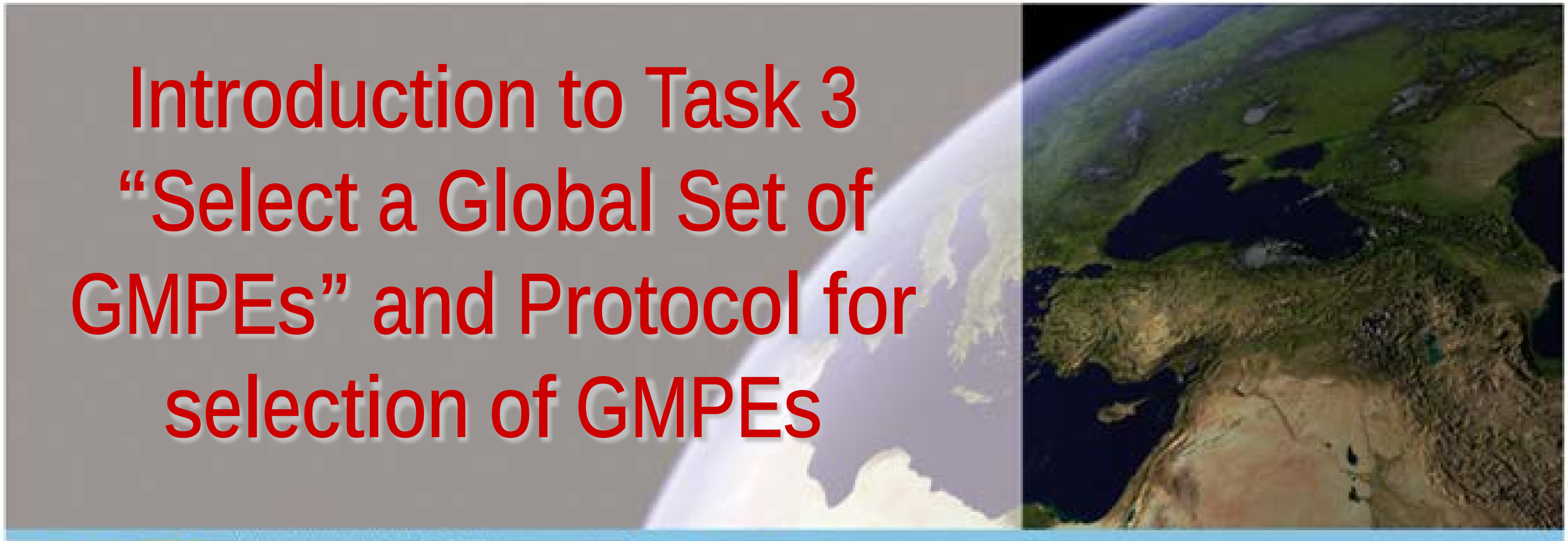

Introduction to Task 3 “Select a Global Set of GMPEs” and Protocol for selection of GMPEs

John Douglas & Jonathan P. Stewart (co-chairs)

C. di Alessandro, D. M. Boore, Y. Bozorgnia
N. A. Abrahamson, E. Delavaud, P. J.
Stafford, K. W. Campbell, M. Erdik &
M. B. Javanbarg

PEER

GEM
GLOBAL EARTHQUAKE MODEL

Consideration of ‘special’ regimes

John Douglas & Jonathan P. Stewart (co-chairs)

C. di Alessandro, D. M. Boore, Y. Bozorgnia
N. A. Abrahamson, E. Delavaud, P. J. Stafford, K. W. Campbell, M. Erdik &
M. B. Javanbarg

+ G. McVerry

Vrancea-type events

- Deep non-subduction events (nests) occur in, e.g.:
  - Vrancea (Romania) – high seismic risk in Bucharest (e.g. 1940, 1977) from these earthquakes
  - Bucaramanga (Colombia)
  - Hindu Kush (Afghanistan)
- Vrancea is the most important for GEM
- It is thought to be the only one with accelerometric data
- Only Sokolov et al. (2008) has published GMPE for spectral ordinates
  - One model not sufficient to model high epistemic uncertainty
  - Model is not ideal for GEM (e.g. azimuthal dependency)
- Proposed plan for a workaround for this zone
  - Using referenced-empirical technique of Atkinson (2008)
  - Collect freely available data
    - Only 4 earthquakes and about 30 records for Vrancea
    - Any data from either of the other locations?
  - Compare observations with the intraslab selected GMPEs using residual plots
  - Propose simple adjustment factors to improve fit between observations and predictions

Oceanic-path events

- Non-subduction earthquakes with oceanic-paths occur, e.g.:
  - Off Portuguese coast, e.g. Lisbon (1755) earthquake
  - Off north Californian coast (Gorda)
- Both these areas have accelerometric data, particularly Gorda
- No GMPEs include terms for this type of path
- Previous studies used SCR and intraslab GMPEs
- Proposed plan for a workaround for this zone
  - Using referenced-empirical technique of Atkinson (2008)
  - Collect freely available data:
    - From Portugal (Vilanova et al., 2012): 6 earthquakes and about 50 records
    - From Gorda (PEER): 8 earthquakes and about 20 records
    - Any others?
  - Compare observations with the intraslab/SCR selected GMPEs using residual plots
  - Propose simple adjustment factors to improve fit between observations and predictions

Volcanic-path

- Additional attenuation from travel paths through volcanic zones, e.g.:
  - New Zealand
  - Iceland
  - Japan

Volcanic GMPEs

-An approach for GEM ground-motion modelling

Graeme McVerry

GEM GMPEs meeting Istanbul
17-18 May 2012

Interpretation of GMPEs for “Volcanic zones”

- Are we dealing with
  - “volcanic earthquakes” (Task 1a & 2 reports) with Mw up to 5.5 & usually much less (de Natale et al 1998; Faccioli et al 2010); or
  - earthquakes with paths through low-Q zones associated with volcanic rifting zones landwards of subducting interfaces (McVerry et al 2006 in New Zealand and Zhao 2010 in Japan i.e. “standard” Mw 5+ earthquakes in “volcanic regions”)

Low-Q and high attenuation rates in volcanic & mantle-wedge zones

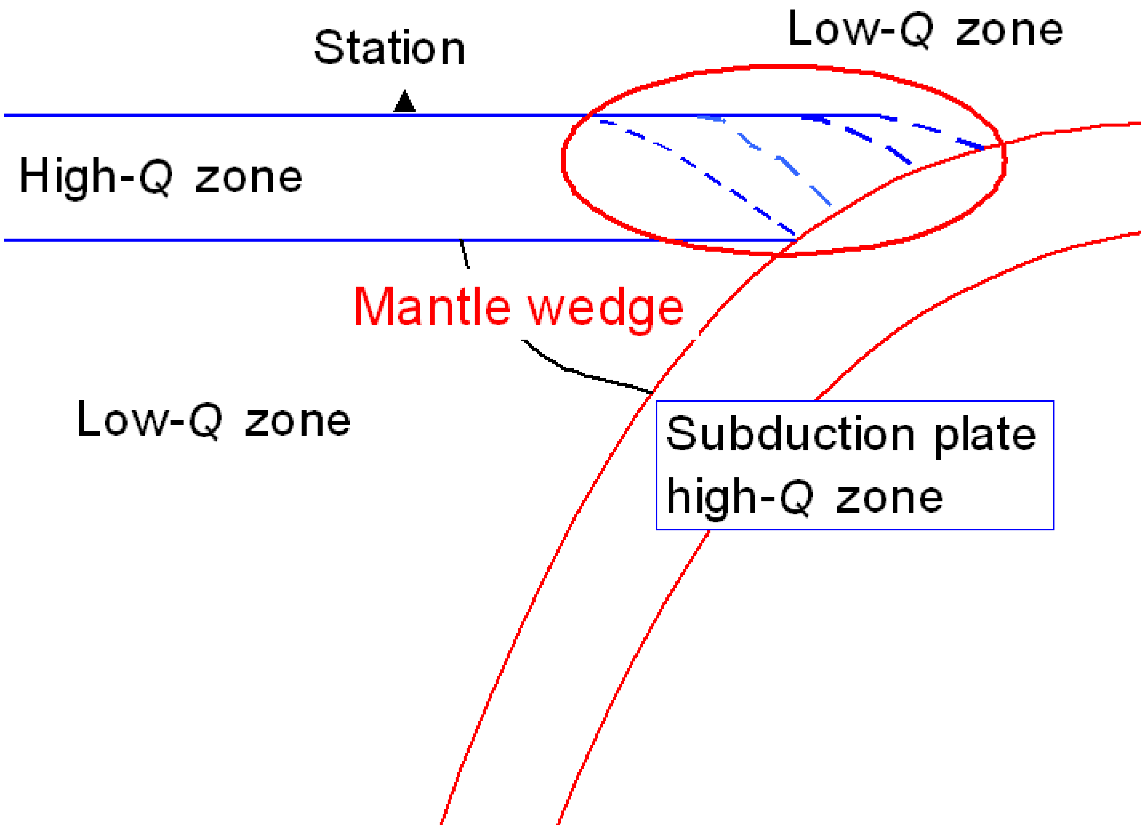
Station
Low-Q zone
High-Q zone
Mantle wedge
Low-Q zone
Subduction plate high-Q zone

Kindly provided by John Zhao, BSSA April 2010

Rapid attenuation in active volcanic regions

- Active volcanic regions often show rapid attenuation i.e. low Q (and Vs)
- Can be handled in GMPEs by the addition of an anelastic attenuation term for the volcanic path length R_{vol}
- Low-attenuation slab, high-attenuation mantle geometries for deeper slab events tend to be more complicated

Functional form

- $\ln SA_{volc}(T,M,R) = \ln SA_{standard}(T,M,R) - C_{vol}(T)R_{vol}$

- Anelastic attenuation term $C_{standard}(T)R$ in standard models often not statistically significant unless data extends beyond about 100 km, & often omitted in GMPEs
- Volcanic path length R_{vol} may be only part of total source-to-site distance R
- “Referenced empirical” approach

High volcanic-path attenuation rates $C_{vol}(T)$

- ~10^{-2} to $4x10^{-2}$ km^{-1} for Taupo Volcanic Zone (TVZ) in New Zealand
- ~10^{-3} to 10^{-2} km^{-1} additional to $C_{standard}$ in Japanese volcanic fronts
- $C_{standard}(T)$~10^{-3} to 10^{-2} km^{-1}
- Volcanic-path attenuation rates greatest at high-frequencies (e.g. pga and short spectral periods 0s-0.5s)
- Additional attenuation small at periods longer than about 2-3s

Effect of volcanic-path term for Taupo Volcanic Zone-path data

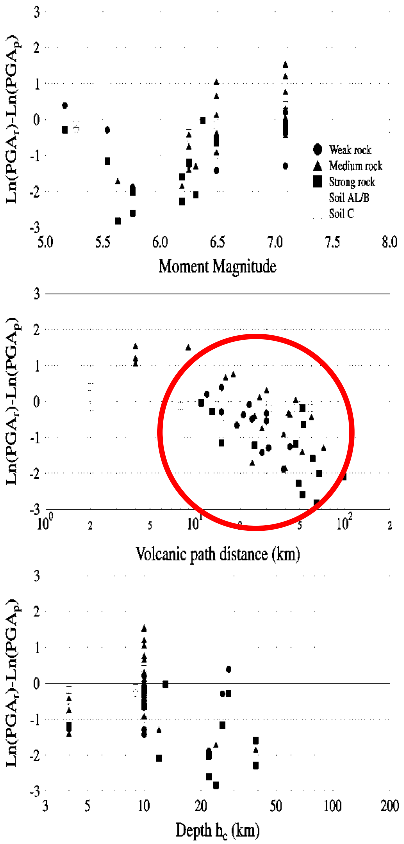

No volcanic-path term – note trend of residuals with volcanic path length

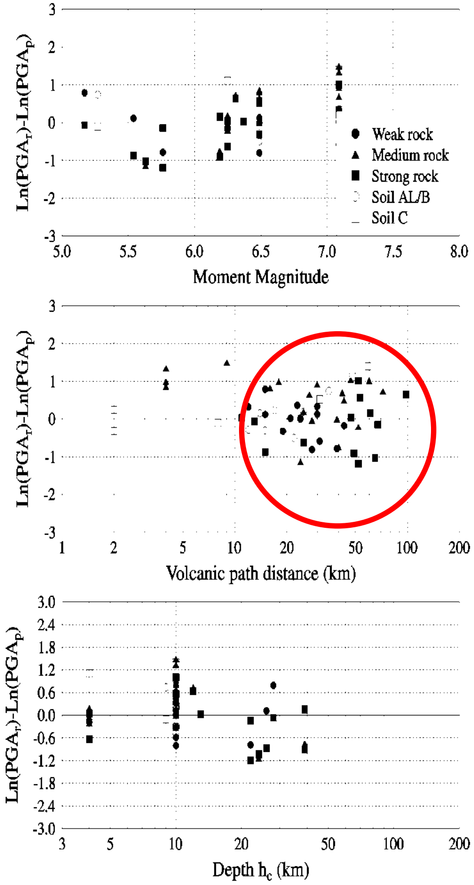

Volcanic-path term - removes trend of residuals with volcanic path length (and depth)

Increased volcanic attenuation

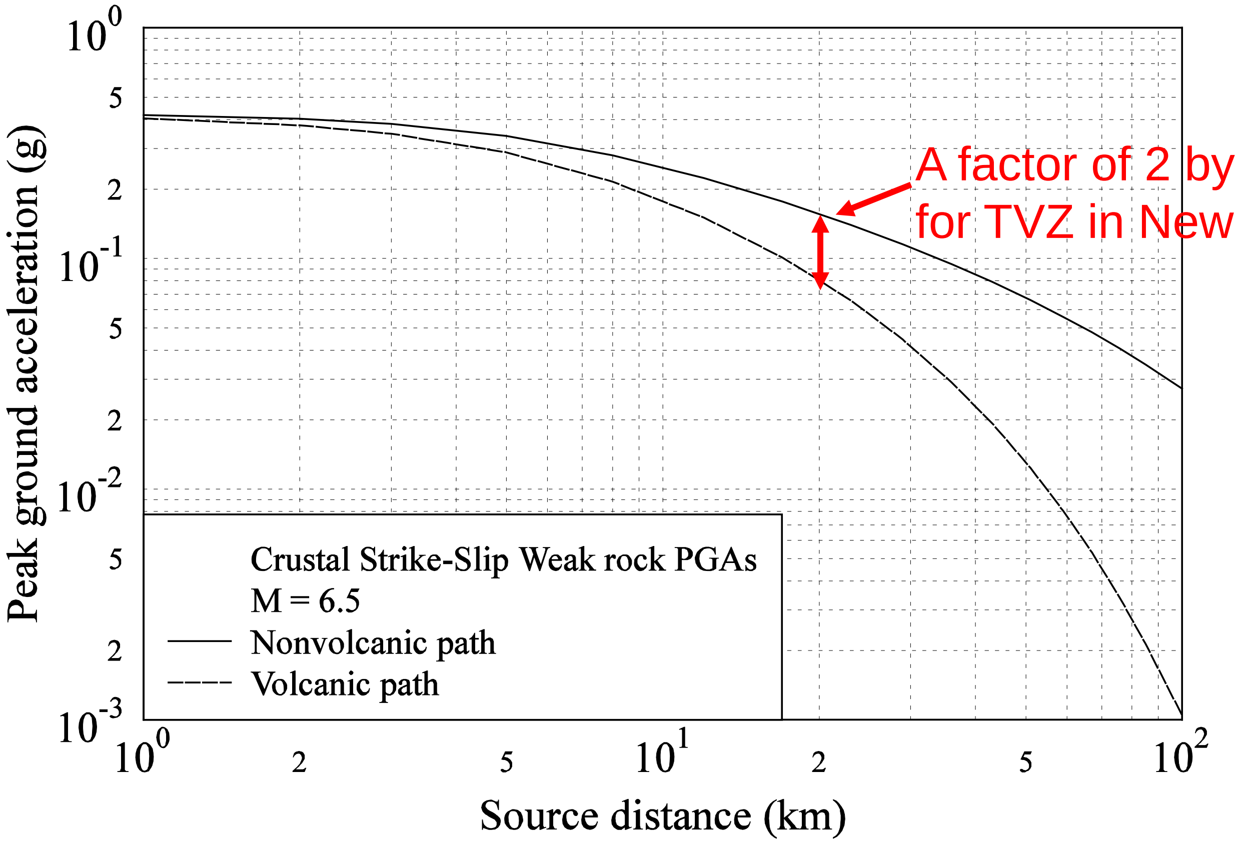

A factor of 2 by 20 km distance for TVZ in New Zealand

Examples of GMPEs including volcanic-path attenuation

- McVerry et al. (BNZSEE, 39(1):1-58, March 2006)
  - implemented for crustal and shallow slab events with paths through Taupo volcanic zone in New Zealand
- Zhao (BSSA, 100(2):712-732, April 2010)
  - Functional forms and plots but no coefficients for active volcanic fronts in Japan
- Dhakal, Takai & Sasatani (Eq. Eng. & Struct. Dynamics, 39:443-461, 2010)
- Ghofrani & Atkinson (BSSA 101(6), 3032-3045, December 2011)
  - Geometrical spreading rates depend on distance, important for determining anelastic attenuation rates
- Kanno et al (BSSA 96(3),879-897, June 2006)
  - Depends on distance from trench and depth
- Bradley (2010) modified Chiou et al (2010) for New Zealand to include volcanic-path attenuation among other changes

PSHA modelling including volcanic path effect

- In New Zealand, volcanic path effect is most important for limiting ground-motion estimates arising from the high seismicity volcanic zone
- Avoid calculating volcanic path length by approximate treatment of applying volcanic attenuation to full-path length for events occurring in volcanic region

Consideration of ‘special’ regimes

John Douglas & Jonathan P. Stewart (co-chairs)
C. di Alessandro, D. M. Boore, Y. Bozorgnia
N. A. Abrahamson, E. Delavaud, P. J. Stafford, K. W. Campbell, M. Erdik &
M. B. Javanbarg
+ G. McVerry

PEER

GEM
GLOBAL EARTHQUAKE MODEL

Preliminary selected GMPEs for Subduction Regions

Jonathan P. Stewart & John Douglas (co-chairs)

C. di Alessandro, D. M. Boore, Y. Bozorgnia
N. A. Abrahamson, E. Delavaud, P. J.
Stafford, K. W. Campbell, M. Erdik &
Mohammad B. Javanbarg

PEER

GEM
GLOBAL EARTHQUAKE MODEL

Pre-selected GMPEs

1. **BC Hydro [2012]:**
   Worldwide
2. **Arroyo *et al*. [2010]:**
   Interface model for Mexico (complementary to Garcia *et al*. [2005])
3. **Atkinson & Boore [2003]:**
   Worldwide
4. **Garcia *et al*. [2005]:**
   Intraslab model for Mexico (complementary to Arroyo *et al*. [2010])
5. **Kanno *et al*. [2006]:**
   Japan
6. **Lin & Lee [2008]:**
   Taiwan
7. **McVerry *et al*. [2006]:**
   New Zealand
8. **Youngs *et al*. [1997]:**
   Worldwide
9. **Zhao *et al*. [2006]:**
   Japan

Reminder of procedure

- **Principles previously agreed upon:**

1. Giving more weight to GMPEs derived from international data sets than from local data sets. Exceptions can be made when a GMPE derived from a local data set has been checked internationally and found to perform well.

2. Giving more weight to GMPEs that have attributes to their functional form that we consider desirable, including saturation with magnitude, magnitude dependent distance scaling and anelastic attenuation terms.

3. If we have multiple GMPEs that are well constrained by data but exhibit different trends, it is desirable to capture those trends in the selected GMPEs to properly represent epistemic uncertainty.

- **Trellis plots**
- **Results of (quantitative) testing of models against independent sets of data**
- **Circulation of available plots and results of testing**
- **Independent selections (of ~3 models) sent to WG facilitators**
- **Discussion of selections and consensus decision taken within core**

- **Today we would like your feedback and suggestions**

Subduction GMPEs pre-selected (page 1)

MODEL	RECORDS	EVENTS	M_w	DIST. (km)	H (km)	SITE Parameters
BC Hydro (2012)	Interface 1378 Intraslab 3946	Interface 46 Intraslab 76	Interface 6.5 - 8.4 Intraslab 5 - 7.9	Interface 5 - 551 Intraslab 34 – 991	Interface < 30 Intraslab > 30	Continuous (V_{s30})
Arroyo et al (2010)	Interface 418	Interface 40	Interface 5.0 - 8.0	Interface 20 - 400	Interface 10 – 29	N/A (NEHRP B only)
Atkinson & Boore (2003)	Interface 349 Intraslab + crustal 761	Interface 49 Intraslab + crustal 30	Interface 5.5 - 8.3 Intraslab 5 - 7.9	Interface 5 – 420 Intraslab 34 – 575 (r300)	Interface < 50 Intraslab 50 – 100	4 (Vs30; NEHRP B to E)
Garcia et al. (2005)	Intraslab 267	Intraslab 16	Intraslab 5.2 - 7.4	Intraslab 40 – 400	Intraslab 35 - 138 (m75)	N/A (NEHRP B only)
Kanno et al. (2006)	Interf. + cr. 3769 Intraslab 8150	Interf. + cr. 83 Intraslab 111	Interf.+ cr. 5.2 - 8.2 Intraslab 5.5 – 8	Interface 1 - 400 Intraslab 30 – 500	Shallow < 30 Deep 30 - 180	Continuous (V_{s30})

Subduction GMPEs pre-selected (page 2)

MODEL	RECORDS	EVENTS	M_w	DIST. (km)	H (km)	SITE Parameters
Lin & Lee (2008)	Interface 873 Intraslab 3950	Interface 17 Intraslab 37	Interface 5.3 - 8.1 Intraslab 4.1 – 6.7	Interface 20 - 40 Intraslab 40 - 600	Interface 4 - 30 Intraslab 43 - 161	2 (Vs30; NEHRP B,C or D,E)
McVerry et al. (2006)	535 Subduct. + crustal	Interface 6 Intraslab 19	5.08 – 7.09	6 - 400	Interf. 15 – 24 Intrasl. 26 - 50 50 - 149	3 (NZ classes)
Youngs et al. (1997)	Interface 181 Intraslab 53	Interface 57 Intraslab 26	Interface 5 - 8.2 Intraslab 5 - 7.8	Interface 8.5 - 551 Intraslab 45 – 774	10 – 229 (not distinguished)	2 (Rock/Soil)
Zhao et al. (2006)	Interface 1508 Intraslab 1725 Crustal 1285	289 (not distinguished)	5.0 - 8.3 (not distinguished)	0 - 300 (not distinguished)	Interf. 10 - 50 Intraslab 15–162 (c125)	5 (HR + 4 Jap. Rail. Ass., Tg)

Trellis plots (PSA on rock)

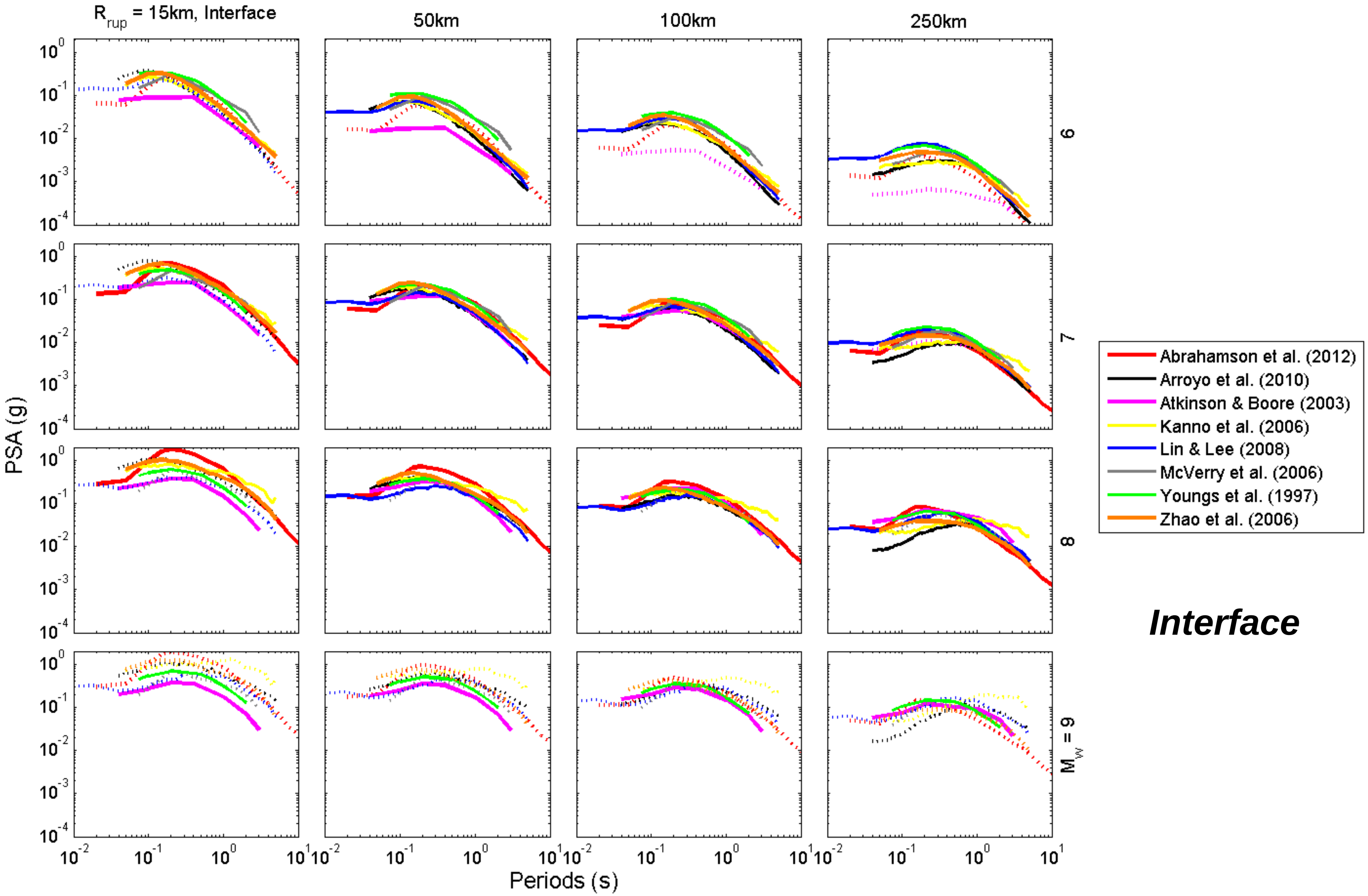

Interface

Trellis plots (PSA on rock)

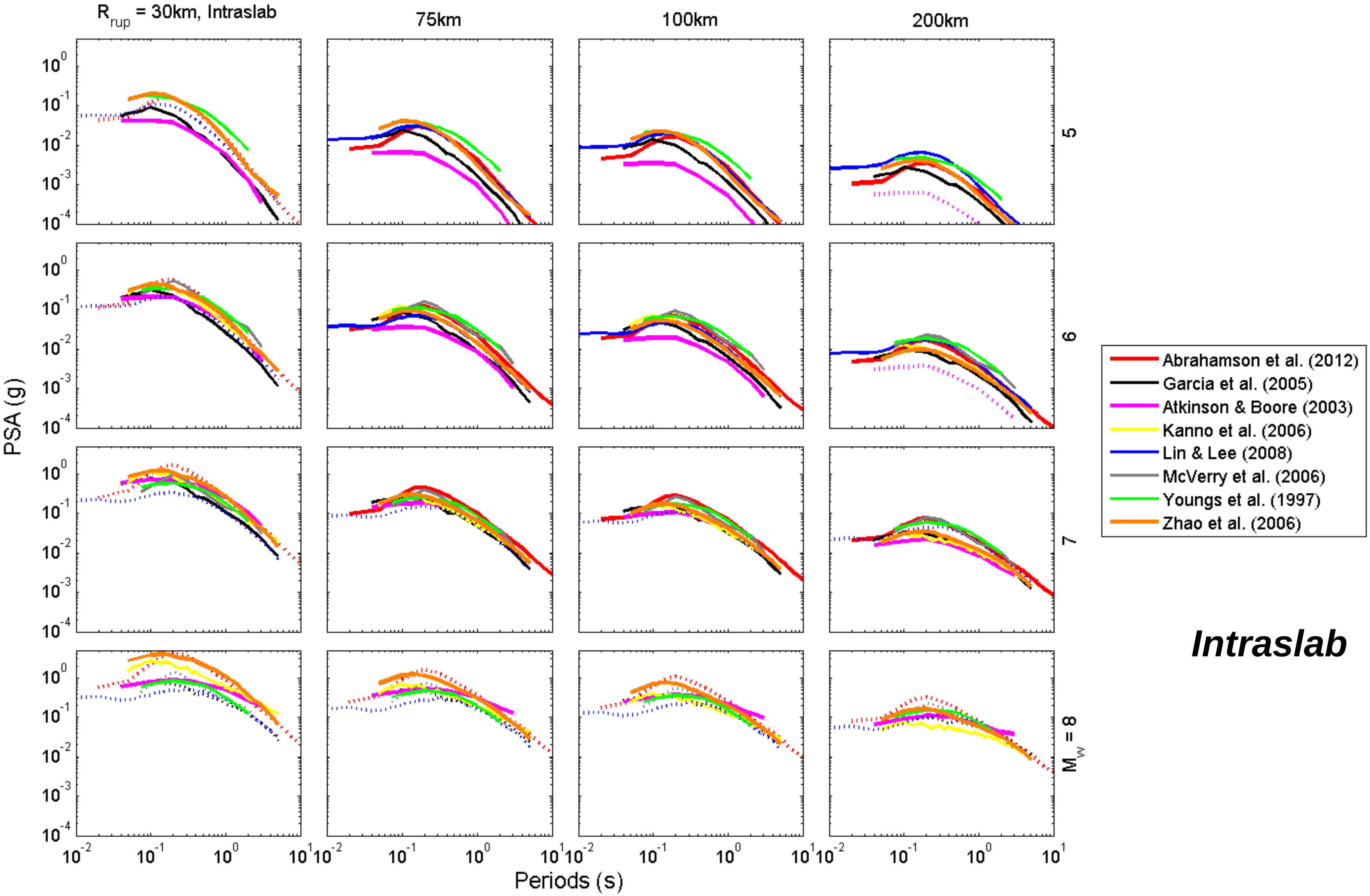

Intraslab

Sigma for rock

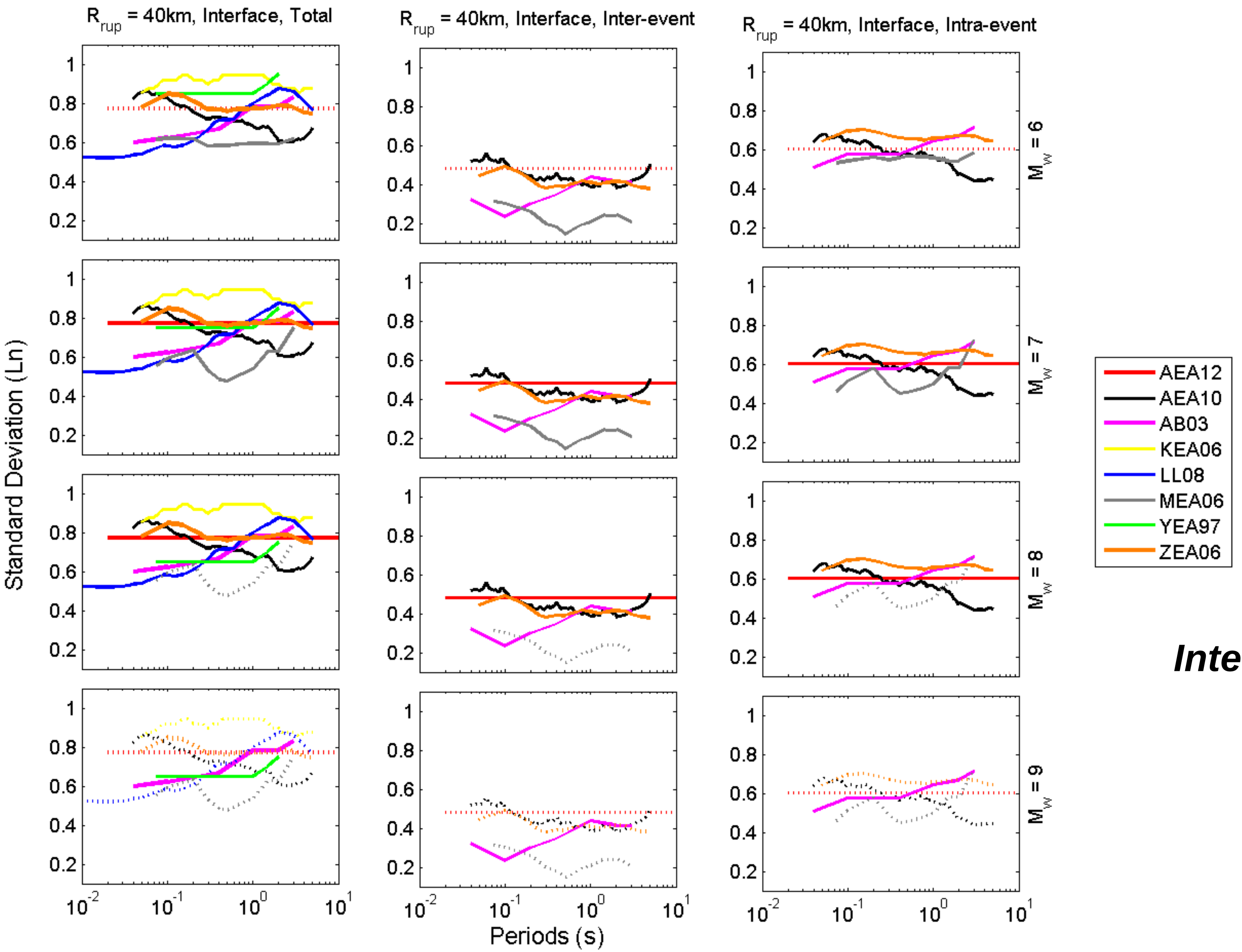

Interface

Sigma for rock

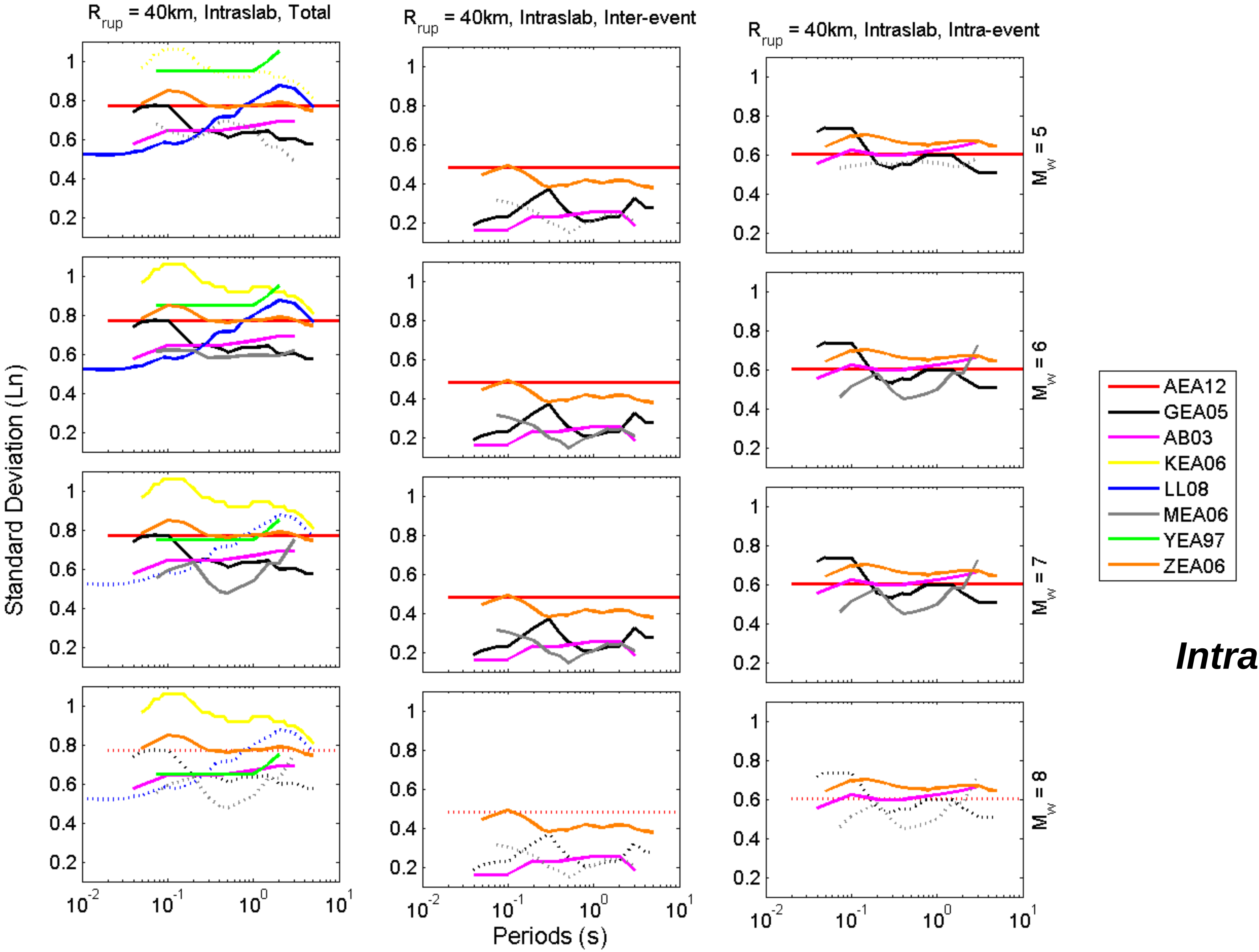

Intraslab

MAGNITUDE TERM SYNTHESIS

MODEL	MAGNITUDE TERM(s)	NOTES	Mw RANGE
Abrahamson et al. (2012)	$\theta_1' + (\theta_4$ or $\theta_5)\,[M-(C1+\Delta C1)] + \theta_{13}(10-M)^2$ (linear M term with change of slope at $M=C_1+\Delta C_1$ and quadratic M) plus linear magnitude-dependent geometric spreading with magnitude-dependent distance saturation $[(\theta_2' + \theta_3(M-7.8))\ln(R+C_4 \exp[(M-6)\,\theta_9])]$	Models change of scaling at $M=C_1+\Delta C_1$ (C_1 is 7.8 and ΔC_1 captures epistemic uncertainty in break in scaling)	Interface: 6.5-8.4 Intraslab: 5.0-7.9
Arroyo et al. (2010)	$\alpha_1 + \alpha_2 M$ (linear M term) plus magnitude-dependent distance saturation in geometric spreading term $[\alpha_3 \ln[(E_1(\alpha_4 R) - E_1(\alpha_4 \mathrm{sqrt}(R^2+r_0^2)))/r_0^2]$ where $r_0^2 = a \exp(bM)$ and E_1 is the exponential integral function]	Simple M dependency but based on solution of a circular finite-source	5.0-8.0
Atkinson & Boore (2003)	$c_1 + c_2 M$ (linear M term) plus magnitude-dependent distance saturation $[-g \log \mathrm{sqrt}(R^2 + a\, 10^{bM})]$	Simple M dependency. Similar to Garcia et al. (2005), Lin & Lee (2008)	Interface: 55.5-8.3 Intraslab: 5.0-7.9
Garcia et al. (2005)	C1+c2M (linear M term) plus magnitude-dependent distance saturation $[-c4 \log \mathrm{sqrt}(R^2 + a\, 10^{bM})]$	Simple M dependency. Similar to Atkinson & Boore (2003), Lin & Lee (2008)	5.2-7.4
Kanno et al. (2006)	C1+a1M (linear M term) plus magnitude-dependent distance saturation $[-\log(X + d_1 10^{0.5M})]$ for shallow events (interface) (no distance saturation for deep (intraslab) events)	Simple M dependency.	Interface: 5.2-8.2 Intraslab: 5.5-8.0

MAGNITUDE TERM SYNTHESIS

MODEL	MAGNITUDE TERM(s)	NOTES	Mw RANGE
Lin & Lee (2008)	C_1+C_2M (linear M term) plus magnitude-dependent distance saturation $[C_3\ln(R+C_4\exp(C_5M)]$		Interface: 5.3-8.1 Intraslab: 4.1-6.7
McVerry et al.	$C_{11}'+(C_{12Y}+[C_{15}'-C_{17}']C_{19Y})(M-6)+C_{13Y}(10-M)^3$ (linear and cubic M terms) plus magnitude-dependent distance saturation $[C_{17}'\ln(r+C_{18Y}\exp(C_{19Y}M))]$	Simple M dependency	5.08-7.09
Youngs et al. (1997)	$C_1{}^{*\prime}+C2'M+B_3'(10-M)^3$ (linear and cubic M terms) plus magnitude-dependent distance saturation $[B3'\ln(R+\exp(\alpha1'+\alpha2'M))]$. Scaling for rock and soil sites allowed to be different.		Interface: 5.0-8.2 Intraslab: 5.0-7.8
Zhao et al. (2006)	$C_k'+aM+Q(M-M)^2$ (linear and quadratic M terms) plus magnitude-dependent distance saturation $[-\log(x+c\exp(dM)]$	Coefficients with subscript Y taken from Youngs et al. (1997). Form adopted from Youngs et al. (1997)	5.08-7.09

PEER

Magnitude-scaling for rock

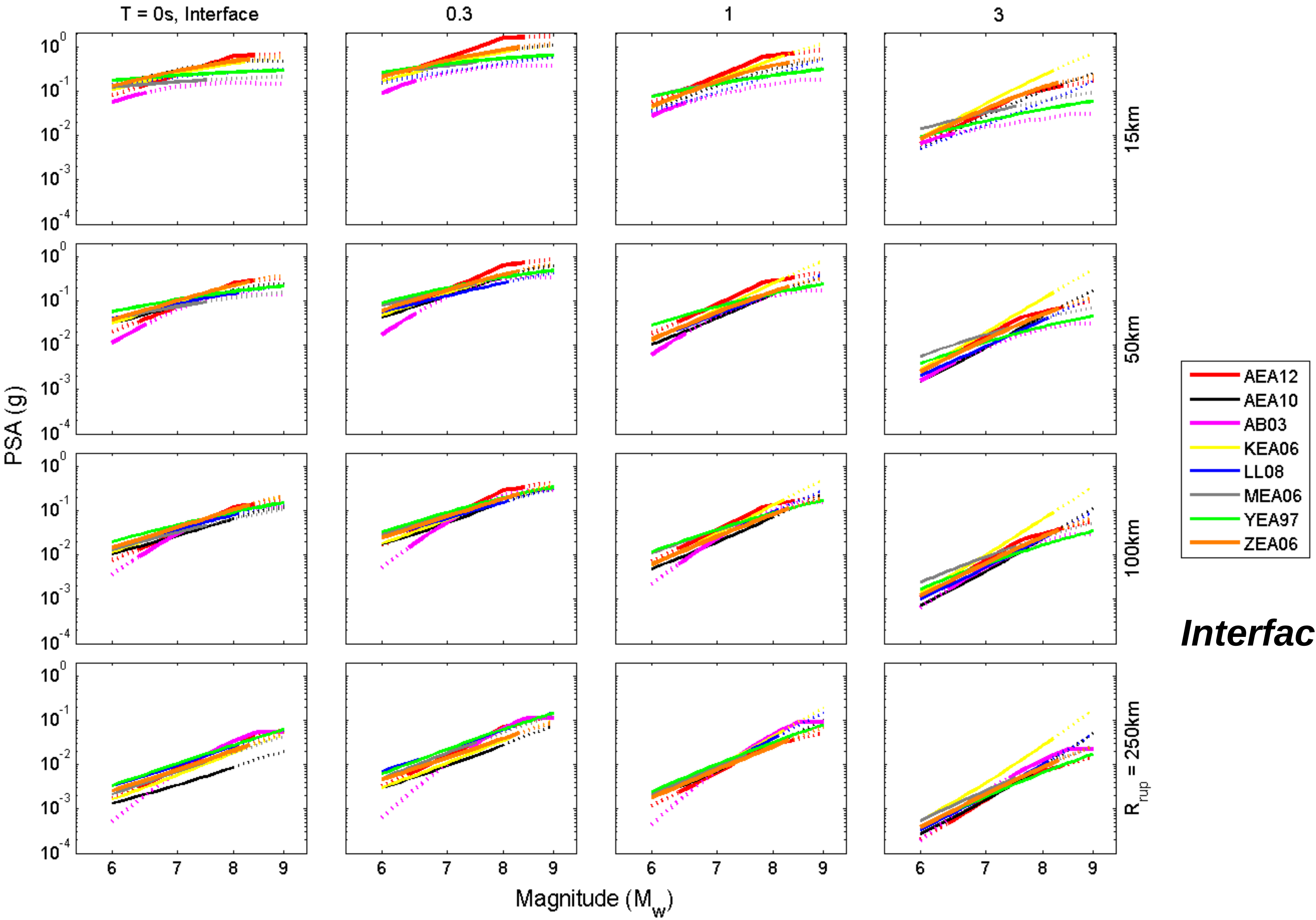

Interface

Magnitude-scaling for rock

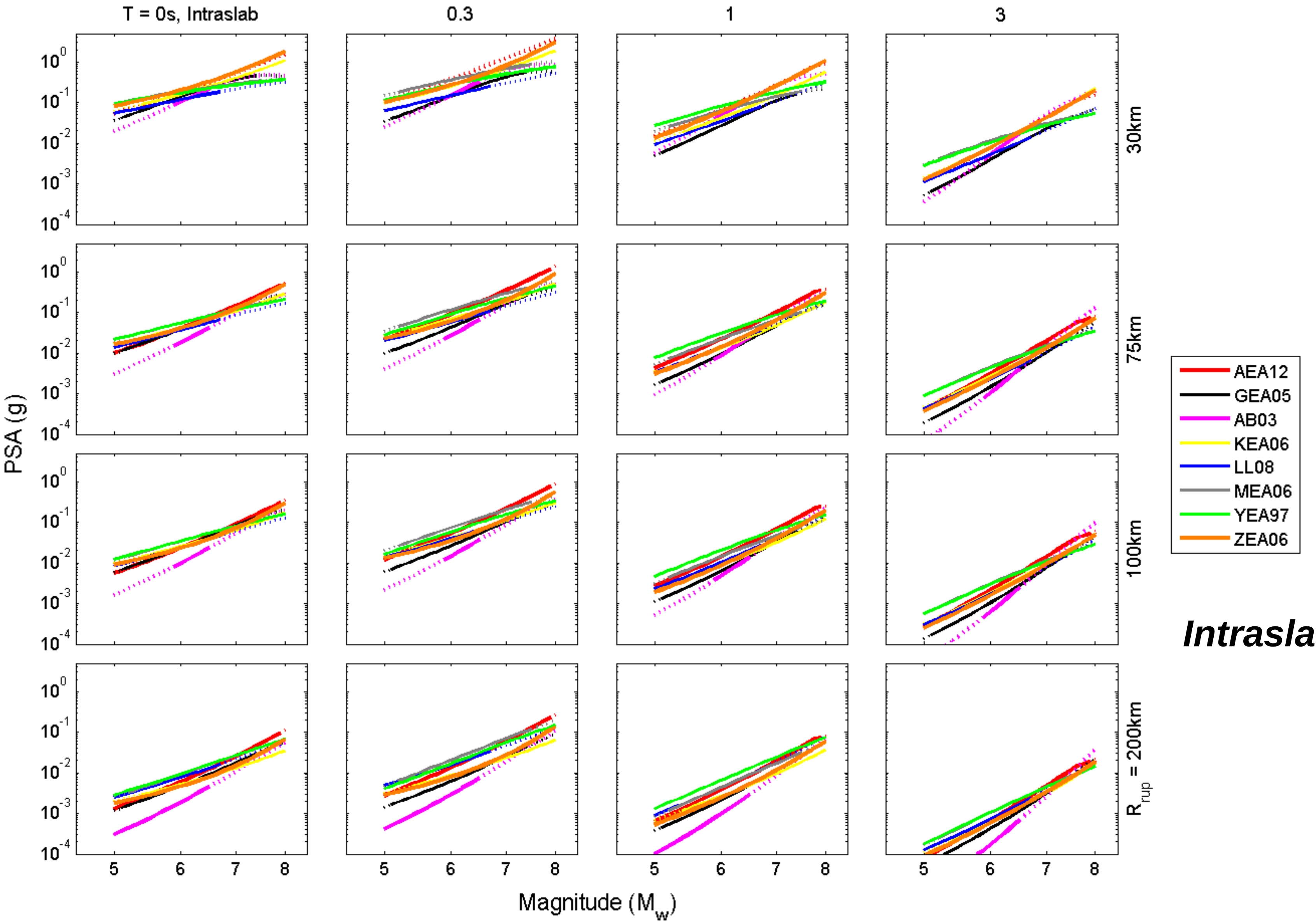

Intraslab

DISTANCE TERM SYNTHESIS

MODEL	DISTANCE TERM(s)	NOTES	DISTANCE RANGE (km)
Abrahamson et al. (2012)	$[(\theta_2' + \theta_3(M-7.8))\ln(R+C_4 \exp[(M-6)\ \theta_9])]$ (linear magnitude-dependent geometric decay with magnitude-dependent distance saturation) plus anelastic attenuation ($\theta_6 R$) plus additional (earthquake-type-dependent) geometric decay for backarc sites.	Models differences in forearc/backarc attenuation	Interface: 5-551 Intraslab: 34-991
Arroyo et al. (2010)	Magnitude-dependent distance saturation in geometric spreading term $[\alpha_3 \ln[(E_1(\alpha_4 R)-E_1(\alpha_4 \mathrm{sqrt}(R^2+r_0^2)))/r_0^2]$ where r_0^2=a exp(bM) and E_1 is the exponential integral function]	Functional form based on solution of a circular finite-source	20-400
Atkinson & Boore (2003)	$-g \log \mathrm{sqrt}(R^2 + a\ 10^{bM})$ (geometric decay with magnitude-dependent distance saturation) plus c_3 R (anelastic attenuation)	Similar to Garcia et al. (2005),	Interface: 5-420 Intraslab: 34-300
Garcia et al. (2005)	$c_4 \log \mathrm{sqrt}(R^2 + a\ 10^{bM})$ (geometric decay with magnitude-dependent distance saturation) plus c_4 R (anelastic attenuation)	Similar to Atkinson & Boore (2003),	40-400
Kanno et al. (2006)	$-\log(X + d_1 10^{0.5M})$ (1/R geometric spreading with magnitude-dependent distance saturation) for shallow (interface) events and $-\log(X)$ (1/R geometric spreading) for deep (intraslab) events plus $b_1 X$ (anelastic attenuation) for both types	Simple distance dependence. Similar to Zhao et al. (2006)	Interface: 1-400 Intraslab: 30-500

DISTANCE TERM SYNTHESIS

MODEL	DISTANCE TERM(s)	NOTES	DISTANCE RANGE (km)
Lin & Lee (2008)	C_3 log (R+a 10^{bM}) (geometric decay with magnitude-dependent distance saturation)	Similar to McVerry et al. (2006), Youngs et al. (1997)	Interface: 20-300 Intraslab: 40-600
McVerry et al. (2006)	C_3 ln (R+a 10^{bM}) (geometric decay with magnitude-dependent distance saturation)	Form adopted from Youngs et al. (1997). Similar to Lin & Lee (2008).	6-400
Youngs et al. (1997)	B_3' ln (R+a 10^{bM}) (geometric decay with magnitude-dependent distance saturation). Scaling for rock and soil sites allowed to be different.	Similar to Lin & Lee (2008) and McVerry et al. (2006)	Interface: 8.5-551 Intraslab: 45-744
Zhao et al. (2006)	-log(r) where r=x+cexp(dM) (1/R geometric spreading with magnitude-dependent distance saturation) +bx (anelastic attenuation)	Simple distance dependence. Similar to Kanno et al. (2006)	0-300

Distance-scaling for rock

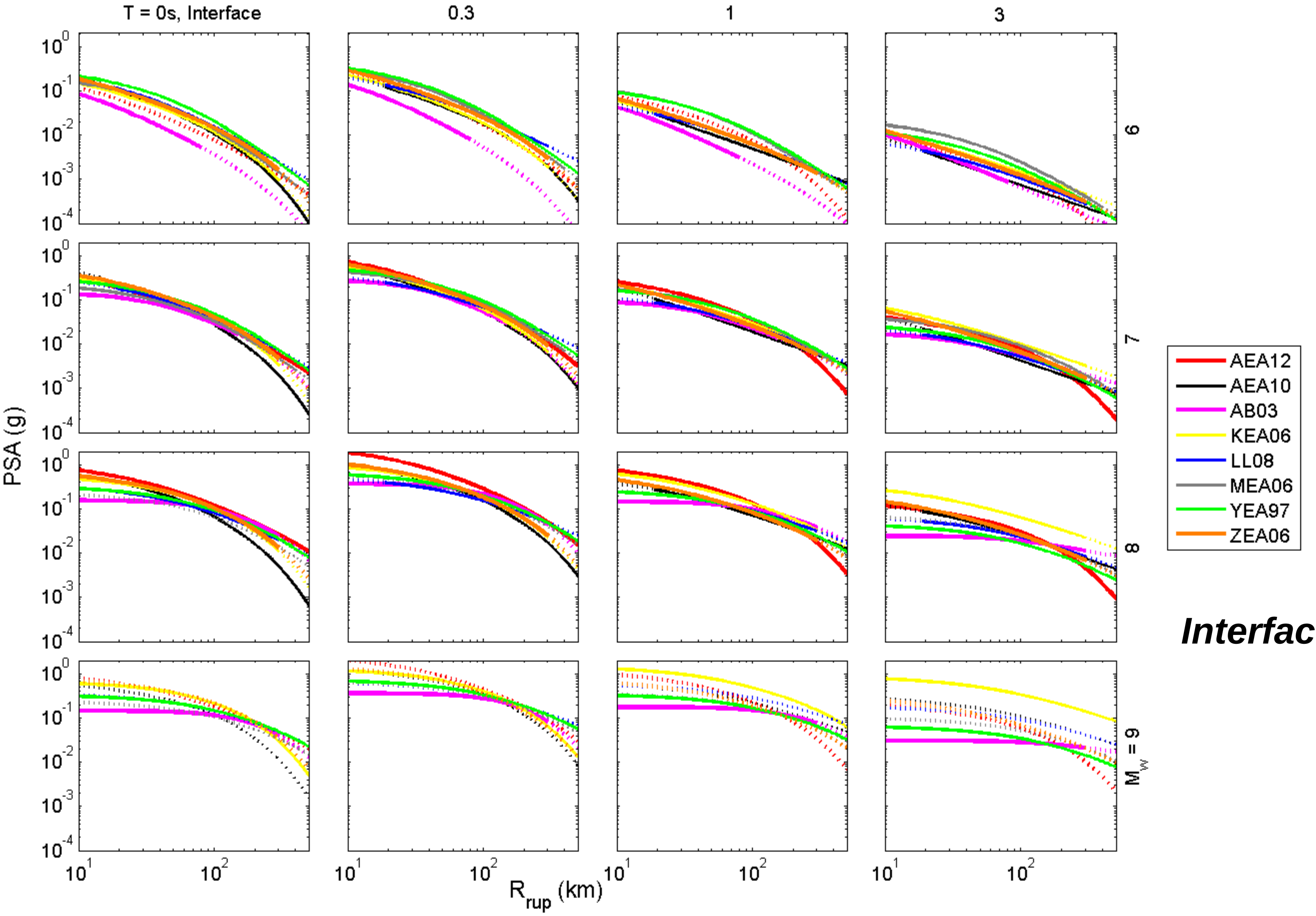

Interface

Distance-scaling for rock

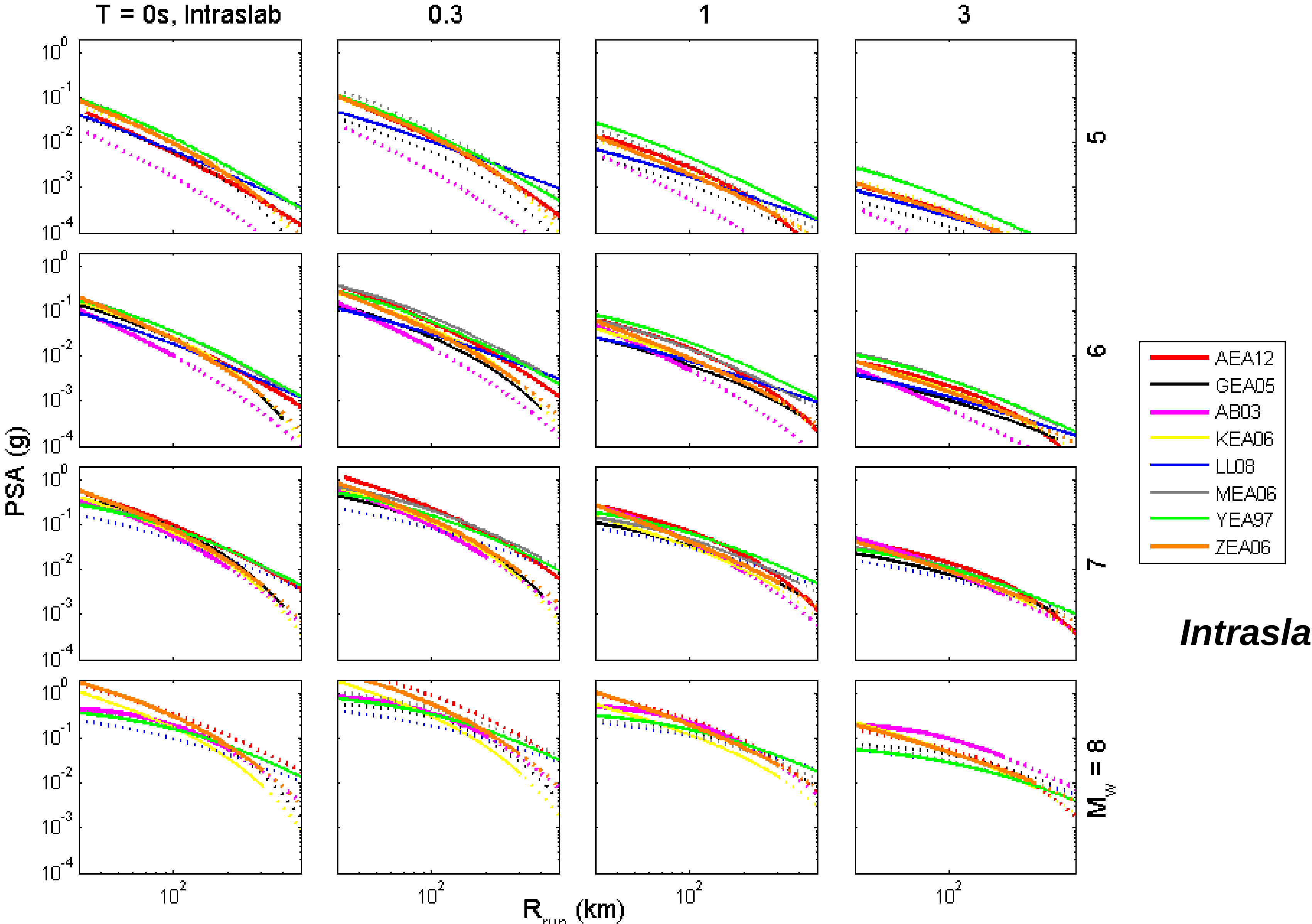

SITE TERM SYNTHESIS

MODEL	SITE TERM	NOTES	SITEs CLASSIFICATION
BC Hydro (2012)	$f_{site}(PGA_{1000}, Vs30m) = \begin{cases} \theta_{12} * Ln(\frac{V_s^*}{V_{lin}}) - b * Ln(PGA_{1000} + c) + \\ \quad b * Ln(PGA_{1000} + c * (\frac{V_s^*}{V_{lin}})^n) & for \quad V_{S30} < V_{lin} \\ \theta_{12} * Ln(\frac{V_s^*}{V_{lin}}) + b * n * Ln(\frac{V_s^*}{V_{lin}}) & for \quad V_{S30} \geq V_{lin} \end{cases}$	Non linear, dependent on the spectral amplitude at PGA_rock(1000)	Continuous (Vs30)
Arroyo et al (2010)	NA		N/A (Sites NEHRP B)
Atkinson & Boore (2003)	$c_5\ sl\ S_C + c_6\ sl\ S_D + c_7\ sl\ S_E,$ $sl = 1.$ for $PGA_{rx} \leq 100$ cm/sec^2 or frequencies ≤ 1 Hz $sl = 1. - (f - 1)(PGA_{rx} - 100.)/400.$ for $100 < PGA_{rx} < 500$ cm/sec^2 (1 Hz $< f < 2$ Hz) $sl = 1. - (f - 1)$ for $PGA_{rx} \geq 500$ cm/sec^2 (1 Hz $< f < 2$ Hz) $sl = 1. - (PGA_{rx} - 100.)/400.$ for $100 < PGA_{rx} < 500$ cm/sec^2 ($f \geq 2$ Hz and PGA) $sl = 0.$ for $PGA_{rx} \geq 500$ cm/sec^2 ($f \geq 2$ Hz and PGA);	“add-on term” to the functional form with linear and amplitude (PGA_rock(NEHRP B)) dependent soil-non linearity	4 (Vs30; NEHRP B to E)
Kanno et al. (2006)	$G = \log(obs/pre) = p \log AVS30 + q,$	“add-on term” to the functional form as log-linear term. Derive p and q by regression analysis on residuals averaged at intervals of every 100m/s in Vs,30. Note that the equation without site correction predicts ground motions at sites with Vs,30 ≈ 300m/s	Cont. (Vs30)

SITE TERM SYNTHESIS

MODEL	SITE TERM	NOTES	SITEs CLASSIFICATION
Lin & Lee (2008)	Rock&Soil: $\ln(y) = C_1 + C_2 M + C_3 \ln(R + C_4 e^{C_5 M}) + C_6 H + C_7 Z_t$ where H=0 and Z_t=0 $\text{Site term} = \exp\left[\ln(Soil) - \ln(Rock)\right]$	Same functional form but entire coefficients ensemble is different according to whether it refers to rock (NEHRP B or C), or to soil (NEHRP D or E)	2 (Vs30; NEHRP B,C or D,E)
McVerry et al. (2006)	*For site class D:* $AMP_D(T) = SA_D(T) / SA_{rock}(T) = AMP_D(T, PGA_r = 0) / (1 + PGA_r / PGA_{ref})^p$ $AMP_D(T, PGA_r = 0) = \exp(C_{43}(T)) / PGA_{ref})^p$ where PGA_{ref} =0.03g and p=-C_{30}(T)	Add on term for Class B to the estimate for rock. Non linear, dependent on the spectral amplitude at PGA_rock for Class C	3 (NZ classes)
Youngs et al. (1997)	Rock: $\ln(Y) = 0.2418 + 1.414M + C_1 + C_2(10 - M)^3 + C_3 \ln(r_{rup} + 1.7818e^{0.554M})...$ $... + 0.00607H + 0.3846Z_T$ Soil: $\ln(Y) = -0.6687 + 1.438M + C_1 + C_2(10 - M)^3 + C_3 \ln(r_{rup} + 1.097e^{0.617M})...$ $... + 0.00648H + 0.3643Z_T$ $\text{Site term} = \exp\left[\ln(Soil) - \ln(Rock)\right]$	H=Z_t=0 (interface eqk.)	2 (Rock/Soil)
Zhao et al. (2006)	$C_k - C_1$	"add-on term" to the functional form	5 (HR + 4 Jap. Rail. Ass., Tg)

Site response (V_{s30} scaling)

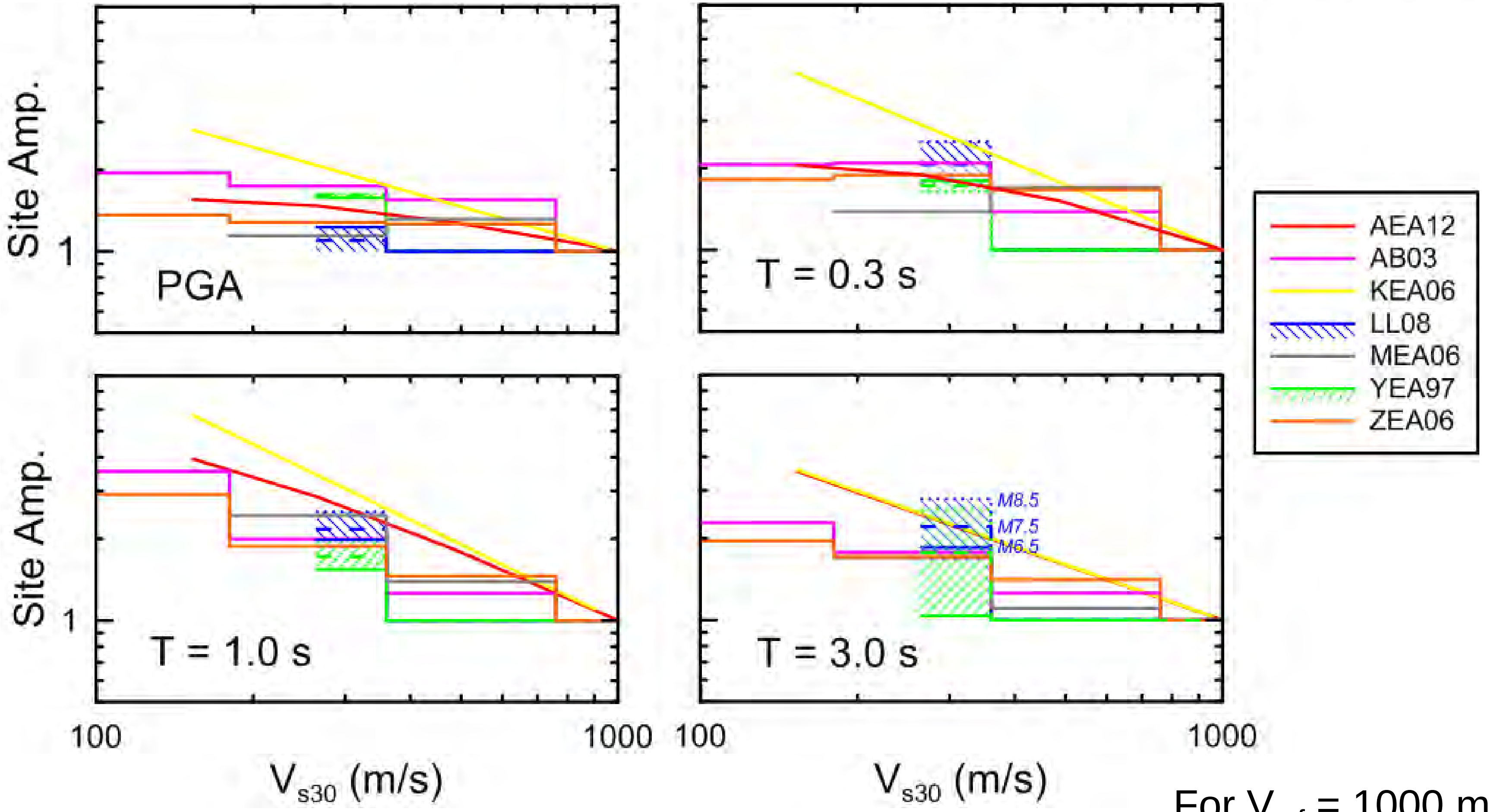

For V_{ref} = 1000 m/s;
PGA_r = 0.1 g

Site response (nonlinearity)

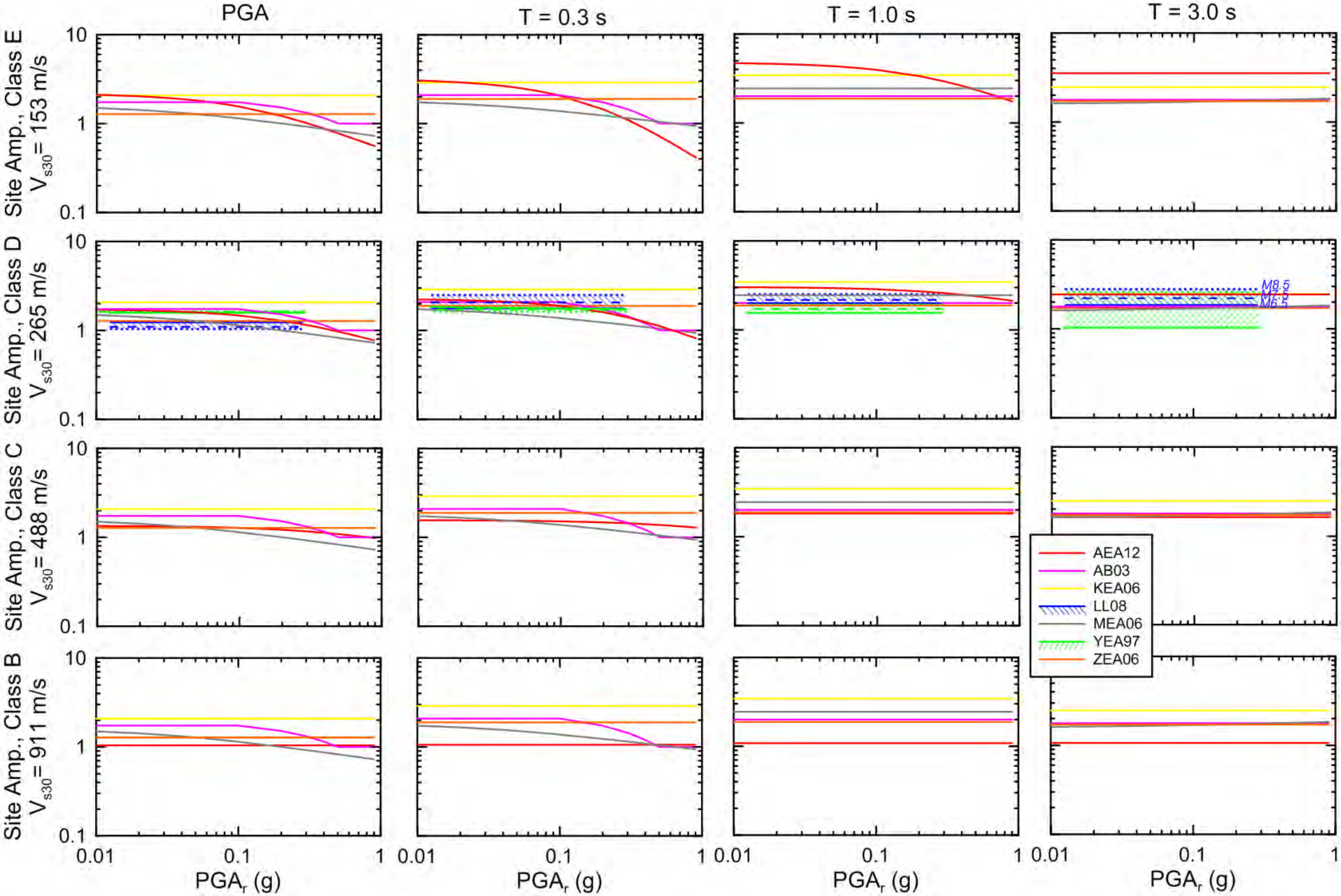

Site response

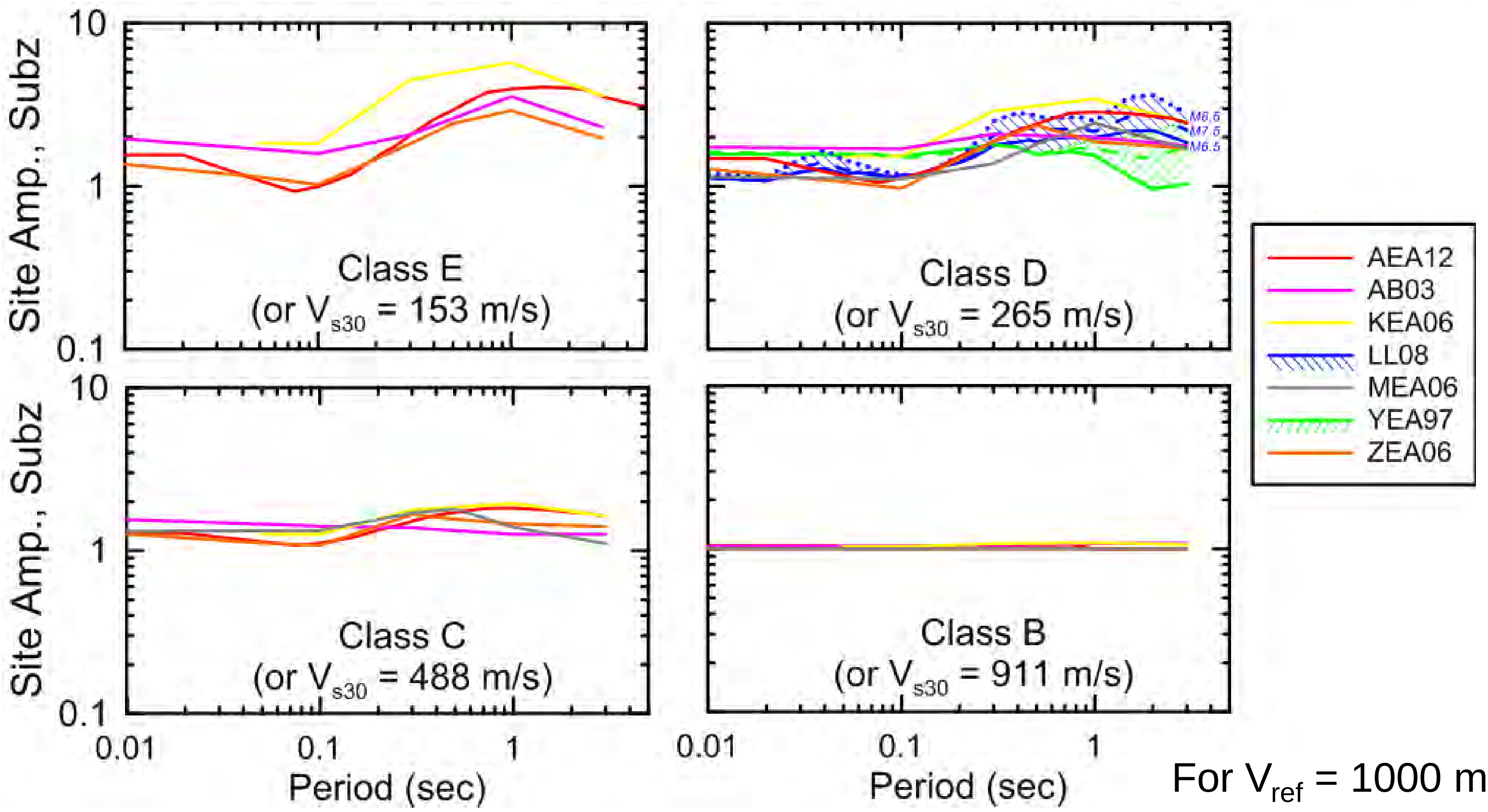

For V_{ref} = 1000 m/s;
PGA_r = 0.1 g

Summary of GMPE-data comparisons

	AEA 2012	AEA2010	AB 2003	GEA 2005	KEA 2006	LL 2008	MEA 2006	YEA 1997	ZEA 2006
A (So. Am.)	x	x	x	x			x	x	x
B (L. Antiles)			x	x	x	x	x	x	x
C (India-Burma)			x						
D (Greece)			x		x	x	x	x	x
E (Worldwide)	x	x	x		x	x	x	x	x
F (NZ)			x				x		x
G(Chile)			x						x
H (Japan)			x						x

List of models pre-selected

AEA 2012 = Abrahamson *et al.* (2012-*submitted*), BC Hydro: International
AEA 2010 = Arroyo *et al.* (2010): Mexico Interface (complementary to GAR 2005)
AB 2003 = Atkinson & Boore (2003): International
GEA 2005 = Garcia *et al.* (2010): Mexico Intraslab (complimentary to AEA 2010)
KEA 2006 = Kanno *et al.* (2006): Japan
LL 2008 = Lin & Lee (2008): Taiwan
MEA 2006 = McVerry *et al.* (2006): New Zealand
YEA 1997 = Youngs *et al.* (1997): International
ZEA 2006 = Zhao *et al.* (2006): Japan

Case study A

Title	“An Evaluation of the Applicability of Current Ground-motion Models to the South and Central American Subduction Zones” *BSSA, 102:1, 143–168, 2012, doi: 10.1785/0120110078*									
Authors	Maria Cristina Arango, Fleur Strasser, Julian J Bommer, Jose M Cepeda,, Ruben Boroschek, Douglas A. Hernandez, Hernando Tavera									
GMPEs tested	AEA 2012	AEA 2010	AB 2003	GEA 2005	KEA 2006	LL 2008	MEA 2006	YEA 1997	ZEA 2006	ZHA2010
	x	x	x	x			x	x	x	
Geog. Areas	Peru’–Chile and CAM: *interface*	Peru’–Chile and CAM: *interface*	Peru’–Chile and CAM: *interface*				Peru’–Chile and CAM: *interface*	Peru’–Chile and CAM: *interface*	Peru’–Chile and CAM: *interface*	
	Peru’–Chile and CAM: *intraslab*		Peru’–Chile and CAM: *intraslab*	Peru’–Chile and CAM: *intraslab*			Peru’–Chile and CAM: *intraslab*	Peru’–Chile and CAM: *intraslab*	Peru’–Chile and CAM: *intraslab*	

Method of performance assessment: Overall goodness of fit from Scherbaum et al. (2004) extended to include inter- and intra-event variability.

Database used for test: 98 records from Peru and Chile (S Am data set) and 554 records from El Salvador, Costa Rica, Nicaragua, and Guatemala

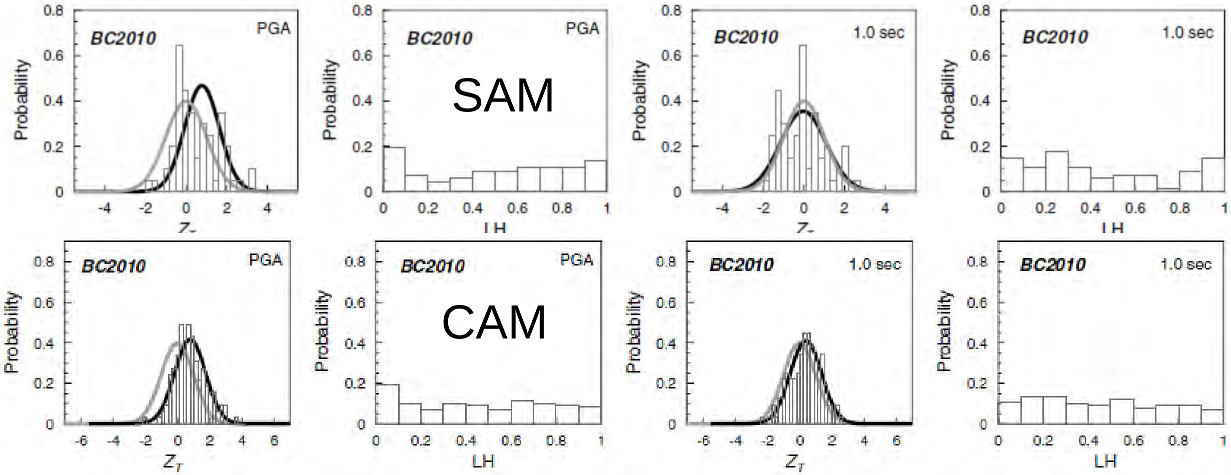

General results: AEA2010 and ZEA2006 models, are suitable for the ground motion prediction in the Peru-Chile and Central American subduction zones.

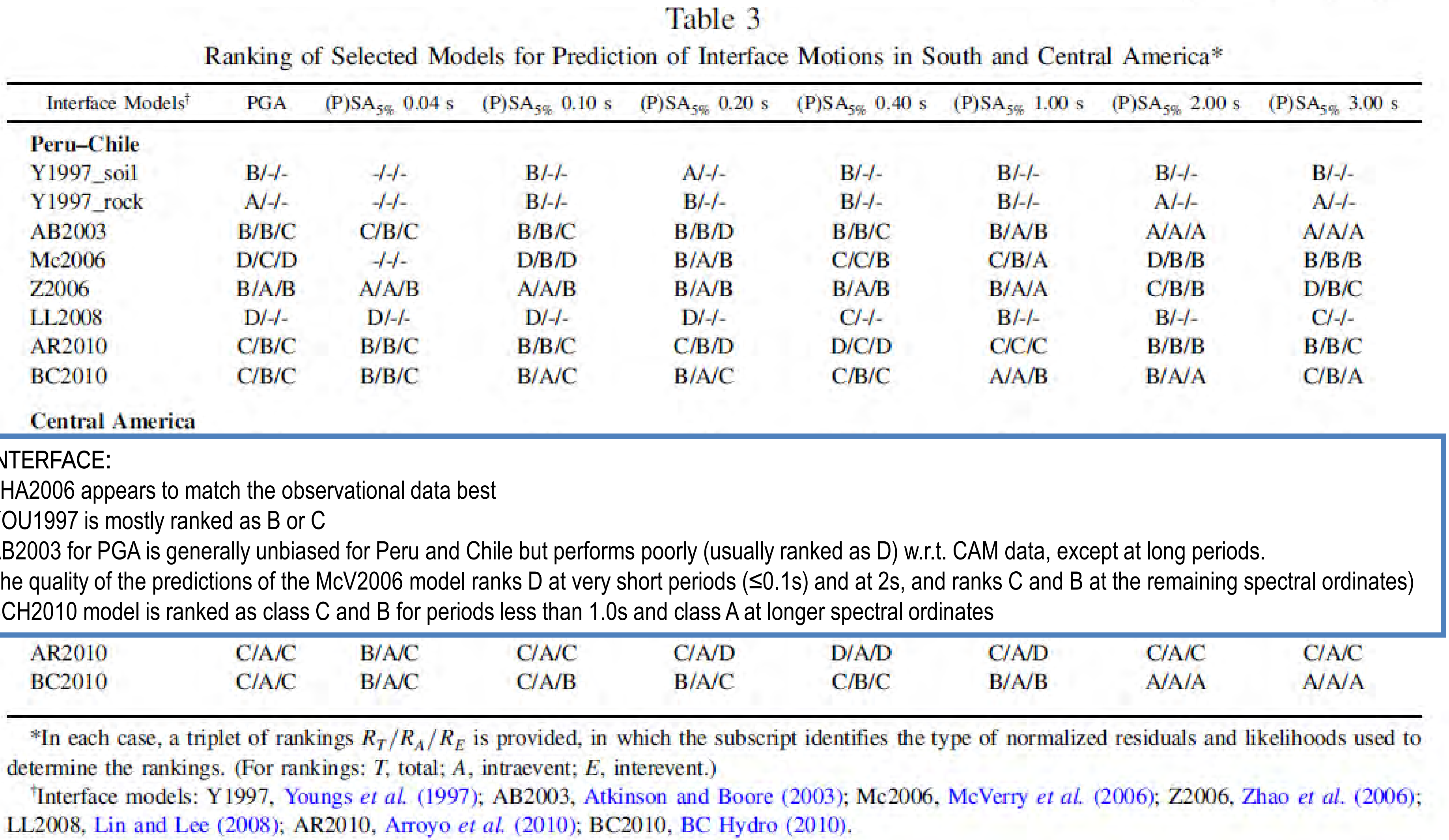

Table 3

Ranking of Selected Models for Prediction of Interface Motions in South and Central America*

Interface Models†	PGA	(P)SA$_{5\%}$ 0.04 s	(P)SA$_{5\%}$ 0.10 s	(P)SA$_{5\%}$ 0.20 s	(P)SA$_{5\%}$ 0.40 s	(P)SA$_{5\%}$ 1.00 s	(P)SA$_{5\%}$ 2.00 s	(P)SA$_{5\%}$ 3.00 s
Peru–Chile								
Y1997_soil	B/-/-	-/-/-	B/-/-	A/-/-	B/-/-	B/-/-	B/-/-	B/-/-
Y1997_rock	A/-/-	-/-/-	B/-/-	B/-/-	B/-/-	B/-/-	A/-/-	A/-/-
AB2003	B/B/C	C/B/C	B/B/C	B/B/D	B/B/C	B/A/B	A/A/A	A/A/A
Mc2006	D/C/D	-/-/-	D/B/D	B/A/B	C/C/B	C/B/A	D/B/B	B/B/B
Z2006	B/A/B	A/A/B	A/A/B	B/A/B	B/A/B	B/A/A	C/B/B	D/B/C
LL2008	D/-/-	D/-/-	D/-/-	D/-/-	C/-/-	B/-/-	B/-/-	C/-/-
AR2010	C/B/C	B/B/C	B/B/C	C/B/D	D/C/D	C/C/C	B/B/B	B/B/C
BC2010	C/B/C	B/B/C	B/A/C	B/A/C	C/B/C	A/A/B	B/A/A	C/B/A
Central America								
AR2010	C/A/C	B/A/C	C/A/C	C/A/D	D/A/D	C/A/D	C/A/C	C/A/C
BC2010	C/A/C	B/A/C	C/A/B	B/A/C	C/B/C	B/A/B	A/A/A	A/A/A

*In each case, a triplet of rankings $R_T/R_A/R_E$ is provided, in which the subscript identifies the type of normalized residuals and likelihoods used to determine the rankings. (For rankings: T, total; A, intraevent; E, interevent.)

†Interface models: Y1997, Youngs *et al.* (1997); AB2003, Atkinson and Boore (2003); Mc2006, McVerry *et al.* (2006); Z2006, Zhao *et al.* (2006); LL2008, Lin and Lee (2008); AR2010, Arroyo *et al.* (2010); BC2010, BC Hydro (2010).

INTERFACE:

ZHA2006 appears to match the observational data best

YOU1997 is mostly ranked as B or C

AB2003 for PGA is generally unbiased for Peru and Chile but performs poorly (usually ranked as D) w.r.t. CAM data, except at long periods.

The quality of the predictions of the McV2006 model ranks D at very short periods (≤0.1s) and at 2s, and ranks C and B at the remaining spectral ordinates)

BCH2010 model is ranked as class C and B for periods less than 1.0s and class A at longer spectral ordinates

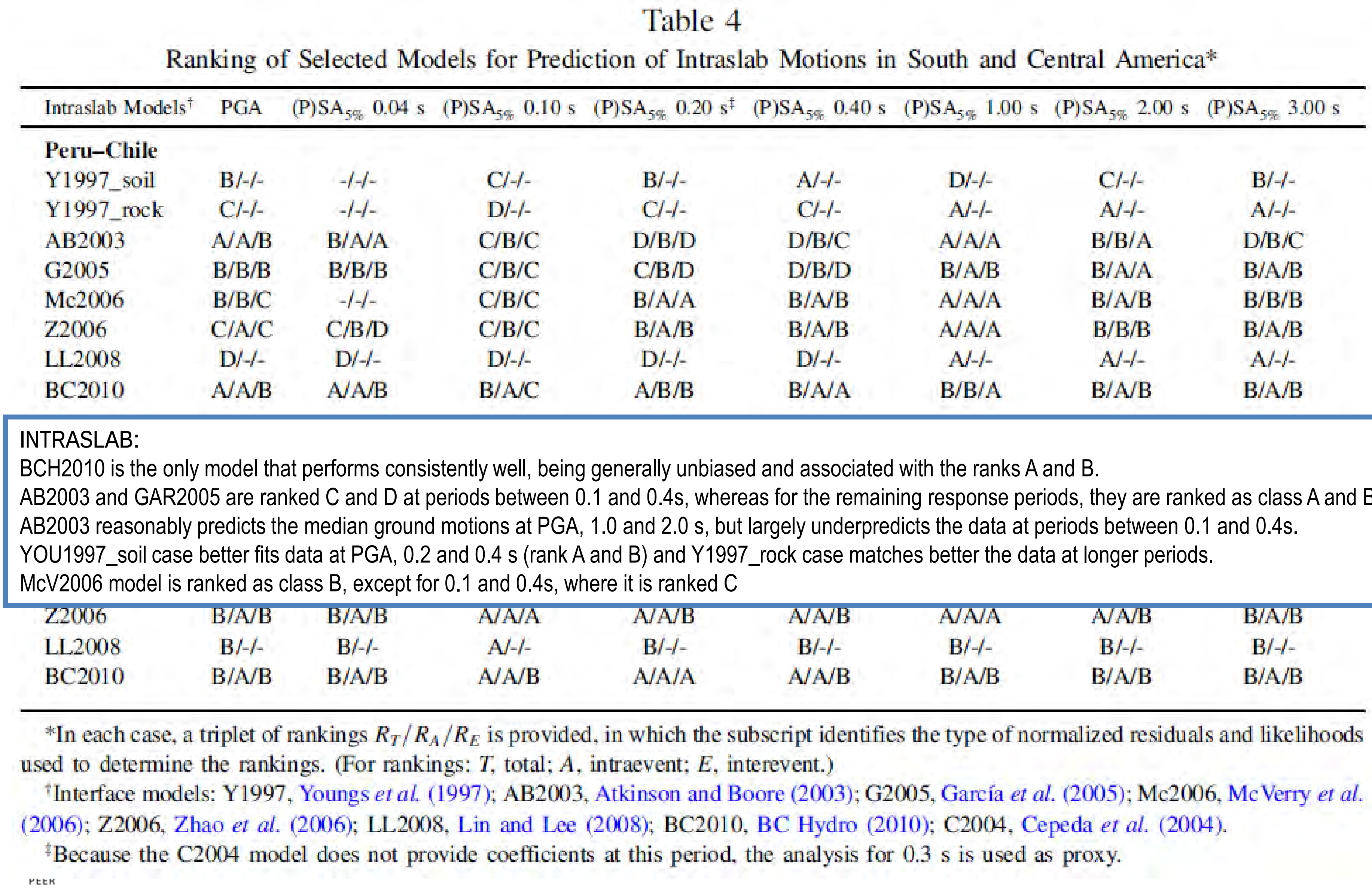

Table 4

Ranking of Selected Models for Prediction of Intraslab Motions in South and Central America*

Intraslab Models†	PGA	(P)SA$_{5\%}$ 0.04 s	(P)SA$_{5\%}$ 0.10 s	(P)SA$_{5\%}$ 0.20 s‡	(P)SA$_{5\%}$ 0.40 s	(P)SA$_{5\%}$ 1.00 s	(P)SA$_{5\%}$ 2.00 s	(P)SA$_{5\%}$ 3.00 s
Peru–Chile								
Y1997_soil	B/-/-	-/-/-	C/-/-	B/-/-	A/-/-	D/-/-	C/-/-	B/-/-
Y1997_rock	C/-/-	-/-/-	D/-/-	C/-/-	C/-/-	A/-/-	A/-/-	A/-/-
AB2003	A/A/B	B/A/A	C/B/C	D/B/D	D/B/C	A/A/A	B/B/A	D/B/C
G2005	B/B/B	B/B/B	C/B/C	C/B/D	D/B/D	B/A/B	B/A/A	B/A/B
Mc2006	B/B/C	-/-/-	C/B/C	B/A/A	B/A/B	A/A/A	B/A/B	B/B/B
Z2006	C/A/C	C/B/D	C/B/C	B/A/B	B/A/B	A/A/A	B/B/B	B/A/B
LL2008	D/-/-	D/-/-	D/-/-	D/-/-	D/-/-	A/-/-	A/-/-	A/-/-
BC2010	A/A/B	A/A/B	B/A/C	A/B/B	B/A/A	B/B/A	B/A/B	B/A/B
Z2006	B/A/B	B/A/B	A/A/A	A/A/B	A/A/B	A/A/A	A/A/B	B/A/B
LL2008	B/-/-	B/-/-	A/-/-	B/-/-	B/-/-	B/-/-	B/-/-	B/-/-
BC2010	B/A/B	B/A/B	A/A/B	A/A/A	A/A/B	B/A/B	B/A/B	B/A/B

---

[*] In each case, a triplet of rankings $R_T/R_A/R_E$ is provided, in which the subscript identifies the type of normalized residuals and likelihoods used to determine the rankings. (For rankings: T, total; A, intraevent; E, interevent.)

[†] Interface models: Y1997, Youngs *et al.* (1997); AB2003, Atkinson and Boore (2003); G2005, García *et al.* (2005); Mc2006, McVerry *et al.* (2006); Z2006, Zhao *et al.* (2006); LL2008, Lin and Lee (2008); BC2010, BC Hydro (2010); C2004, Cepeda *et al.* (2004).

[‡] Because the C2004 model does not provide coefficients at this period, the analysis for 0.3 s is used as proxy.

PEER

INTRASLAB:
BCH2010 is the only model that performs consistently well, being generally unbiased and associated with the ranks A and B.
AB2003 and GAR2005 are ranked C and D at periods between 0.1 and 0.4s, whereas for the remaining response periods, they are ranked as class A and B.
AB2003 reasonably predicts the median ground motions at PGA, 1.0 and 2.0 s, but largely underpredicts the data at periods between 0.1 and 0.4s.
YOU1997_soil case better fits data at PGA, 0.2 and 0.4 s (rank A and B) and Y1997_rock case matches better the data at longer periods.
McV2006 model is ranked as class B, except for 0.1 and 0.4s, where it is ranked C

Case study B

Title	"Comparing predicted and observed ground motions from subduction earthquakes in the Lesser Antilles" *J Seismol (2009) 13:577–587*									
Authors	John Douglas and Rosemarie Mohais									
GMPEs tested	AEA 2012	AEA 2010	AB 2003	GEA 2005	KEA 2006	LL 2008	MEA 2006	YEA 1997	ZEA 2006	ZHA2010
			x	x	x	x	x	x	x	
Geog. Areas	Islands of the Lesser Antilles (Guadeloupe, Martinique, Trinidad, and Dominica)									

Method of performance assessment: Overall goodness of fit from Scherbaum et al. (2004). Total residuals. Some analysis of residuals wrt M and R

Database used for test: ground motions recorded on the French Antilles (Caribbean), consisting of 156 records from 13 interface earthquakes (M 4.9-5.8) and 146 records from nine intraslab earthquakes (M 4.8-7.4)

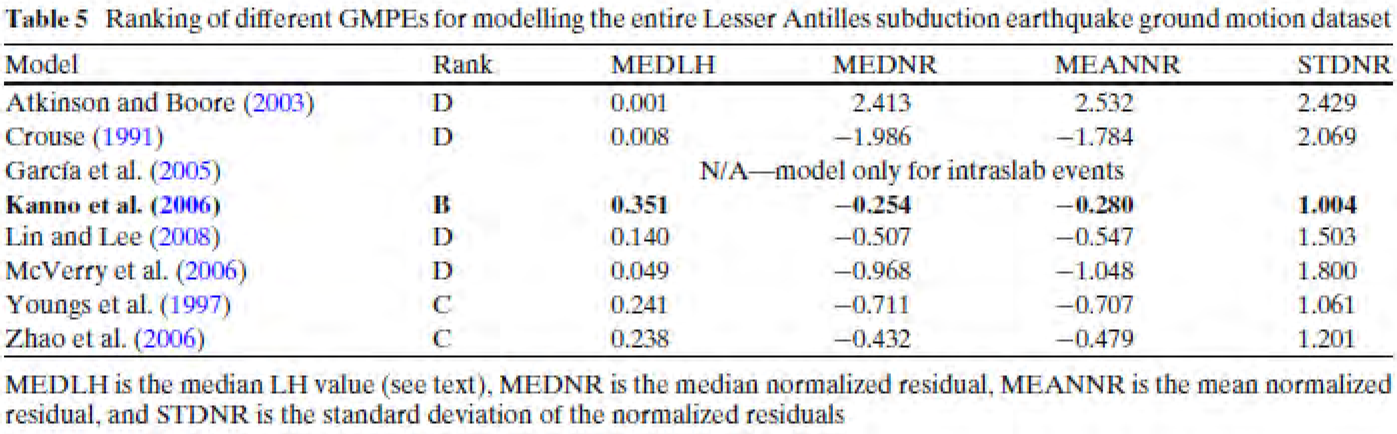

Table 5 Ranking of different GMPEs for modelling the entire Lesser Antilles subduction earthquake ground motion dataset

Model	Rank	MEDLH	MEDNR	MEANNR	STDNR
Atkinson and Boore (2003)	D	0.001	2.413	2.532	2.429
Crouse (1991)	D	0.008	−1.986	−1.784	2.069
García et al. (2005)		N/A—model only for intraslab events			
Kanno et al. (2006)	**B**	**0.351**	**−0.254**	**−0.280**	**1.004**
Lin and Lee (2008)	D	0.140	−0.507	−0.547	1.503
McVerry et al. (2006)	D	0.049	−0.968	−1.048	1.800
Youngs et al. (1997)	C	0.241	−0.711	−0.707	1.061
Zhao et al. (2006)	C	0.238	−0.432	−0.479	1.201

MEDLH is the median LH value (see text), MEDNR is the median normalized residual, MEANNR is the mean normalized residual, and STDNR is the standard deviation of the normalized residuals

General results: KEA 2006 and ZEA2006 models provide good predictions of observed earthquake ground motions and their variabilities in the Lesser Antilles

Case study D

Title	“Toward a ground-motion logic tree for probabilistic seismic hazard assessment in Europe” *J Seismol (2012) DOI 10.1007/s10950-012-9281-z*									
Authors	Elise Delavaud · Fabrice Cotton · Sinan Akkar · Frank Scherbaum · Laurentiu Danciu · Céline Beauval · Stéphane Drouet · John Douglas · Roberto Basili · M. Abdullah Sandikkaya · Margaret Segou · Ezio Faccioli · Nikos Theodoulidis									
GMPEs tested	AEA 2012	ARR 2010	AB 2003	GAR 2005	KEA 2006	LL 2008	McV 2006	YEA 1997	ZEA 2006	ZHA2010
			x	x	x	x	x	x	x	
Geog. Areas	Hellenic Arc (Greece)									

Method of performance assessment: Overall goodness-of-fit from Scherbaum et al. (2009), LLH total residuals. Rankings for PSAs at T=0.05-2 s.

Database used for test: 65 recordings from inslab strike-slip earthquakes along the Hellenic arc. Moment magnitudes range from 5.2 to 6.7, their depth mainly varies from 40 to 90 km, and the hypocentral distances are mostly from 70 to 300 km.

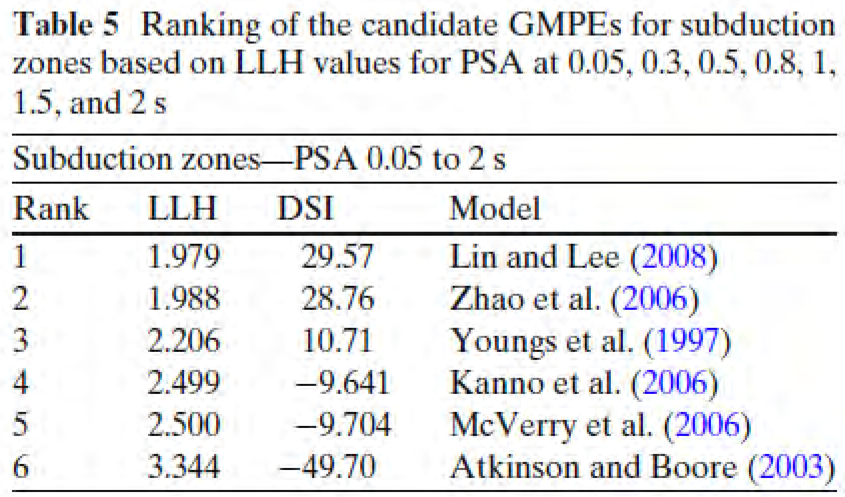

Table 5 Ranking of the candidate GMPEs for subduction zones based on LLH values for PSA at 0.05, 0.3, 0.5, 0.8, 1, 1.5, and 2 s

Subduction zones—PSA 0.05 to 2 s

Rank	LLH	DSI	Model
1	1.979	29.57	Lin and Lee (2008)
2	1.988	28.76	Zhao et al. (2006)
3	2.206	10.71	Youngs et al. (1997)
4	2.499	−9.641	Kanno et al. (2006)
5	2.500	−9.704	McVerry et al. (2006)
6	3.344	−49.70	Atkinson and Boore (2003)

General results: Top-ranked models are LL 2008 and ZEA 2006. AB 2003 performs poorly at long periods but ok for T < 0.16 s.

Case study E

Title	"Regional differences in subduction ground motions" *Presented at the 2011 COSMOS meeting – technical session – November 2011, Emeryville, CA, USA and submitted to 15th World Conference on Earthquake Engineering*									
Authors	Celine Beauval, Fabrice Cotton, Norm Abrahamson, Nikos Theodulidis, Elise Delavaud, Luis E. Rodriguez, F. Scherbaum, A. Haendel									
GMPEs tested	AEA 2012	AEA 2010	AB 2003	GEA 2005	KEA 2006	LL 2008	MEA 2006	YEA 1997	ZEA 2006	ZHA2010
	x	x	x		x	x	x	x	x	
Geog. Areas	*Interface:* Japan, Taiwan, Central + South America, Mexico									
	Intraslab: Greece, Japan, Taiwan									

Method of performance assessment: Overall goodness-of-fit from Scherbaum et al. (2009), LLH total residuals. Intra- and inter-event standard deviations of residuals.

Database used for test: Japan: 7 interface earthquakes, 800 recordings with R < 300km. 7 intraslab earthquakes, 844 recordings.
Taiwan: 3 interface earthquakes, 1 intraslab.
Central and South America: 15 interface earthquakes,115 recordings, R < 300 km.
Greece: 7 intraslab earthquakes, 68 recordings, R = 70-300 km

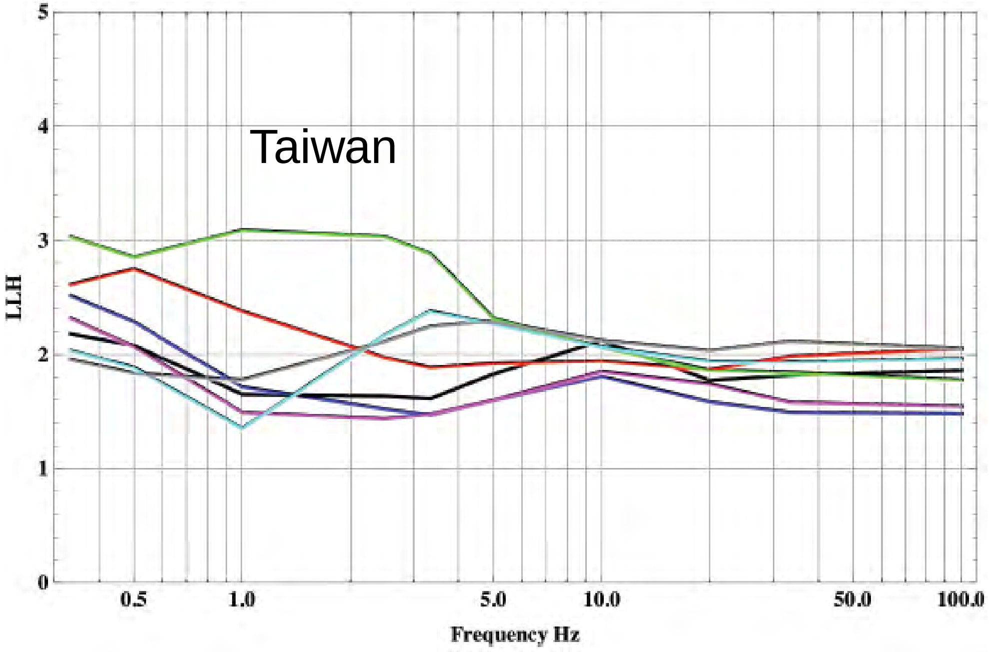

BCHydro, Zhao et al., Lin and Lee, Kanno et al., Youngs et al., Atkinson and Boore, McVerry et al.

INTERFACE:

Japan: close LLH for all models. Good fit up to 0.5 sec for KEA. Best fit for global AEA12 and ZEA06.

Taiwan: large LLH for all models above 0.5 sec. Worst model: global Youngs et al.

Central and South America: good fit with low LLH for YEA, AB2003, AEA12, ZEA. Best fitting for AEA10. (rock only).

Mexico: good fit with low LLH over the whole period range for KEA, AEA12, AEA10. and ZEA06. Best fitting models are AEA and ZEA.

INTRASLAB:

Greece: close LLH for all models, except poor fit for MEA + AB03. Best fitting: AEA12, ZEA06., LL.

Japan: close LLH for all models, except poor fit for MEA + LL. Good fit for AEA12 (lower LLH if accounting for back-arc and fore-arc) / AB03 (no big improvement if Japan specific coefficients are used). Best fit: ZEA06.

Taiwan: large difference in LLH depending on the GMPEs. Poor fit for most models, even LL. Best fit for AEA12 and YEA97.

General results: • Are global models well predicting the ground motion? – AEA12 in most cases (never yielding large LLH / stable with frequency) – YEA97 in most cases (never yielding very large LLH) – AB2003 depending on the region

• Is the ground motion regionally dependent? – Regional models are best fitting models in Japan/Mexico, MEA is not fitting any data, no model is correctly predicting ground motions in Taiwan (M6+) – But, global models AEA12 (and YEA97) are usually predicting well the ground motions, sometimes equally well as the regional models. One reason might be the scaling in magnitude/distance which is better modeled in the AEA12 equations..

Case study F

Title	“NZ-Specific Pseudo-Spectral Acceleration Ground Motion Prediction Equations Based on Foreign Models” (2010), *Research report 2010-03, Department of Civil Engineering, University of Canterbury, Christchurch, New Zealand, 22 September 2010*									
Authors	Brendon A. Bradley									
GMPEs tested	AEA 2012	AEA 2010	AB 2003	GEA 2005	KEA 2006	LL 2008	MEA 2006	YEA 1997	ZEA 2006	ZHA2010
			x				x		x	
Geog. Areas	New Zealand									

Method of performance assessment: Analysis of inter- and intra-event residuals, Scasserra et al. (2009).

Database used for test: 2437 records from NZ, 62% from intra-slab events. Many of the Subduction slab events have normal oblique focal mechanism).

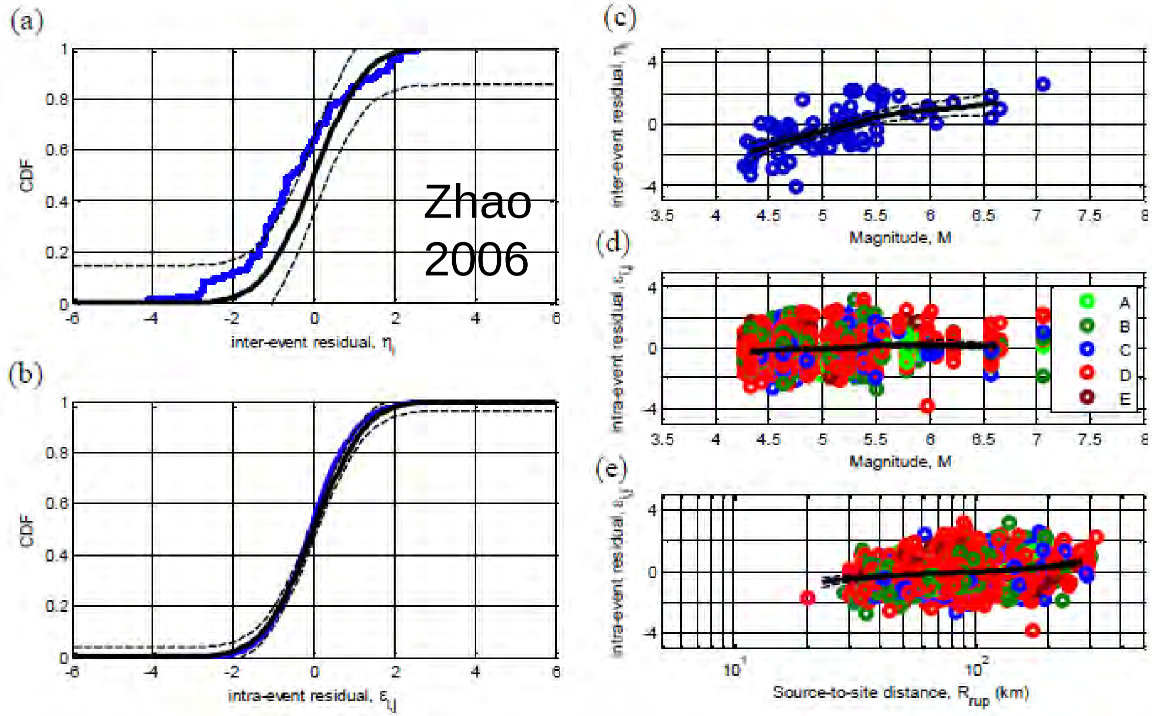

Zhao 2006

General results:

Interface: best model is Zhao 2006

Intraslab: all models bias. NZ-specific model developed by modifying Zhao 2006

Case study G

Title	“Strong Ground Motion Attributes of the 2010 Mw8.8 Maule Chile Earthquake” *Earthquake Spectra, 28 (S1), S19-38. (2012)*									
Authors	Rubén Boroschek, Víctor Contreras, Dong Youp Kwak and Jonathan P. Stewart									
GMPEs tested	AEA 2012	AEA 2010	AB 2003	GEA 2005	KEA 2006	LL 2008	MEA 2006	YEA 1997	ZEA 2006	ZHA2010
			x						x	
Geog. Areas	Chile (M_w 8.8 Maule earthquake)									

Method of performance assessment: Analysis of inter- and intra-event residuals, Scasserra et al. (2009).

Database used for test: 31 strong motion recordings of the M_w 8.8 Maule Chile earthquake over a rupture distance range of 30 to 700 km

General results:
Nonlinear M-scaling

R-scaling consistent with AB 2003

Sigma generally consistent with GMPE

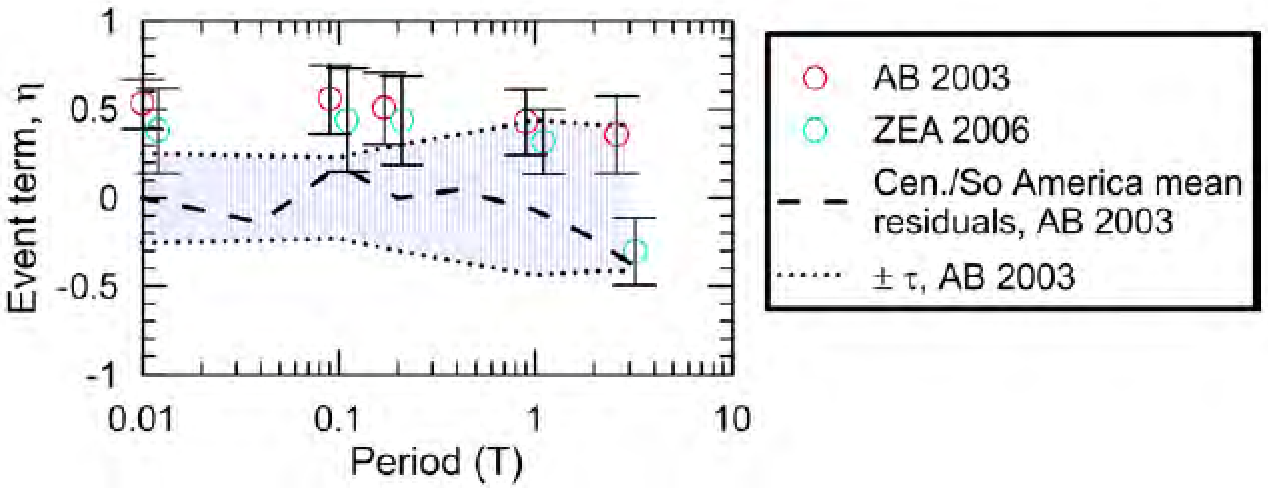

$$R_i = \ln\left(IM_i\right)_{rec} - \ln\left(IM_i\right)_{GMPE}$$

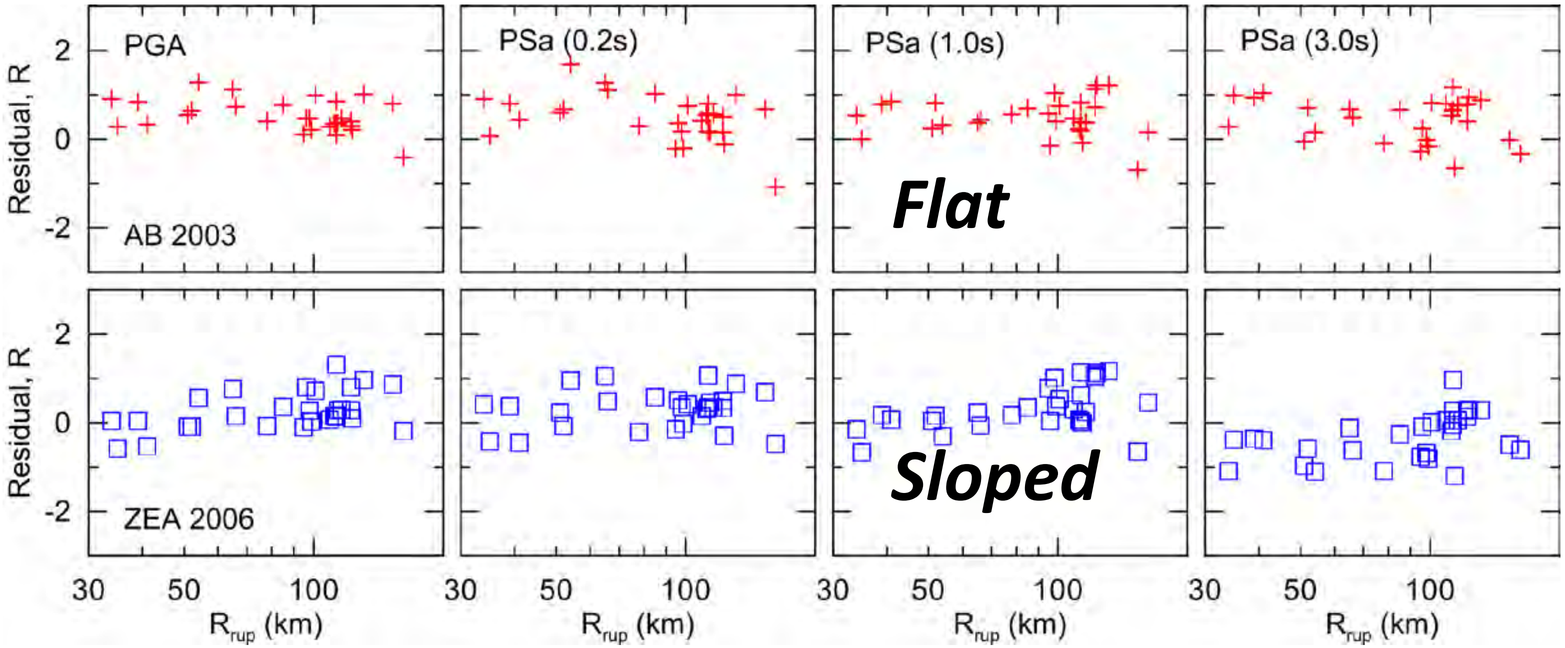

Flat

Sloped

Case study H

Title	“Implications of Mw 9.0 Tohoku-oki Japan earthquake for ground motion scaling with source, path, and site parameters” *Earthquake Spectra (2012-in review)*									
Authors	Jonathan P. Stewart, Suburoh Midorikawa, Robert W. Graves, Khatareh Khodaverdi, Hiroyuki Miura, Yousef Bozorgnia, Kenneth W. Campbell									
GMPEs tested	AEA 2012	AEA 2010	AB 2003	GEA 2005	KEA 2006	LL 2008	MEA 2006	YEA 1997	ZEA 2006	ZHA2010
	x		x						x	
Geog. Areas	Japan (M_w 9.0 Tohoku earthquake)									

Method of performance assessment: Analysis of inter- and intra-event residuals, Scasserra et al. (2009).

Database used for test: 477 strong motion recordings of the M_w 9.0 Tohoku-oki Japan earthquake over a rupture distance range of 50 to 500 km

General results:

Nonlinear M-scaling (saturation at short periods)

Fast R-scaling. ZEA2006 better than AB 2003

Little V_{s30}-scaling at high frequencies.

Lower intra-event sigma than ZEA 2006

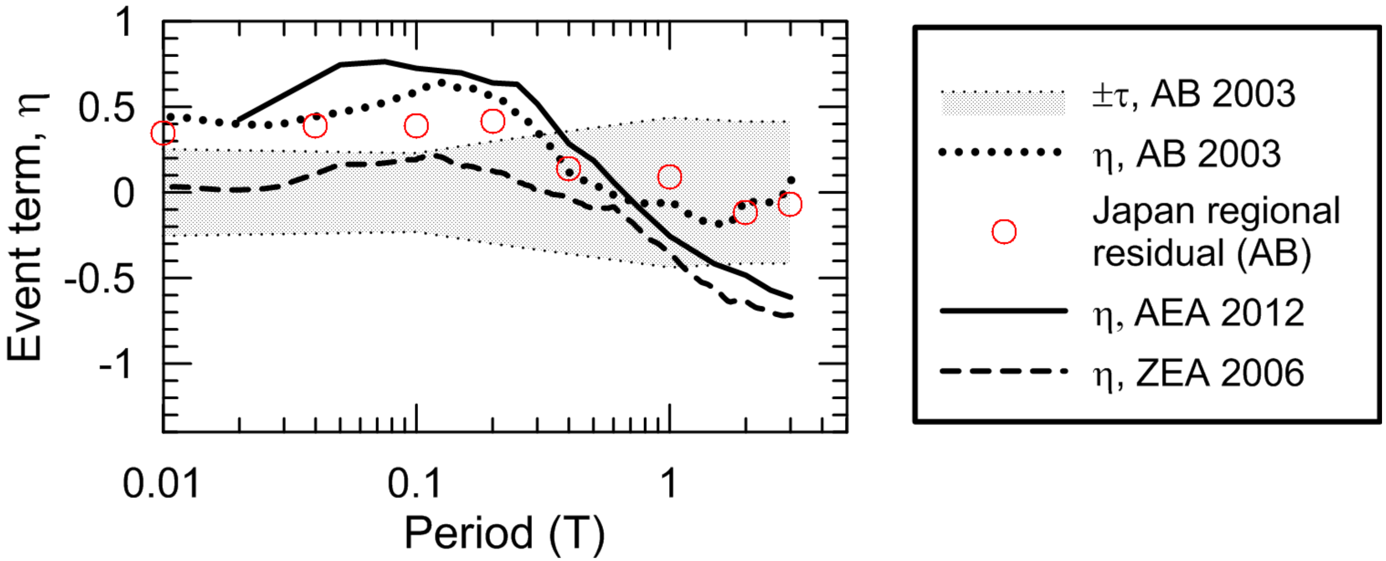

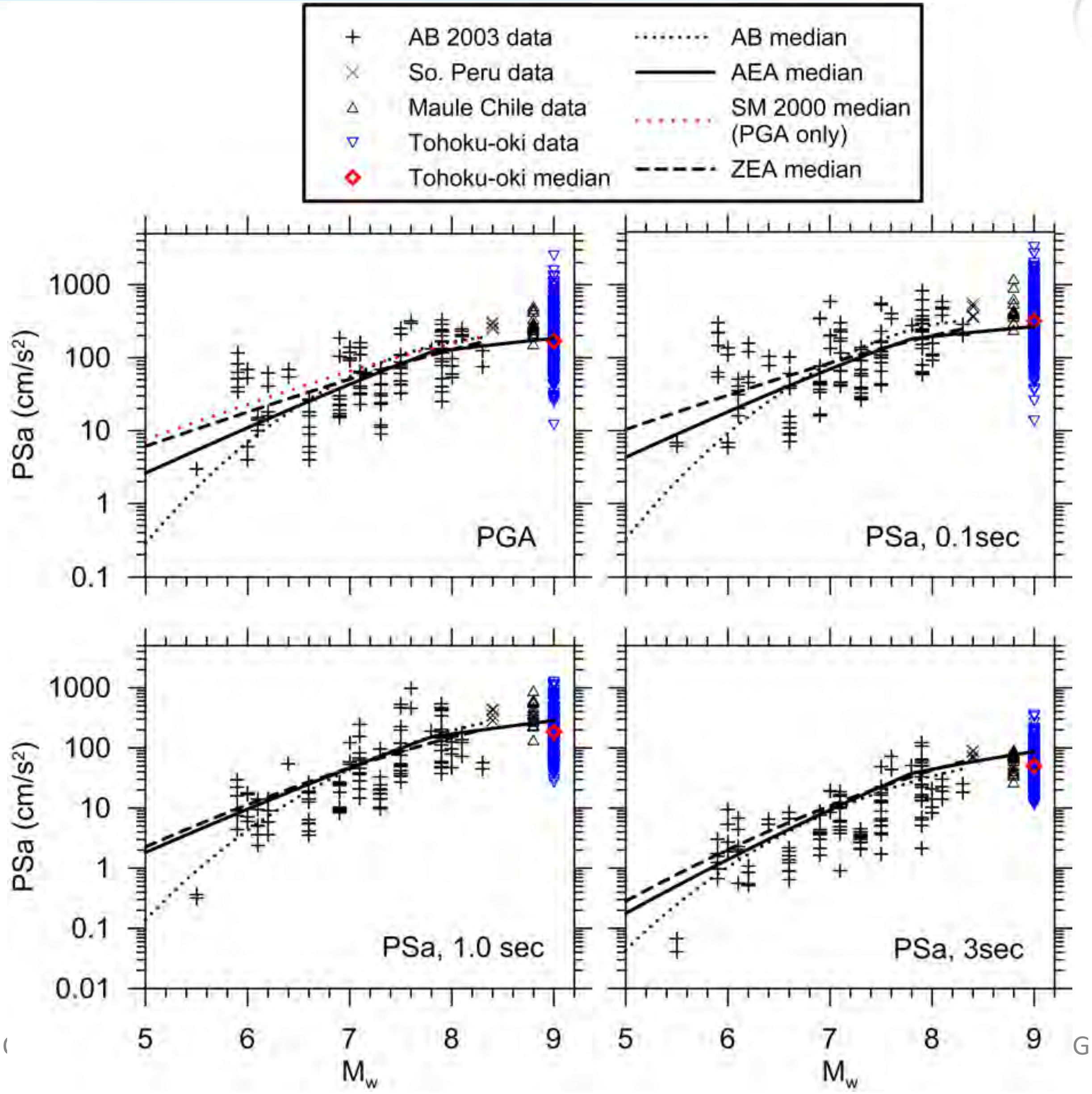
AB 2003 data
So. Peru data
Maule Chile data
Tohoku-oki data
Tohoku-oki median
AB median
AEA median
SM 2000 median (PGA only)
ZEA median
PSa (cm/s²)
1000
100
10
1
0.1
0.01
PGA
PSa, 0.1sec
PSa, 1.0 sec
PSa, 3sec
5
6
7
8
9
Mw

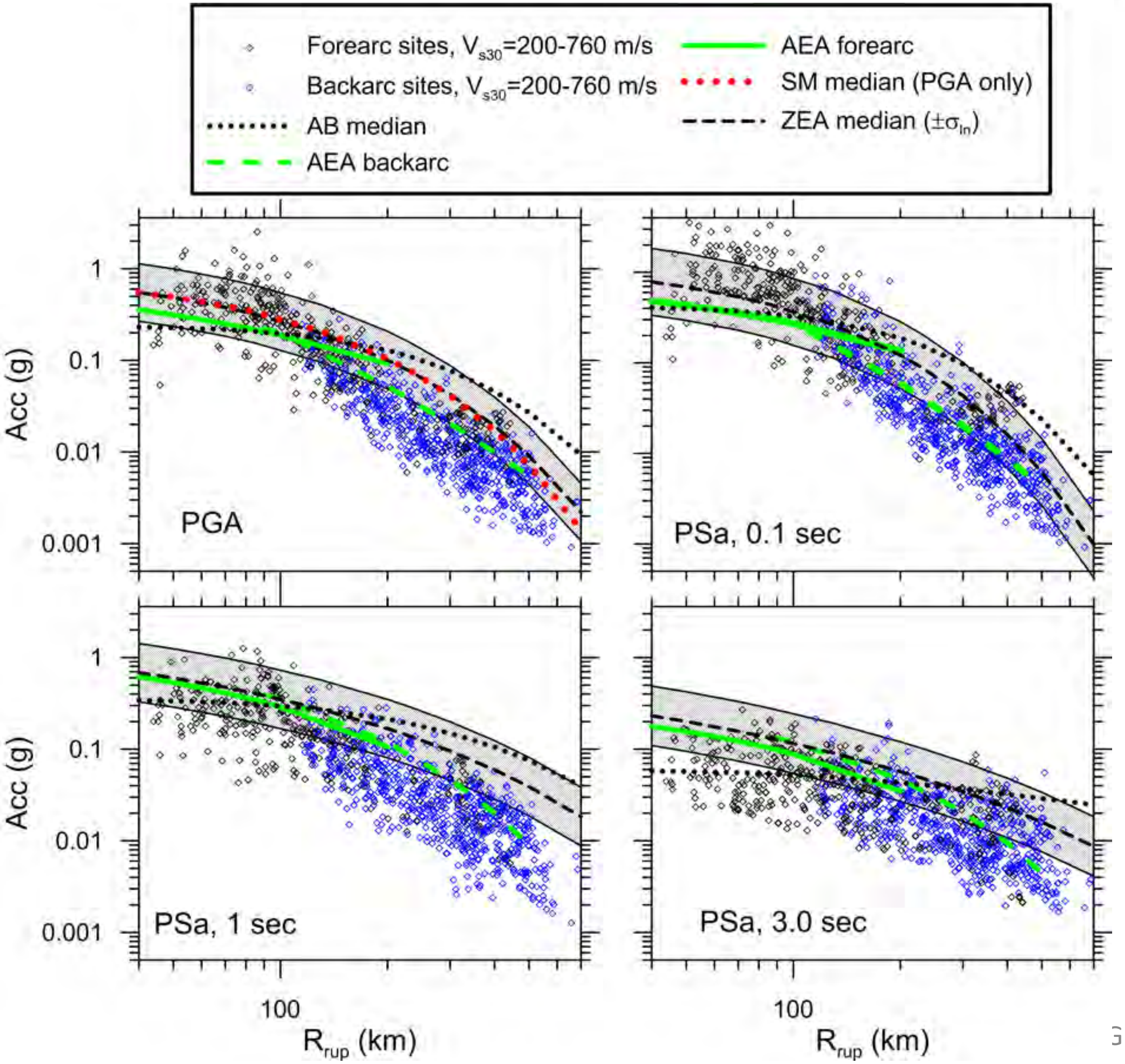
Forearc sites, V$_{s30}$=200-760 m/s
Backarc sites, V$_{s30}$=200-760 m/s
AB median
AEA backarc
AEA forearc
SM median (PGA only)
ZEA median ($\pm\sigma_{ln}$)
PGA
PSa, 0.1 sec
PSa, 1 sec
PSa, 3.0 sec
Acc (g)
1
0.1
0.01
0.001
100
R$_{rup}$ (km)

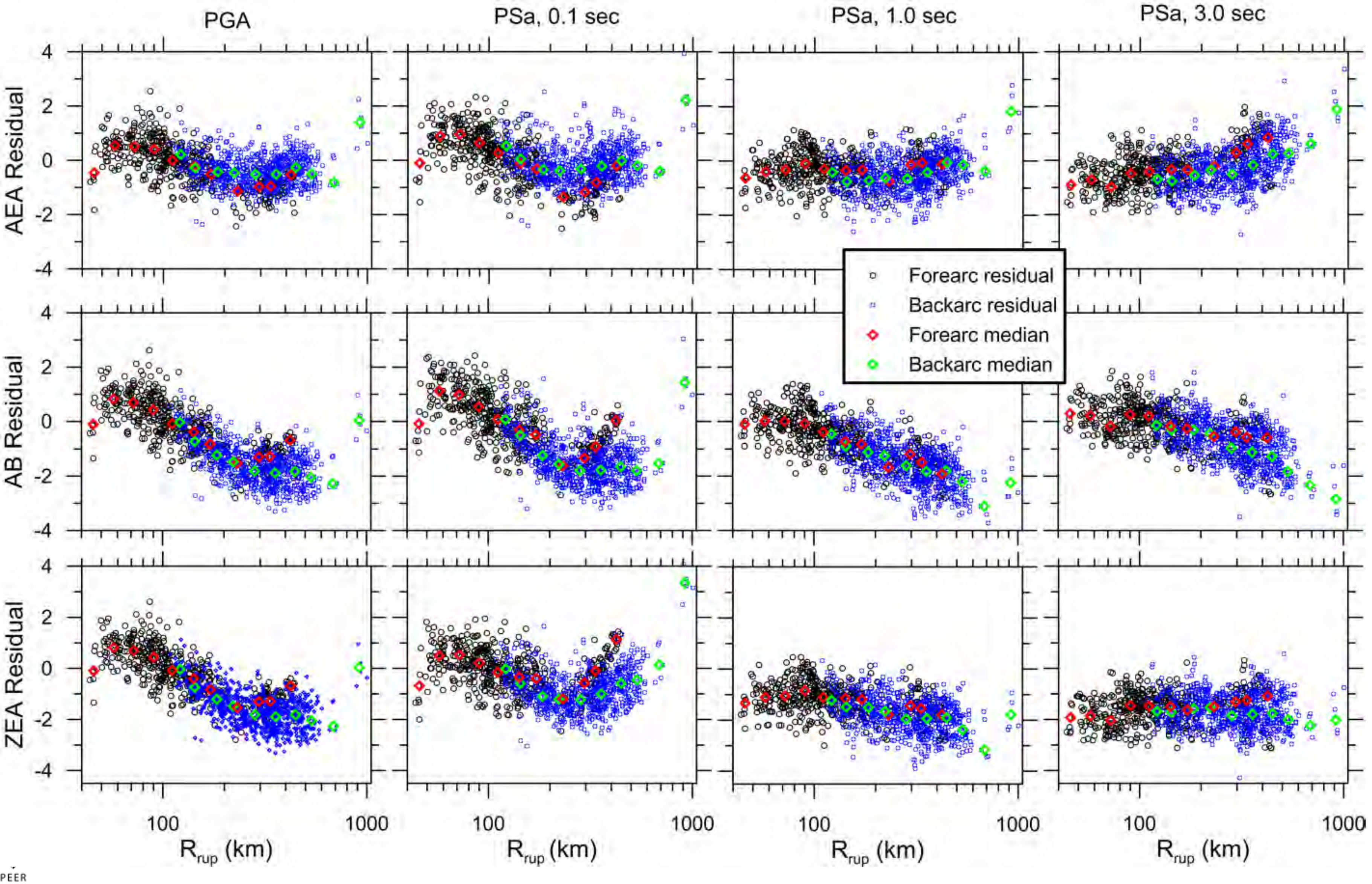
PGA
PSa, 0.1 sec
PSa, 1.0 sec
PSa, 3.0 sec
AEA Residual
AB Residual
ZEA Residual
4
2
0
-2
-4
100
1000
R_{rup} (km)
○ Forearc residual
□ Backarc residual
◇ Forearc median
◇ Backarc median

Proposed selection

- **Following two webconferences and numerous email exchanges the core proposes:**
  - Atkinson & Boore (2003)
    - Large international database
    - Sophisticated functional form
    - Perform well for recent large events (e.g. Maule 2010)
    - Models relatively *slow* attenuation rate, as in Chile
  - Abrahamson et al. (2012)
    - Largest and most recent database
    - International applicability
    - Sophisticated functional form
  - Zhao et al. (2006)
    - Large international database
    - Sophisticated functional form
    - Performs well for recent large events (e.g. Tohoku 2011)
    - Models relatively *fast* attenuation rate, as in Japan
- **Reasonably easy to come to final decision within the core**

Spectra for proposed GMPEs

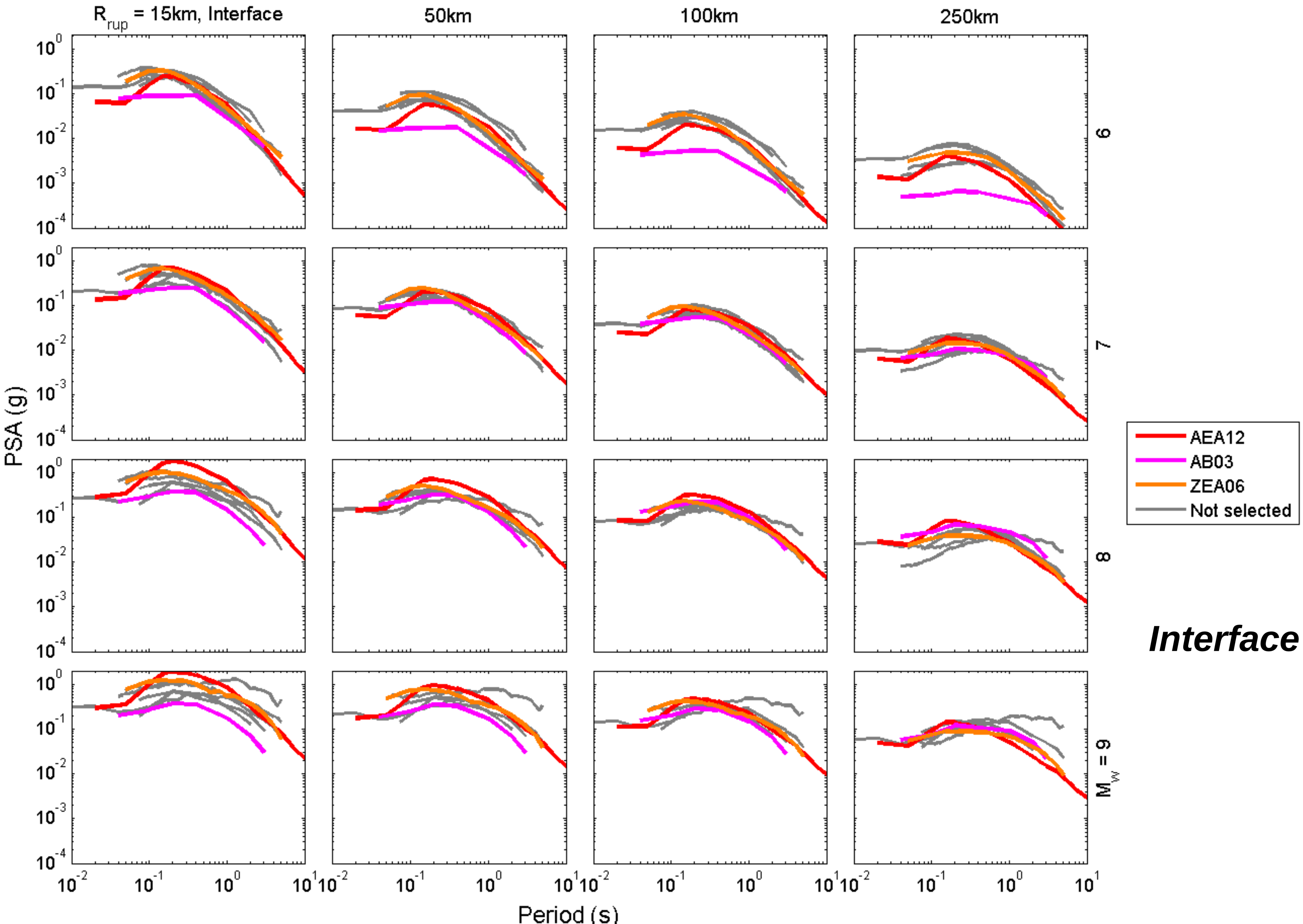

Interface

Spectra for proposed GMPEs

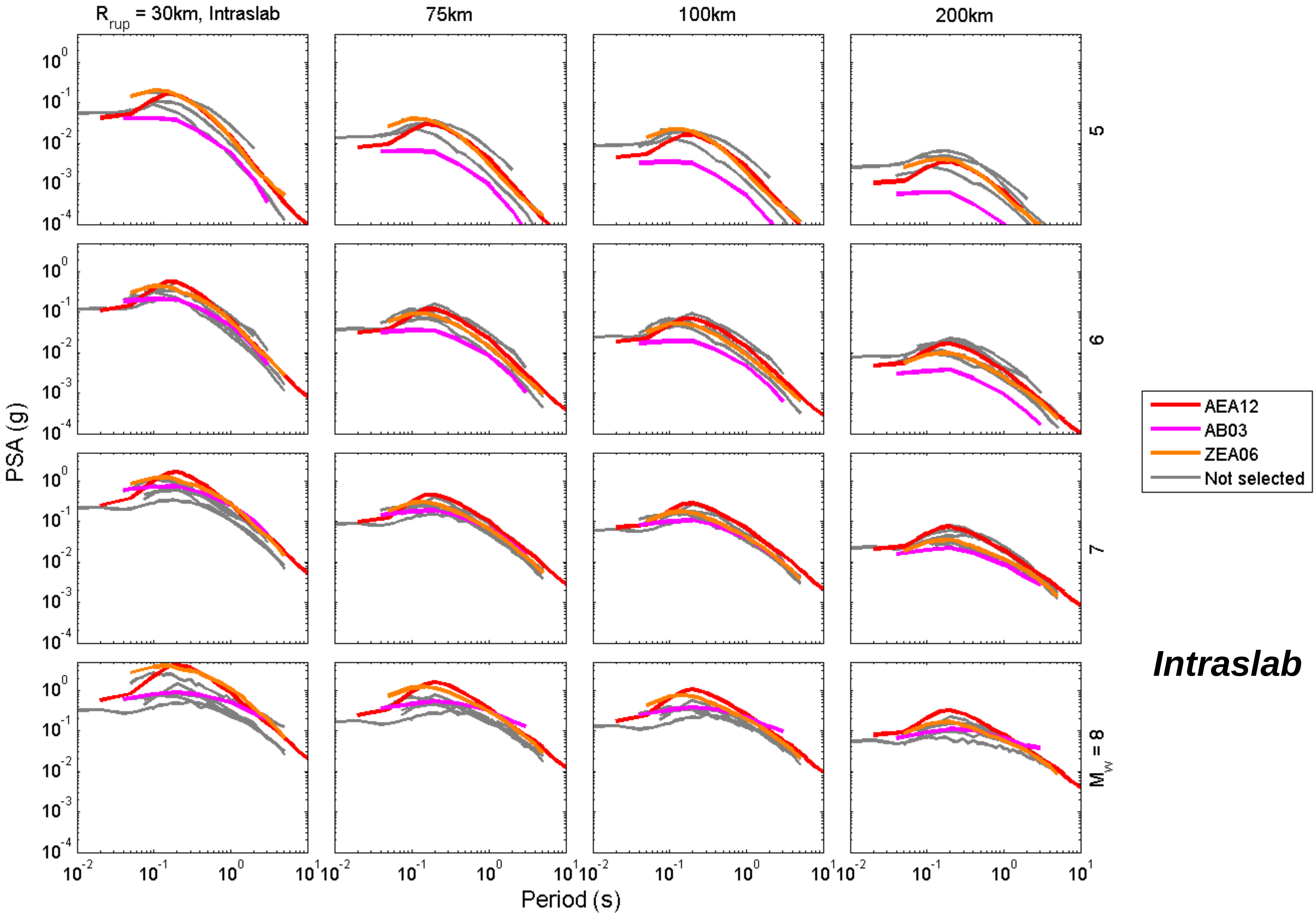

Intraslab

M-scaling of proposed GMPEs

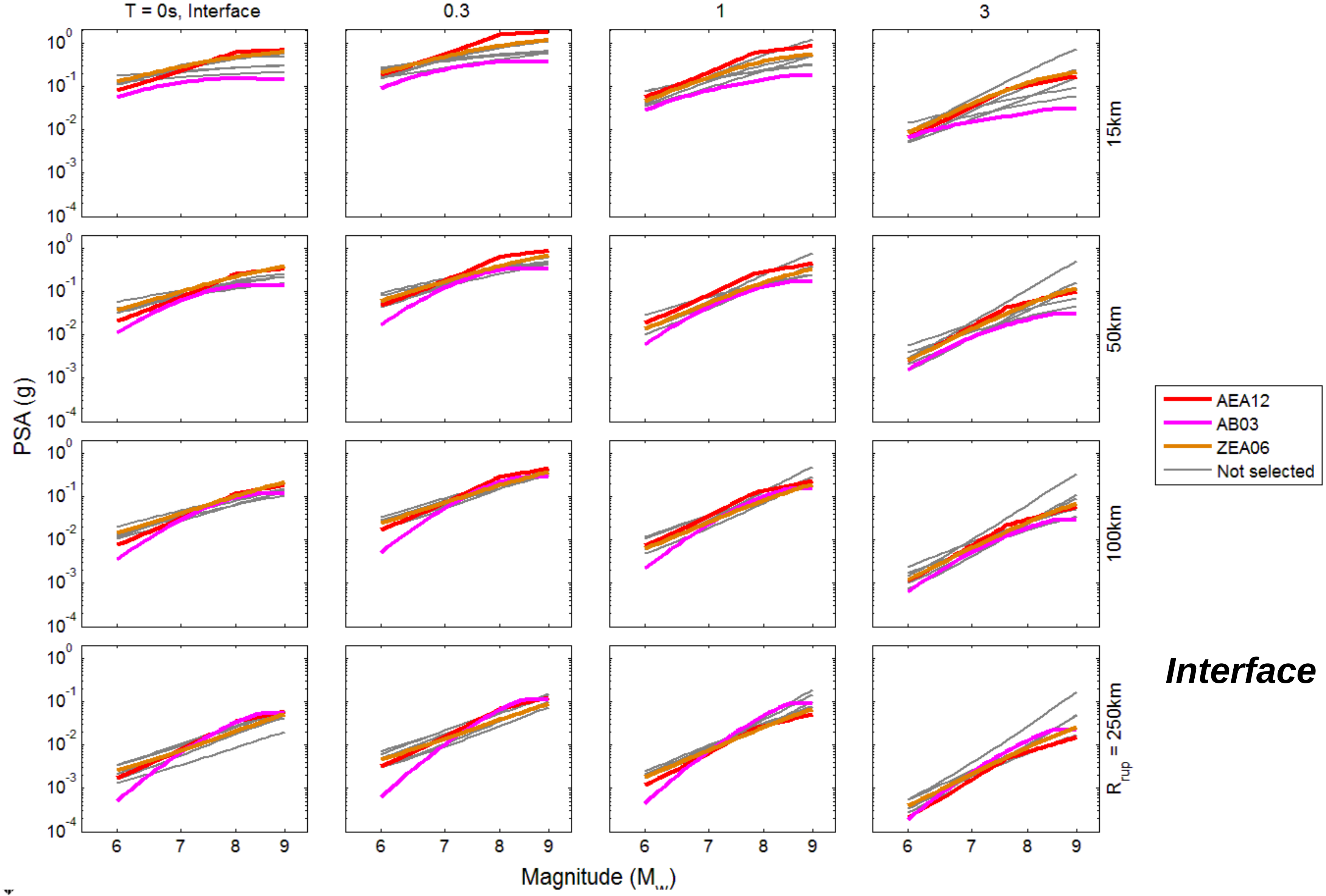

Interface

M-scaling of proposed GMPEs

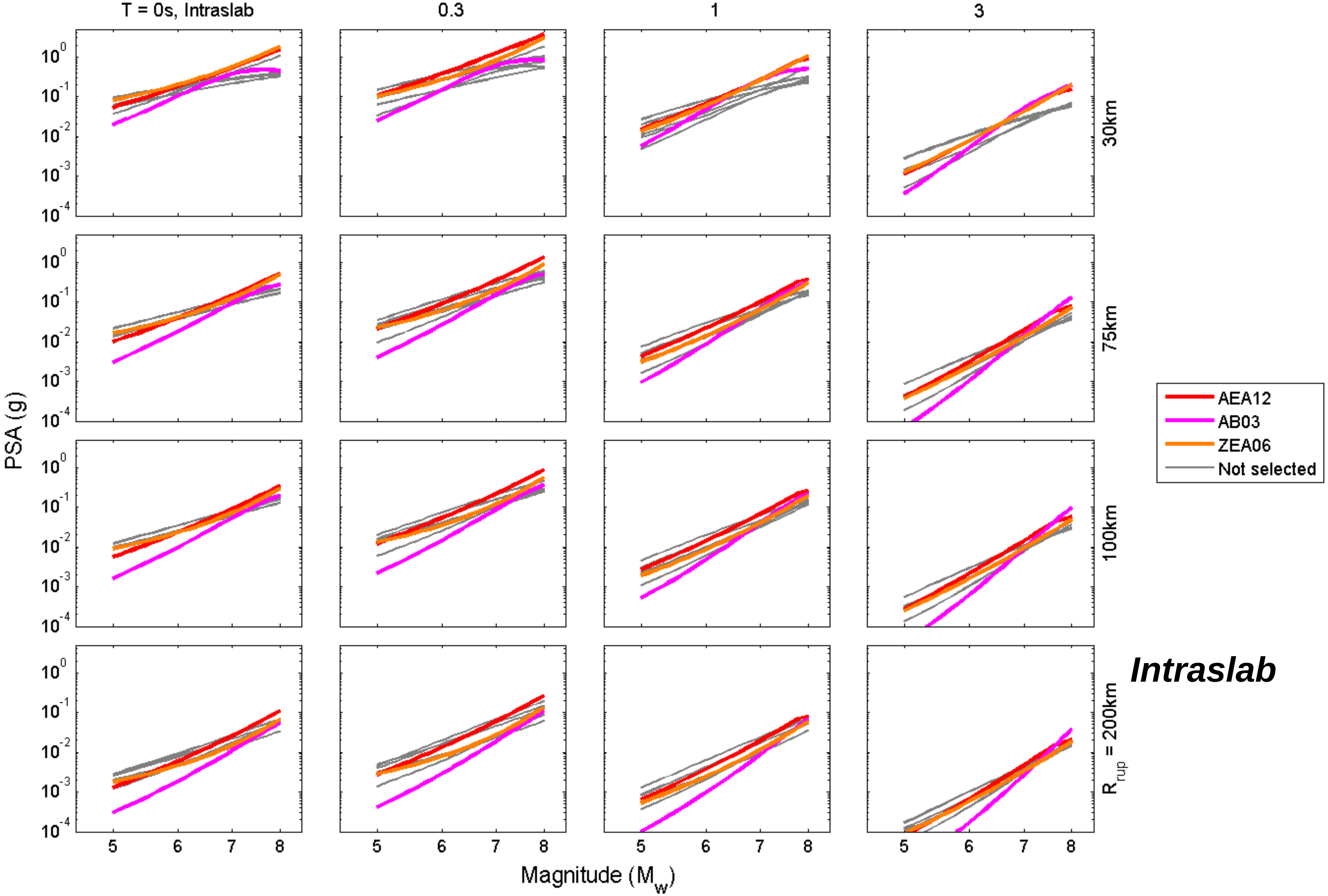

Intraslab

R-scaling of proposed GMPEs

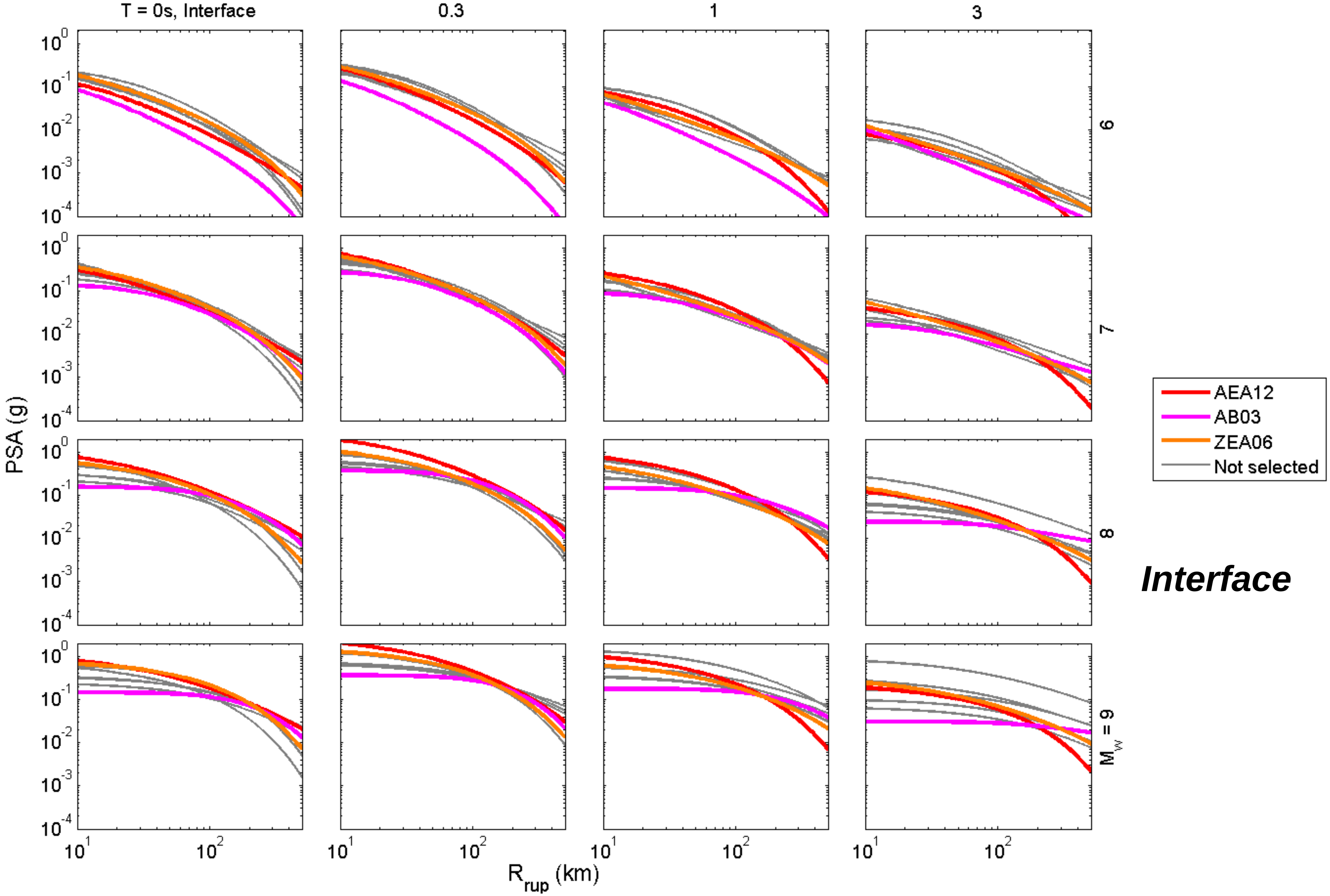

Interface

R-scaling of proposed GMPEs

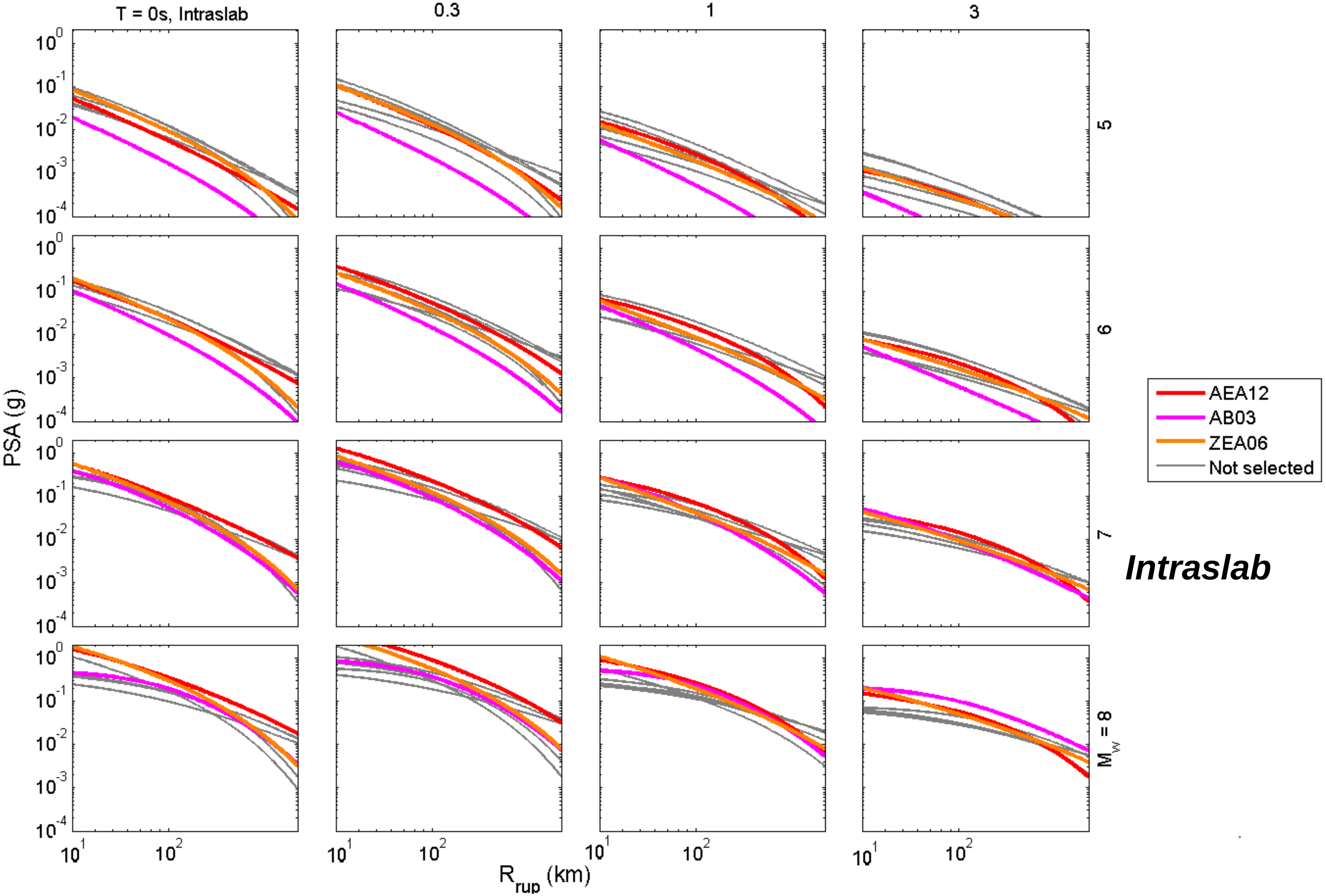

Intraslab

Sigma of proposed GMPEs

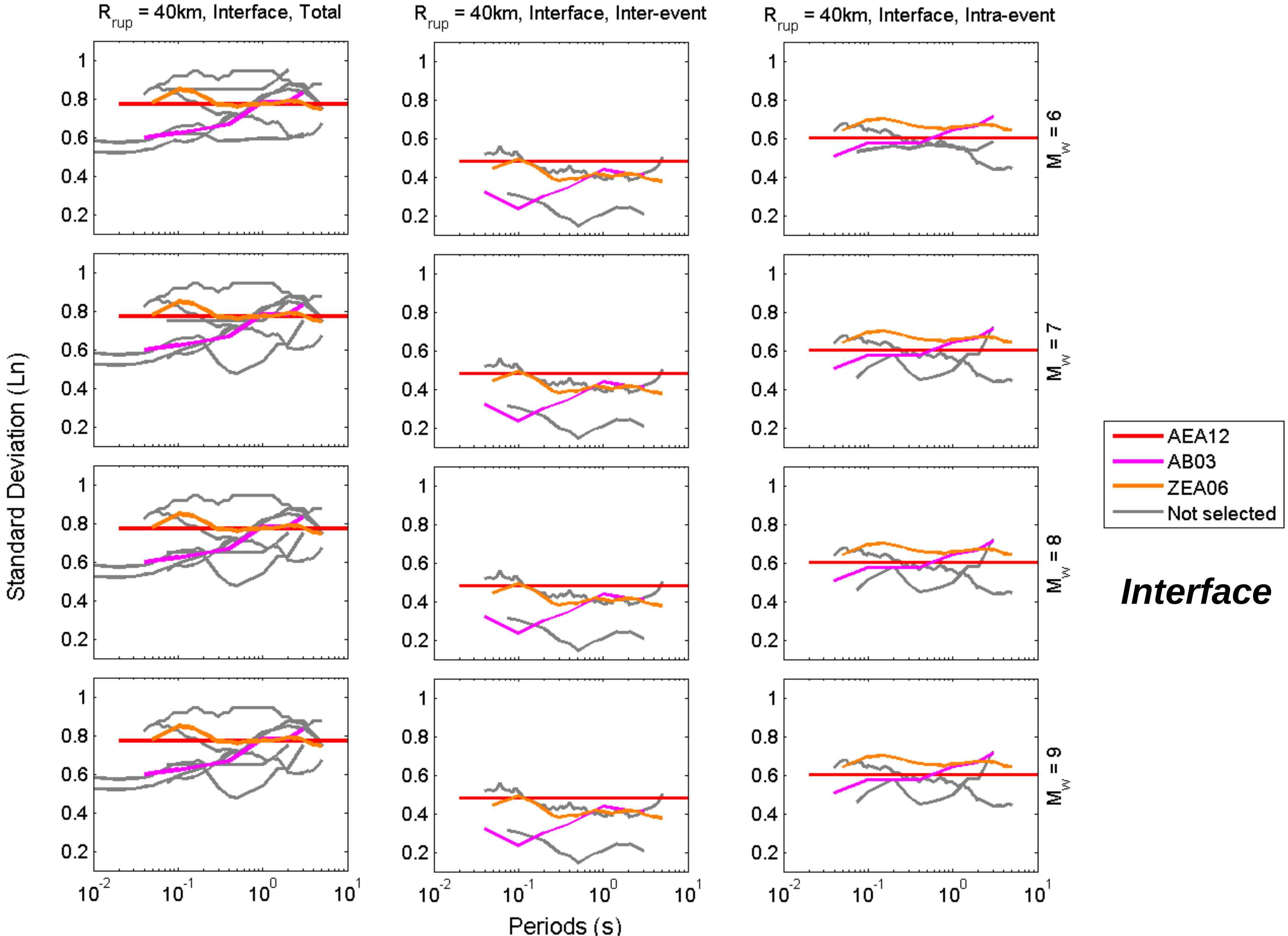

Interface

Sigma of proposed GMPEs

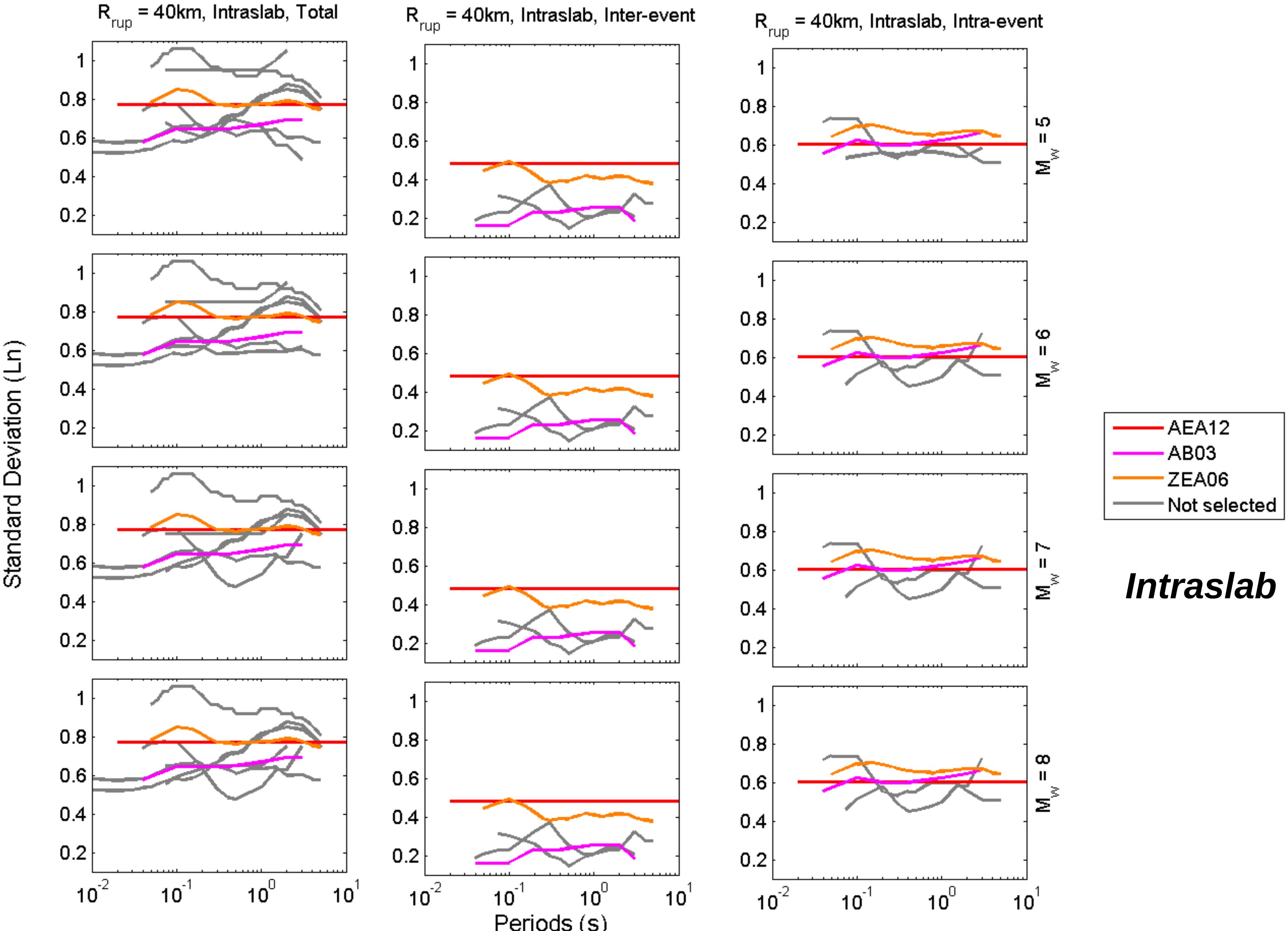

Intraslab

Preliminary selected GMPEs for Subduction Regions

Jonathan P. Stewart & John Douglas (co-chairs)

C. di Alessandro, D. M. Boore, Y. Bozorgnia
N. A. Abrahamson, E. Delavaud, P. J.
Stafford, K. W. Campbell, M. Erdik &
M. B. Javanbarg

PEER

GEM
GLOBAL EARTHQUAKE MODEL

Preliminary selected GMPEs for Stable Continental Regions

John Douglas & Jonathan P. Stewart (co-chairs)

C. di Alessandro, D. M. Boore, Y. Bozorgnia
N. A. Abrahamson, E. Delavaud, P. J.
Stafford, K. W. Campbell, M. Erdik &
Mohammad B. Javanbarg

PEER

GEM
GLOBAL EARTHQUAKE MODEL

Pre-selected GMPEs

1. **Atkinson [2008] as modified by Atkinson & Boore [2011]:**
   Referenced empirical model for eastern North America
2. **Atkinson & Boore [2006] as modified by Atkinson & Boore [2011]:**
   Extended stochastic model for eastern North America
3. **Campbell [2003]:**
   Hybrid model for eastern North America
4. **Douglas *et al*. [2006]:**
   Hybrid model for southern Norway
5. **Frankel *et al*. [1996] as parameterized by EPRI [2004]:**
   Stochastic model for eastern North America
6. **Raghu Kanth & Iyengar [2006, 2007]:**
   Stochastic model for peninsular India
7. **Silva *et al*. [2002]:**
   Stochastic model for eastern North America
8. **Somerville *et al*. [2009]:**
   Simulation-based models for Australia
9. **Pezeshk *et al*. [2011]:**
   Hybrid model for eastern North America
10. **Toro *et al*. [1997] modified by Toro [2002]:**
    Stochastic model for eastern North America

+ various variants to account for epistemic uncertainty or different regions

Reminder of procedure

- **Principles agreed (slightly different to those for subduction and active):**

1. SCR GMPEs are derived principally from the results of numerical simulations. However, the manner in which the limited available data is used to constrain the input parameters used in the simulations is critical. The empirical calibration may influence, for example, stress drop parameters and kappa. **We give more weight to GMPEs judged to effectively use the available data to constrain model parameters.**
2. **We give more weight to GMPEs that have attributes to their functional form that we consider desirable, including saturation with magnitude, magnitude dependent distance scaling and anelastic attenuation terms.** Since the data is very limited for SCRs, it is especially important that the selected models extrapolate in a reasonable manner beyond the data range.
3. **We seek GMPEs that meet the above criteria and which collectively: (i) represent diverse geographic regions and (ii) use alternate simulation methodologies.** This is intended to capture epistemic uncertainty in the selected GMPEs.

- Trellis plots
- Results of (quantitative) testing of models against independent sets of data (very few)
- Circulation of available plots and results of testing (two rounds after discussions)
- Independent selections (of ~3 models) sent to WG facilitators
- Discussion of selections and consensus decision taken within core

- **Today we would like your feedback and suggestions**

SCR GMPEs pre-selected (page 1)

Reference	Area	H	E	*M* min	*M* max	*M* scale	*r* min	*r* max	*R* scale	S	*T*s	*T* min	*T* max	C	R	M
Atkinson [2008] as modified by Atkinson & Boore [2011]	Eastern North America	ENA observations from Atkinson & Boore (2006)		4.3	7.6	Mw	10	1000+	Rjb	1 - Vs30= 760 m/s	6, PGA, PGV	0.1	5	Referenced Empirical Approach		
Atkinson & Boore [2006] as modified by Atkinson & Boore [2011]	Eastern North America	34800[1]	10	3.5	8	Mw	1	1000	Rrup	1, C	24, PGA, PGV	0.025	5	G	1	R
Campbell [2003]	Eastern North America	Hybrid Empirical GM simulations		+5	8.2	Mw	0	1000	Rrup	1 - Vs30= 2.8 km/s	16, PGA (0.01 s)	0.02	4	G	1	R
Douglas *et al*. [2006]	Southern Norway	Hybrid Empirical GM simulations		+4.5	7.5	Mw	1	1000	Rjb	1 – rock sites	14	0.02	2	G	1	R, N, S
Frankel *et al*. [1996] as parameterized by EPRI[2004]	Central Eastern North America	Stochastic simulations		5	8	Mw	10	500	Rhyp	1 – Vs30= 2800m/s	7	0	2	G	1	R

[1] simulated records

SCR GMPEs pre-selected (page 2)

Reference	Area	H	E	*M* min	*M* max	*M* scale	*r* min	*r* max	*R* scale	S	*Ts*	*T* min	*T* max	C	R	M
Raghu Kanth & Iyengar [2006, 2007]	Peninsular India	900	9[2]	4[2]	8[2]	Mw	1[2]	300[2]	Rhypo	1 – bedrock Vs_{30} ~ 3600 m/sec + conversion for NEHRP A,B,C and D	27, PGA	0.01	4	U	2	A
Silva *et al.* [2002]	Central and Eastern North America, Mid-Continent and Gulf Coast Areas	300[3]	5[3]	4.5[3]	7.5[3]	Mw	1[3]	400[3]	Rrup	[4]	26, PGA, PGV, PGD	0.01	10	U	U	A
Somerville *et al.* [2009]	Australia (cratonic and non-cratonic)			5	7.5	Mw	0	500	Rjb	1 - rock Vs_{30}= 865 m/s	22, PGA, PGV	0.01	10	U[5]	1 M	T[6]

[2] Spectral acceleration values are simulated for moment magnitude (Mw) ranging from 4 to 8 in increments of 0.5 units. The distance parameter is varied in intervals of log10(repi) = 0.13

[3] 300 stochastic point-source simulations reflecting parametric variability are made at distances of 1, 5, 10, 20, 50, 75, 100, 200, and 400 km. At each distance, five magnitudes are used: M 4.5, 5.5, 6.5, 7.5, and 8.5.

[4] random vibration theory (RVT) used to assess the site response, where a profile randomization scheme has been developed which varies both layer velocity and thickness

[5] fault locations and orientations are not known. Probably the geometric mean.

[6] Source model developed for Thrust-faulting: the style of faulting in Australia is predominantly reverse, with strike-slip faulting occurring together with thrust faulting

SCR GMPEs pre-selected (page 3)

Reference	Area	H	E	*M* min	*M* max	*M* scale	*r* min	*r* max	*R* scale	S	*Ts*	*T* min	*T* max	C	R	M
Pezeshk *et al.* [2011]	Eastern North America		7[7]	5[7]	8[7]	Mw	1[7]	1000[6]	Rrup	1 – hard rock $Vs_{30} \geq$ 2000 m/s or NEHRP A	22, PGA	0.01	10	I50	1	A[8]
Toro *et al.* [1997] modified by Toro [2002]	Eastern North America	Stochastic simulations		5	8	Mw	1	1000	Rjb	1 - Vs_{30} = 2.8 km/s	7, PGA	0.05	4	G	1	R

[7] hybrid empirical method, moment magnitudes 5.0 to 8.0 in 0.5 magnitude unit increments, and for 24 rupture distances (Rrup) logarithmically spaced from 1 to 1000 km.

[8] generic style of faulting for NGA models

10 models but variants for 4 GMPEs hence 26 models in total

Spectra (rock sites)

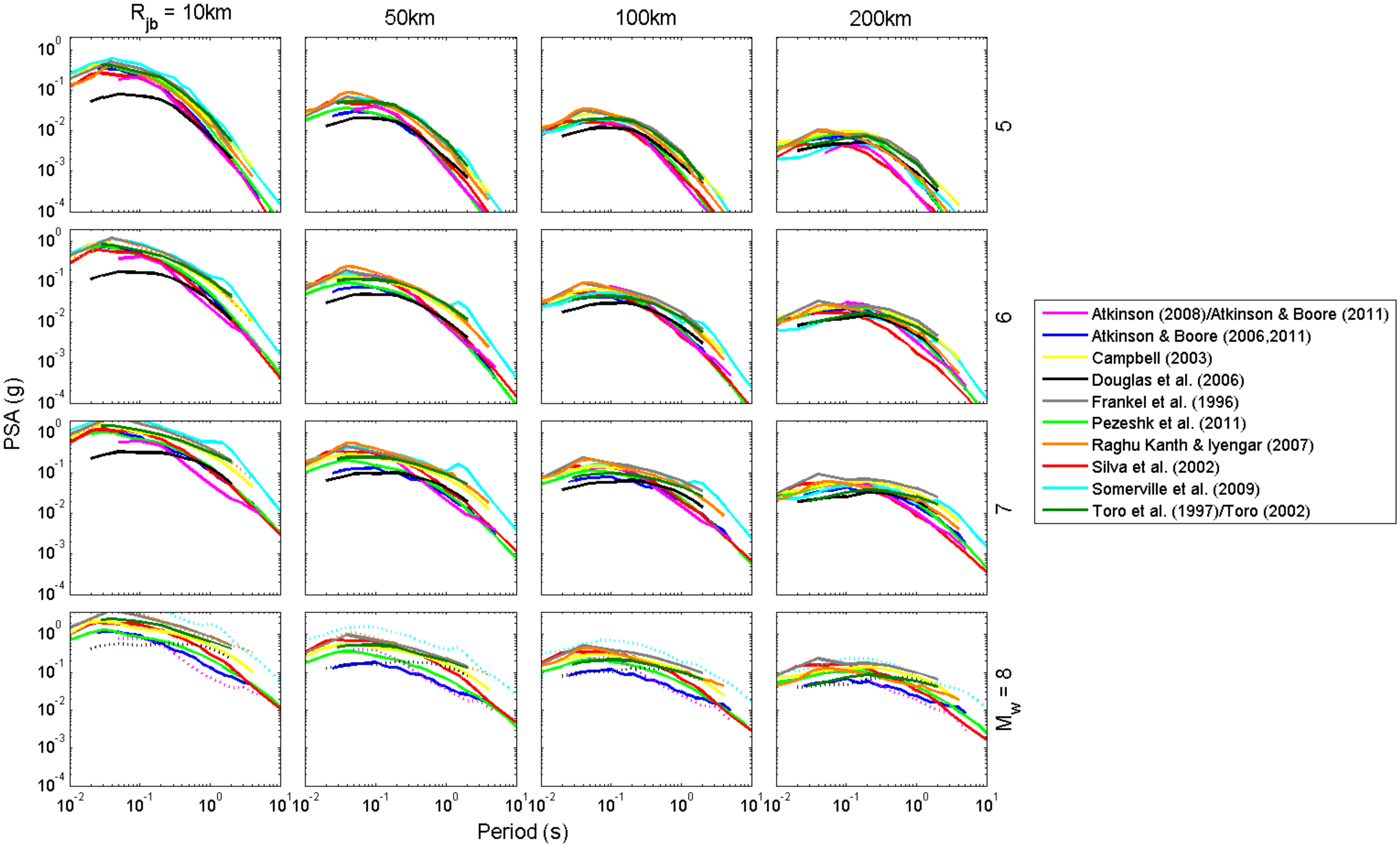

Sigma for rock

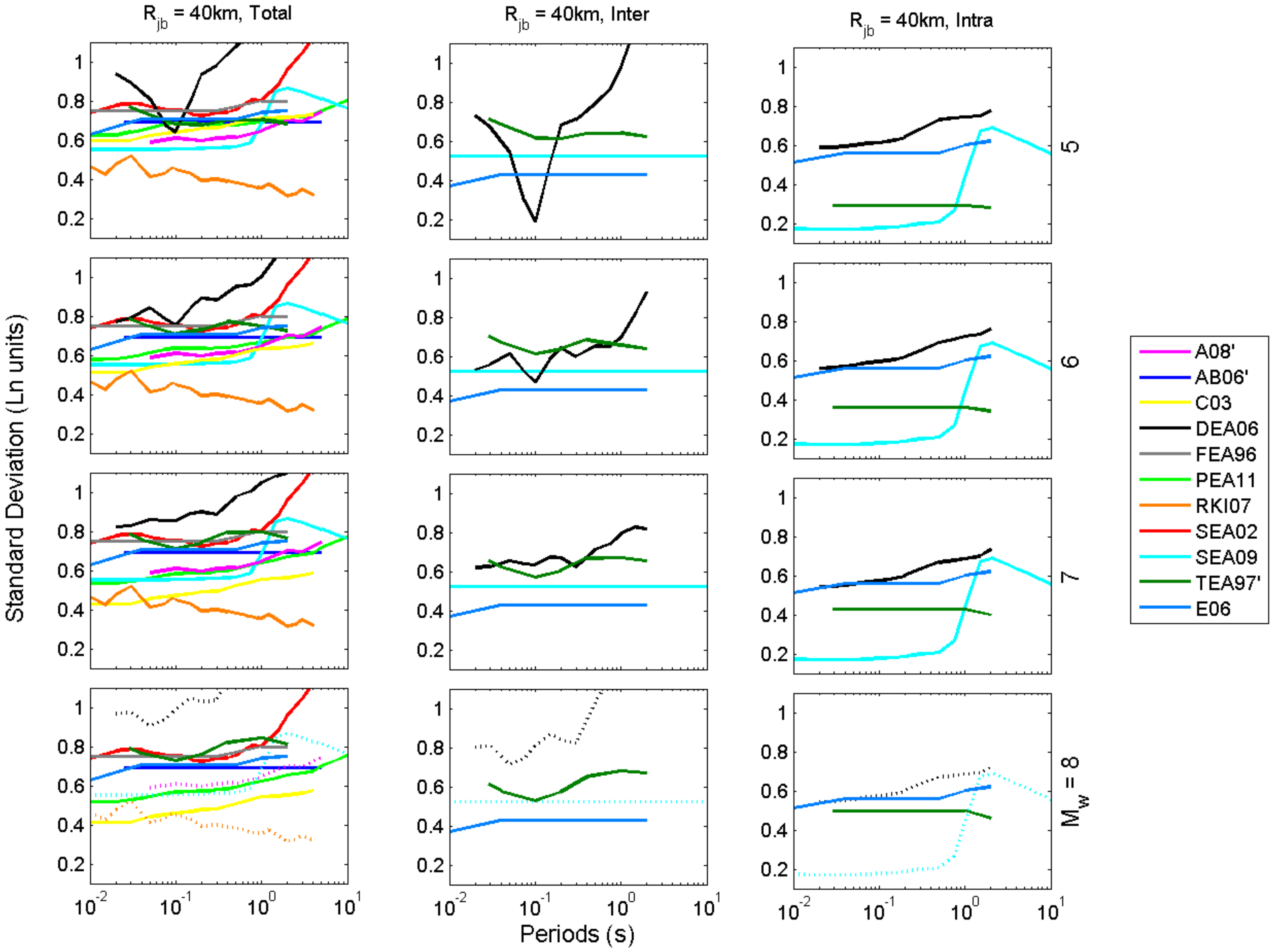

MAGNITUDE TERM SYNTHESIS

MODEL	MAGNITUDE TERM(s)	NOTES	Mw RANGE
Atkinson (2008) as modified by Atkinson & Boore (2011)	$e_5(M-M_h)+e_6(M-M_h)^2$ (linear and quadratic M terms) for $M<M_h$ and $e_7(M-M_h)^2$ (linear M term) for $M>M_h$ where $M_h=6.75$ plus linear magnitude-dependent geometric decay $[(c_1+c_2(M-M_{ref}))\ln(R/R_{ref})]$	Assumes the same magnitude-scaling as Boore & Atkinson (2008) for active regions. Break in magnitude-scaling at 6.75	4.3-7.6
Atkinson & Boore (2006) as modified by Atkinson & Boore (2011)	$c_2M+c_3M^2$ (linear and quadratic M term) plus linear magnitude-dependent decay $[(c_6+c_7M)R'$ where R' are various distance functions accounting for crustal structure]	Same as Frankel et al. (1996)/EPRI (2004)	3.5-8
Campbell (2003)	$c_2M+c_3(8.5-M)^2$ (linear and quadratic M term) plus linear magnitude-dependent anelastic decay $[(c_5+c_6M)r_{rup}]$ and magnitude-dependent distance-saturation geometric spreading term $[R=\mathrm{sqrt}(r_{rup}{}^2+(c_7\exp(c_8M))^2)]$	Same as Douglas et al. (2006)	+5-8.2
Douglas et al. (2006)	$c_2M+c_3(8.5-M)^2$ (linear and quadratic M term) plus linear magnitude-dependent anelastic decay $[(c_5+c_6M)r_{JB}]$ and magnitude-dependent distance-saturation geometric spreading term $[R=\mathrm{sqrt}(r_{JB}{}^2+(c_7\exp(c_8M))^2)]$	Adopted form of Campbell (2003)	+4.5-7.5
Frankel et al. (1996) as parameterized by EPRI (2004)	$c_2M+c_3M^2$ (linear and quadratic M term) plus linear magnitude-dependent decay $[(c_6+c_7M)R'$ where R' are various distance functions accounting for crustal structure] and magnitude-dependent distance saturation $[r'=\mathrm{sqrt}(r_{JB}{}^2+(\exp(C_{11}+C_{12}M))^2)]$	Same as Atkinson & Boore (2006, 2011)	+5-8

MAGNITUDE TERM SYNTHESIS

MODEL	MAGNITUDE TERM(s)	NOTES	Mw RANGE
Raghu Kanth & Iyengar (2006, 2007)	$c_2(M-6)+c_3(M-6)^2$ (linear and quadratic M term)	Very simple form	4-8
Silva et al. (2002)	$C_2M+C_{10}(M-6)^2$ (linear and quadratic M term) plus linear magnitude-dependent geometric spreading term $[(C_6+C_7M)\ln(R+e^{C4})]$		4.5-7.5
Somerville et al. (2009)	(c_2 or c_7)$(M-m_1)+c_8(8.5-M)^2$ (linear and quadratic M term) with different linear slopes (c_2 and c_7) below and above magnitude threshold ($m_1=6.4$) plus linear magnitude-dependent geometric spreading term	Break in magnitude-scaling at 6.4	5-7.5
Pezeshk et al. (2011)	$c_2M+c_3(8.5-M)^2$ (linear and quadratic M term) plus linear magnitude-dependent geometric decay $[(c_4+c_5M)R'$ where R' are various distance functions accounting for crustal structure]	Similar to Atkinson & Boore (2006, 2011)	5-8
Toro et al. (1997) modified by Toro (2002)	$c_2(M-6)+c_3(M-6)^2$ (linear and quadratic M terms) plus magnitude-dependent distance saturation term (either $R_M=\mathrm{sqrt}(r_{rup}{}^2+C_7{}^2[\exp(-1.25+0.227M)]^2)$ in the empirical approach or $R_M=r_{JB}+0.089\exp(0.6M)$ in the modelling approach)		5-8

Magnitude-scaling for rock sites

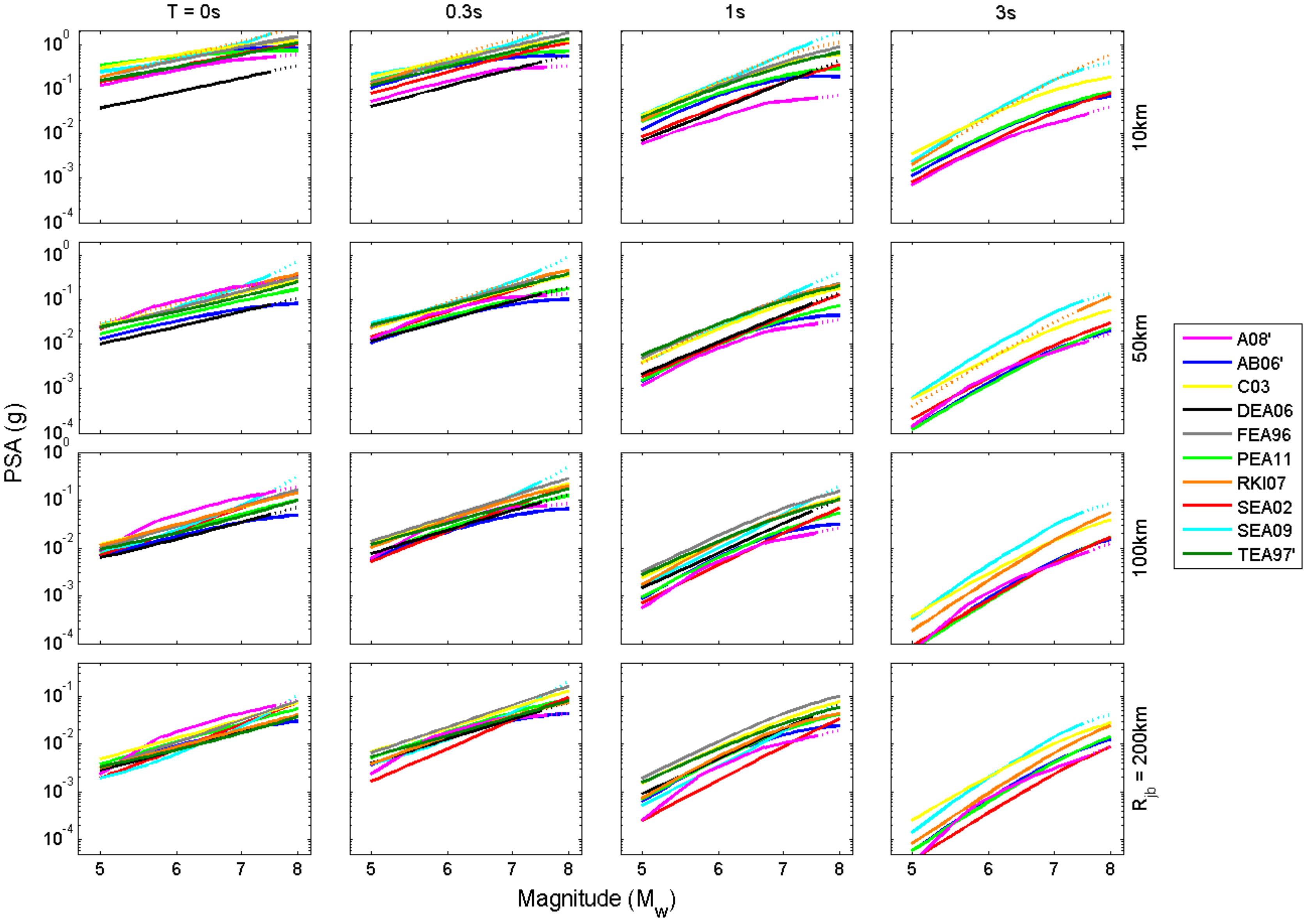

DISTANCE TERM SYNTHESIS

MODEL	DISTANCE TERM(s)	NOTES	DISTANCE RANGE (km)
Atkinson (2008) as modified by Atkinson & Boore (2011)	$[c_1+c_2(M-M_{ref})]\ln(R/R_{ref})+c_3(R-R_{ref})$ where $R=\text{sqrt}(R_{JB}^2+h^2)$ (Boore & Atkinson, 2008) plus $(c_0+c)+(c_1+d)R_{JB}+c^2R_{JB}^2$ (adjustment factors of Aktinson (2008)/Atkinson & Boore (2011)) (linear magnitude-dependent geometric spreading term with distance saturation and anelastic attenuation term)	Modifies the distance-scaling of Boore & Atkinson (2008) by a quadratic distance dependency (modification of anelastic attenuation)	10-1000+
Atkinson & Boore (2006) as modified by Atkinson & Boore (2011)	$(c_4+c_5M)f_1+(c_6+c_7M)f_2+(c_8+c_9M)f_0+c_{10}R_{cd}$ where $f_0=\max[\log(R_0/R_{cd}),0]$, $f_1=\min(\log R_{cd},\log R_1)$ and $f2=\max[\log(R_{cd}/R_2),0]$ where $R_0=10$, $R_1=70$ and $R_2=140$km (three-branched geometric spreading term with anelastic attenuation term)	Models change of decay rate due to crustal structure (Moho bounce) at 70km and 140km	1-1000
Campbell (2003)	$c_4\ln R+(c_5+c_6M_w)r_{rup}+f_3$ where $R=\text{sqrt}(r_{rup}^2+(c_7\exp(c_8M))^2)$ and $f_3=0$ for $r_{rup}<r_1$, $c_7(\ln r_{rup}-\ln r_1)$ for $r_1<r_{rup}<r_2$ and $c_7(\ln r_{rup}-\ln r_1)+c_8(\ln r_{rup}-\ln r_2)$ for $r_{rup}>r_2$ with $r_1=70$ and $r_2=130$km (three-branched geometric spreading term with linear magnitude-dependent anelastic attenuation term and magnitude-dependent distance-saturation)	Models change of decay rate due to crustal structure (Moho bounce) at 70km and 130km	0-1000
Douglas et al. (2006)	$c_4\ln R+(c_5+c_6M_w)r_{rup}+f_3$ where $R=\text{sqrt}(r_{rup}^2+(c_7\exp(c_8M))^2)$ and $f_3=0$ for $r_{rup}<r_1$, $c_7(\ln r_{rup}-\ln r_1)$ for $r_1<r_{rup}<r_2$ and $c_7(\ln r_{rup}-\ln r_1)+c_8(\ln r_{rup}-\ln r_2)$ for $r_{rup}>r_2$ with $r_1=70$ and $r_2=130$km (three-branched geometric spreading term with linear magnitude-dependent anelastic attenuation term and magnitude-dependent distance-saturation)	Adopted form of Campbell (2003)	1-1000
Frankel et al. (1996) as parameterized by EPRI (2004)	$(C4+C5M)\min[\ln(r'),\ln(70)]+(C6+C7M)\max[\min(\ln(r'/70),\ln(130/70)),0]+(C8+C9M)\max[\ln(r'/130),0]+C10r'$ where $r'=\text{sqrt}(r_{JB}^2+(\exp(C_{11}+C_{12}M))^2)$ (three-branched magnitude-dependent geometric spreading terms plus magnitude-dependent distance saturation term)	Similar to form of Atkinson & Boore (2006). Models change of decay rate due to crustal structure (Moho bounce) at 70km and 130km	10-500

DISTANCE TERM SYNTHESIS

MODEL	DISTANCE TERM(s)	NOTES	DISTANCE RANGE (km)
Raghu Kanth & Iyengar (2006, 2007)	$-\ln(r)-c_4r$ (1/R geometric spreading and anelastic attenuation)	Very simple form	1-300
Silva et al. (2002)	$(C_6+C_7M)\ln(R+e^{C4})$ (magnitude-dependent geometric spreading)	No modelling of Moho bounce or anelastic attenuation	1-400
Somerville et al. (2009)	$c_3\ln R+c_4(M-m_1)\ln R+c_5r$ where $R=\mathrm{sqrt}(r^2+6^2)$ for $r<r_1$ and $c_3\ln R_1+c_4(M-m_1)\ln R+c_5r+c_6(\ln R-\ln R_1)$ where $R=\mathrm{sqrt}(r_1^2+6^2)$ and r_1=50km for $r>r_1$ (two-branched linear magnitude-dependent geometric spreading with distance saturation and anelastic attenuation)	Models change of decay rate at 50km	0-500
Pezeshk et al. (2011)	(c4+c5M)min[log(R), log(70)]+ (c6+c7M)max[min(log(R/70),log(140/70),0]+ (c8+c8M)max(log(R/140),0)+c10R where $R=\mathrm{sqrt}(R_{rup}^2+c_{11}^2)$ (three-branch linear magnitude-dependent geometric spreading with distance saturation and anelastic attenuation)	Models Moho bounce between 70 and 140km.	1-1000
Toro et al. (1997) modified by Toro (2002)	$-c_4\ln R_M-(c_5-c_4)\max[\ln(R_M/100),0]-c_6R_M$ (either $R_M=\mathrm{sqrt}(r_{rup}^2+C_7^2[\exp(-1.25+0.227M)]^2)$ in the empirical approach or $R_M=r_{JB}+0.089\exp(0.6M)$ in the modelling approach) (two-branch geometric spreading with magnitude-dependent distance saturation and anelastic attenuation)	Models change of decay rate at 100km	1-1000

PEER

Distance-scaling (decay) for rock sites

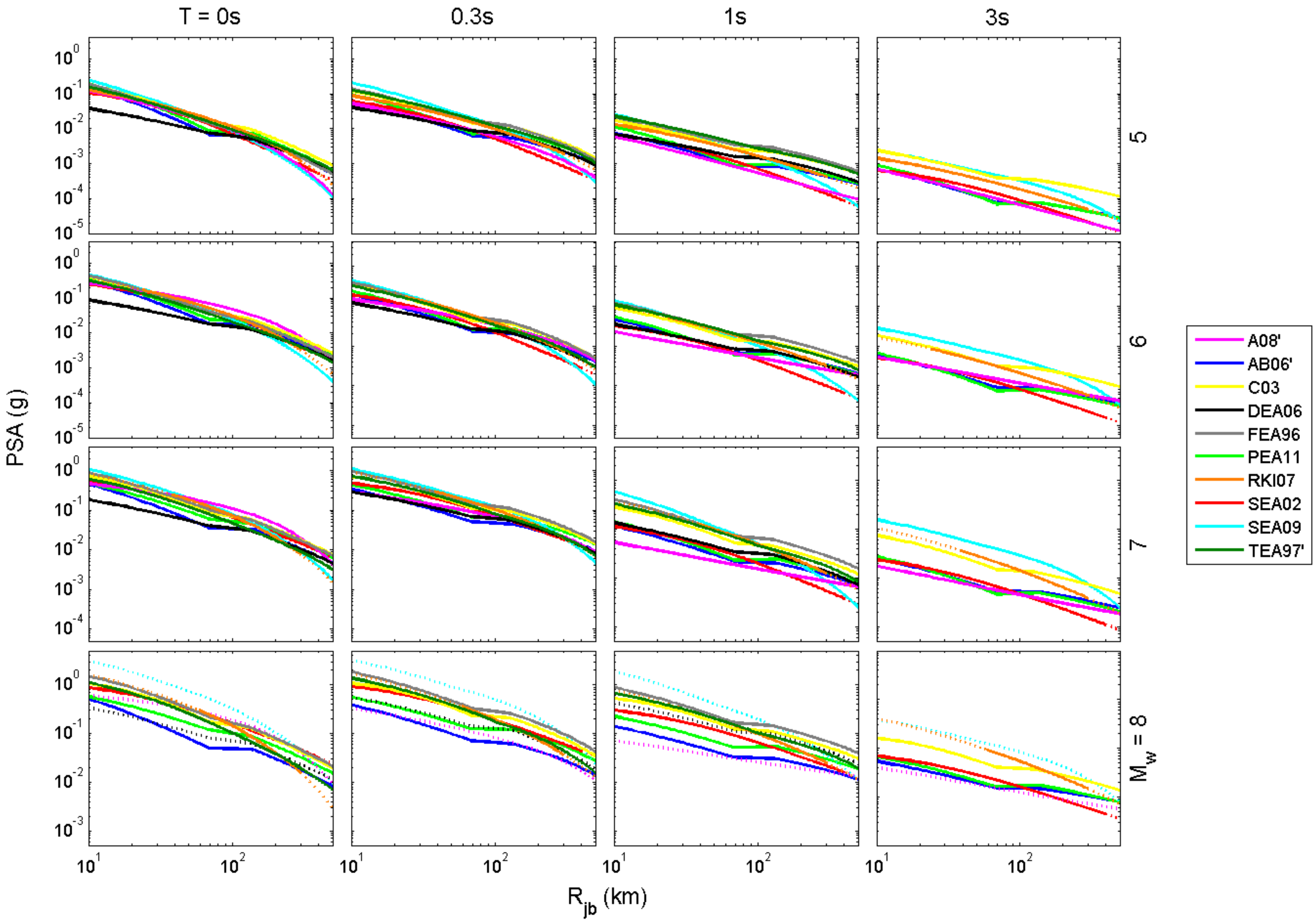

Site response functions

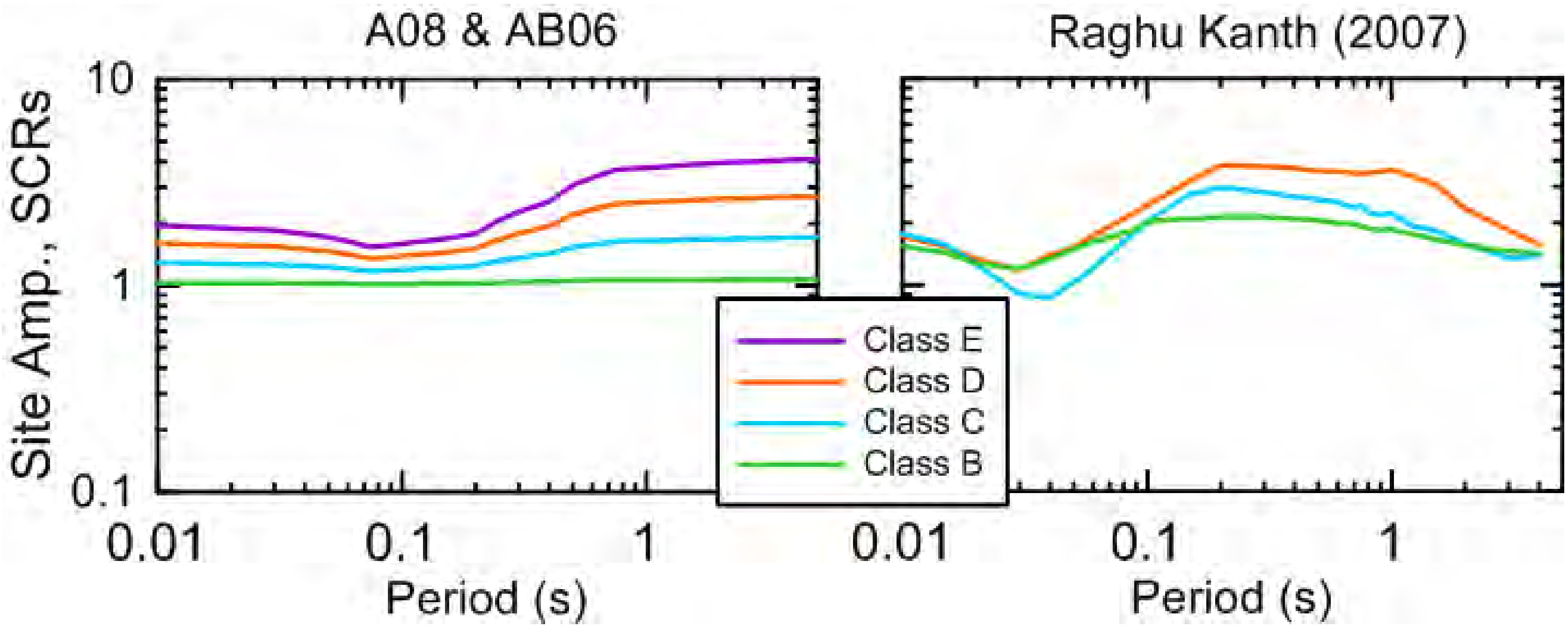

Site response functions

AB06’

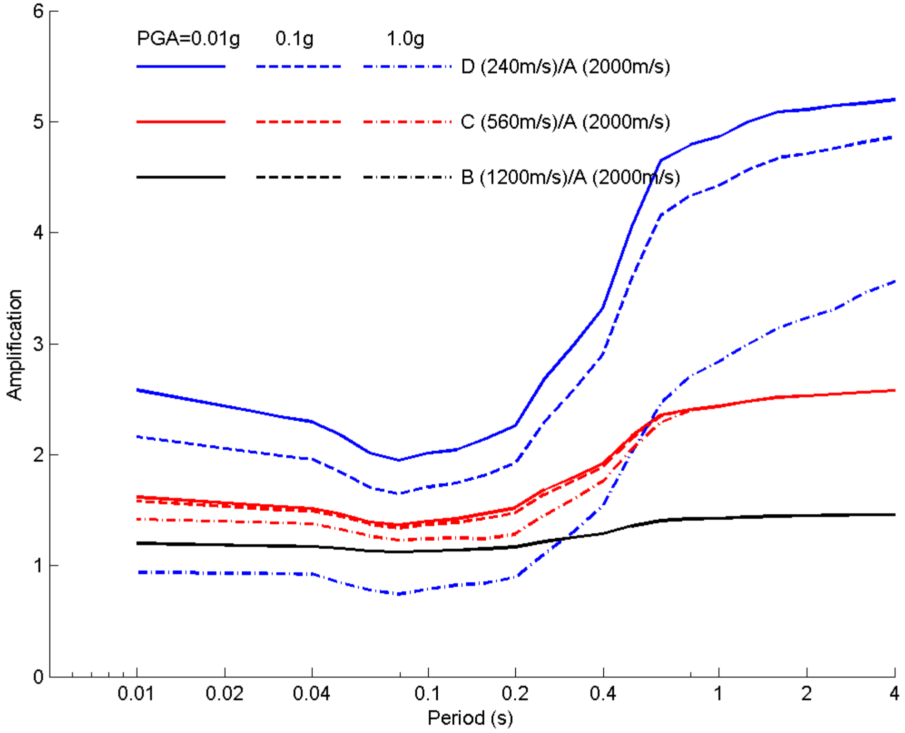

RKI07

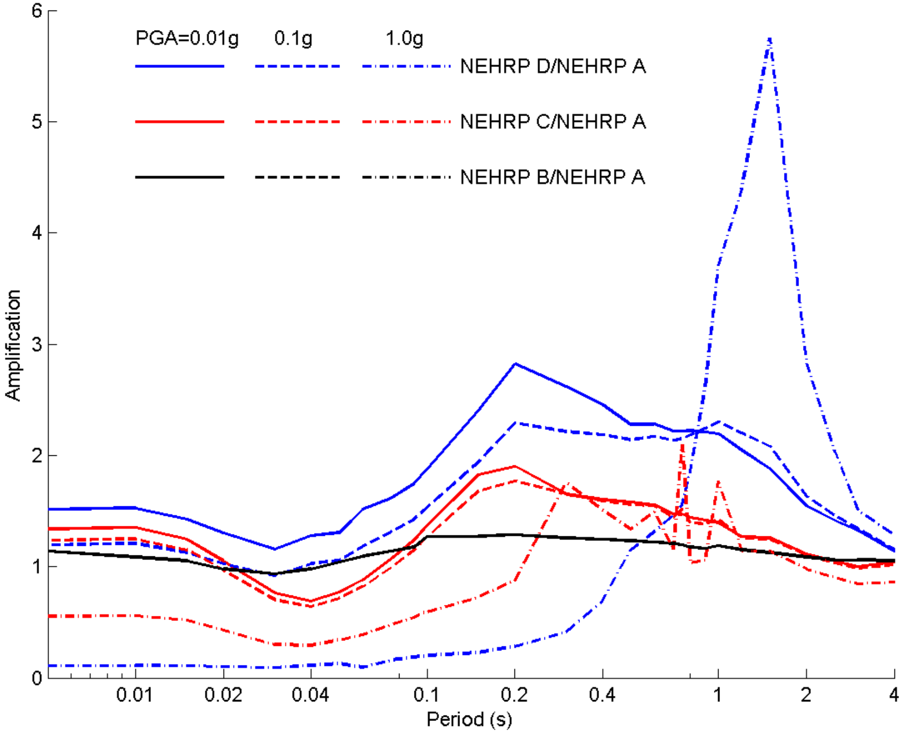

Summary of GMPE-data comparisons

	A2008’	AB 2006’	C2003	DEA 2006	FEA 96-04	RKI 2007	SEA 2002	SEA 2009	PEA 2011	TEA 97-02
A (global)		x	x							x
B (Portugal)	x	x	x							
C (Virginia)		x	x				x			x
D (Virginia)	x	X								
E (Thailand)										x

List of models pre-selected

A 2008’ = Atkinson (2008) as modified by Atkinson & Boore (2011): Referenced empirical model for eastern North America
AB 2006’ = Atkinson & Boore (2006) as modified by Atkinson & Boore (2011): Extended stochastic model for eastern North America
C 2003 = Campbell (2003): Hybrid model for eastern North America
DEA 2006 = Douglas *et al*. (2006): Hybrid model for southern Norway
FEA 96-04 = Frankel *et al*. (1996) as parameterized by EPRI (2004): Stochastic model for eastern North America
RKI2007 = Raghu Kanth & Iyengar (2006, 2007): Peninsular India
SEA 2002 = Silva *et al*. (2002): Stochastic model for eastern North America
SEA 2009 = Somerville *et al*. (2009): Simulation-based models for Australia
PEA 2011 = Pezeshk *et al*. (2011): Hybrid model for eastern North America
TEA 97-02 = Toro *et al*. (1997) modified by Toro (2002): Stochastic model for eastern North America

Case study A

Title	“Evaluation of Ground-Motion Modeling Techniques for Use in Global ShakeMap—A Critique of Instrumental Ground-Motion Prediction Equations, Peak Ground Motion to Macroseismic Intensity Conversions, and Macroseismic Intensity Predictions in Different Tectonic Settings” *US Geological Survey, Open-File Report 2009–1047, 114p.*									
Authors	Trevor I. Allen and David J. Wald									
GMPEs tested	A 2008’	AB 2006 (not 2011)	C 2003	DEA 2006	FEA 96-04	RKI2007	SEA 2002	SEA 2009	PEA 2011	TEA 97-02
		x	x							x
Geog. Areas	Atlas of ShakeMaps - global									

Method of performance assessing: They plot individual ground-motion residuals vs. Rrup for each GMPE, color-coded by earthquake magnitude.
They use NEHRP site-class amplification factors (Borcherdt, 1994) and topographically based VS30 estimates (Wald and Allen, 2007) to correct the observed ground-motion amplitudes to BC rock conditions when comparing these SCR GMPEs.

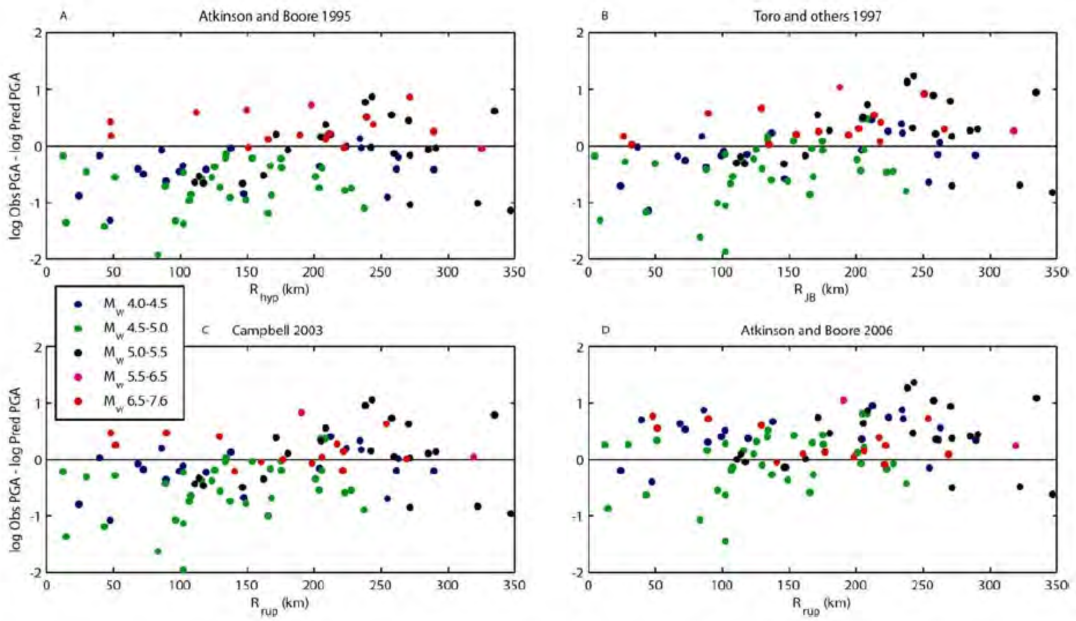

Database used for test: strong ground-motion and macroseismic intensity datasets gathered to calibrate the Atlas of ShakeMaps (Allen and others, 2008, 2009b). The classification between active (both shallow crust and subduction zone) and stable crustal events was achieved using polygons of stable continents defined by Johnston and others (1994).

General results: Atkinson and Boore (2006) relation provides the lowest residuals for PGA, particularly in the near-source region (less than Rrup 150 km). The other stable continent GMPEs tend to overestimate PGA at near-source distances. The Campbell (2003) GMPE appears to predict PGA quite well at distances larger than approximately 150 km from the earthquake source.

Case study B

Title	"Ground-motion models for seismic-hazard assessment in western Iberia; constraints from instrumental data and intensity observations" *Bulletin of the Seismological Society of America* (2012), 102(1):169-184									
Authors	Susana P. Vilanova, Joao F. B. D. Fonseca, and Carlos S. Oliveira									
GMPEs tested	A 2008'	AB 2006	C 2003	DEA 2006	FEA 96-04	RKI2007	SEA 2002	SEA 2009	PEA 2011	TEA 97-02
	x	x	x							
Geog. Areas	Western Iberia (i.e. Portugal)									

Method of performance assessment: Overall goodness-of-fit from Scherbaum et al. (2004) for T= 0.01-2.0 sec.

Database used for test: M 4.8-7.8, R 100-400 km, 1969-2009

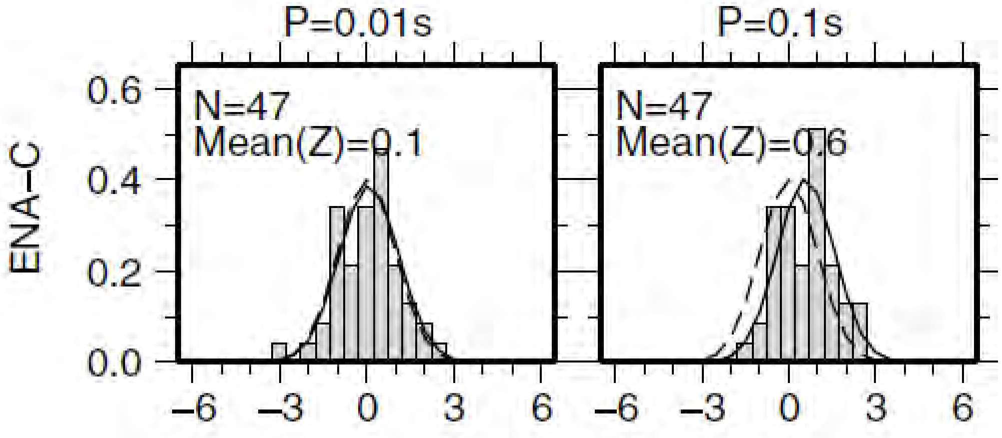

General results: SCR models better than ACR models. A 2008', AB 2006' and C 2003 models underpredict the response spectra ordinates, except for the C 2003 model at the longest periods analyzed (1.0 s and 2.0 s), which overestimates the regional motions.

Case study C

Title	The 2011 Mineral, VA M5.8 Earthquake Ground Motions and Stress Drop: An Important Contribution to the NGA East Ground Motion Database, *Presented at Eastern Section SSA Meeting, Little Rock, AR, October 18 2011*.									
Authors	Cramer, C., J. Kutliroff, and D. Dangkuas									
GMPEs tested	A 2008’	AB 2006	C 2003	DEA 2006	FEA 96-04	RKI2007	SEA 2002	SEA 2009	PEA 2011	TEA 97-02
		x	x				x			x
Geog. Areas	Virginia (US)									

f_c = 0.6-0.7 Hz

Brune $\Delta\sigma$ =

20-30 MPa

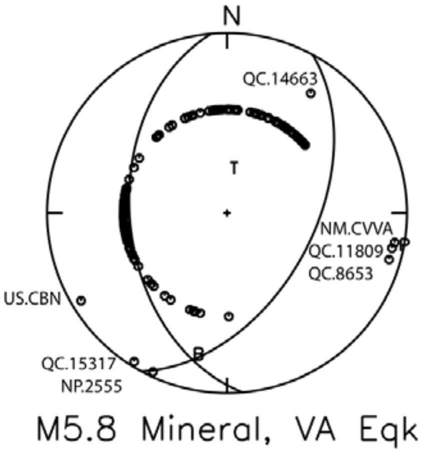

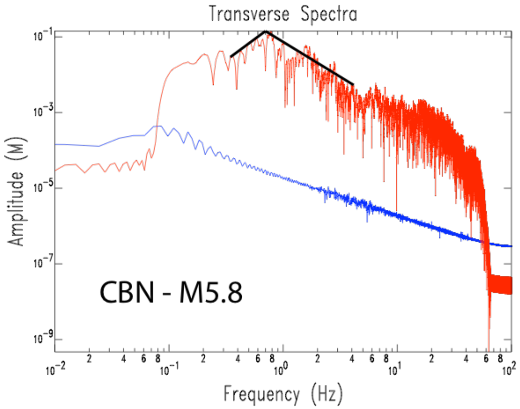

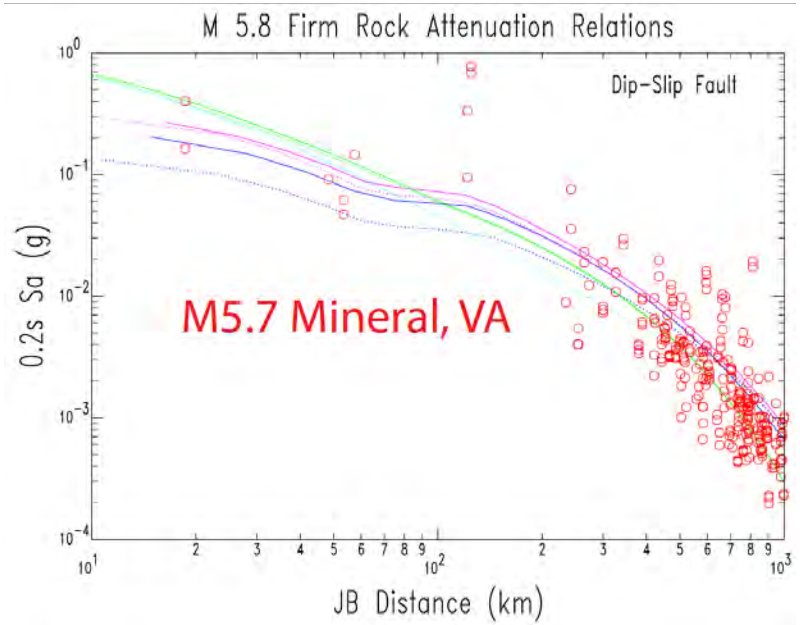

General results: The Mineral, VA M5.8 earthquake is an important contributor of records and current GMPEs as a group predict the short period values but over predict the long period values. Comparison of the Mineral, VA M5.8 to the 1988 Saguenay M5.9 earthquake shows similarities in ground motion, directivity, and radiation pattern. f_c ~ 0.7 Hz implying a Brune stress drop of ~30 MPa, but site and SSI effects add to uncertainty. Regional data suggest that Virginia earthquake were average stress event, 150 – 300 bars. The EGF study appear to suggest much higher stress drops.

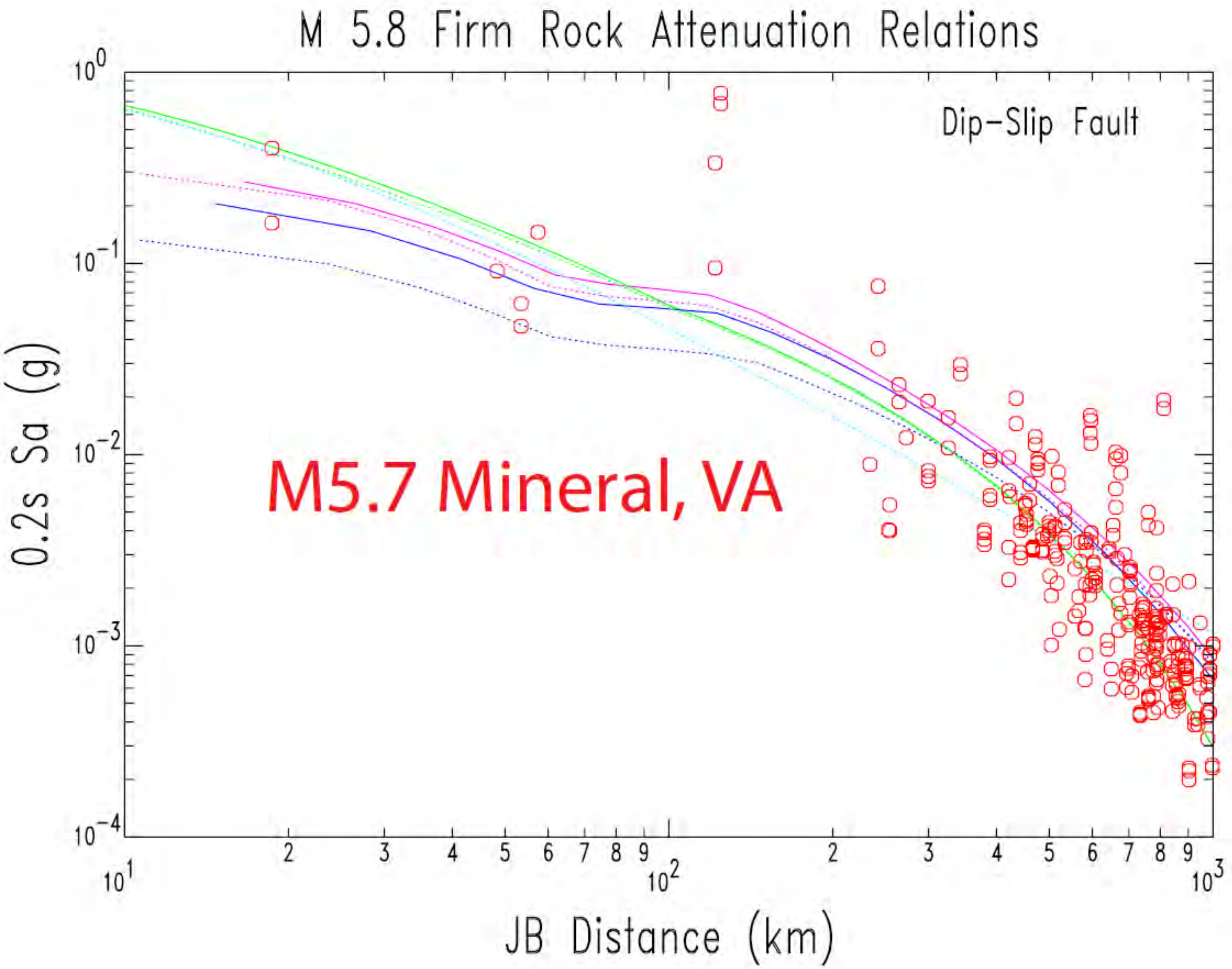

M5.7 Mineral, VA

Case study D

Title	2011 M5.8 Mineral VA earthquake, *Presented at NGA-East Meeting, November 2011.*									
Authors	G.M. Atkinson									
GMPEs tested	A 2008’	AB 2006	C 2003	DEA 2006	FEA 96-04	RKI2007	SEA 2002	SEA 2009	PEA 2011	TEA 97-02
	x	x								
Geog. Areas	Virginia (US)									

Method of performance assessment:
Simple data-GMPE comparison

Database used for test: Records from single earthquake

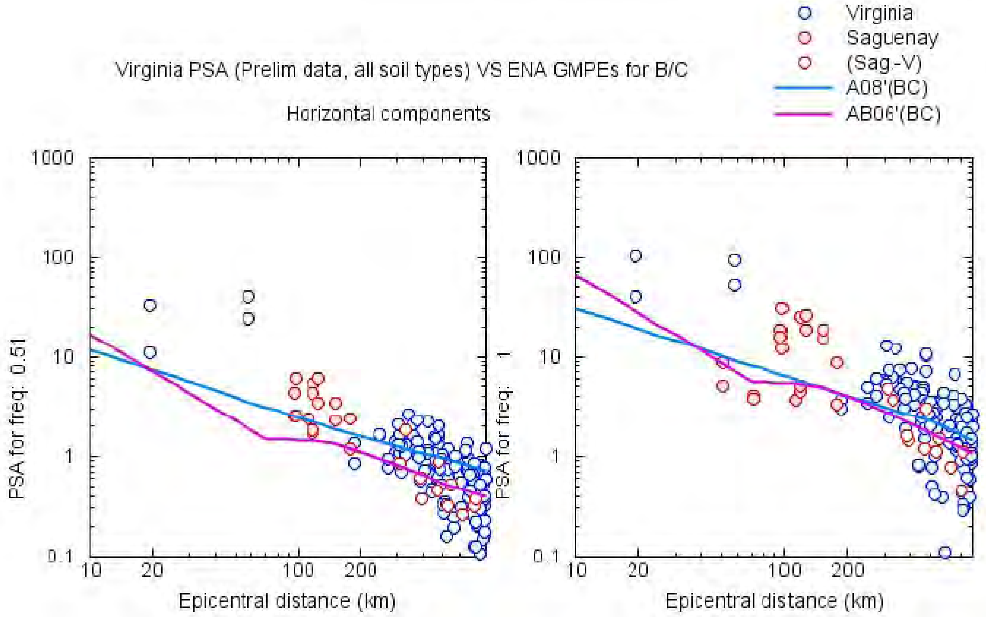

General results: Data generally consistent with A 08’ and AB 06’ GMPEs

Case study E

Title	"Suitable attenuation model for Thailand" *Proc 14 WCEE*, (2008), Article 14/2-0088.									
Authors	C. Chintanapakdee, M.E. Naguit and M. Charoenyuth									
GMPEs tested	A 2008'	AB 2006	C 2003	DEA 2006	FEA 96-04	RKI2007	SEA 2002	SEA 2009	PEA 2011	TEA 97-02
	x	x								
Geog. Areas	Thailand									

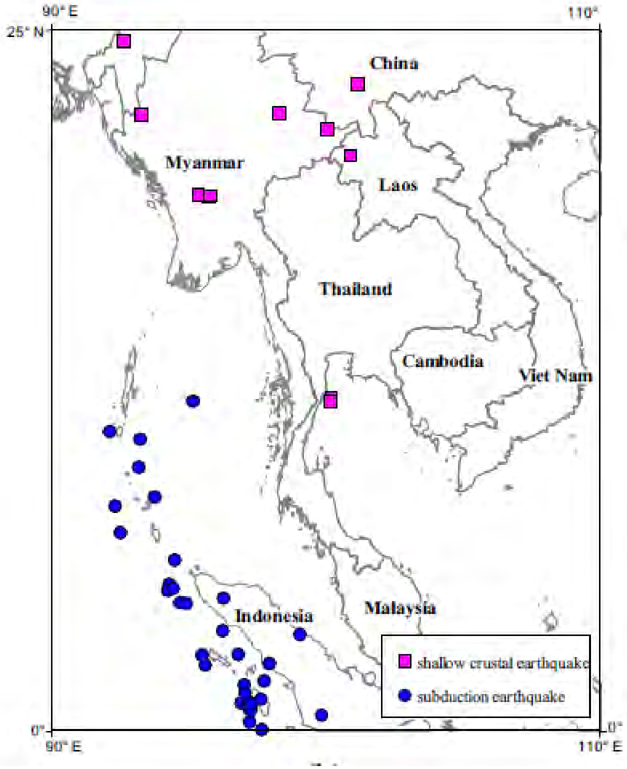
90° E
110°
25° N
China
Myanmar
Laos
Thailand
Cambodia
Viet Nam
Indonesia
Malaysia
■ shallow crustal earthquake
● subduction earthquake
0°
90° E
110° E
0°

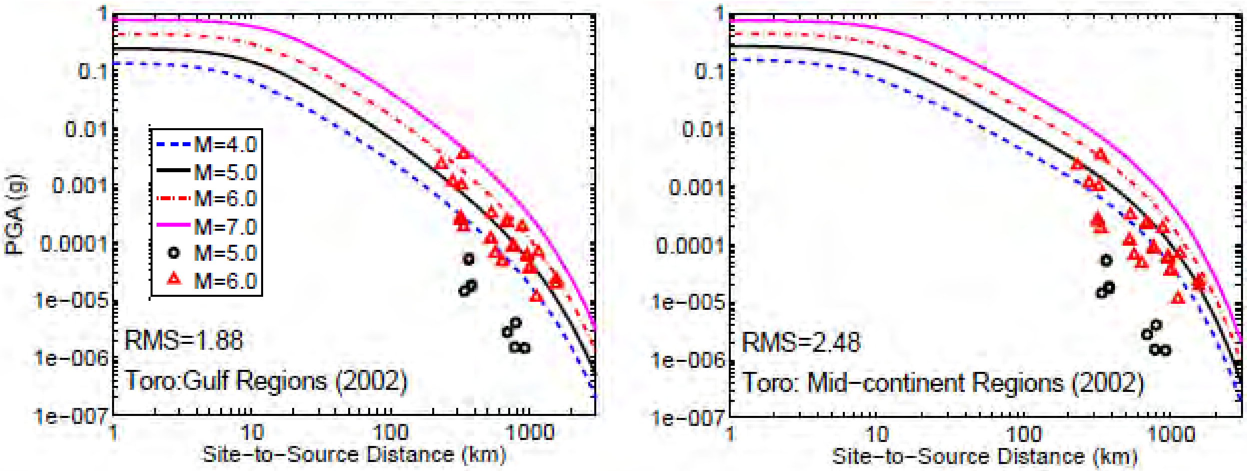

Method of performance assessment: Simple data-GMPE comparison and calculation of RMS error

General results: Four SCR GMPEs considered, but only Toro 2002 is among the GEM pre-selected models. Toro identified as best model.

Database used for test: 163 records from 45 events in Thailand between 2006 and 2007. Mostly subduction. 55 SCR recordings. M > 4

Particular difficulties for SCR GMPEs

- **Lack of (or non-optimal) aleatory variability (sigma) models for some GMPEs**
  - Should we recommend the adoption of sigmas from other GMPEs?
  - Sigmas lacking or with potential problems:
    1. Raghu Kanth & Iyengar (2006, 2007) - only parametric variability and not the modelling variability coming from the fit to observations
    2. Atkinson & Boore (2006) – 0.69 given without explanation
  - Many models only give total sigma not inter- and intra-event components separately
- **Which model to select when more than one model presented to model epistemic uncertainty?**
  1. Douglas et al. (2006): Seven models (different empirical GMPEs)
  2. Silva et al. (2002): Five models (different source spectra)
  3. Somerville et al. (2009): Two models (non-cratonic/Yilgarn craton)
  4. Toro et al. (1997)/Toro (2002): Two models (different crustal regions)
- **Lack of quantitative tests of applicability of models against observations**
- **Lack of site amplification functions**
  - For soil not really a problem since could use independent site amplification functions
  - But converting from different rock conditions to common Vs30-kappa pair could be difficult

Summary of discussions of core

- More difficult to get a consensus than for subduction zone GMPEs
- Potential problems with all models
  - Reason for on-going NGA-East project
- Very large spread (about factor 10) in predictions, particularly for M 7 and 8
  - Probably not realistic
  - Because of models that extrapolate poorly
  - Need to be careful not to over-estimate epistemic uncertainty
- Select more than three models since epistemic uncertainty high?
- Scale up and down a robust model to add in extra epistemic uncertainty?
- Desire to include non-eastern North American models because of global scope of project
- Somerville et al. (2009)'s long-period (>1s) bump may not be 'typical' of SCRs
- Discarded Toro (2002), Frankel et al. (1996) and Campbell (2003) since considered superseded by Silva et al. (2002), Atkinson & Boore (2006) and Pezeshk et al. (2011)
- Douglas et al. (2006) not selected since $\Delta\sigma$ used are not based on observations but mainly arbitrary decision
- Raghu Kanth & Iyengar (2007) does not extrapolate well to large near-source events
- Atkinson (2008) is a simple empirical adjustment from weak-motion data

Proposed selection

- **Following two webconferences and numerous emails the core proposes:**
  - Atkinson & Boore (2006, 2011)
    - Effective calibration of input parameters for stochastic simulations using observations
    - Extensive use in previous studies (e.g. US National Hazard Maps)
    - Performed reasonably well in tests of Allen & Wald (2009) and Vilanova et al. (2012)
    - Well documented
    - However, similar predictions to Pezeshk et al. (2011) so perhaps do not need both
  - Pezeshk et al. (2011)
    - Hybrid-empirical technique
    - Recent and fairly complete database for eastern North America
  - Silva et al. (2002) (double corner with saturation)
    - Double corner means that long-periods not overpredicted
    - Good modeling of uncertainties
- **We are considering adding epistemic uncertainty by scaling up and down one or two base models**

Spectra for proposed GMPEs

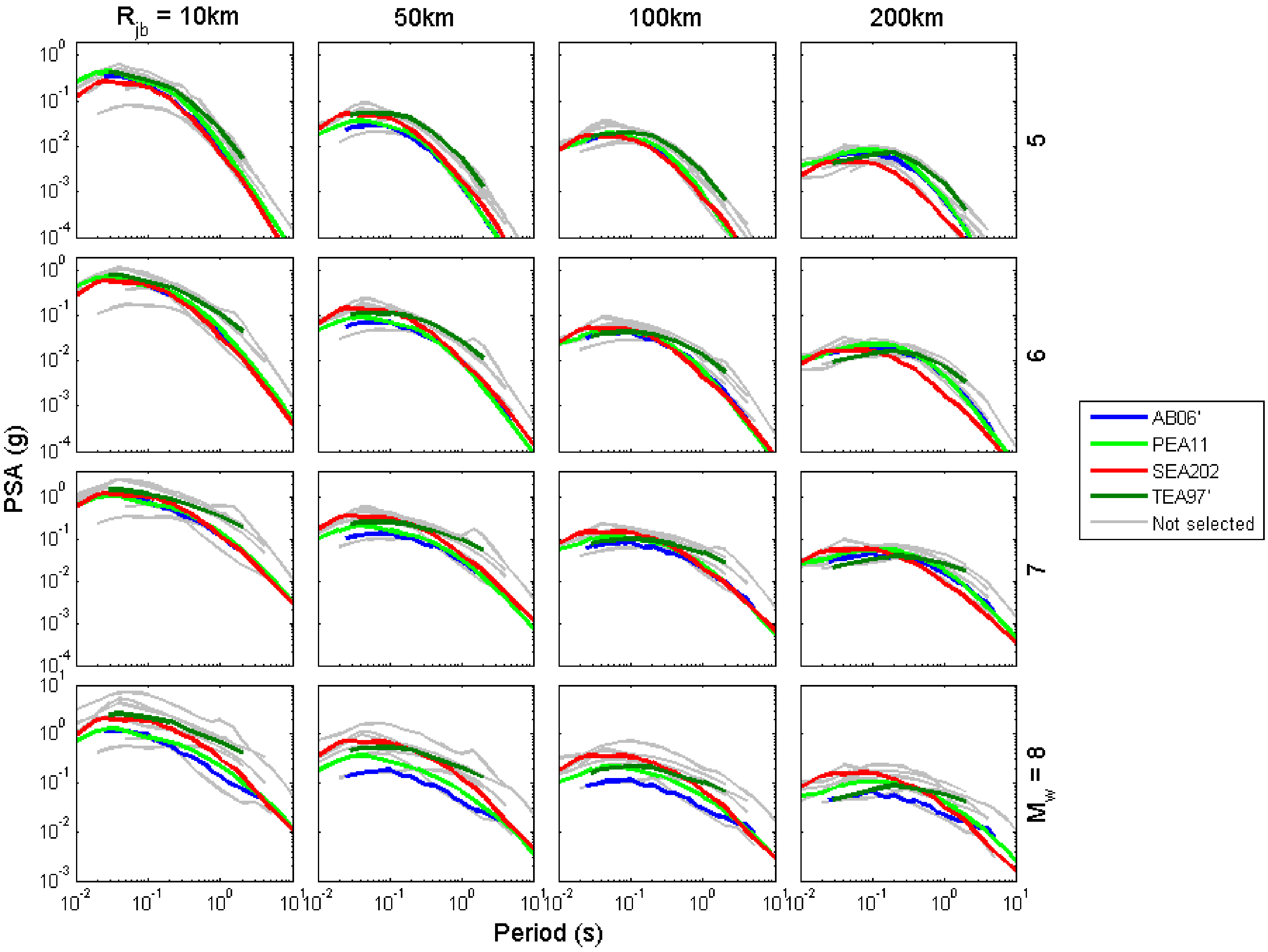

PEER

Magnitude-scaling for proposed GMPEs

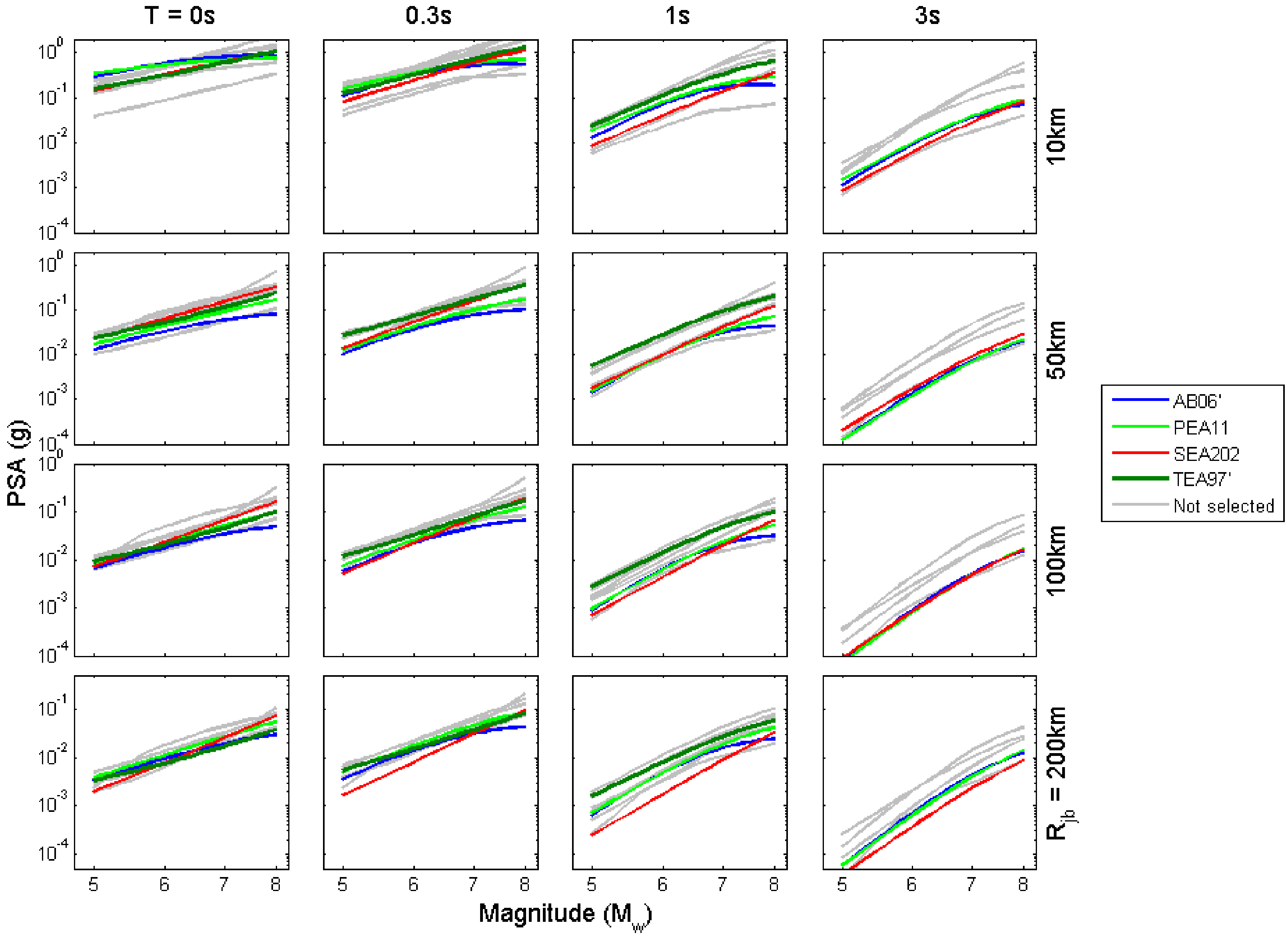

Distance-scaling for proposed GMPEs

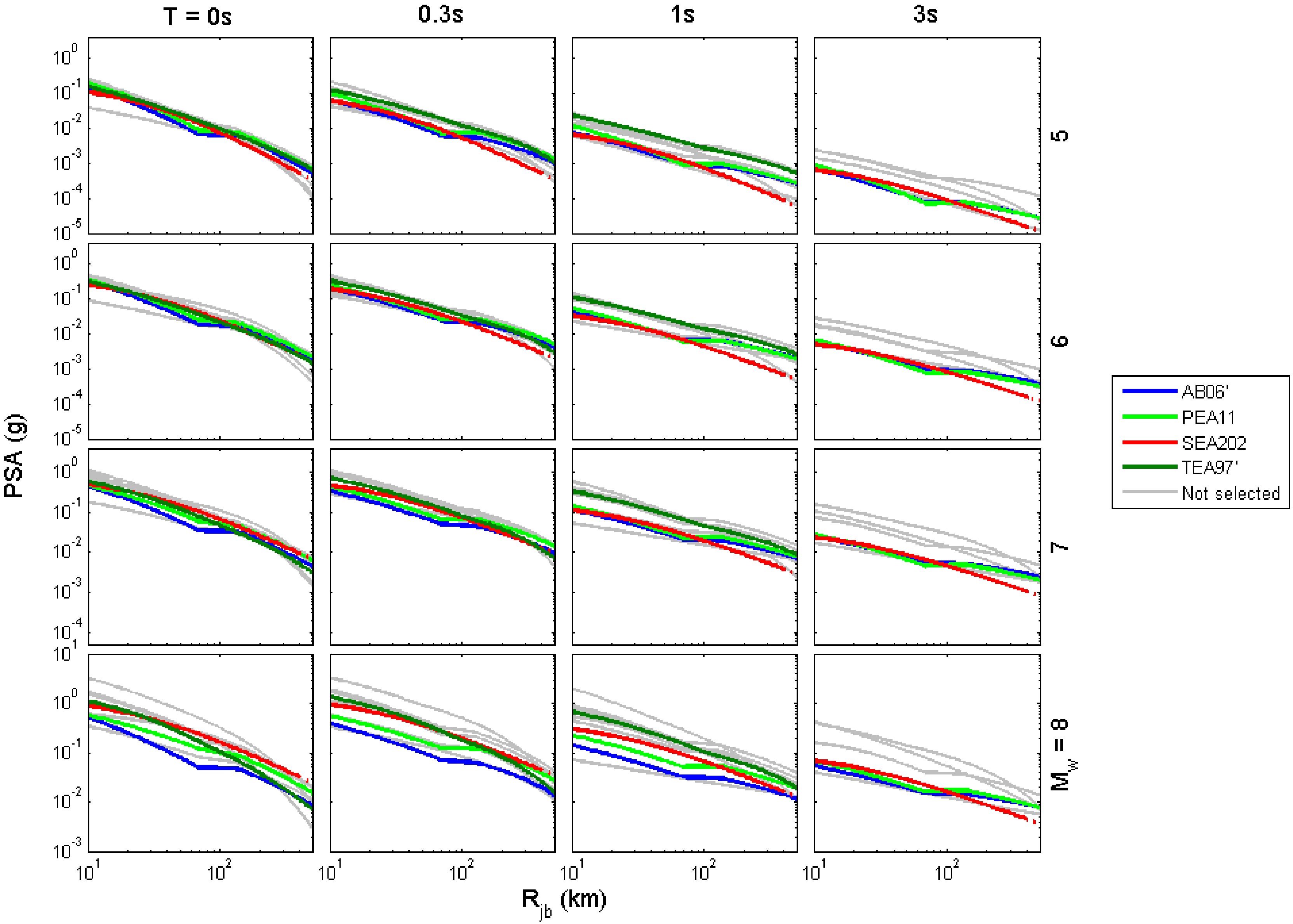

Sigma for proposed GMPEs

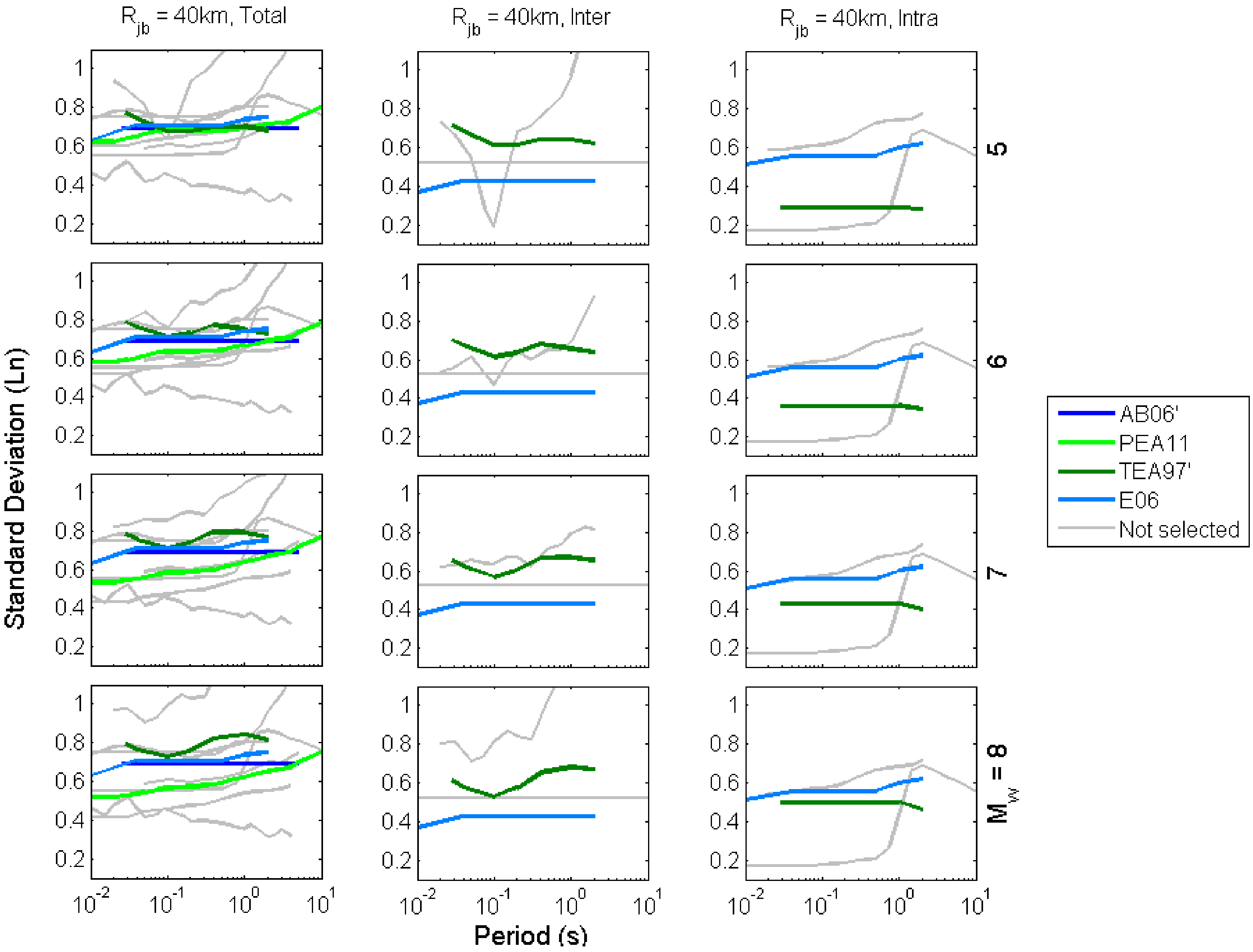

PEER

Preliminary selected GMPES for Stable Continental Regions

John Douglas & Jonathan P. Stewart (co-chairs)

C. di Alessandro, D. M. Boore, Y. Bozorgnia
N. A. Abrahamson, E. Delavaud, P. J.
Stafford, K. W. Campbell, M. Erdik &
M. B. Javanbarg

PEER

GEM
GLOBAL EARTHQUAKE MODEL

Preliminary selected GMPEs for Shallow Crustal Seismicity Regions

John Douglas & Jonathan P. Stewart (co-chairs)

C. di Alessandro, D. M. Boore, Y. Bozorgnia
N. A. Abrahamson, E. Delavaud, P. J.
Stafford, K. W. Campbell, M. Erdik &
Mohammad. B. Javanbarg

Pre-selected GMPEs

1. **Abrahamson & Silva [2008]:**
   NGA model using worldwide data
2. **Akkar & Bommer [2010]:**
   Model using Mediterranean and Middle Eastern data
3. **Boore & Atkinson [2008] as modified by Atkinson & Boore [2011]:**
   NGA model using worldwide data
4. **Campbell & Bozorgnia [2008]:**
   NGA model using worldwide data
5. **Cauzzi & Faccioli [2008]: updated by Faccioli *et al*. [2010]:**
   Model using worldwide data (mainly Japanese)
6. **Chiou & Youngs [2008]:**
   NGA model using worldwide data
7. **Kanno *et al*. [2006]:**
   Model using mainly Japanese data
8. **McVerry *et al*. [2006]:**
   Model using mainly New Zealand data
9. **Zhao *et al*. [2006]:**
   Model using mainly Japanese data

Reminder of procedure

- **Principles previously agreed:**

1. Giving more weight to GMPEs derived from international data sets than from local data sets. Exceptions can be made when a GMPE derived from a local data set has been checked internationally and found to perform well.

2. Giving more weight to GMPEs that have attributes to their functional form that we consider desirable, including saturation with magnitude, magnitude dependent distance scaling and anelastic attenuation terms.

3. If we have multiple GMPEs that are well constrained by data but exhibit different trends, it is desirable to capture those trends in the selected GMPEs to properly represent epistemic uncertainty.

- **Trellis plots**
- **Results of (quantitative) testing of models against independent sets of data**
- **Circulation of available plots and results of testing**
- **Independent selections (of ~3 models) sent to WG facilitators**
- **Discussion of selections and consensus decision taken within core**

- **Today we would like your feedback and suggestions**

ACR GMPEs pre-selected (page 1)

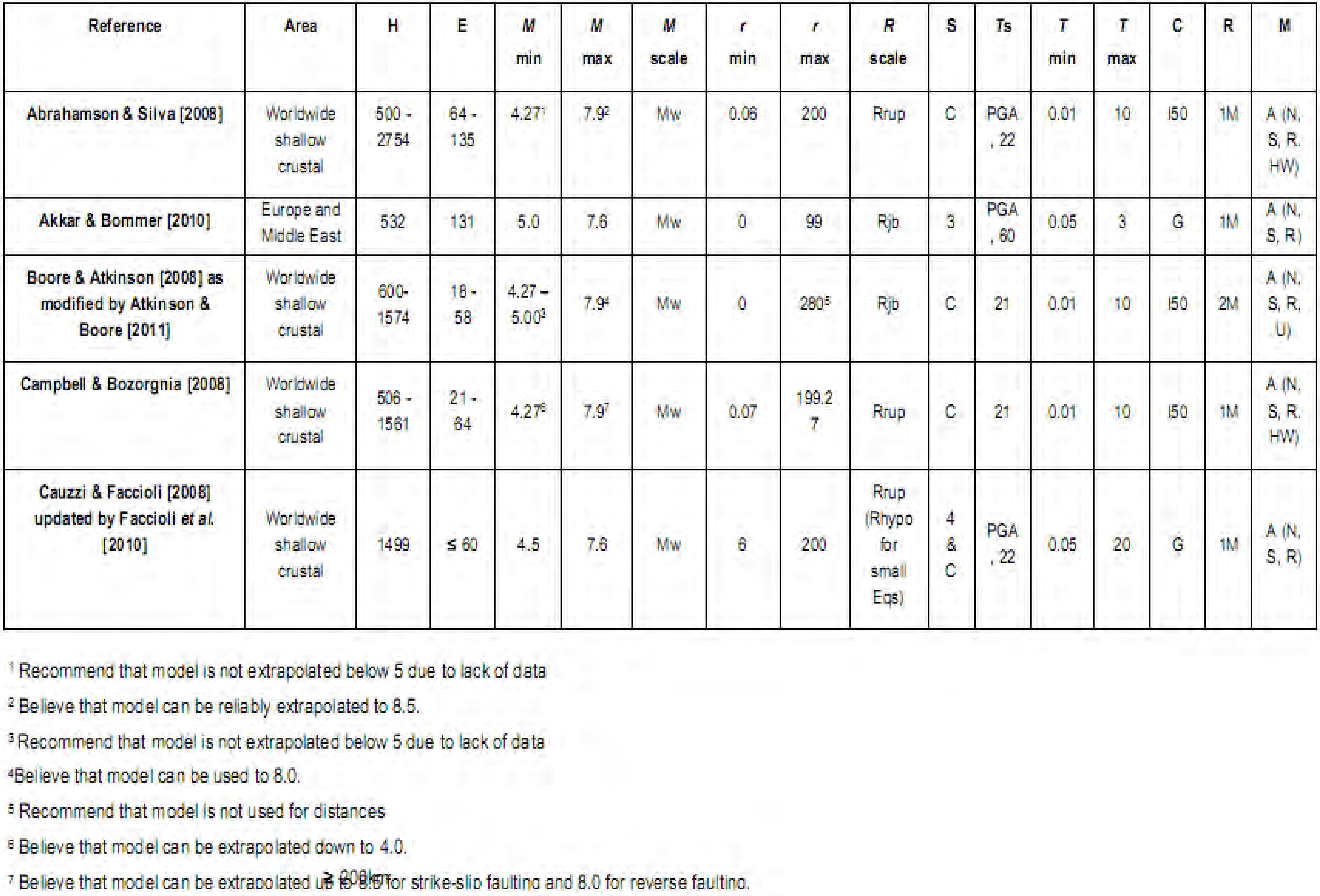

Reference	Area	H	E	*M* min	*M* max	*M* scale	*r* min	*r* max	*R* scale	S	Ts	*T* min	*T* max	C	R	M
Abrahamson & Silva [2008]	Worldwide shallow crustal	500 - 2754	64 - 135	4.27[1]	7.9[2]	Mw	0.06	200	Rrup	C	PGA, 22	0.01	10	I50	1M	A (N, S, R, HW)
Akkar & Bommer [2010]	Europe and Middle East	532	131	5.0	7.6	Mw	0	99	Rjb	3	PGA, 60	0.05	3	G	1M	A (N, S, R)
Boore & Atkinson [2008] as modified by Atkinson & Boore [2011]	Worldwide shallow crustal	600-1574	18 - 58	4.27 – 5.00[3]	7.9[4]	Mw	0	280[5]	Rjb	C	21	0.01	10	I50	2M	A (N, S, R, U)
Campbell & Bozorgnia [2008]	Worldwide shallow crustal	506 - 1561	21 - 64	4.27[6]	7.9[7]	Mw	0.07	199.27	Rrup	C	21	0.01	10	I50	1M	A (N, S, R, HW)
Cauzzi & Faccioli [2008] updated by Faccioli *et al.* [2010]	Worldwide shallow crustal	1499	≤ 60	4.5	7.6	Mw	6	200	Rrup (Rhypo for small Eqs)	4 & C	PGA, 22	0.05	20	G	1M	A (N, S, R)

[1] Recommend that model is not extrapolated below 5 due to lack of data

[2] Believe that model can be reliably extrapolated to 8.5.

[3] Recommend that model is not extrapolated below 5 due to lack of data

[4] Believe that model can be used to 8.0.

[5] Recommend that model is not used for distances

[6] Believe that model can be extrapolated down to 4.0.

[7] Believe that model can be extrapolated up to 8.5 for strike-slip faulting and 8.0 for reverse faulting.

≥ 200km

ACR GMPEs pre-selected (page 2)

Reference	Area	H	E	*M* min	*M* max	*M* scale	*r* min	*r* max	*R* scale	S	Ts	*T* min	*T* max	C	R	M
Chiou & Youngs [2008]	Worldwide shallow crustal	≤ 1950[8]	≤ 125	4.265[9]	7.90[10]	Mw	0.2[11]	70[12]	Rrup	C	PGA, 22	0.01	10	I50	1M	A (N, S, R. HW, AS)
Kanno *et al*. [2006]	Japan + foreign data	Interface + crustal = 3769; Intraslab = 8150	Interface = 83; Intraslab = 111	Interface + crustal = 5.2; Intraslab = 5.5	Interface + crustal = 8.2; Intraslab = 8.0	Mw	Interface + crustal =1; Intraslab = 30	Interface + crustal = 400 Intraslab = 500	Rhypo	C (Vs30)	PGA, PGV, 36	0.05	5	R	2M	A
McVerry *et al*. [2006]	New Zealand + 66 foreign	535[10]	Interface = 6?; Intraslab = 19 ?	5.08 (or 5,2?)	7.09 (or 6.8?)	Mw	6 (or 30?)	400	Rc (Rrup)	3[3]	PGA, 11	0.075	3	L, G	1M	C (R, OR, S & N) & F, B
Zhao *et al*. [2006] modified by Zhao [2010]	Japan+ 208 foreign crustal near-source records	Interface =1508; Intraslab = 1725 crustal = 1285	289[12]	5	8.3	Mw	0	300	Rrup	4[13]	PGA, 20	0.05	5	G	1M	C(R, S/N) & F,B

[8] Due to filtering number of records and earthquakes depends on period.
[9] Believe that model can be extrapolated down to 4.0.
[10] Believe that model can be extrapolated up to 8.5 for strike-slip faulting and 8.0 for reverse faulting.
[11] Believe that model valid to 0km.
[12] Believe that model valid to 200km.

Trellis plots (PSA on rock, V_{s30}=1000m/s, SS)

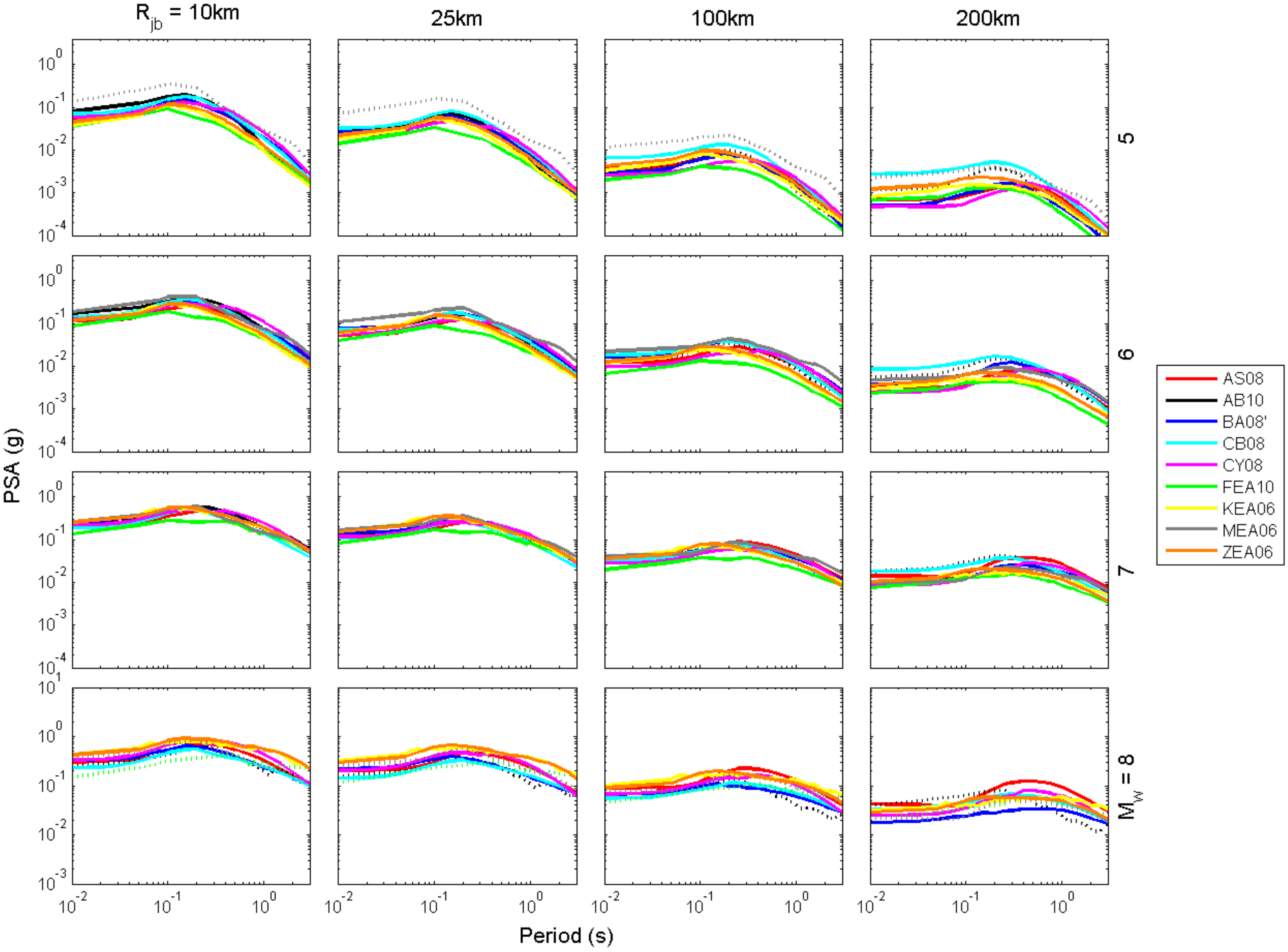

Trellis plots (PSA on rock, V_{s30}=1000m/s, SS)

🟥	AS08
⬛	AB10
🟦	BA08'
🟦	CB08
🟪	CY08
🟩	FEA10
🟨	KEA06
⬜	MEA06
🟧	ZEA06

🟥	Abrahamson & Silva (2008)
⬛	Akkar & Bommer (2010)
🟦	Boore & Atkinson (2008)/Atkinson & Boore (2011)
🟦	Campbell & Bozorgnia (2008)
🟪	Chiou & Youngs (2008)
🟩	Faccioli et al. (2010)
🟨	Kanno et al. (2006)
⬜	McVerry et al. (2006)
🟧	Zhao et al. (2006)

Sigma (R_{JB}=20km, V_{s30}=1000m/s, strike-slip)

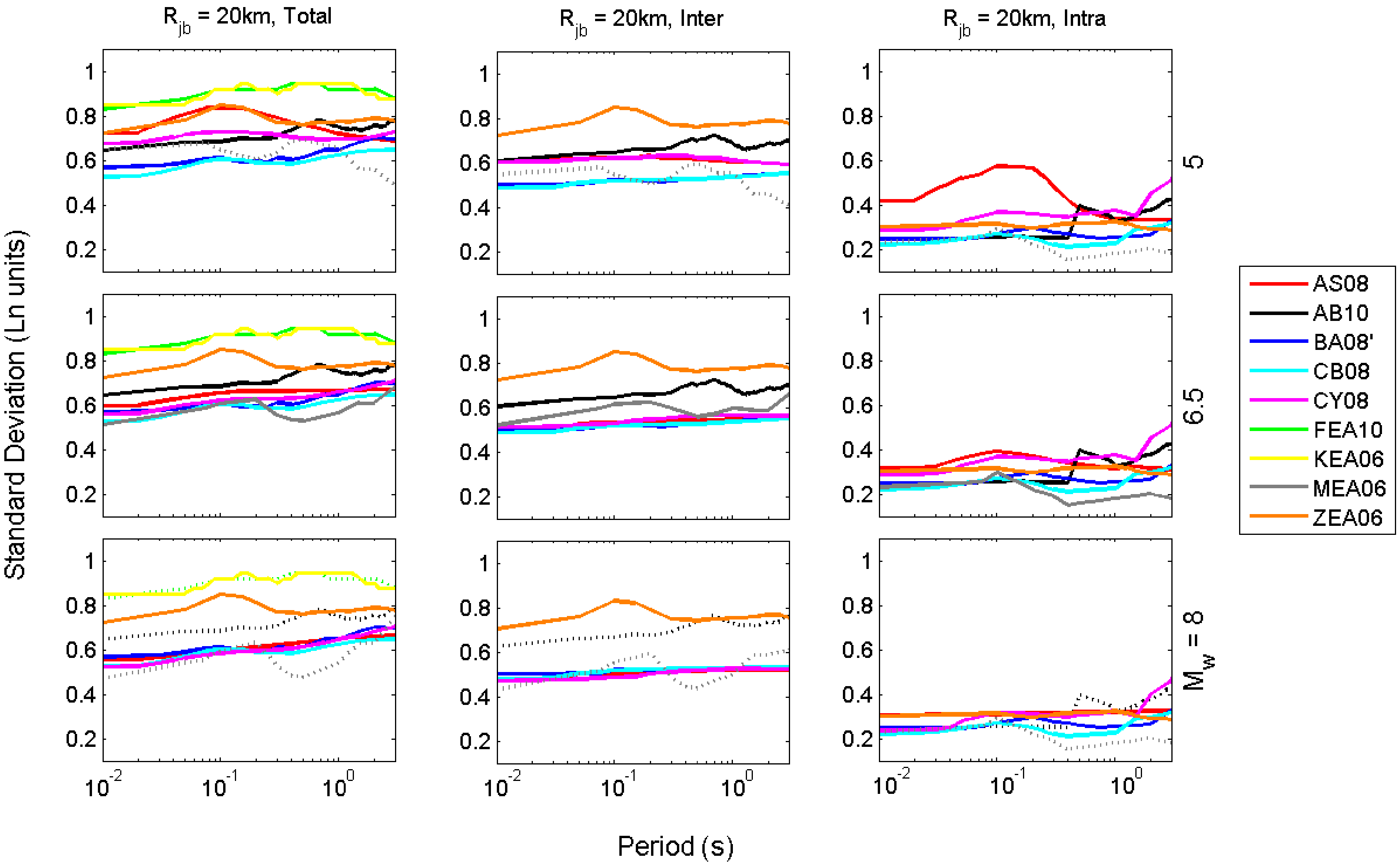

MAGNITUDE TERM SYNTHESIS

MODEL	MAGNITUDE TERM(s)	NOTES	Mw RANGE
Abrahamson & Silva (2008)	$a_1+(a_4$ or $a_5)(M-c_1)+a_8(8.5-M)^2$ (linear with different slopes (a4 or a5) above and below threshold magnitude c1=6.75 and quadratic M term) plus linear magnitude-dependent geometric decay term ($[a_2+a_3(M-c_1)]\ln(R)$)	Models change of M-scaling at M 6.75	5.0-8.5
Akkar & Bommer (2010)	$b_1+b_2M+b_3M^2$ (linear and quadratic M terms) plus linear magnitude-dependent geometric spreading term ($[b_4+b_5M]\log R'$)		5.0-7.6
Boore & Atkinson (2008) as modified by Atkinson & Boore (2011)	$e'+e_5(M-Mh)+e_6(M-Mh)^2$ (linear and quadratic M terms) for $M<M_h$ and $e'+e_7(M-M_h)$ (linear M term) for $M>M_h$ plus linear magnitude-dependent geometric spreading ($[c_1+c_2(M-M_{ref})]\ln(R/R_{ref})$). In 2011 revision adjustment in linear M- and R-scaling below M 5.75.	Models change in M-scaling at M 6.75 and below M 5.75	5.0-8.0
Campbell & Bozorgnia (2008)	c_0+c_1M below M 5.5, $c_0+c_1M+c_2(M-5.5)$ between M 5.5 and 6.5 and $c_0+c_1M+c_2(M-5.5)+c_3(M-6.5)$ above M 6.5 (trilinear M-scaling with breaks at 5.5 and 6.5) plus linear magnitude-dependent geometric spreading $[(c_4+c_5M)\ln(R')]$	Models change in M-scaling at M 5.5 and M 6.5	4.0-8.5 for SS and 8.0 for R

MAGNITUDE TERM SYNTHESIS

MODEL	MAGNITUDE TERM(s)	NOTES	Mw RANGE
Chiou & Youngs (2008)	$c_1' + c_2(M-6) + (c_2 - c_3)/c_n \ln[1+\exp(c_n(c_M - M))]$ (linear M term and complex M dependency) plus magnitude-dependent distance saturation $(c_4 \ln(R_{rup} + c_5 \cosh[c_6 \max(M - c_{HM}, 0)])$ plus magnitude-dependent anelastic attenuation $[c_{\gamma 1} + 1/\cosh(\max(M - c_{\gamma 3}, 0))]r_{rup}$	M-scaling based on theoretical physical model	4.0-8.5 for SS and 8.0 for R
Faccioli et al. (2010)	$a_1 + a_2 M$ (linear M term) plus magnitude-dependent distance saturation $[a_3 \log(R_{rup} + a_4 10^{a5M})]$	Simple M dependency. Notes that inclusion of M^2 term has negligible impact on sigma but improves predictions for large M	4.5-7.6
Kanno et al. (2006)	C1+a1M (linear M term) plus magnitude-dependent distance saturation $[-\log(X + d_1 10^{0.5M})]$	Simple M dependency	5.2-8.2
McVerry et al. (2006)	$C_1' + C_{4AS}(M-6) + C_{3AS}(8.5-M)^2$ (linear and quadratic M terms) plus linear magnitude-dependent geometric spreading $[(C_8' + C_{6AS}(M-6))\ln(R')]$	Coefficients labelled AS taken from Abrahamson & Silva (1997)	5.08-7.09
Zhao et al. (2006)	$Ck' + aM + Q_c(M - M_C)^2$ (linear and quadratic M terms) plus magnitude-dependent distance saturation $[-\log(x + c\exp(dM))]$	Quadratic M dependency derived based on residuals	5.0-8.3

Magnitude-scaling for rock (SS)

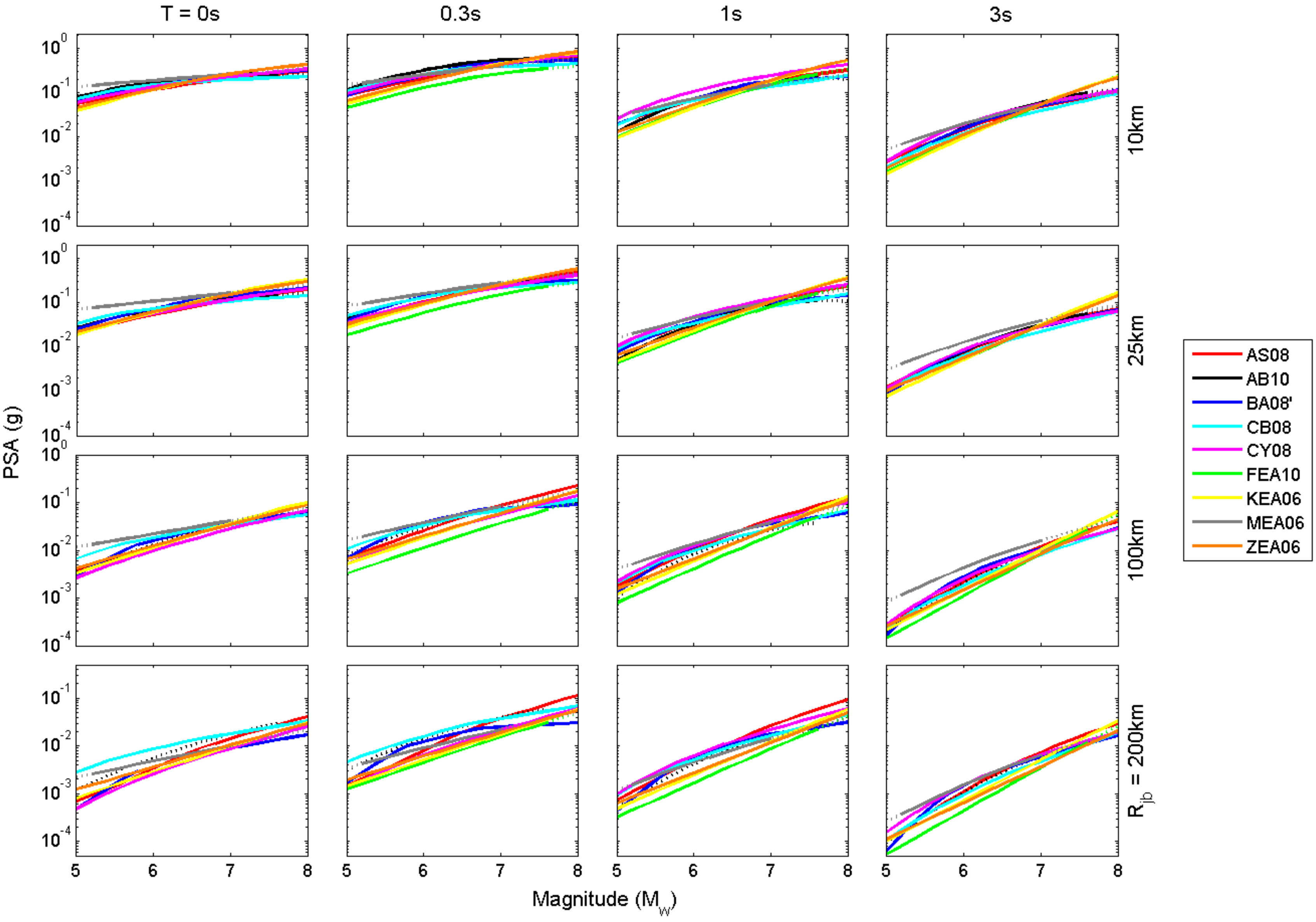

DISTANCE TERM SYNTHESIS

MODEL	DISTANCE TERM(s)	NOTES	DISTANCE RANGE (km)
Abrahamson & Silva (2008)	$[a_2+a_3(M-c_1)]\ln \mathrm{sqrt}(R_{rup}{}^2+c_4{}^2)$ (linear magnitude-dependent geometric spreading with distance saturation) plus magnitude-dependent anelastic attenuation for R>100km $[a_{18}(R_{rup}-100)T_6(M)$ where $T_6(M)=1$ for $M<5.5$, $0.5(6.5-M)+0.5$ for $5.5<M<6.5$ and 0.5 for $M>6.5]$		0-200
Akkar & Bommer (2010)	$(b_4+b_5M)\log \mathrm{sqrt}(R_{JB}{}^2+b_6{}^2)$ (linear magnitude-dependent geometric spreading with distance saturation)		0-99
Boore & Atkinson (2008) as modified by Atkinson & Boore (2011)	$[c_1+c_2(M-M_{ref})]\ln(R/R_{ref})$ where $R=\mathrm{sqrt}(R_{JB}{}^2+h^2)$ (linear magnitude-dependent geometric spreading with distance saturation) plus anelastic attenuation $[c_3(R-R_{ref})]$. In 2011 revision adjustment in R-scaling below M 5.75.	Models change in geometric decay below M 5.75	0-200
Campbell & Bozorgnia (2008)	$(c_4+c_5M)\ln \mathrm{sqrt}(R_{rup}{}^2+c_6{}^2)$ (linear magnitude-dependent geometric spreading with distance saturation)		0-200

DISTANCE TERM SYNTHESIS

MODEL	DISTANCE TERM(s)	NOTES	DISTANCE RANGE (km)
Chiou & Youngs (2008)	$c_4\ln(R_{rup}+c_5\cosh[c_6\max(M-c_{HM},0)])+(c_{4a}-c_4)\ln(\mathrm{sqrt}(R_{rup}+c_{RB}^2))$ (geometric spreading with magnitude-dependent distance saturation)+ $[c_{\gamma1}+1/\cosh(\max(M-c_{\gamma3},0))]r_{rup}$ (magnitude-dependent anelastic attenuation)		0-200
Faccioli et al. (2010)	$a_3\log(R_{rup}+a_4 10^{a5M})$ (geometric spreading with magnitude-dependent distance saturation)		6-200
Kanno et al. (2006)	$-\log(X+d_1 10^{0.5M})$ (1/R geometric spreading with magnitude-dependent distance saturation) + b_1X (anelastic attenuation)	Simple distance dependence. Similar to Zhao et al. (2006)	1-400
McVerry et al. (2006)	$[C_8'+C_{6AS}(M-6)]\ln \mathrm{sqrt}(r^2+C_{10AS}^2)]$ (linear magnitude-dependent geometric spreading with distance saturation) $+C_5'r$ (anelastic attenuation)	Coefficients labelled AS taken from Abrahamson & Silva (1997)	6-400
Zhao et al. (2006)	$-\log(r)$ where $r=x+c\exp(dM)$ (1/R geometric spreading with magnitude-dependent distance saturation) $+bx$ (anelastic attenuation)	Simple distance dependence. Similar to Kanno et al. (2006)	0-300

Distance-scaling (decay) for rock (SS)

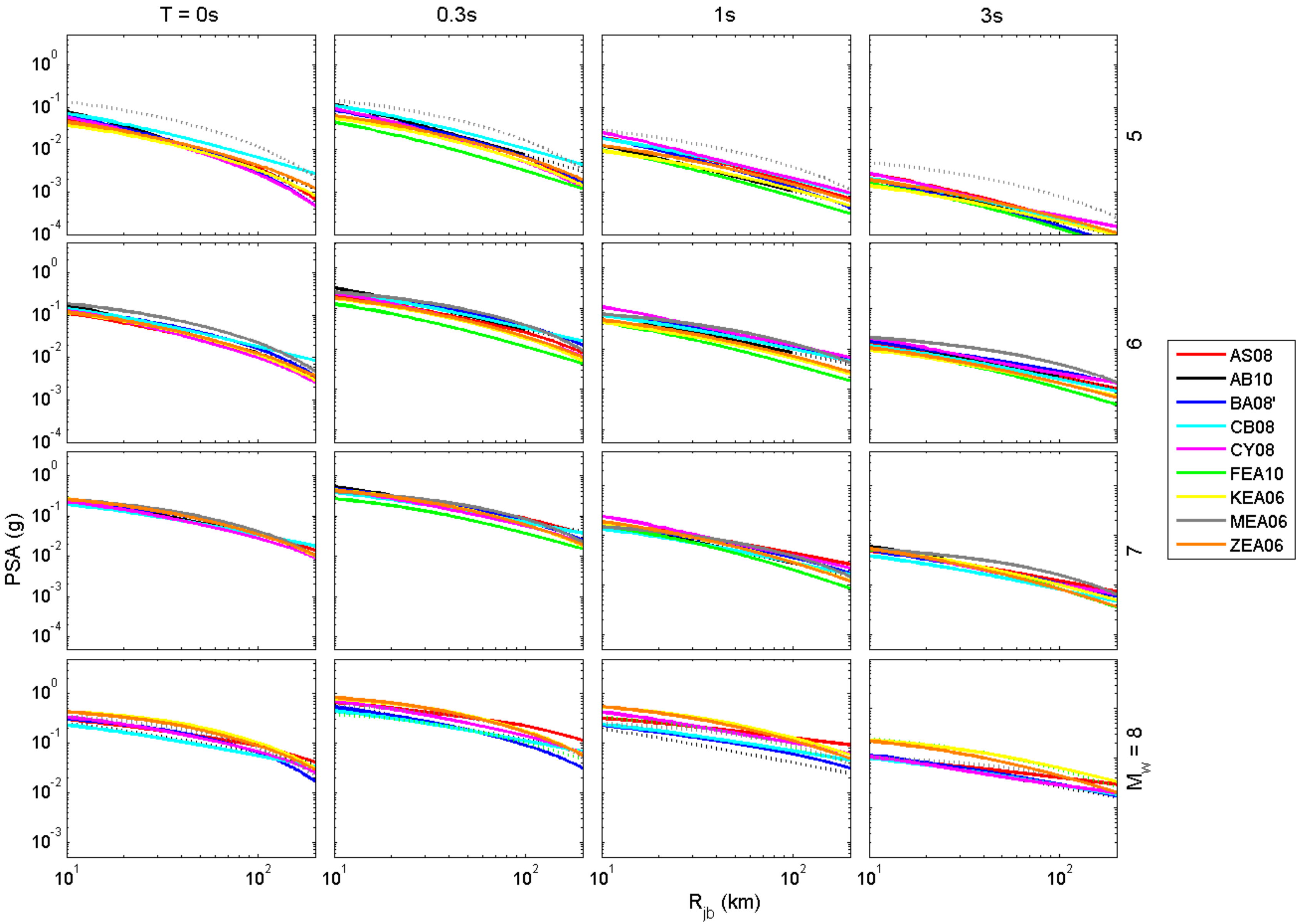

Site response functions

- Site response computed relative to V_{ref} = 1000 m/s or nearest category (for category-based site models)
- Scaling with V_{s30} and reference motion amplitude investigated for PGA to 3.0 sec S_a.

	Reference	Application Region	Site Parameters		Site Amplification Function	
			Discrete categories[1]	Continuous Variables	Non-linearity	Reference site condition[2]
Active tectonic regions	Abrahamson & Silva (2008)	Global	-	V_{s30}, $Z_{1.0}$	Yes	V_{s30} = 1100 m/s
	Akkar & Bommer (2010)	Europe & Middle East	*Three* : rock, stiff & soft soil	-	No	Rock
	Boore & Atkinson (2008, 2011)	Global	-	V_{s30}	Yes	V_{s30}=760 m/s
	Campbell & Bozorgnia (2008)	Global	-	V_{s30}, $Z_{2.5}$	Yes	V_{s30} = 1100 m/s
	Cauzzi & Faccioli (2008); Faccioli et al. (2010)	Global	CEN A-D	V_{s30}	No	CEN A
	Chiou & Youngs (2008)	Global	-	V_{s30}, $Z_{1.0}$	Yes	V_{s30}=1130 m/s
	Kanno et al. (2006)	Japan	-	V_{s30}	No	$V_{s30}\approx$300 m/s
	McVerry et al. (2006)	New Zealand	*Five* : strong rock to v soft soil	-	Yes	Strong rock and rock
	Zhao et al. (2006)	Japan	*Four* : hard rock to soft soil	-	No	Not defined

Site response functions

Summary of ACR Site Models

Site Models	***Linear Site Response Terms***	***Functional Form***	***Nonlinear Site Response Terms***
Akkar & Bommer (2010)	b_7 (T), b_8(T)	$\ln(F) = b_7\,(T)S_S + b_8\,(T)S_A$	-
Abrahamson & Silva (2008)	a10 (T),b,n	$\ln(F) = (a_{10}\,(T)+bn)*\ln(V_{s30}/V_{lin})$	b, c, n, V_{lin}
Boore & Atkinson (2008)	b_{lin} (T)	$\ln(F_{lin}) = b_{lin}(T)*\ln(V_{s30}/V_{ref})$	b_{nl}
Campbell & Bozorgnia (2008)	c_{10} (T), k_2 (T), n	$\ln(F_{lin}) = [c_{10}(T)+k_2(T)*n]*\ln(V_{s30}/k_1(T))$	k_2, c, n, k1
Chiou & Youngs (2008)	ϕ_1 (T)	$\ln[a(V_{s30},T)] = \phi_1\,(T)*\ln(V_{s30}/V_{ref})$	$b(V_{s30},T)$
Faccioli et al. (2010)	b_v(T)	$\ln(f_s) = b_v\,(T)*\ln(V_{s30}/V_a)$	-
Kanno et al. (2006)	p (T)	ln(G) = p(T)*ln(AVS30)+q	-
McVerry et al. (2006)	C_{30} (T)	See the paper p. 37	Amp_k (T)
Zhao et al. (2006)	C_k, C_H	$\ln(F) = C_k - C_1$	-

Site response functions (V_{s30} scaling)

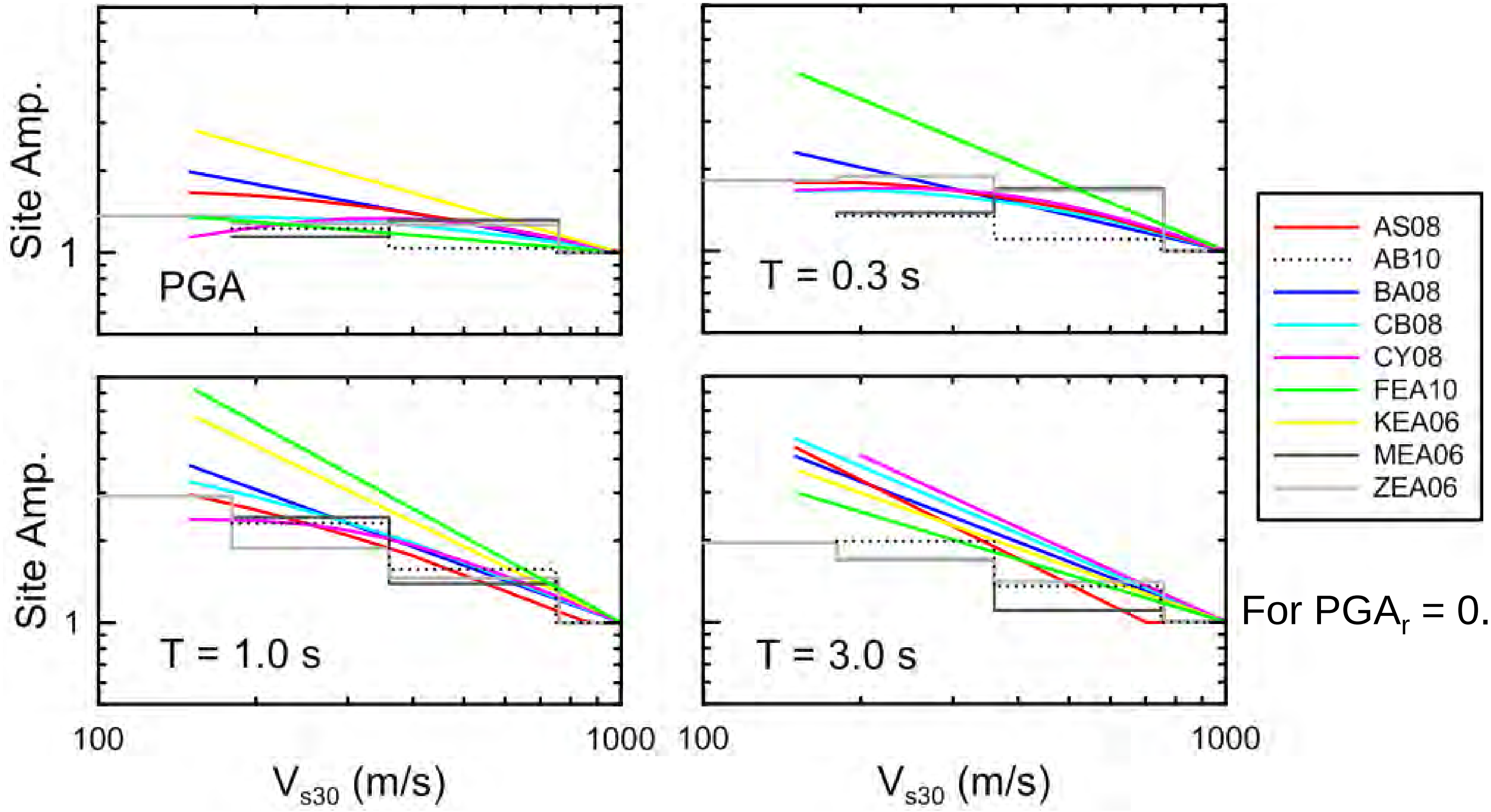

For PGA_r = 0.1 g

Site response functions (V_{s30} scaling)

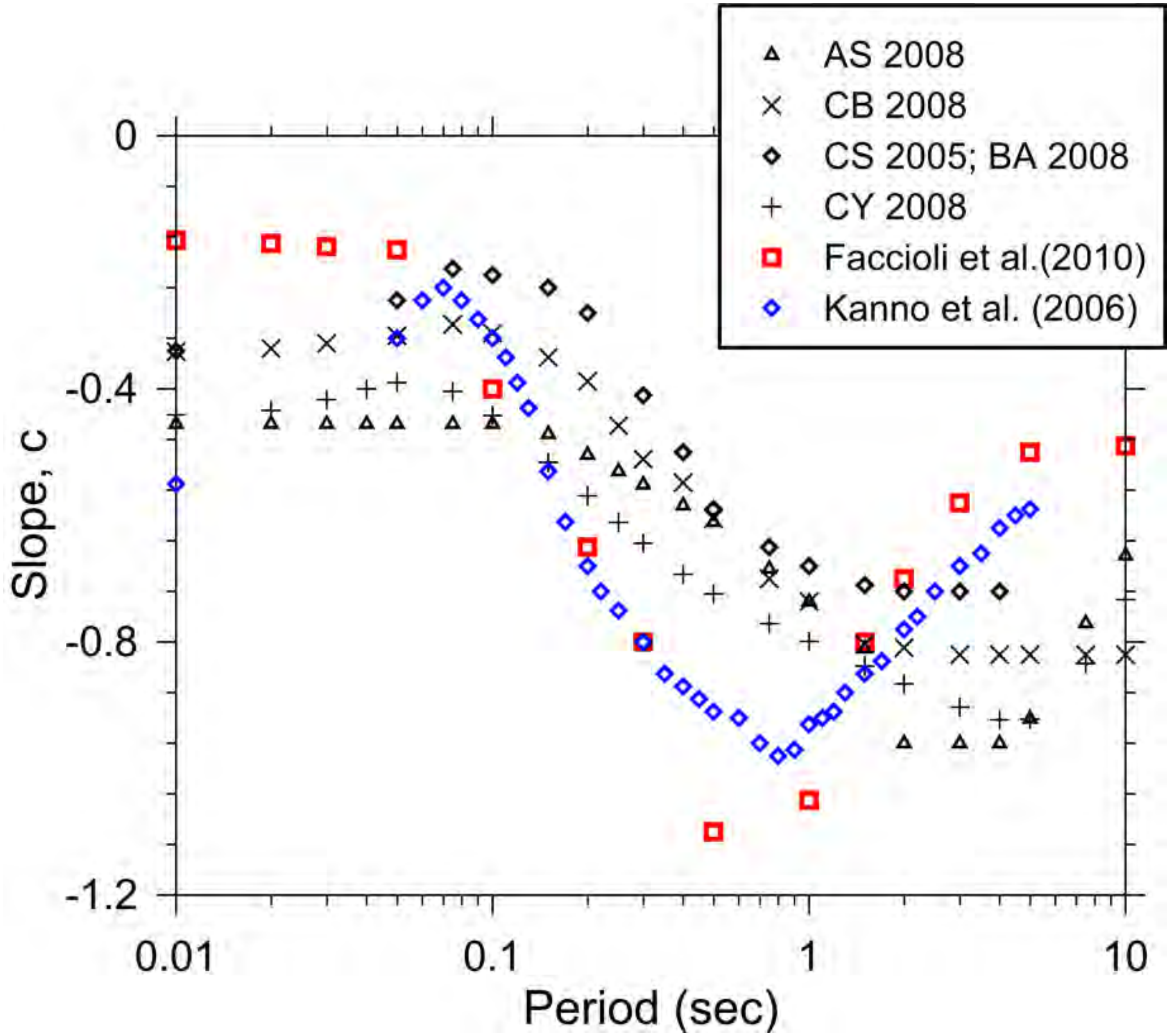

$$F_{lin} = \left(\frac{V_{s30}}{V_{ref}} \right)^{c}$$

Site response functions (nonlinearity)

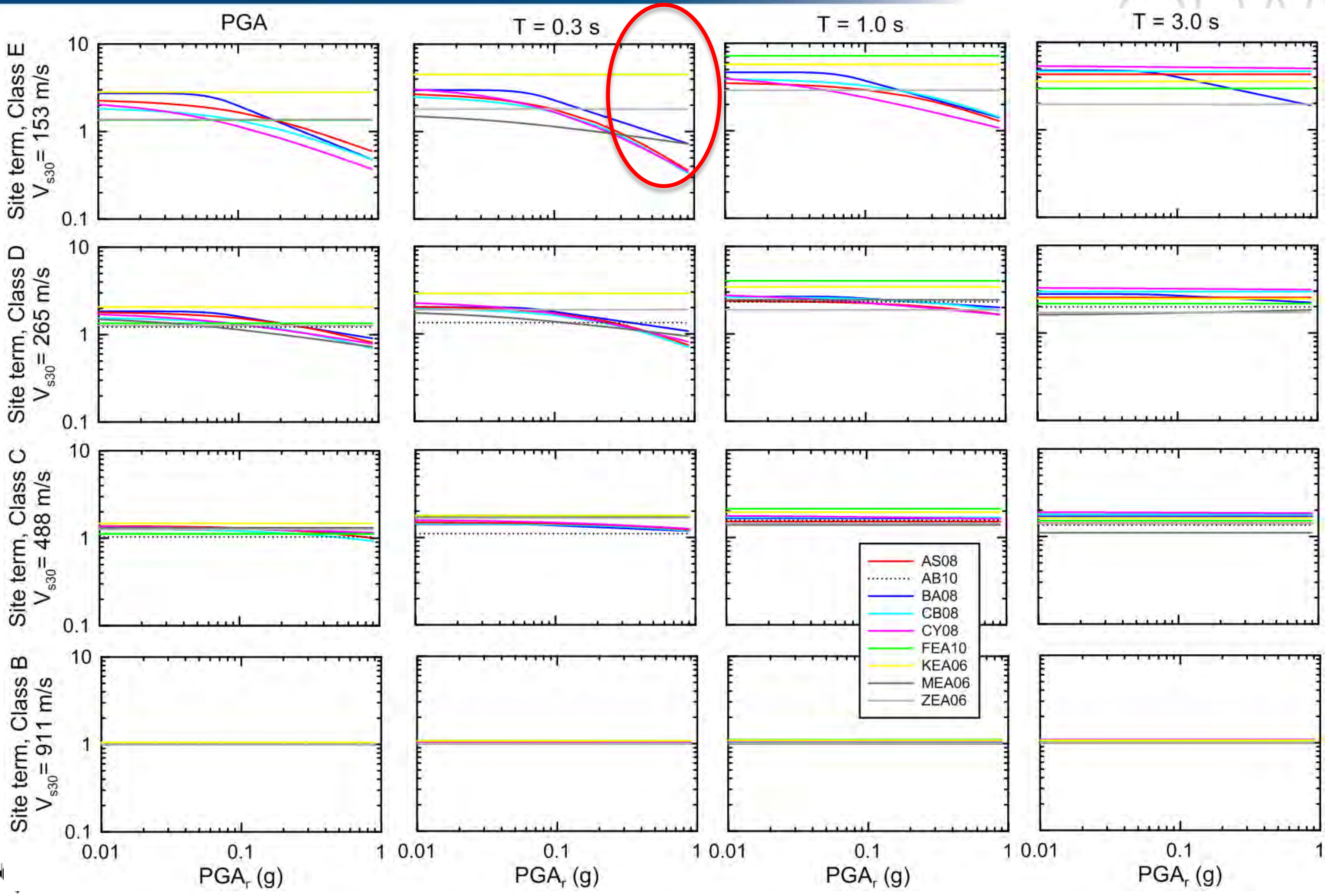

PEER

Site response functions

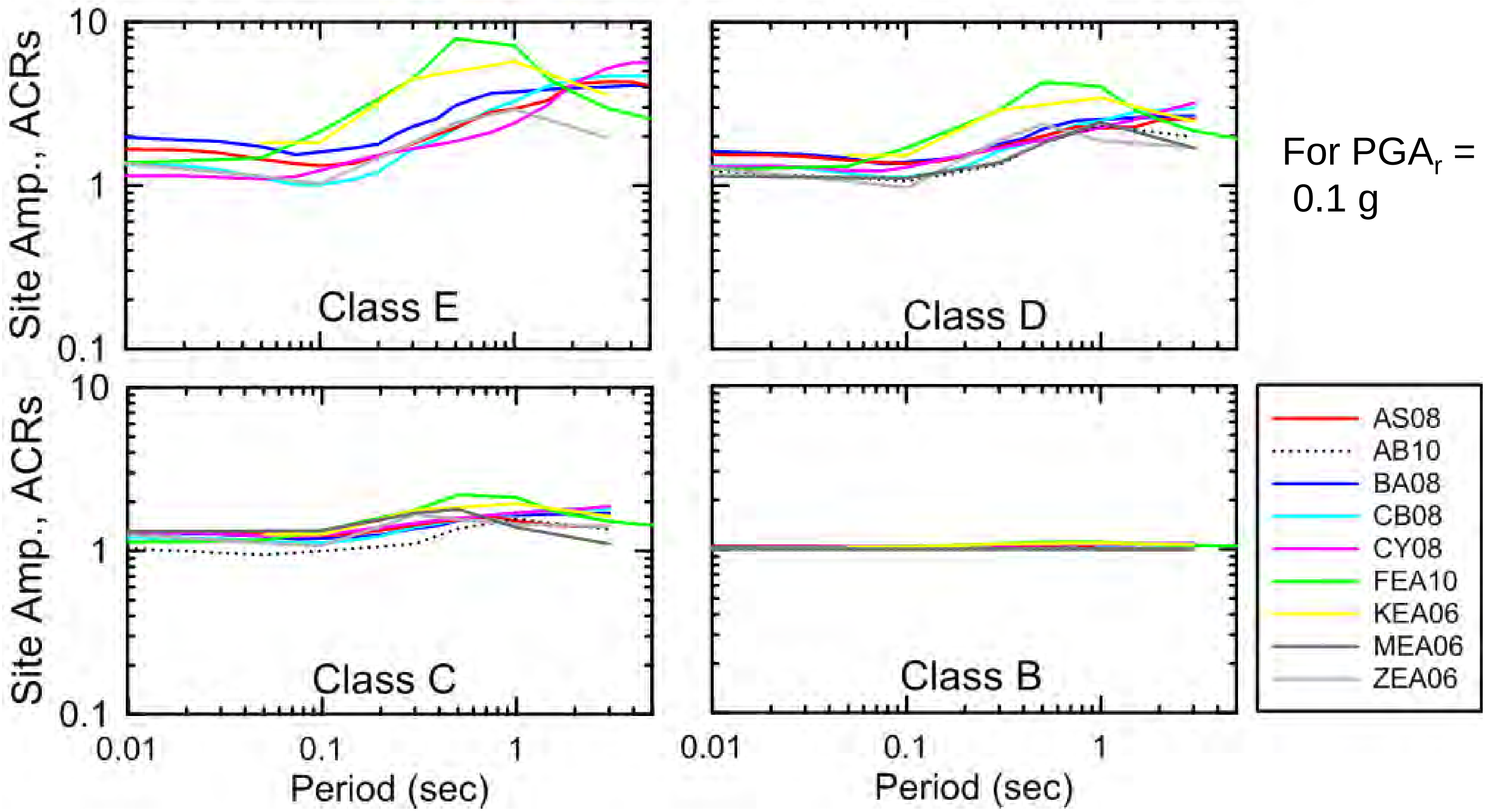

For PGA$_r$ = 0.1 g

Summary of GMPE-data comparisons

	AS 2008	AB 2010	BA 2008	CB 2008	FEA10	CY 2008	KEA 2006	MEA 2006	ZEA 2006
A (Eur-Med)		X	X						
B (Iran)			X	X		X			
C (Worldwide)	X	X	X	X	X (CF08)	X	X		X
D (CA)	X		X	X		X			
E (Japan)	X		X	X		X			
F (Portugal)		X	X			X			
G (Japan)	X	X	X		X (CF08)	X	X		X
H (Italy)	X	x (07)	X	X		X			
I (Greece)			X						
J (Iran)			X	X		X			
K (Japan)	X		X	X		X	X		
L (New Zeal.)			X			X		X	X
M (CA)	X		X	X		X			

List of models pre-selected
AS2008 = Abrahamson & Silva (2008): NGA
AB2010 = Akkar and Bommer (2010): Europe
BA2008 = Boore & Atkinson (2008): NGA. Modifie
CB2008 = Campbell & Bozorgnia (2008): NGA
CF08/FEA10 = Cauzzi and Faccioli (2008) as updated by Faccioli *et al*. (2010): International data, mostly Japan
CY2008 = Chiou and Youngs (2008): NGA
KEA2006 = Kanno *et al*. (2006): Japan
McV2006 = McVerry *et al*. (2006): New Zealand
Zhao2006 = Zhao *et al*. (2006): International, mostly Japan

We first present 'overall goodness of fit' studies. Then 'residuals analysis' studies.

Case study A

Title	"An evaluation of the applicability of the NGA models to ground-motion prediction in the Euro- Mediterranean region", Bull Earthquake Eng (2008) 6:149–177								
Authors	Peter J. Stafford · Fleur O. Strasser · Julian J. Bommer								
GMPEs tested	AS2008	AB2010	BA2008	CB2008	CF08-FEA10	CY2008	KEA2006	MEA 2006	ZEA 2006
		X (2007 ver)	x (2007 ver)						
Geog. Areas	Euro-Mediterranean Region								

Method of performance assessment: Overall goodness of fit from Scherbaum et al. (2004) extended to include inter- and intra-event variability.

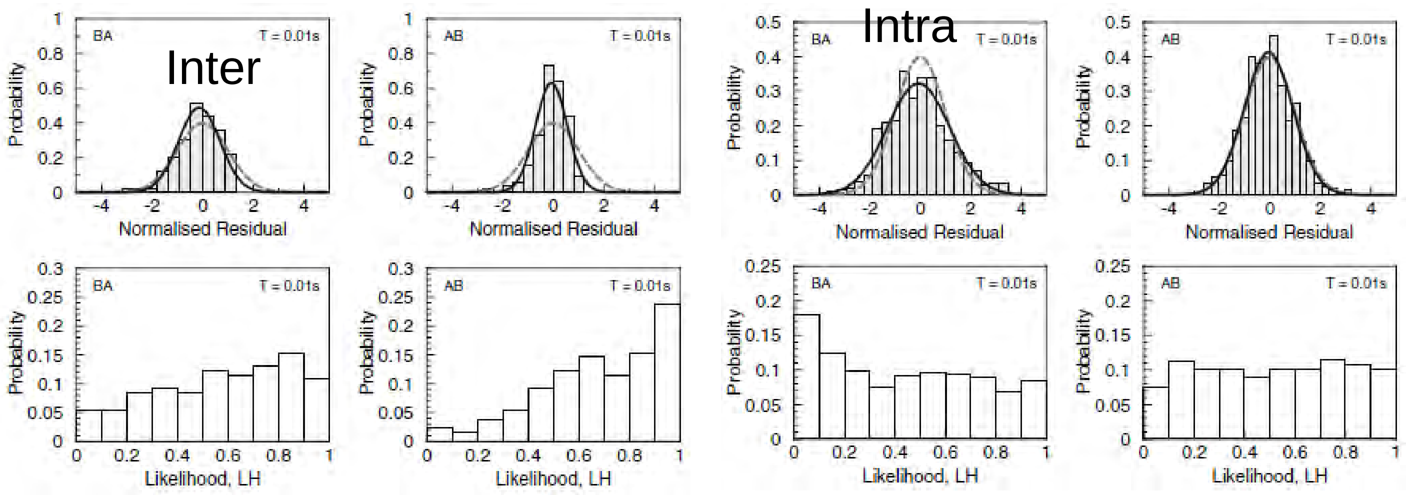

Database used for test: strong ground-motion data from Euro-Mediterranean region used by Akkar and Bommer (2007). Similar to Ambrasseys et al. (2005).

General results: As expected, Akkar and Bommer (2007) receives A classification for all periods. BA2007 model receives C classifications for periods below 0.8 s, B for periods between 0.8 and 1.5 s, and A at longer periods. BA means are close to zero, but model standard deviations are smaller than data.

Case study B.1

Title	"Ranking of several ground-motion models for seismic hazard analysis in Iran", *J. Geophys. Eng.*, 5 (2008) 301–310								
Authors	H Ghasemi, M Zare and Y Fukushima								
GMPEs tested	AS2008	AB2010	BA2008	CB2008	CF08-FEA10	CY2008	KEA2006	MEA 2006	ZEA 2006
			X (2007 ver)	x (2007 ver)		x (2007 ver)			
Geog. Areas	Iran								

Method of performance assessment: Overall goodness-of-fit from Scherbaum et al. (2004)

Database used for test: The strong motions recorded during the 2002 Avaj, 2003 Bam, 2004 Kojour and 2006 Silakhor earthquakes are considered. M 6.1-6.4 (*sic*). Bam magnitude is 6.7.

General results: All models rejected by strict interpretation of the statistical tests. CB ranks C. BA and CY rank D.

Local GMPEs from ISMN recommended.

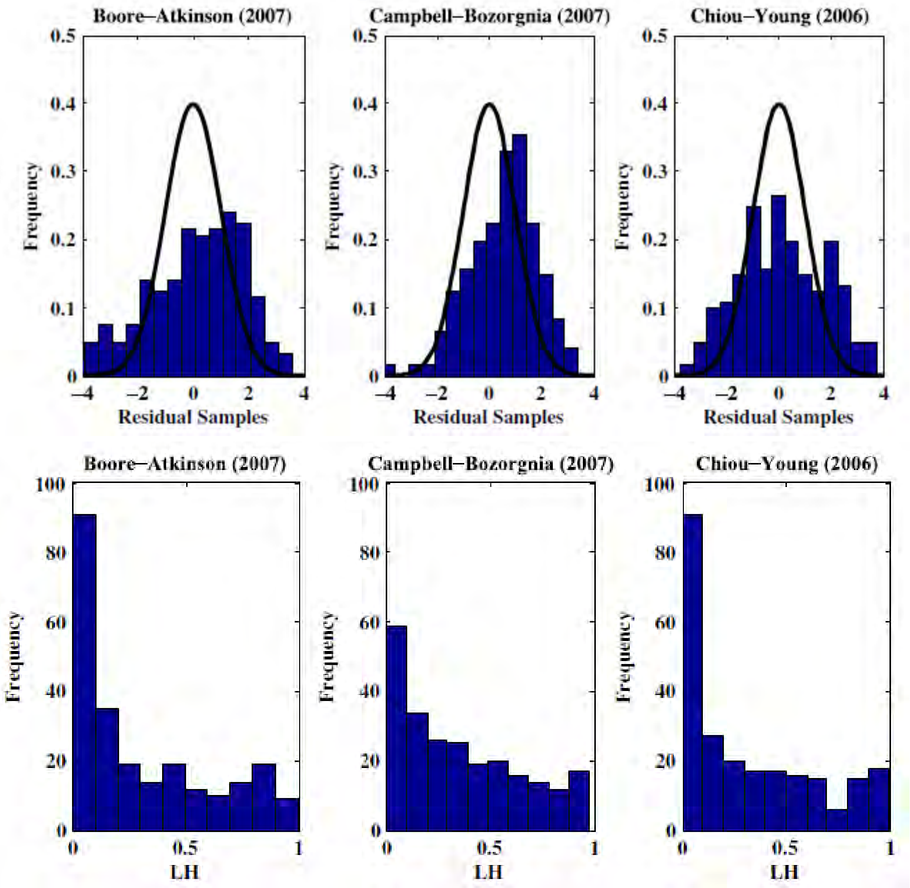

Case study B.2

Title	"An empirical spectral ground-motion model for Iran", *Journal of Seismology*, 13 (2009) 499–515, doi: 10.1007/s10950-008-9143-x								
Authors	H Ghasemi, M Zare and Y Fukushima and K. Koketsu								
GMPEs tested	AS2008	AB2010	BA2008	CB2008	CF08-FEA10	CY2008	KEA2006	MEA 2006	ZEA 2006
			X	X		X			
Geog. Areas	Iran								

Method of performance assessment: Overall goodness-of-fit from Scherbaum et al. (2004)

Database used for test: 69 records from distances 9-150km and Mw 5.6-7.3 (see table for the complete dataset, which includes soil records). Only rock records used for this analysis

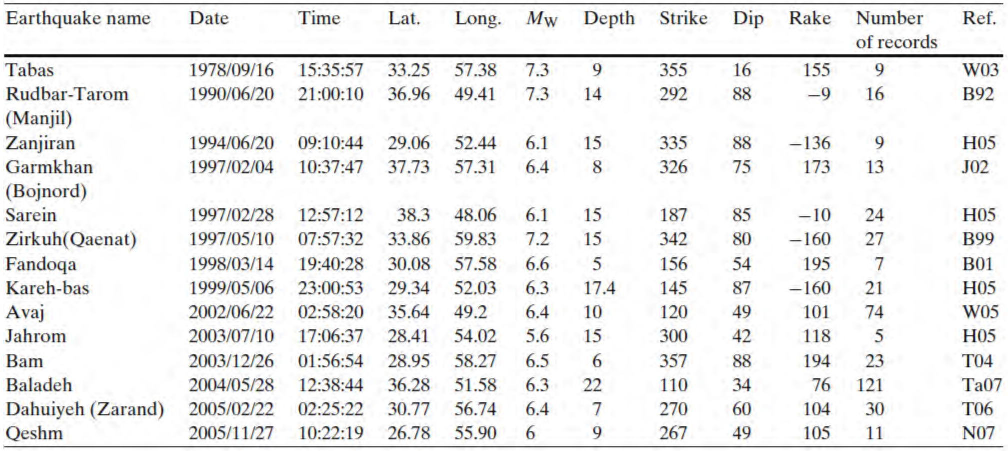

Earthquake name	Date	Time	Lat.	Long.	M_W	Depth	Strike	Dip	Rake	Number of records	Ref.
Tabas	1978/09/16	15:35:57	33.25	57.38	7.3	9	355	16	155	9	W03
Rudbar-Tarom (Manjil)	1990/06/20	21:00:10	36.96	49.41	7.3	14	292	88	−9	16	B92
Zanjiran	1994/06/20	09:10:44	29.06	52.44	6.1	15	335	88	−136	9	H05
Garmkhan (Bojnord)	1997/02/04	10:37:47	37.73	57.31	6.4	8	326	75	173	13	J02
Sarein	1997/02/28	12:57:12	38.3	48.06	6.1	15	187	85	−10	24	H05
Zirkuh(Qaenat)	1997/05/10	07:57:32	33.86	59.83	7.2	15	342	80	−160	27	B99
Fandoqa	1998/03/14	19:40:28	30.08	57.58	6.6	5	156	54	195	7	B01
Kareh-bas	1999/05/06	23:00:53	29.34	52.03	6.3	17.4	145	87	−160	21	H05
Avaj	2002/06/22	02:58:20	35.64	49.2	6.4	10	120	49	101	74	W05
Jahrom	2003/07/10	17:06:37	28.41	54.02	5.6	15	300	42	118	5	H05
Bam	2003/12/26	01:56:54	28.95	58.27	6.5	6	357	88	194	23	T04
Baladeh	2004/05/28	12:38:44	36.28	51.58	6.3	22	110	34	76	121	Ta07
Dahuiyeh (Zarand)	2005/02/22	02:25:22	30.77	56.74	6.4	7	270	60	104	30	T06
Qeshm	2005/11/27	10:22:19	26.78	55.90	6	9	267	49	105	11	N07

General results: See table. Campbell & Bozorgnia (2008) ranked B, Boore & Atkinson (2008) ranked C and Chiou & Youngs (2008) ranked D. Observed ground motions more variable than predicted by the NGA models.

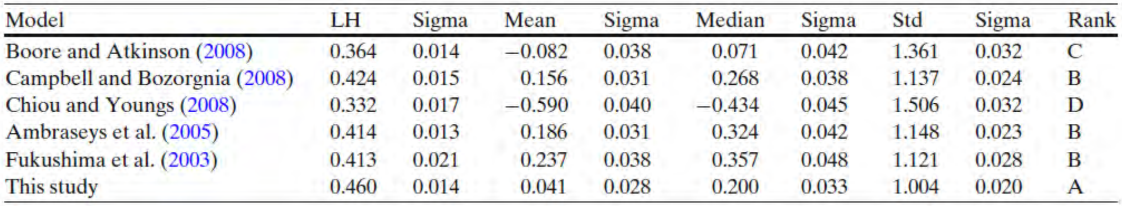

Model	LH	Sigma	Mean	Sigma	Median	Sigma	Std	Sigma	Rank
Boore and Atkinson (2008)	0.364	0.014	−0.082	0.038	0.071	0.042	1.361	0.032	C
Campbell and Bozorgnia (2008)	0.424	0.015	0.156	0.031	0.268	0.038	1.137	0.024	B
Chiou and Youngs (2008)	0.332	0.017	−0.590	0.040	−0.434	0.045	1.506	0.032	D
Ambraseys et al. (2005)	0.414	0.013	0.186	0.031	0.324	0.042	1.148	0.023	B
Fukushima et al. (2003)	0.413	0.021	0.237	0.038	0.357	0.048	1.121	0.028	B
This study	0.460	0.014	0.041	0.028	0.200	0.033	1.004	0.020	A

Case study C

Title	"Testing the global applicability of ground-motion prediction equations for active shallow crustal regions", *BSSA*, 102 (2012) 707–721								
Authors	Elise Delavaud, Frank Scherbaum, Nicolas Kuehn, and Trevor Allen								
GMPEs tested	AS2008	AB2010	BA2008	CB2008	CF08-FEA10	CY2008	KEA2006	MEA 2006	ZEA 2006
	x	x	x	x	x	x	x		x
Geog. Areas	California, Japan, Europe								

Method of performance assessment: Overall goodness-of-fit from Scherbaum et al. (2009), LLH. 11 GMPEs considered, 8 are pre-selected GEM GMPEs. Total residuals considered.

Database used for test: Global dataset by Allen and Wald (2009). Three focus regions: CA, Japan, Europe. M > 5, R < 200 km

General results: Tabulated values of LLH organized by region and IM.

No strong evidence for regionalization was found, except Japan.

AB2010 and Chiou et al. (2010) consistently performed the best across IMs and regions.

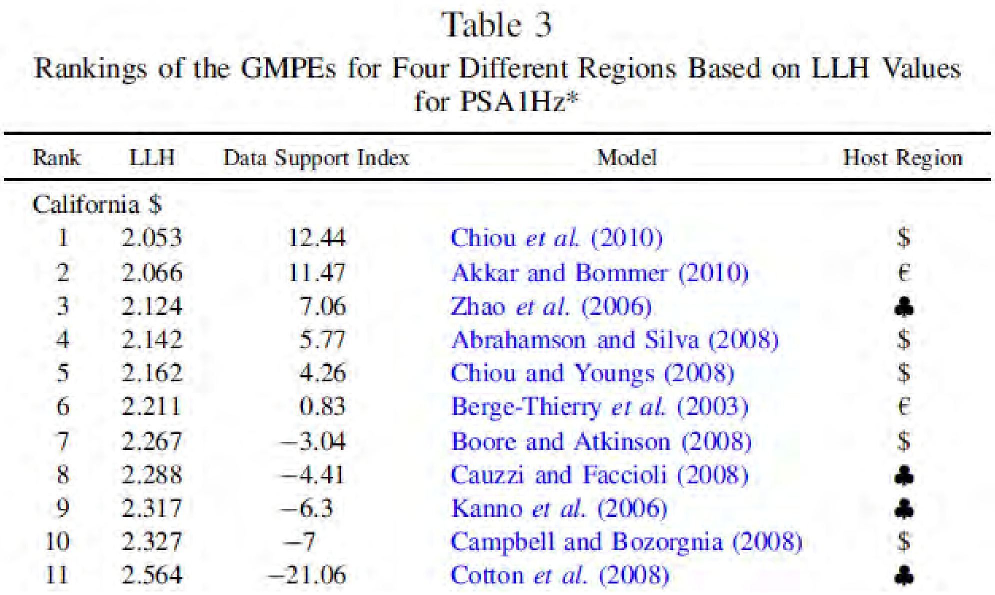

Table 3

Rankings of the GMPEs for Four Different Regions Based on LLH Values for PSA1Hz*

Rank	LLH	Data Support Index	Model	Host Region
California $				
1	2.053	12.44	Chiou *et al.* (2010)	$
2	2.066	11.47	Akkar and Bommer (2010)	€
3	2.124	7.06	Zhao *et al.* (2006)	♣
4	2.142	5.77	Abrahamson and Silva (2008)	$
5	2.162	4.26	Chiou and Youngs (2008)	$
6	2.211	0.83	Berge-Thierry *et al.* (2003)	€
7	2.267	−3.04	Boore and Atkinson (2008)	$
8	2.288	−4.41	Cauzzi and Faccioli (2008)	♣
9	2.317	−6.3	Kanno *et al.* (2006)	♣
10	2.327	−7	Campbell and Bozorgnia (2008)	$
11	2.564	−21.06	Cotton *et al.* (2008)	♣

Case study D

Title	"Model validations and comparisons of the next generation attenuation of ground motions (NGA–West) project", *BSSA*, 101 (2011) 160–175								
Authors	James Kaklamanos and Laurie G. Baise								
GMPEs tested	AS2008	AB2010	BA2008	CB2008	CF08-FEA10	CY2008	KEA2006	MEA 2006	ZEA 2006
	x		x	x		x			
Geog. Areas	California (seven earthquakes)								

Method of performance assessment: Overall goodness-of-fit. Metrics: (1) Nash–Sutcliffe model efficiency coefficient, E (higher values indicate better models); (2) median LH value from Scherbaum et al. 2004 (values close to 50% are best)

Database used for test: Seven CA events, M_w 5.2-7.2. All are post-NGA-W1 database. 1060 records.

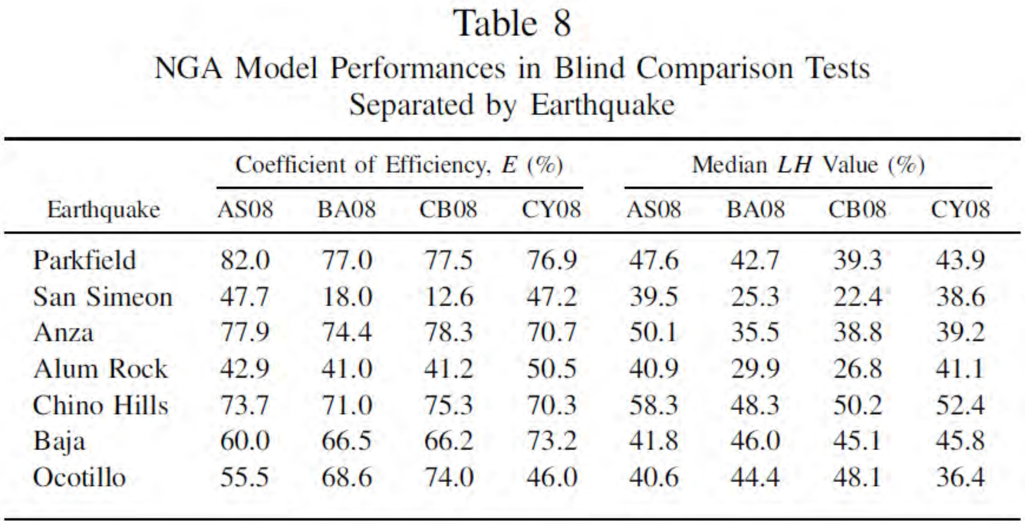

Table 8

NGA Model Performances in Blind Comparison Tests Separated by Earthquake

	Coefficient of Efficiency, *E* (%)				Median *LH* Value (%)			
Earthquake	AS08	BA08	CB08	CY08	AS08	BA08	CB08	CY08
Parkfield	82.0	77.0	77.5	76.9	47.6	42.7	39.3	43.9
San Simeon	47.7	18.0	12.6	47.2	39.5	25.3	22.4	38.6
Anza	77.9	74.4	78.3	70.7	50.1	35.5	38.8	39.2
Alum Rock	42.9	41.0	41.2	50.5	40.9	29.9	26.8	41.1
Chino Hills	73.7	71.0	75.3	70.3	58.3	48.3	50.2	52.4
Baja	60.0	66.5	66.2	73.2	41.8	46.0	45.1	45.8
Ocotillo	55.5	68.6	74.0	46.0	40.6	44.4	48.1	36.4

General results: Pre-NGA models less effective than NGA models. Including aftershocks in GMPE development can produce bias, especially at small M. More complex functional forms do not necessarily lead to better model performance.

Relative GMPE performance not recommended for use in ranking.

Case study E

Title	"Conformity of the attenuation relationships in Japan with those by the NGA-project", *Summaries of Technical Papers of Annual Meeting of Architectural Institute of Japan (Hokuriku), September 2010*								
Authors	Toshimitsu Nishimura								
GMPEs tested	AS2008	AB2010	BA2008	CB2008	CF08-FEA10	CY2008	KEA2006	MEA 2006	ZEA 2006
	x		x	x		x			
Geog. Areas	Japan								

Method of performance assessment: Standard deviation of residuals. Appears to be a total standard deviation, but not clear.

Database used for test: K-NET and KiK-net data from 7 shallow Japanese earthquakes occured from 1997 to 2008, with M 6.1-6.8 & strike-slip or reverse faulting.

General results: Japanese models have lowest standard deviations.

Best performing of the NGA models is CY2008

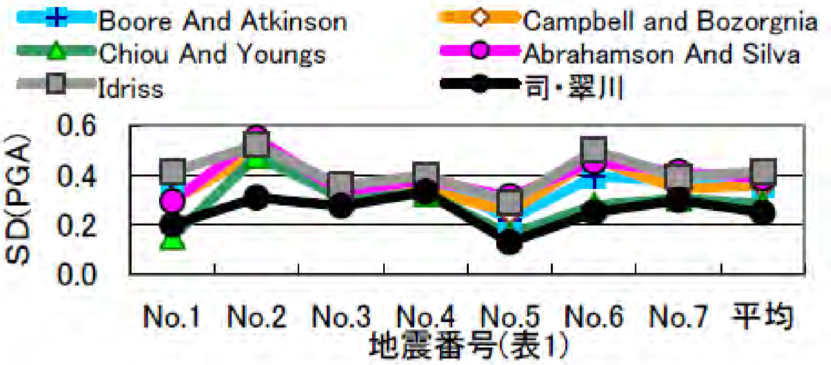

図 3 断層最短距離 30km 以下の対数標準偏差(PGA)

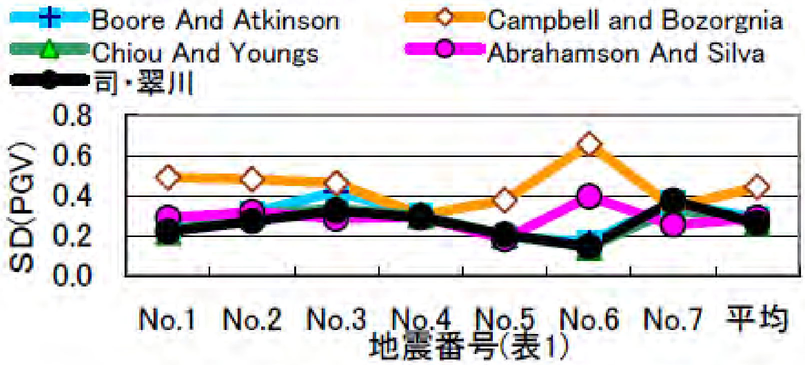

Case study F

Title	“Ground-motion models for seismic-hazard assessment in western Iberia; constraints from instrumental data and intensity observations” *Bulletin of the Seismological Society of America* (2012), 102(1):169-184								
Authors	Susana P. Vilanova, Joao F. B. D. Fonseca, and Carlos S. Oliveira								
GMPEs tested	AS2008	AB2010	BA2008	CB2008	CF08-FEA10	CY2008	KEA2006	MEA 2006	ZEA 2006
		x	x			X			
Geog. Areas	Western Iberia (i.e. Portugal)								

Method of performance assessment: Overall goodness-of-fit from Scherbaum et al. (2004) for T= 0.01-2.0 sec.

Database used for test: M 4.8-7.8, R 100-400 km, 1969-2009

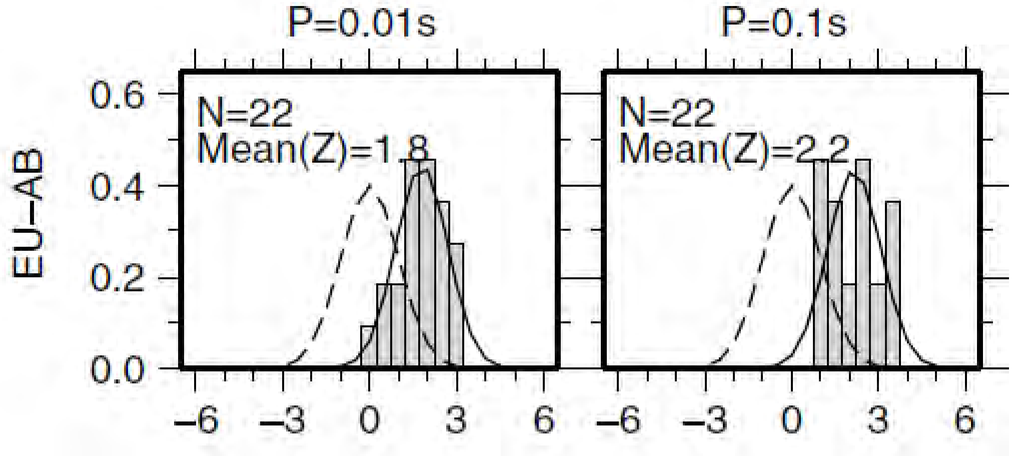

General results: Models developed for stable continental regions perform significantly better than models developed for active tectonic regions.

All three GMPEs for active regions greatly underestimate the observed ground motions at all examined periods (positive mean residual). But note that this comparison requires extrapolation of GMPEs beyond their distance range of applicability.

Case study G

Title	“On the testing of ground--motion prediction equations against small magnitude data”, accepted in *Bulletin of the Seismological Society of America* (2012)								
Authors	C. Beauval, H. Tasan, A. Laurendeau, E. Delavaud, F. Cotton, Ph. Gueguen, and N. Kuehn								
GMPEs tested	AS2008	AB2010	BA2008	CB2008	CF08-FEA10	CY2008	KEA2006	MEA 2006	ZEA 2006
	X	X	X		X (CF08)	X	X		X
Geog. Areas	Japan (also study French data but only for M<4.6 so not considered here)								

Method of performance assessing: Overall goodness-of-fit from Scherbaum et al. (2009), LLH.

Database used for test: About 1200 records from earthquakes with at least 10 records from 5≤Mw ≤7 from K-Net and KiK-Net. Only records from earthquakes located by F-Net and with focal depths less than 25km. Only records from sites with Vs30≥500m/s. Apply M-dependent filter to remove records beyond the edge of triggering (like Kanno et al., 2006). Consider frequencies between 0.25 and 10Hz (0.1 and 4s).

General results: Of GMPEs considered here, Kanno et al. (2006) is best performing followed by Zhao et al. (2006) and Chiou & Youngs (2008). Cauzzi & Faccioli (2008) (forerunner of Faccioli et al., 2010) also performs well.

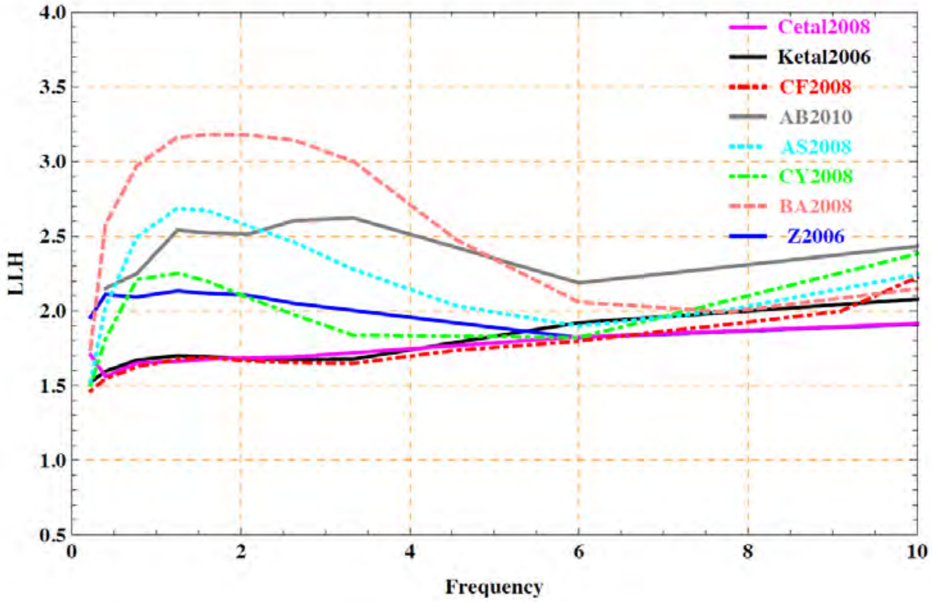

Case study H

Title	"A comparison of NGA ground-motion prediction equations to Italian data", *BSSA*, 99 (2009) 2961–2978								
Authors	Giuseppe Scasserra, Jonathan P Stewart, Paolo Bazzurro, Giuseppe Lanzo, and Fabrizio Mollaioli								
GMPEs tested	AS2008	AB2010	BA2008	CB2008	CF08-FEA10	CY2008	KEA2006	MEA 2006	ZEA 2006
	x	x (2007 ver)	x	x		x			
Geog. Areas	Italy								

Method of performance assessment:
Compute data – model residuals and separate into inter- and intra-event components. Use intra-event residuals to evaluate site amplification and distance attenuation. Use inter-event residuals (event terms) to evaluate M-scaling.

Database used for test: Italian dataset processed using PEER-NGA procedures by Scasserra et al. (2009a)

General results:

- Faster distance attenuation for high-frequency IMs; consistent M-scaling. Nonlinear site response.
- Higher intra-event standard deviation.

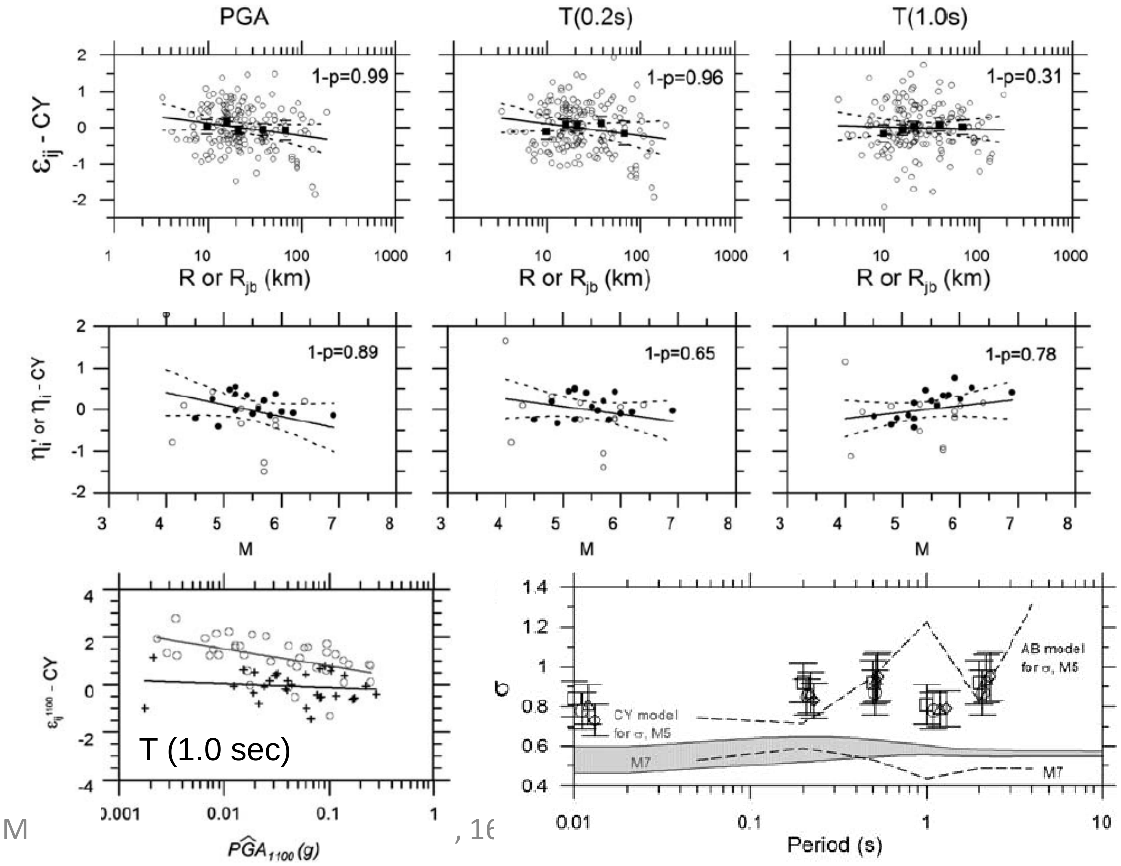

Case study I

Title	“The 8 June 2008 Mw6.4 Achaia–Elia, Greece Earthquake: Source Characteristics, Ground Motions, and Ground Failure,” *Earthquake Spectra*, 26:399–422, 2010								
Authors	Basil Margaris, George Athanasopoulos, George Mylonakis, Christos Papaioannou, Nikolaos Klimis, Nikolaos Theodulidis, Alexandros Savvaidis, Vicky Efthymiadou, and Jonathan P. Stewart								
GMPEs tested	AS2008	AB2010	BA2008	CB2008	CF08-FEA10	CY2008	KEA2006	MEA 2006	ZEA 2006
			x						
Geog. Areas	Greece								

Method of performance assessment: Analysis of inter- and intra-event residuals.

Database used for test: Data for single earthquake. 27 records.

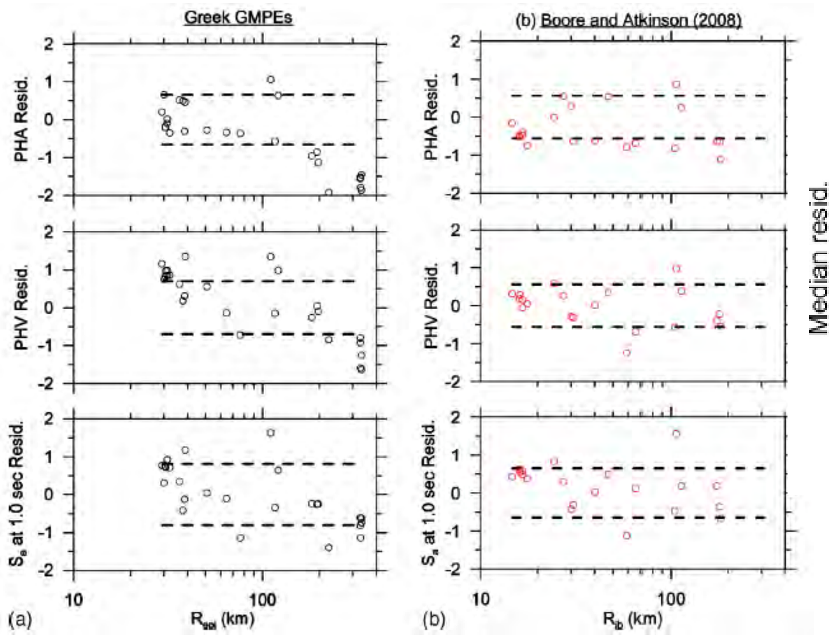

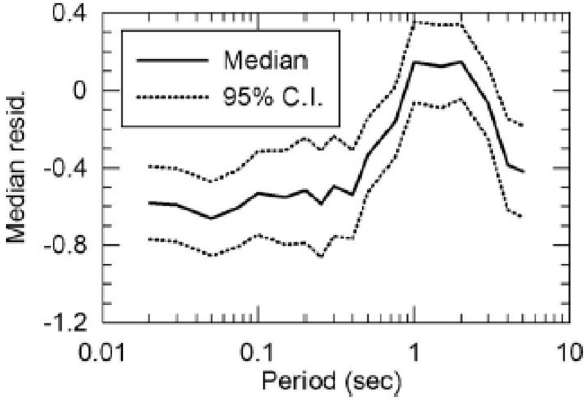

General results: Distance attenuation trends of BA model improved relative to Greek GMPEs. Negative event terms at high frequencies.

Case study J

Title	"A Test of the Applicability of NGA Models to the Strong Ground-Motion Data in the Iranian Plateau", *Journal of Earthquake Engineering*, 14:278–292, 2010								
Authors	J. Shoja–Taheri, S. Naserieh, And G. Hadi								
GMPEs tested	AS2008	AB2010	BA2008	CB2008	CF08-FEA10	CY2008	KEA2006	MEA 2006	ZEA 2006
			x	x		x			
Geog. Areas	Iran								

Method of performance assessment: Analysis of residuals. Similar to Scasserra et al. 2009, but no formal random effects modeling (event term from data means)

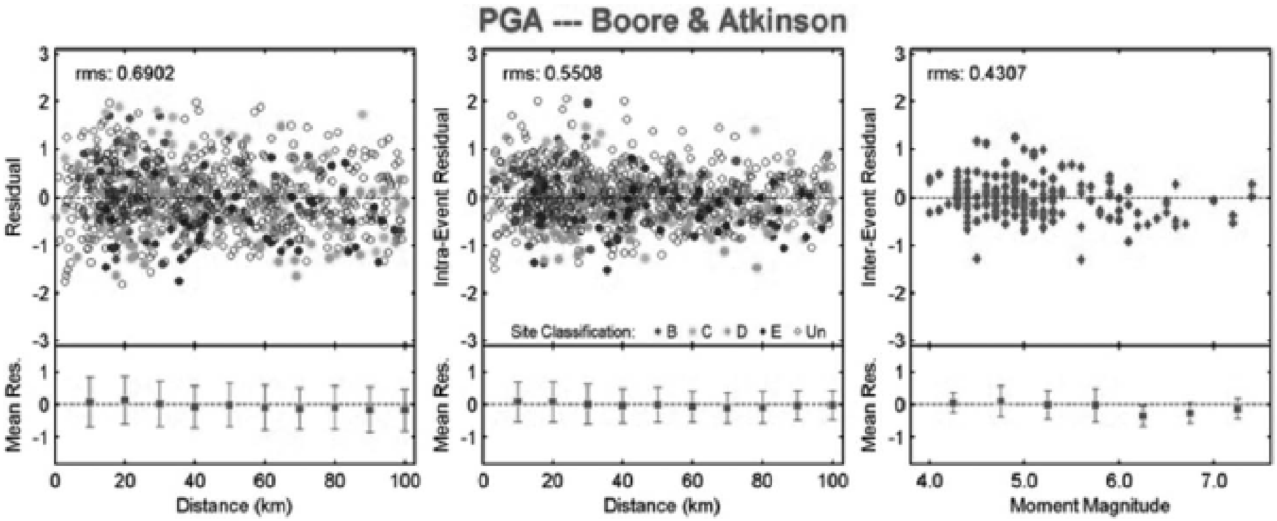

Database used for test: Iranian strong-motion database. Comprises 863 two-component horizontal acceleration time series recorded within 100 km of epicentral distances for 166 earthquakes in Iran with magnitudes ranging from 4.0–7.4 occurred between 1973 and 2006

General results: Residuals for PGA, PGV, and 0.2 sec Sa do not have significant trends with distance or magnitude. NGA models found to be applicable to Iran.

Case study K

Title	"A Study of the Applicability of NGA Models to Strike-Slip Earthquakes in Japan", *Summaries of Technical Papers of Annual Meeting of Architectural Institute of Japan (Kanto), August 2011*								
Authors	Yasuo Uchiyama and Saburoh Midorikawa								
GMPEs tested	AS2008	AB2010	BA2008	CB2008	CF08-FEA10	CY2008	KEA2006	MEA 2006	ZEA 2006
	x		x	x		x	x		
Geog. Areas	Japan								

Method of performance assessment: Analysis of residuals. Similar to Scasserra et al. 2009, but no formal random effects modeling (event term from data means)

Database used for test: K-NET and KiK-net data from 5 shallow crustal strike-slip Japanese earthquakes from 1997 to 2005, with M 5.8-6.8

General results: Distance attenuation bias -- GMPEs tend to underestimate at close distances (Fig.3). Trends with V_{s30} too.

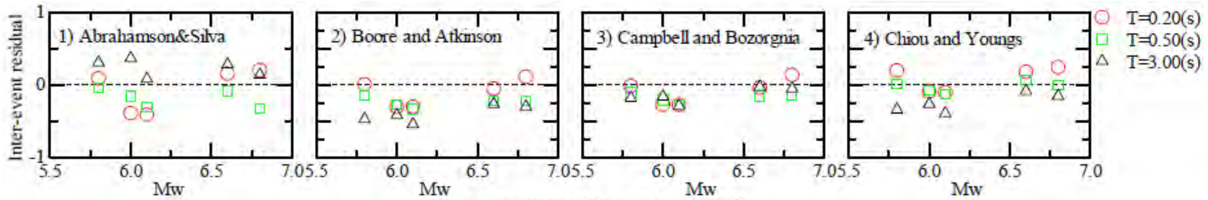

図 2　地震間誤差と Mw の関係

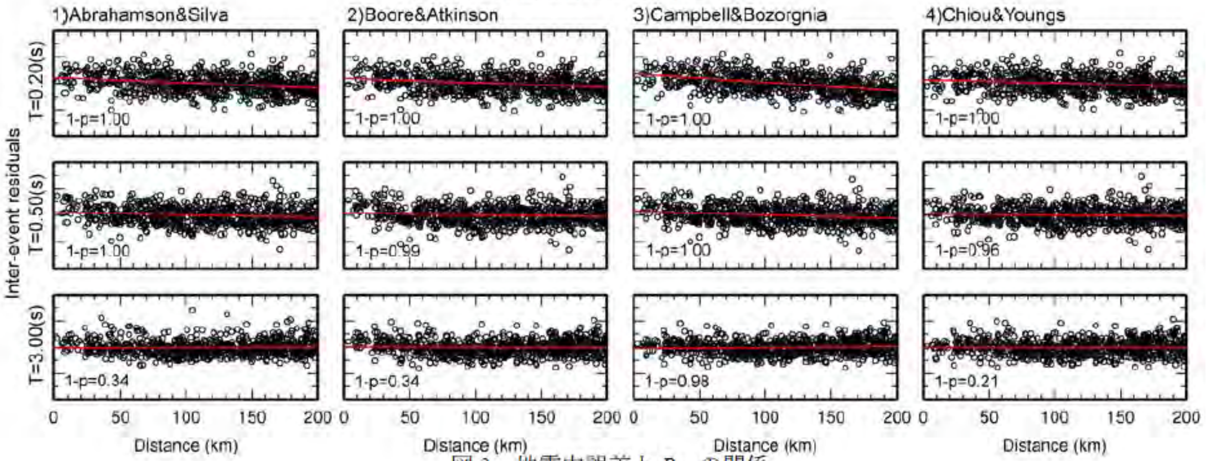

図 3　地震内誤差と R_{rup} の関係

Case study L

Title	"A New Zealand-specific pseudo-spectral acceleration ground motion prediction equation for active shallow crustal earthquakes based on foreign models ," *BSSA.* Submitted, 2012 (used with permission)								
Authors	Brendon A. Bradley								
GMPEs tested	AS2008	AB2010	BA2008	CB2008	CF08-FEA10	CY2008	KEA2006	MEA 2006	ZEA 2006
			X			X		X	X
Geog. Areas	New Zealand								

Method of performance assessment: Analysis of inter- and intra-event residuals, Scasserra et al. (2009).

Database used for test: NZ data set compiled in the study. 2437 recs.,

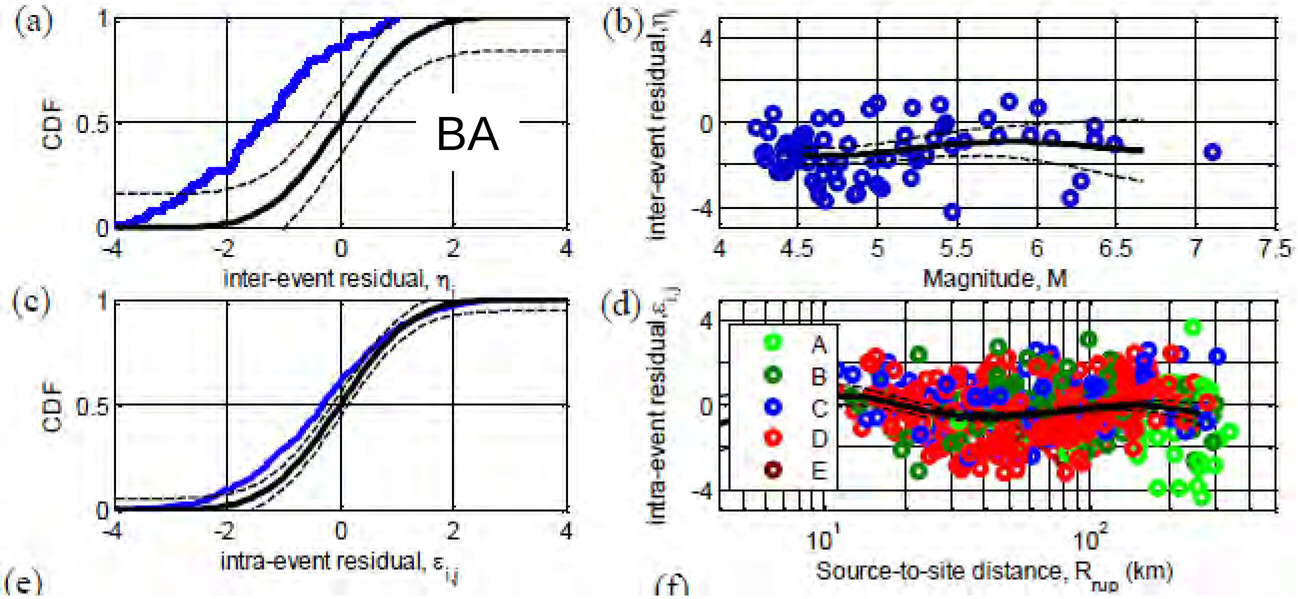

General results: NGA, McV, and ZEA GMPEs over-predict, especially at small magnitudes. Chiou et al. (2010) was the best model. NZ-specific model developed by modifying Chiou et al. (2010) model. Issues with volcanic path distance addressed.

Case study M

Title	“Comparison of ground motions from the 2010 Mw 7.2 El Mayor–Cucapah earthquake with the next generation attenuation ground motion prediction equations ,” *Bull Eqk. Engineering*. Published online May 19 2012, DOI 10.1007/s10518-012-9358-7								
Authors	Yun Liao · Jorge Meneses								
GMPEs tested	AS2008	AB2010	BA2008	CB2008	CF08-FEA10	CY2008	KEA2006	MEA 2006	ZEA 2006
	x		X	x		X			
Geog. Areas	California and Northern Mexico								

Method of performance assessment: Analysis of inter- and intra-event residuals.

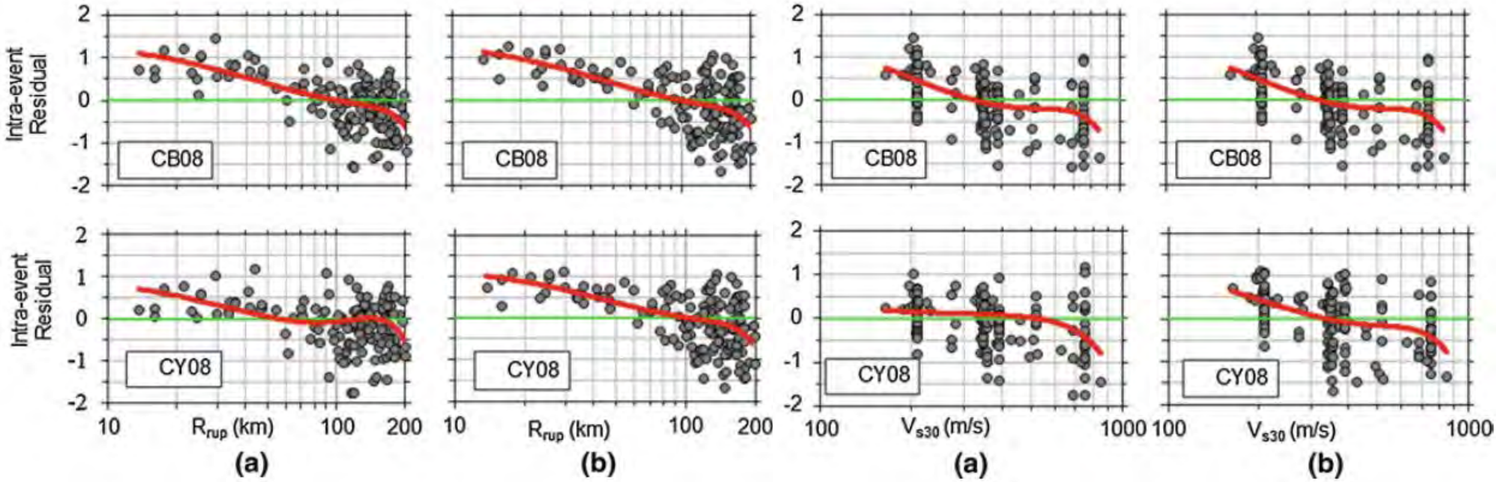

Database used for test: Data for single earthquake. 144 records, Mw 7.0, R < 200 km

General results: Negative trends of residuals with distance for R < 40 km, indicating faster distance attenuation in data than in models. Mixed trends with Vs30, indicating stronger Vs30 scaling in data than model. Intra-event sigma not looked at.

Proposed selection

- **Following one in-person meeting:**
    - Chiou & Youngs (2008): International
        - Large and international database
        - Good metadata
        - Sophisticated functional form
    - Akkar & Bommer (2010): Europe & Middle East
        - Distinct region
        - Large database
        - Higher sigma
        - Functional form modeling M-saturation and M-dependent distance decay
    - Zhao et al. (2006): Mostly Japan
        - Distinct region
        - Large database
        - Higher sigma
        - Functional form modeling M-saturation and M-dependent distance decay
- **We do not recommend application of linear site response in AB 2010 or ZEA 2006**

Trellis plots (PSA on rock, V_{s30}=1000m/s, SS)

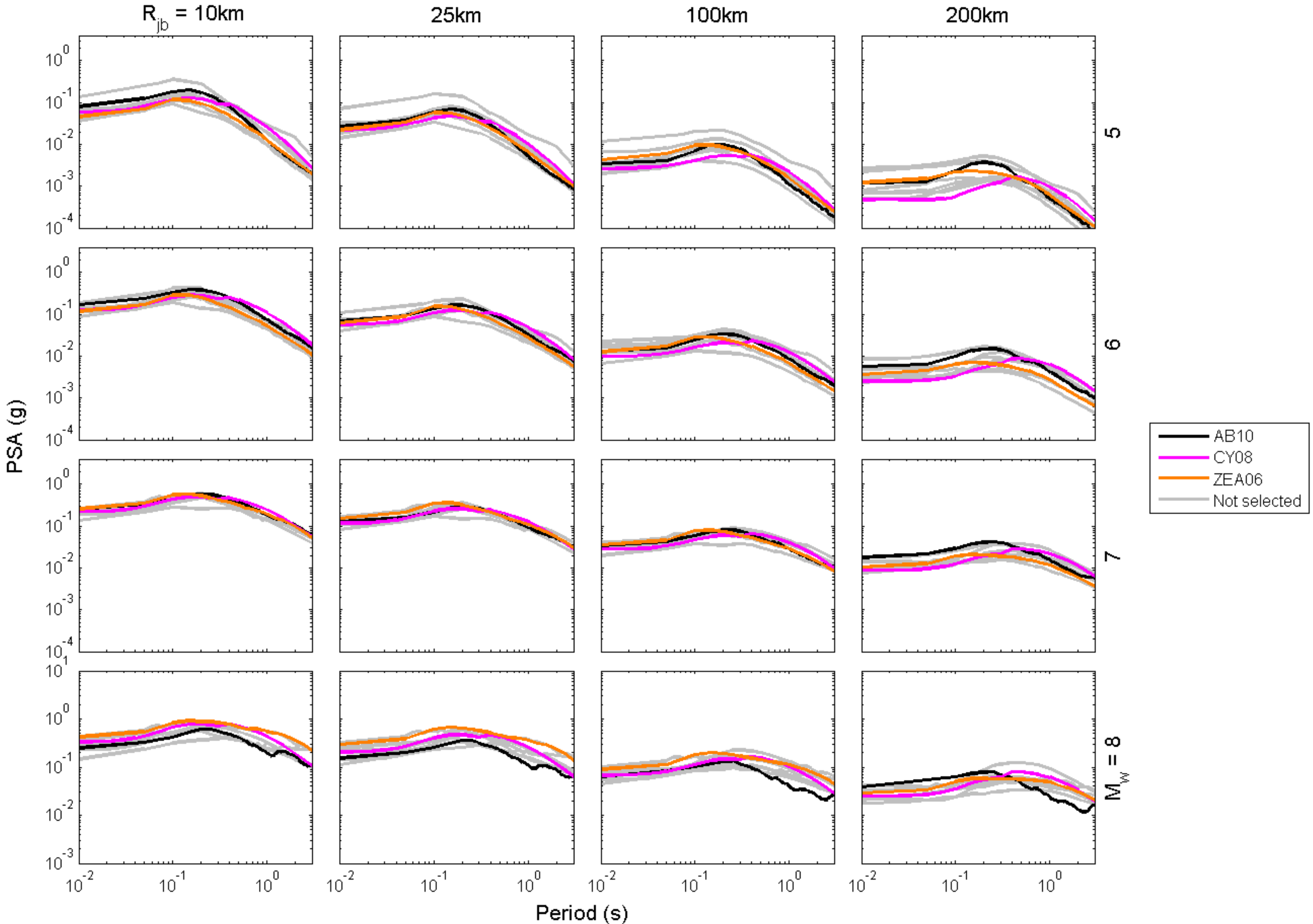

Magnitude-scaling for rock (SS)

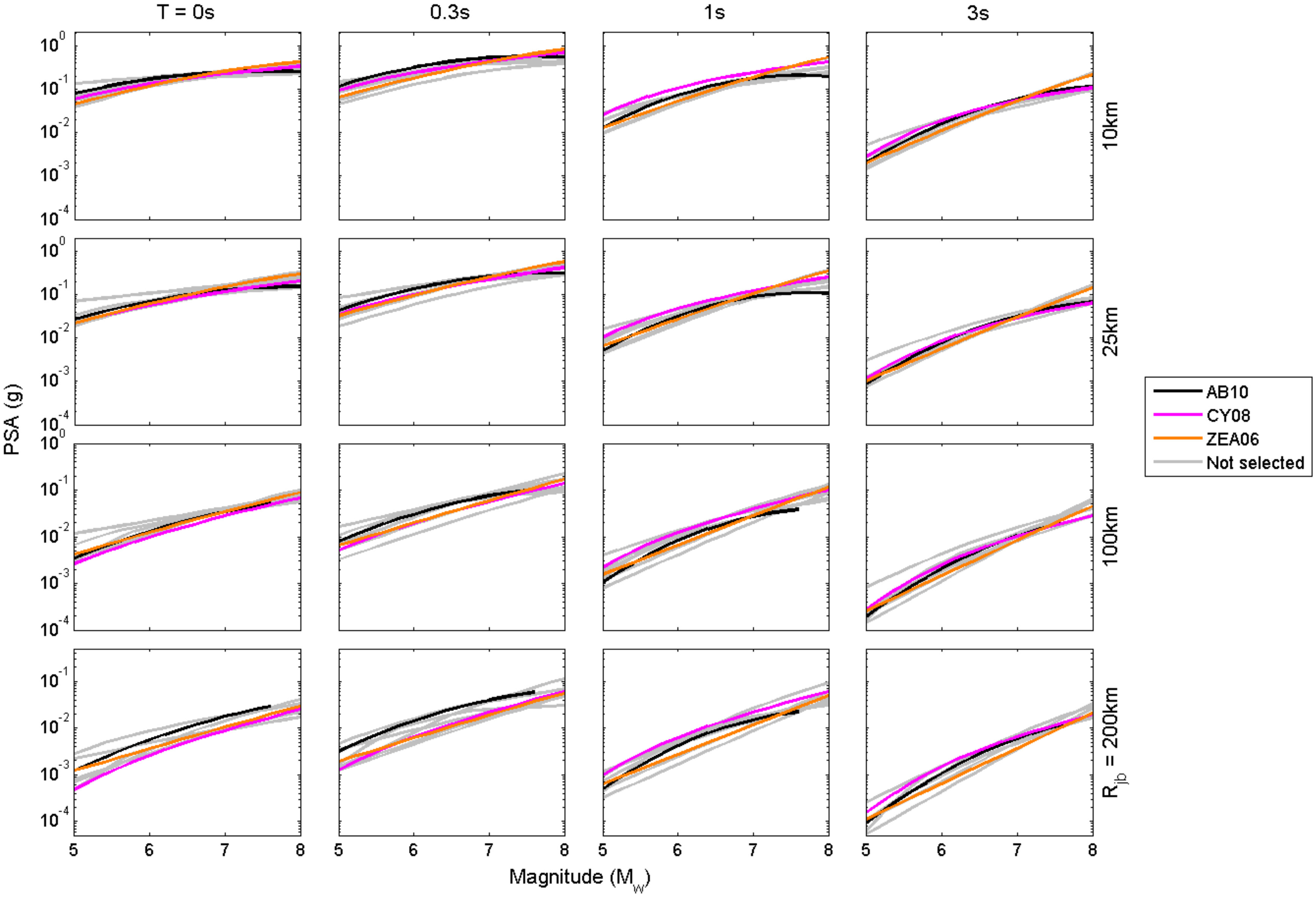

Distance-scaling (decay) for rock (SS)

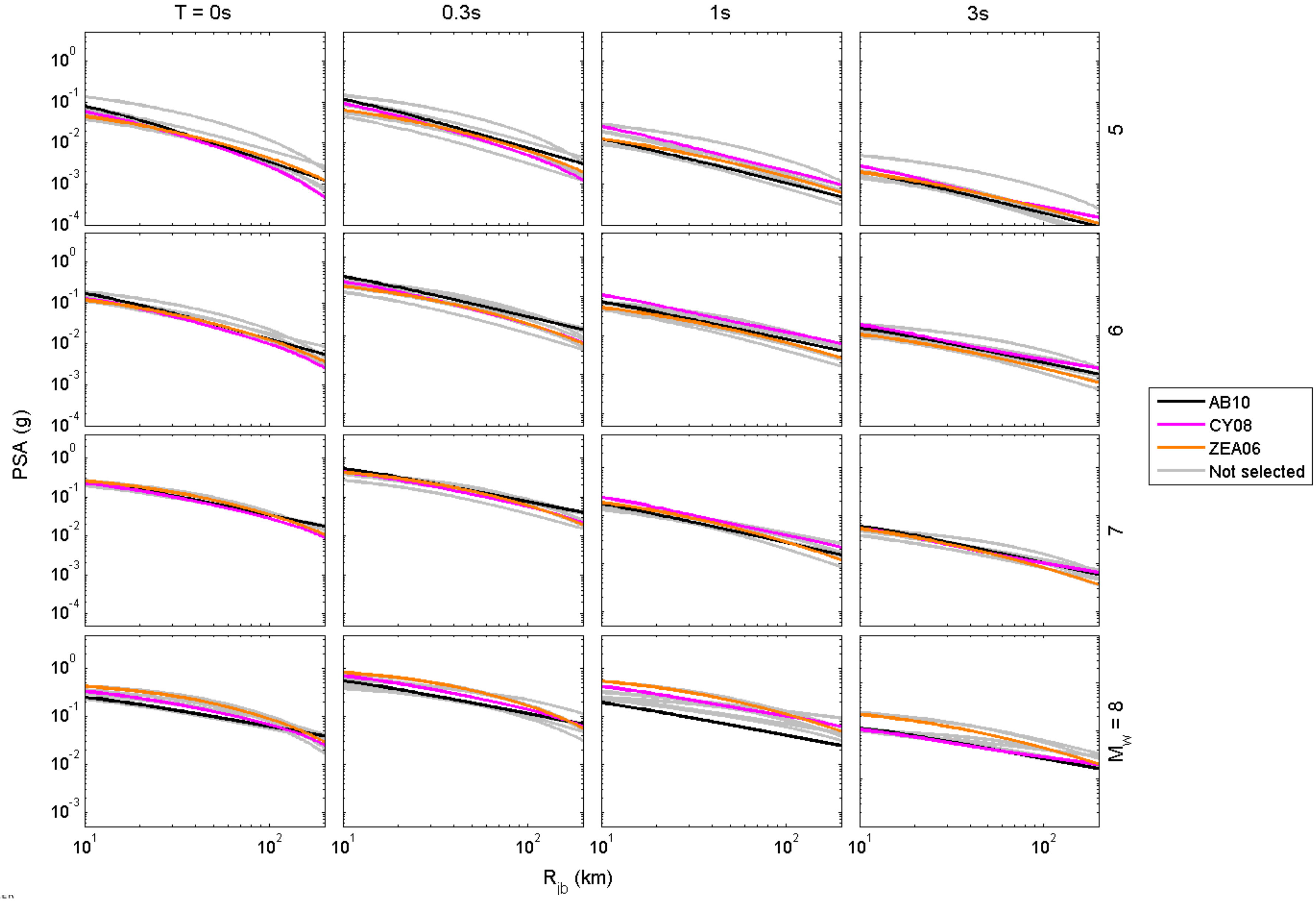

Sigma for rock

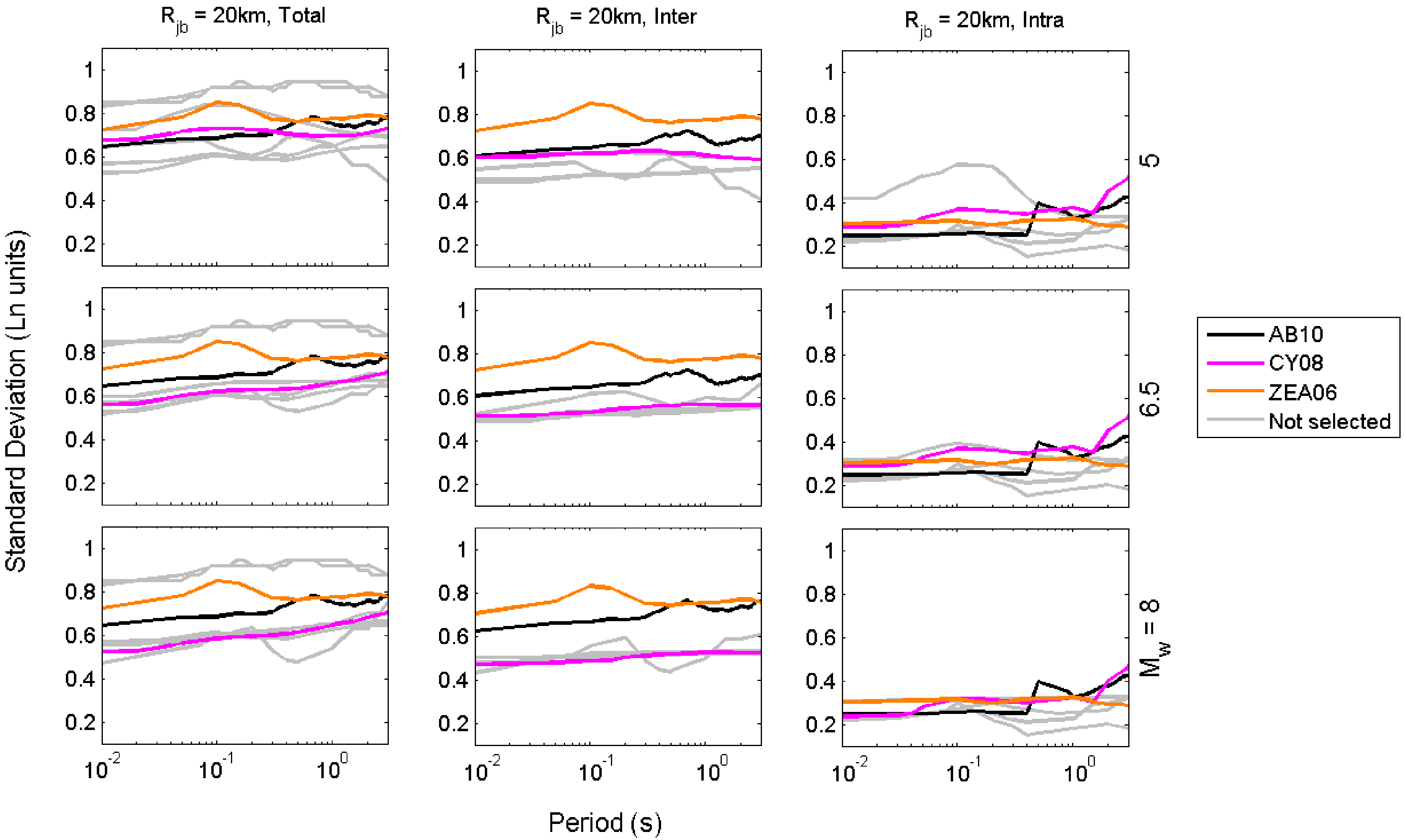

Preliminary selected GMPEs for Shallow Crustal Seismicity Regions

John Douglas & Jonathan P. Stewart (co-chairs)

C. di Alessandro, D. M. Boore, Y. Bozorgnia
N. A. Abrahamson, E. Delavaud, P. J.
Stafford, K. W. Campbell, M. Erdik &
M. B. Javanbarg

PEER

GEM
GLOBAL EARTHQUAKE MODEL

The Pacific Earthquake Engineering Research Center (PEER) is a multi-institutional research and education center with headquarters at the University of California, Berkeley. Investigators from over 20 universities, several consulting companies, and researchers at various state and federal government agencies contribute to research programs focused on performance-based earthquake engineering.

These research programs aim to identify and reduce the risks from major earthquakes to life safety and to the economy by including research in a wide variety of disciplines including structural and geotechnical engineering, geology/seismology, lifelines, transportation, architecture, economics, risk management, and public policy.

PEER is supported by federal, state, local, and regional agencies, together with industry partners.

PEER Core Institutions:
University of California, Berkeley (Lead Institution)
California Institute of Technology
Oregon State University
Stanford University
University of California, Davis
University of California, Irvine
University of California, Los Angeles
University of California, San Diego
University of Southern California
University of Washington

PEER reports can be ordered at http://peer.berkeley.edu/publications/peer_reports.html or by contacting

Pacific Earthquake Engineering Research Center
University of California, Berkeley
325 Davis Hall, mail code 1792
Berkeley, CA 94720-1792
Tel: 510-642-3437
Fax: 510-642-1655
Email: peer_editor@berkeley.edu

ISSN 1547-0587X